

Effect of Thiourea on the Radical Polymerization of Vinyl Monomers. Part II. Effect of Diphenyl Thiourea on the Polymerization of Methyl Methacrylate with Benzoyl Peroxide as Initiator

YUJI MINOURA and TAKA AKI SUGIMURA,
*Department of Chemistry, Osaka City University,
Kita-ku, Osaka, Japan*

Synopsis

The polymerization of methyl methacrylate (MMA) initiated by benzoyl peroxide (BPO) in the presence of diphenyl thiourea (DPTU) has been studied. It was found that the BPO-DPTU catalyst system was not an effective accelerating system but showed a relatively strong retarding effect. With DPTU derivatives, the polymerization rate was found to decrease with the increase in the electron-attracting forces of substituents attached to the phenyl groups of DPTU. In the polymerization of MMA initiated by AIBN, the addition of DPTU to the reaction systems affected neither the polymerization rate nor the degree of polymerization. From this fact, it might be concluded that DPTU itself serves as a radical scavenger. It seems most probable from the results of kinetic studies, iodometric titration, and from the effect of an oxidation product of DPTU (diphenyl formamidine disulfide) that the retardation effect observed is attributable to the action of the disulfide (DPFDS). By extending the Alfrey-Price scheme for the copolymerization reactions to the chain-transfer reactions, the Q and e values of DPFDS were determined. The apparent chain-transfer constants for DPTU and its derivatives were calculated by means of rate measurements and were correlated with substituent constants. The mechanism of the polymerization is discussed on the basis of these results.

INTRODUCTION

Benzoyl peroxide (BPO) is commonly used as a radical initiator for vinyl monomers. Its decomposition is strongly accelerated by the addition of reducing agents, such as amine compounds,^{1,2} to produce free radicals due to one-electron transfer with concomitant cleavage of the —O—O— bond under attack by these nucleophiles. The polymerizations with these catalyst systems are referred to as redox polymerization.

On the other hand, it was also reported that the decomposition of BPO was accelerated by phenol compounds, but in these occasions the reaction proceeded via a nonradical mechanism, so the BPO-C₆H₅OH catalyst system is not an effective polymerization catalyst.³ Thus, it is known that there are two different types of decomposition of BPO, i.e., radical and nonradical mechanisms.

In a previous paper,⁴ it was found that acrylonitrile polymerization initiated by hydrogen peroxide in an aqueous solution was effectively accelerated by the addition of thiourea, while preliminary studies showed that the BPO-diphenyl thiourea (DPTU) catalyst system produced no effective acceleration and decreased the polymerization rate.

In this paper, studies of the polymerization of methyl methacrylate (MMA) initiated by the BPO-DPTU system are reported. The polymerization of MMA was carried out at 50°C. in benzene. The polymerization rate was calculated from results of gravimetric analysis and was found to decrease with addition of DPTU. It might be considered that the retardation effect was not due to the action of DPTU itself but could be attributed to the effect of its oxidation product, namely, diphenyl formamidine disulfide (DPFDS). This assumption was consistent with the results of kinetic studies, iodometric titration, and of the effect of DPFDS. Disulfides, in general, tended to retard the polymerization, since the radicals derived from them were so often of lower reactivity than the polymer radicals.

By using the transfer data of two monomers, whose Q and e values have been reported in the literature,⁵ Q_{tr} and e_{tr} for DPFDS were calculated according to the Alfrey-Price $Q-e$ scheme⁶ and the modified equation.⁷ Apparent chain-transfer constants for these retarded polymerizations were determined by means of rate measurements,⁸ and correlated with the substituent constants. The mechanism of the polymerization is discussed on the basis of these experimental results.

EXPERIMENTAL

Reagents

Methyl Methacrylate. Commercially available monomer was distilled with steam. The inhibitor was removed with care by washings with 10% sodium hydroxide solution and then with water. The monomer was dried over calcium chloride, distilled under nitrogen at reduced pressure, and its middle fraction was collected and kept in a dark place at 0°C. This fraction was freshly distilled at 45–45.5°C.

Styrene. Commercial monomer was purified by distillation under nitrogen after removing the inhibitor and drying; b.p. 70–71°C./61 mm. Hg.

Benzene. Analytical grade reagent was washed with concentrated sulfuric acid and with water. It was distilled twice over sodium wire after drying over calcium chloride and refluxing with sodium metal.

Diphenyl Thiourea. Commercial product was purified by recrystallization twice from ethanol; m.p. 151–152°C.

Preparation of Diphenyl Thiourea Derivatives

***N,N'*-Bis(*p*-tolyl)thiourea.**⁹ *p*-Toluidine (100 g.) was dissolved in a mixture of carbon disulfide (18.5 g.) and ethanol (300 ml.) together with a

small amount of sulfur. The reaction mixture was gently refluxed until evolution of hydrogen sulfide gas ceased. The reaction product was filtered off and recrystallized three times from ethanol; m.p. 178–179°C.

ANAL. Calcd. for $C_{13}H_{16}N_2S$: C, 70.2%; H, 6.3%; N, 10.9%. Found: C, 70.2%; H, 6.4%; N, 10.5%.

***N,N'*-Bis(*p*-chlorophenyl)thiourea.** According to the method of Fry,¹⁰ *p*-chloroaniline and pyridine were dissolved in 200 ml. of carbon disulfide, and iodine dissolved in 100 ml. of carbon disulfide was added to the solution. The reaction mixture was warmed for several hours, then distilled with steam. The product was washed with water to remove traces of carbon disulfide, pyridine, and pyridinium salt. The residue was fractionally crystallized from ethanol; m.p. 167–168°C.

ANAL. Calcd. for $C_{13}H_{10}N_2Cl_2S$: C, 52.6%; H, 3.2%; N, 9.4%. Found: C, 51.7%; H, 3.2%; N, 7.9%.

***N,N'*-Bis(*m*-tolyl)thiourea.**¹¹ Similarly to the preparation method of *p*-tolyl derivative, an ethanol solution of *m*-toluidine and carbon disulfide was refluxed for about 5 hr. The product was recrystallized twice from benzene; m.p. 121–122°C.

ANAL. Calcd. for $C_{14}H_{16}N_2S$: C, 70.2%; H, 6.3%; N, 10.9%. Found: C, 70.0%; H, 6.5%; N, 10.7%.

***N,N'*-Bis(*m*-nitrophenyl)thiourea.**¹² *m*-Nitroaniline was mixed with carbon disulfide and ethanol containing pyridine and iodine. The product was recrystallized twice from ethanol; m.p. 160–161°C.

ANAL. Calcd. for $C_{13}H_{10}N_4O_4S$: C, 49.1%; H, 3.2%; N, 17.6%. Found: C, 50.0%; H, 3.2%; N, 17.5%.

Other Thioureas. Preparative methods for *N,N'*-bis(methoxyphenyl)-thiourea¹³ and *N,N'*-bis(*p*-dimethylaminophenyl)thiourea¹⁴ were similar to the above-mentioned methods used to prepare DPTU derivatives. The methoxy derivative of DPTU had m.p. 125–126°C.

ANAL. Calcd. for $C_{15}H_{16}N_2O_2S$: C, 63.0%; H, 5.6%; N, 9.7%. Found: C, 62.6%; H, 5.6%; N, 10.0%.

The dimethylamino derivative of DPTU had m.p. 184–185°C.

ANAL. Calcd. for $C_{17}H_{22}N_2S$: C, 65.0%; H, 7.0%; N, 16.9%. Found: C, 64.7%; H, 7.1%; N, 17.0%.

Diphenyl Formamidine Disulfide. According to the method of Hodoson,¹⁵ fine powders of DPTU (2.7 g.) and benzoyl peroxide (1.3 g.) were added to a 100-ml. three-necked flask containing 25 ml. of petroleum ether. The reaction was carried out at room temperature for 2 hr. under nitrogen. The reaction product was carefully recrystallized from petroleum ether.

ANAL. Calcd. for $C_{26}H_{22}N_4S_2$: C, 68.7%; H, 4.9%; N, 12.3%. Found: C, 68.4%; H, 4.8%; N, 12.4%.

Polymerization

The polymerizations were carried out in benzene at 50°C. (± 0.05) in sealed tubes. The required amounts of reactants were placed into clean tubes, then degassed by repeated freezing and thawing cycles and the tubes were sealed. The polymerization was stopped before the conversion reached 2–10%, then the reaction mixture was poured into a large volume of methanol and the precipitate formed was filtered off and dried *in vacuo* at 40°C. to constant weight.

Molecular Weight Measurement

Solution viscosities of the polymer samples were determined at 30°C. with an Ubbelohde dilution viscometer. The number-average degrees of polymerization were calculated from the relationship:¹⁶

$$\log \bar{P}_n = 3.420 + 1.13 \log [\eta] \quad (1)$$

RESULTS AND DISCUSSION

The effects of monomer, initiator, and DPTU concentration on the polymerization of MMA by BPO were studied. It was found that the rate of polymerization was proportional to the monomer concentration and

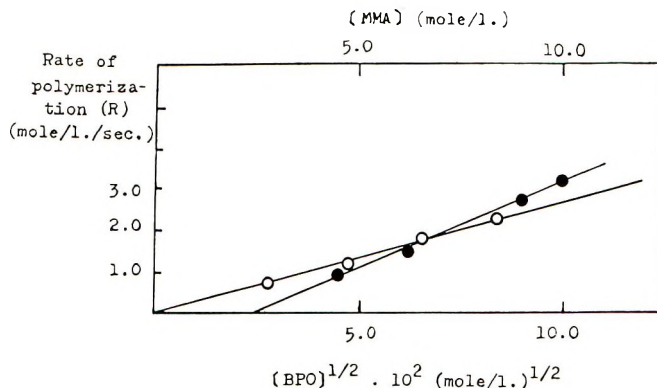


Fig. 1. Dependence of polymerization rate on BPO and monomer concentration at 50°C.: (●) rate of polymerization vs. BPO concentration, [MMA] = 4.68 mole/l., [DPTU] = 1.2 mmole/l.; (○) rate of polymerization vs. MMA concentration, [BPO] = 4.2 mmole/l., [DPTU] = 0.42 mmole/l.

to the square root of the concentration of BPO (Fig. 1). In marked contrast with the results of a previous study,⁴ no acceleration effect was observed for the BPO–DPTU catalyst system. In this case it was found that DPTU acted as an inhibitor and retarder as shown in Figure 2. In this case the polymerization was carried out at fixed concentrations of BPO and monomer with increasing of DPTU. This degradative chain-transfer effect is known for various organic compounds such as disulfides¹⁷ and allyl compounds.¹⁸ However, when the polymerization was carried out

with azobisisobutyronitrile (AIBN) as initiator instead of BPO, no retardation effect was observed and the decrease in the degree of polymerization was found to be low. The chain-transfer constant for DPTU was 8×10^{-3} in this case. It may be considered that the reactivity of DPTU as transfer agent is probably low. It is known that BPO can interact with protic compounds and no free radicals are formed as intermediate in this reaction. It may be considered therefore, that the retardation effect observed for the BPO-DPTU system is not due to the behavior of DPTU itself as a radical scavenger.

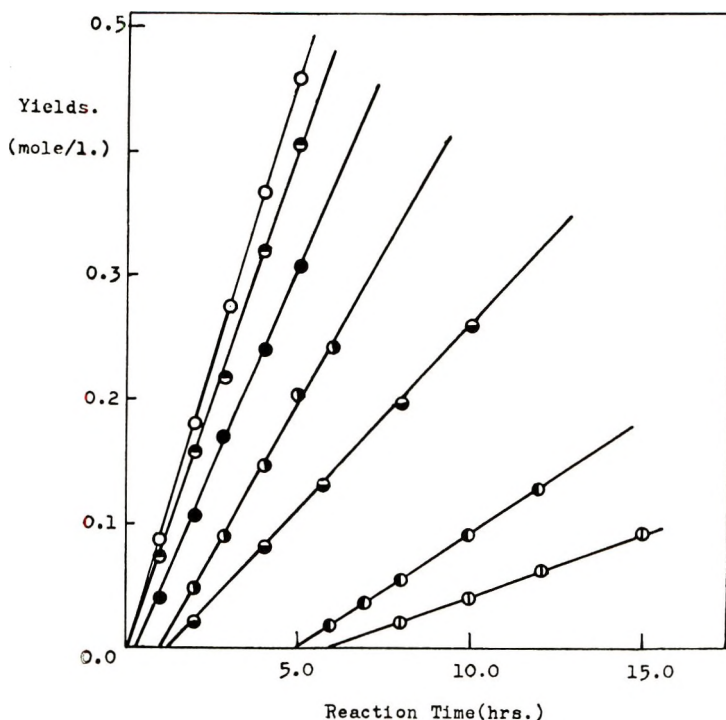


Fig. 2. Effect of DPTU on BPO-initiated polymerization of MMA at 50°C., [BPO] = 4.20 mmole/l., [MMA] = 4.68 mole/l., and various DPTU concentrations: (○) 0.00; (●) 0.42 mmole/l., (●) 0.84 mmole/l.; (◐) 2.10 mmole/l.; (◑) 4.20 mmole/l.; (◒) 8.40 mmole/l.; (◓) 21.0 mmole/l.

The reaction between an organic peroxide and an amine compound proceeds explosively,^{1,2,19} e.g., the BPO-tertiary amine system acts as an effective initiator for the polymerization of vinyl monomers.

The polymerization with diphenyl urea (DPU) instead of DPTU was also studied, and it was found that the addition of DPU had no effects on the polymerization rate (i.e., acceleration and retardation). Although DPTU contains two functional groups, it seems probable that DPTU would interact with BPO not at the nitrogen but at the sulfur of DPTU through a nonradical mechanism to retard polymerization rate. Since it

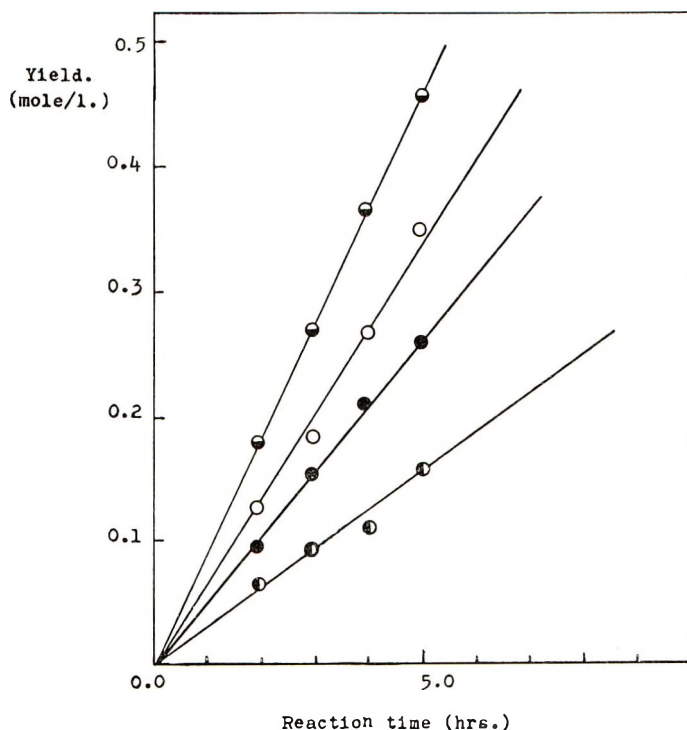
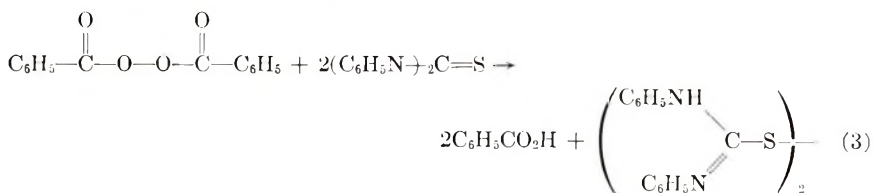


Fig. 3. Effect of DPFDS on BPO-initiated polymerization of MMA at 50°C., [BPO] = 4.20 mmole/l., [MMA] = 4.68 mole/l., and various DPFDS concentrations: (◐) 0.0; (○) 0.42 mmole/l.; (●) 1.05 mmole/l.; (◑) 2.10 mmole/l.

is known that the negative electromeric effect of =S, i.e., the π -electron-attracting force, is stronger than that of =O,²⁰ and since thiourea undergoes a thiolike reaction owing to its tautomerization



BPO may interact with DPTU to produce disulfide which would serve as a transfer agent, followed by the retardation effect [eq. (3)].



Recently, Hodoson and Serban¹⁵ showed that DPFDS is produced by the reaction of BPO with DPTU, although the reaction was carried out in the absence of polymerizable monomers and the mechanism of formation of DPFDS was not clear. The effect of DPFDS prepared according to Hodoson's method on the polymerization of MMA initiated by BPO, is

TABLE I
 Effects of DPTU and DPFDS on the Polymerization of MMA

[DPTU] $\times 10^3$, mole/l.	$R_p \times 10^5$, mole/l.-sec.	[DPFDS] $\times 10^3$, mole/l.	$R_p \times 10^5$, mole/l.-sec.
0.0	2.56	0.0	2.54
0.84	1.82	0.42	1.88
2.10	1.38	1.05	1.42
4.20	0.84	2.10	0.87

shown in Figure 3. On comparing the effect of disulfide with the results shown in Figure 2, it was found that no induction period was observed on the addition of DPFDS, while after addition of DPTU, an induction period was noted (Table I). The degree of retardation was found to be in good agreement with the results shown in Figure 2 for the corresponding concentration of DPTU (DPTU/DPFDS = 2/1).

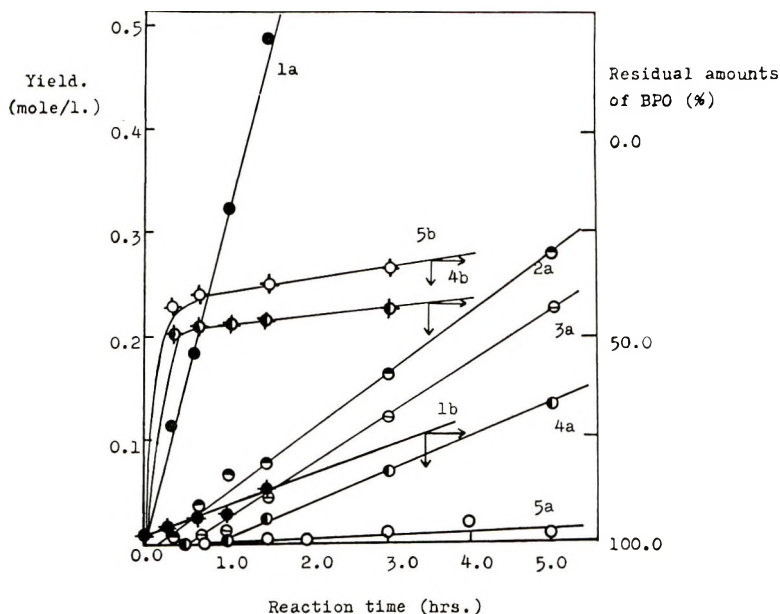
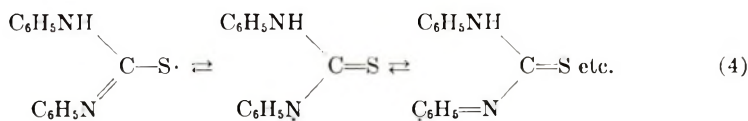


Fig. 4. Effect of DPTU on the polymerization of MMA at [BPO] = 50.0 mmole/l., [MMA] = 4.68 mole/l., and various concentrations of DPTU: (1) 0.0; (2) 16.0 mmole/l.; (3) 24.0 mmole/l.; (4) 32.0 mmole/l.; (5) 40.0 mmole/l. Curves *a* show plots of reaction time vs. yield of PMMA (polymer isolated after titration analysis of BPO); curves *b* show plots of reaction time vs. BPO consumed by DPTU which correspond to the identical numbered curves *a*.

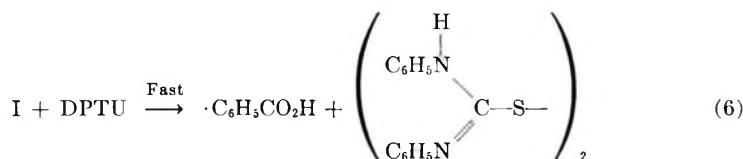
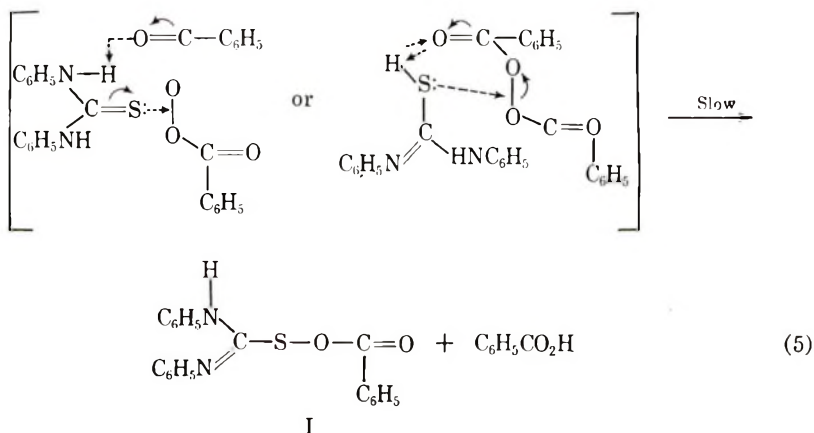
The thermal dissociation of DPFDS to two thiyl radicals and its ability to initiate polymerization are considered. In the experiments on the addition of disulfide as the initiator for the polymerization of MMA and styrene (St), no polymerization took place at 50°C. for both monomers after 10 and 20 hr., respectively. Hence, DPFDS could not initiate poly-

merization of MMA and St, even if it might be dissociated into thiyl radicals. The thiyl radical derived from disulfide was considered to be stabilized due to its many resonance forms [eq. (4)]



Hence the stabilized radical cannot be an initiator for vinyl polymerization. The amount of BPO consumed by the reaction with DPTU in the polymerization systems was determined by means of iodometry in order to assess the amount of BPO consumed in the fast stage of the polymerization. The results are shown in Figure 4.

It seems likely that the results shown in Figures 2-4 demonstrate that DPTU reacts rapidly with BPO through a nonradical mechanism to produce disulfide during the fast stage of polymerization. The interaction mechanism for the formation of disulfide would probably be a four-centered mechanism such as that postulated by Walling et al.³ for the reaction of BPO with phenol [eqs. (5) and (6)].



The DPFDS thus produced would behave as a retarder during polymerization. The induction periods observed are probably due to the following two factors: (a) radical deactivation reactions by DPTU and DPFDS and (b) the decrease in the decomposition rate of BPO accompanying the consumption of BPO by the polar reaction as mentioned above.

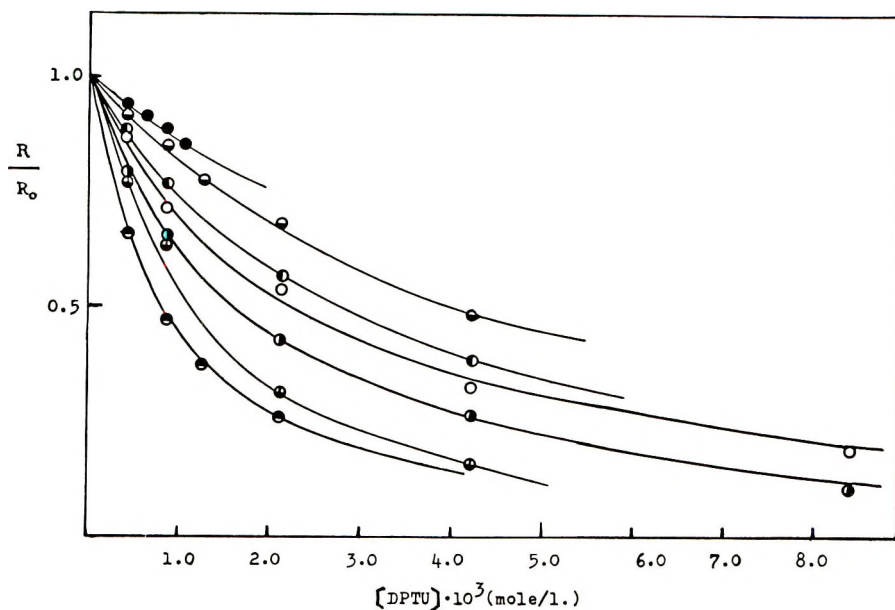
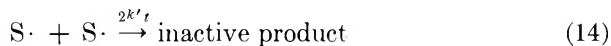
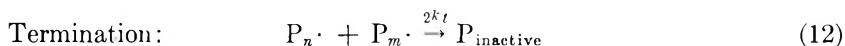
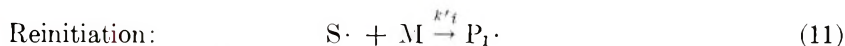
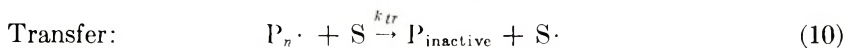
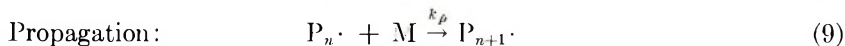
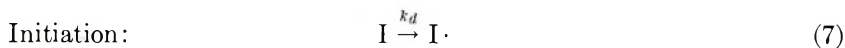


Fig. 5. Effects of substituents of DPTU on polymerization ratio: (●) $p\text{-N}(\text{CH}_3)_2$; (○) $p\text{-CH}_3$; (●) $m\text{-CH}_3$; (○) H; (○) $m\text{-OCH}_3$; (○) $p\text{-Cl}$; (●) $m\text{-NO}_2$.

The polymerization scheme is shown in eqs. (7)–(14).



In this scheme S is the added retarder and $\text{S}\cdot$ is the radical formed by the reaction of $\text{P}\cdot$ with the retarder. This kinetic scheme is similar to Kice's⁸ treatment, in which the chain-transfer constant was determined from the polymerization rate for retarded systems. According to Kice's treatment, eq. (15) was derived from the scheme mentioned above, where, the overall polymerization rate is represented by $R = k_p[\text{R}\cdot][\text{M}]$ in the presence of DPTU and $R_t = k_p[\text{R}\cdot]_0[\text{M}]$ in the presence of DPTU.

$$\frac{A^2[S]}{1-A^2} \left[1 + \sqrt{1 + \frac{c(1-A^2)}{A^2}} \right] = \frac{1}{[M]} \frac{2k_t R}{k_p k_{tr}} \sqrt{1 + \frac{c(1-A^2)}{A^2}} + \left(\frac{2k_t k_i' [M]}{k' k_{tr}} \right) \quad (15)$$

Here A is R/R_0 , R and R_0 are polymerization rates at the presence and absence of retarder, respectively, and $c = 4k_t k_i'' / k_i' {}^2$.

The effects of substituents on the polymerization rate were studied by using *para* or *meta* derivatives of DPTU. The results are shown in Figure 5. As can be seen from Figure 5, the polymerization rate decreased when electron-withdrawing substituents were added to the phenyl groups of DPTU. By using eq. (15), the apparent chain-transfer constants for DPTU and its derivatives based on the above-mentioned assumption, were determined (Fig. 6), and the results are summarized in Table II. The chain-transfer constants were obtained from $1/P_n$ versus $[S]/[M]$ according to the Mayo-Lewis method (Fig. 7), and the results are also shown in Table II.

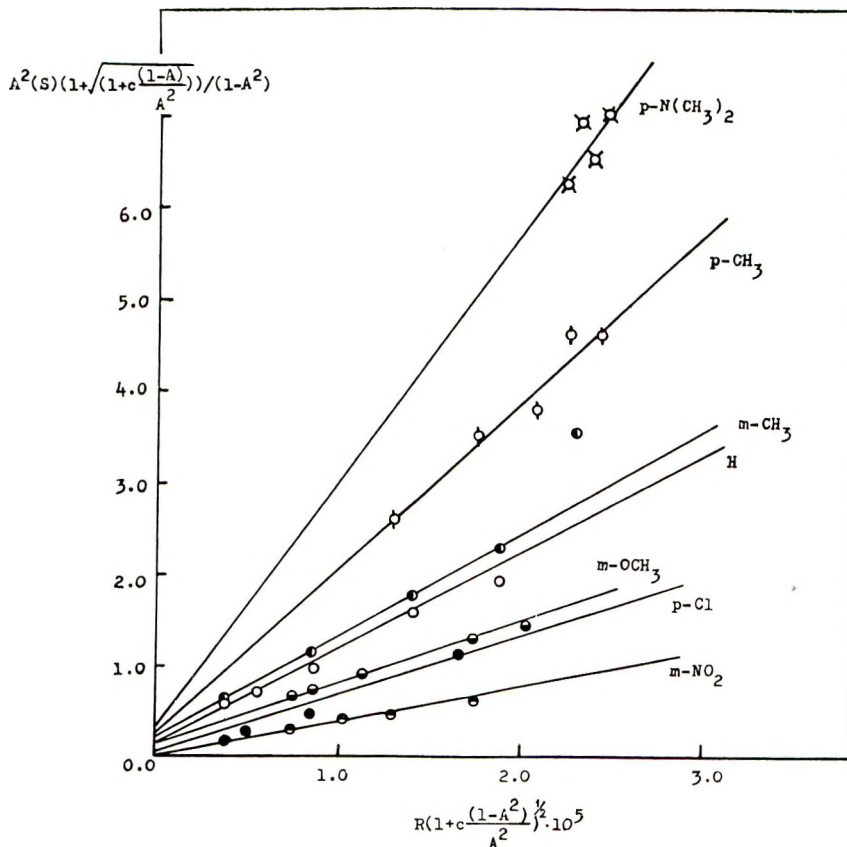


Fig. 6. Determination of chain-transfer constants by means of eq. (15).

TABLE II
Transfer Constants for DPTU and its Derivatives in MMA Polymerization with BPO as Initiator at 50°C.

Substituents of DPTU	k_{tr} , l./mole-sec. ^a	C_{tr} ^b	$k_i'/k_i'' \times 10^5$	c_{tr} from Mayo eq. ^c
<i>p</i> -N(CH ₃) ₂	48	0.09	0.79	0.45
<i>p</i> -CH ₃	72	0.13	0.81	0.17
<i>m</i> -CH ₃	115	0.21	0.98	0.19
H ^d	121	0.22	0.88	0.35
<i>m</i> -OCH ₃	185	0.33	1.36	0.18
<i>p</i> -Cl	197	0.35	0.36	0.09
<i>m</i> -NO ₂	307	0.55	—	0.34

^a k_{tr} calculated by eq. (15) using $c = (4k_i k_i''/k_i') = 10^{-2}$.

^b $C_{tr} = k_{tr}/k_p$, k_p used is the value of Matheson et al.⁵ (i.e., Kice's method).

^c C_{tr} values were determined from the Mayo-Lewis equation.

^d Rate constants for DPTU were calculated from both sets of data, i.e., from data for DPTU and DPFDS.

The relationship between the chain-transfer constant [from eq. (15)] and the substituent constant is shown to be appropriately linear ($\rho = +0.35$) (Fig. 8). Using the radioactive tracer methods for the measurement of transfer constants of vinyl monomers with *n*-butyl mercaptan, Walling²¹ suggested that the polar and resonance factors are also involved

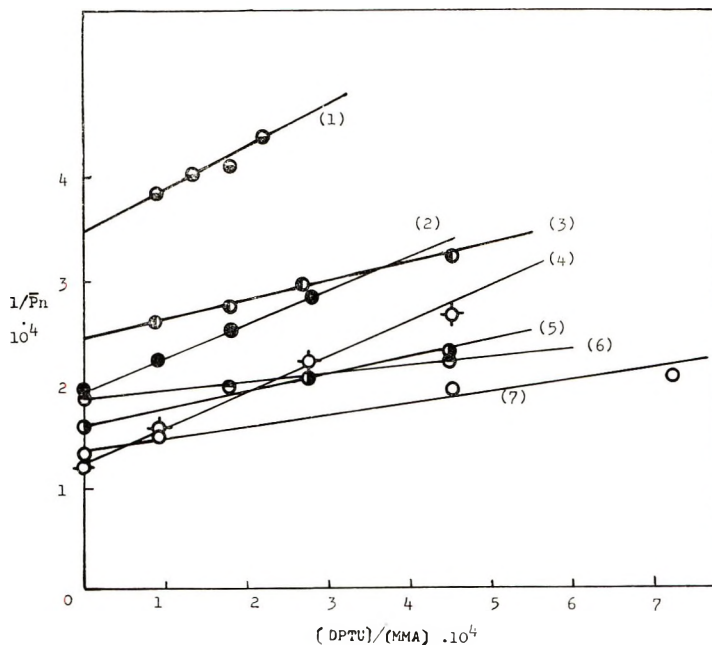


Fig. 7. Determination of chain-transfer constants from the Mayo-Lewis equation for variously substituted DPTU derivatives: (1) *p*-N(CH₃)₂; (2) *m*-NO₂; (3) *p*-CH₃; (4) H; (5) *m*-CH₃; (6) *p*-Cl; (7) *m*-OCH₃.

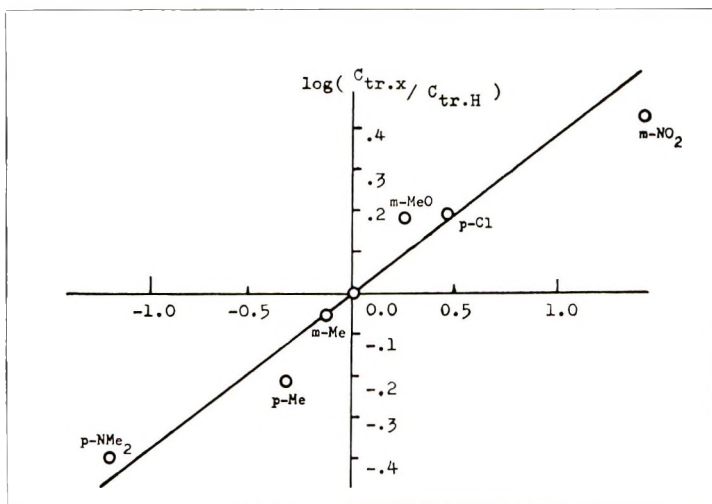
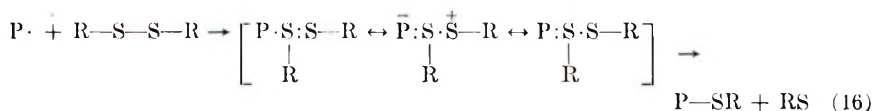


Fig. 8. Relationship between apparent chain-transfer constants calculated from eq. (15) and Hammett's substituents constants.

in the chain-transfer reaction and explained this by the presence of additional ionic forms in the transition state arising from the transfer of one electron from the attacking radical to the transfer reagent, or vice versa.^{21,22} These ionic factors in radical reactions have been discussed in the literature.^{23,24}

In the present study, the transition state of the reaction between the polymeric radical and disulfide would then have the polar contribution shown in eq. (16).



Schaafsma et al.²⁴ have measured the effect of ring substituents in thiophenol on the rate of the transfer reactions with 1-cyano-1-cyclohexyl radicals. The relative reactivity constants for the series of eight thiols studied fit Hammett's equation quite well with a value for ρ of -0.4 . The explanation suggested by the authors, is that the cyanocyclohexyl radical is more electronegative than the thiol. Therefore the polar contribution for transition state in this result is inverse to the above-mentioned scheme. Mesrobian and Fuhrman applied⁷ the Alfrey-Price $Q-e$ scheme⁶ to the transfer reaction:

$$C = k_{tr}/k_{11} = Q_{tr}/Q_1 \exp \{ -e_1(e_{tr} - e_1) \} \quad (17)$$

where Q_{tr} and Q_1 refer to the general reactivity of the transfer agent and monomer, respectively, and e_{tr} and e_1 refer to their polarities.

By using the transfer data of the two monomers whose Q and e values have been reported in literature,⁵ eq. (17) was employed to calculate Q_{tr}

and e_{tr} for nonsubstituted DPFDS. Based on the transfer data obtained from MMA and St at 50°C., the Q_{tr} and e_{tr} values for DPFDS are 0.41 and +2.70, respectively. The chain-transfer constant of St for DPFDS was 6.72, and this value is greater than that of MMA.

The relatively high positive e value of DPFDS indicates that DPFDS serves as an electron acceptor and should exhibit an increased reactivity with electron donor radicals. It is probable that the fact that the e_{tr} value is not so large as expected, is due to the effect of the neighboring amino groups.

References

1. L. Honer, E. Schwenk et al., *Ann.*, **573**, 35 (1961); *ibid.*, **574**, 202 (1951); *J. Polymer Sci.*, **18**, 438 (1955).
2. M. Imoto et al., *J. Polymer Sci.*, **22**, 137 (1956).
3. C. Walling and R. B. Hodgdon, Jr., *J. Am. Chem. Soc.*, **80**, 228 (1958).
4. Y. Minoura, N. Yasumoto, and T. Sugimura, *J. Polymer Sci. A*, **3**, 2935 (1965).
5. M. S. Matheson, E. E. Auer, E. B. Bevilacqua, and E. J. Hart, *J. Am. Chem. Soc.*, **71**, 497 (1949); *ibid.*, **73**, 1700 (1951).
6. T. Alfrey, Jr. and C. C. Price, *J. Polymer Sci.*, **2**, 101 (1947).
7. R. B. Mesrobian and N. Fuhrman; *J. Am. Chem. Soc.*, **76**, 3281 (1954).
8. J. L. Kice, *J. Am. Chem. Soc.*, **76**, 6274 (1954).
9. A. W. Hugershoff, *Ber.*, **32**, 2245 (1899).
10. H. S. Fry, *J. Am. Chem. Soc.*, **35**, 1539 (1913).
11. A. Weith and A. Londolt, *Ber.*, **8**, 718 (1875).
12. H. S. Fry, *J. Am. Chem. Soc.*, **35**, 1544 (1913).
13. G. M. Dyson, H. J. Georg, and R. F. Hunter, *J. Chem. Soc.*, **1927**, 440.
14. A. Bauer, *Ber.*, **12**, 533 (1879).
15. F. Hodoson and N. Serban, *Bull. Soc. Chim. France*, **1960**, 133.
16. A. V. Tobolsky and B. Baysal, *J. Polymer Sci.*, **9**, 171 (1952).
17. W. H. Stockmayer, R. O. Howard, and J. T. Clarke, *Makromol. Chem.*, **44-46**, 427 (1961).
18. P. D. Bartlett and R. Altschul, *J. Am. Chem. Soc.*, **67**, 812, 816 (1945).
19. H. E. de la Mare, *J. Org. Chem.*, **25**, 2114 (1960).
20. C. K. Ingold, *Structure and Mechanism in Organic Chemistry*, 1953, pp. 64-92.
21. C. Walling, *J. Am. Chem. Soc.*, **70**, 256 (1948).
22. R. A. Gregg and F. R. Mayo, *J. Am. Chem. Soc.*, **75**, 3530 (1953).
23. F. R. Mayo and C. Walling, *Chem. Rev.*, **46**, 191 (1950).
24. Y. Schaafsma, A. F. Bickel, and E. C. Kooyman, *Rec. Trav. Chim.*, **76**, 180 (1957).

Résumé

La polymérisation du méthacrylate de méthyle initié par le peroxyde de benzoyl (BPO) en présence de diphénylthiourée (DPTU) a été étudiée. On a trouvé que le système catalyseur BPO-DPTU ne constitue pas un système accélérateur efficace, mais au contraire manifeste un effet retardateur relativement prononcé. Utilisant des dérivés du DPTU, la vitesse de polymérisation décroît avec le caractère électro-capteur croissant des substituants attachés aux groupes phényles du DPTU. Dans la polymérisation du méthacrylate de méthyle initiée par l'azo-bis-isobutyronitrile, l'addition de DPTU n'exerce aucun effet, ni sur la vitesse de polymérisation, ni sur le degré de polymérisation. De ceci on peut conclure que la DPTU elle-même exerce un rôle capteur de radicaux. Il semble très probable sur la base de résultats d'études cinétiques, de titration iodométrique et de l'effet du produits d'oxydation de DPTU (disulfure de formamidoné), que le retardement de la réaction observé doit être attribué à l'action du disulfure (DPFDS).

Par extension du schéma de Alfrey-Price, (Q, e) pour les réactions de copolymérisation aux réactions de transfert de chaînes, les valeurs de Q, e de DPFDS ont été déterminées. Les constantes apparentes de transfert de chaînes pour la DPTU et ses dérivés, ont été calculées au moyen des mesures de vitesse et ont été reliées aux constantes des substituants. Le mécanisme de la polymérisation a été discuté sur la base de ces résultats.

Zusammenfassung

Die durch Benzoylperoxyd (BPO) in Gegenwart von Diphenylthioharnstoff (DPTU) gestartete Polymerisation von Methylmethacrylat (MMA) wurde untersucht. Es zeigte sich, dass das BPO-DPTU-Katalysatorsystem nicht als Beschleuniger, sondern als verhältnismässig starker Verzögerer wirkte. Bei Verwendung von DPTU-Derivaten hatte die Polymerisationsgeschwindigkeit mit steigender Elektronen-Anziehungstendenz der Substituenten an den Phenylgruppen des DPTU ab. Bei der mit AIBN gestarteten Polymerisation von MMA hatte der Zusatz von DPTU zum Reaktionssystem weder auf die Polymerisationsgeschwindigkeit noch auf den Polymerisationsgrad Einfluss. Daraus kann geschlossen werden, dass nicht DPTU selbst als Radikalabfänger wirksam ist. Die Ergebnisse der kinetischen Untersuchungen, der jodometrischen Titration sowie der Einfluss des Oxydationsproduktes von DPTU, Formamidindisulfid, lassen es am wahrscheinlichsten erscheinen, dass der beobachtete Verzögerungseffekt dem Disulfid DPFDS zuzuschreiben ist. Durch eine Erweiterung des Q, e -Kopolymerisationsschemas von Alfrey-Price auf die Kettenübertragung konnten die Q - und e -Werte für DPFDS bestimmt werden. Die scheinbaren Übertragungskonstanten für DPTU und seine Derivate wurden aus Geschwindigkeitsmessungen berechnet und zu Substituentenkonstanten in Beziehung gesetzt. Auf Grundlage der Ergebnisse wurde der Polymerisationsmechanismus diskutiert.

Received January 6, 1966

Revised March 5, 1966

Prod. No. 5112A

Effect of Thiourea on the Radical Polymerization of Vinyl Monomers. Part III. Effect of Diphenyl Thiourea on the Polymerization of Methyl Methacrylate with Various Organic Peroxides as Initiator

TAKA AKI SUGIMURA and YUJI MINOURA, *Department of Chemistry, Osaka City University, Kita-ku, Osaka, Japan*

Synopsis

The effect of diphenyl thiourea (DPTU) on the radical polymerization of methyl methacrylate (MMA) has been studied in benzene solution at 50°C. with the use of cumene hydroperoxide (CHP), *p*-menthane hydroperoxide (PMHP), *tert*-butyl perbenzoate (tBPBz), di-*tert*-butyl peroxide (DBP), and dicumyl peroxide (DCP) as initiators. In the CHP-initiated polymerization, the rate of polymerization increased appreciably on addition of DPTU with a linear dependence on the square root of DPTU concentration up to a maximum which was observed when the ratio of the concentration of CHP to DPTU was 2.5. Then the rate decreased gradually with increasing DPTU concentration in the range greater than the above ratio. It was found from kinetic studies that the overall polymerization rate R_p was expressed by the equation: $R_p = K[\text{peroxide}]^{1/2}[\text{DPTU}]^{\alpha}[\text{MMA}]$, where K is the rate constant, $\alpha = 1.2$ for CHP and $\alpha = 1.0$ for tBPBz. It was thought that the acceleration effect observed was due to a redox reaction caused by the interaction of a peroxide-monomer and/or a peroxide-solvent complex with DPTU, and the decrease in the polymerization rate which was observed over a certain concentration of DPTU was due to the action of the oxidized product of DPTU as a transfer agent. The effect of substituents was studied by using *para* and *meta*-substituted DPTU. It was found that the polymerization rate increased as electron-donating substituents are added to the benzene ring of DPTU with considerable dependence on Hammett's equation ($\rho = -0.36$). The acceleration effect is also observed for PMPH- and tBPBz-initiated polymerizations, whereas the DCP- and DBP-initiated systems show no effects on the polymerization rate.

INTRODUCTION

It has been shown that radical polymerization of vinyl monomers initiated by organic and inorganic peroxides is accelerated by small amounts of reducing agents; this type of reaction is referred to as a redox reaction.

The prototype for this evidence has been the extensively studied hydrogen peroxide-ferrous salt systems¹ and the benzoyl peroxide-amine systems.²

In the previous studies,^{3,4} it was found that thiourea used as a reducing agent caused an increase in the rate of hydrogen peroxide-initiated

polymerization of acrylonitrile whereas for the benzoyl peroxide-initiated polymerization of methyl methacrylate, diphenyl thiourea was found to behave as a retarder. These results seemed sufficiently interesting to merit continuation of the work to clarify these different effects. In this paper, a study of the effect of diphenyl thiourea (DPTU) on the polymerization of methyl methacrylate (MMA) initiated by cumene hydroperoxide (CHP), *p*-menthane hydroperoxide (PMHP), *tert*-butyl perbenzoate (tBPBz), dicumyl peroxide (DCP), and di-*tert*-butyl peroxide (DBP) is reported.

In marked contrast with the benzoyl peroxide-DPTU systems,⁴ DPTU caused a marked acceleration of polymerization rate in CHP-, PMHP-, and tBPBz-initiated polymerization, while with DCP and DBP as initiators, it had no effect on the polymerization rate.

It was found from the kinetic investigation that the overall polymerization rate for the former cases was given by eq. (1):

$$R_p = K[\text{peroxide}]^{1/2} [\text{DPTU}]^{1/2} [\text{MMA}]^\alpha \quad (1)$$

The effect of substituents was investigated by using *para* and *meta* derivatives of DPTU, and the rate ratios were then correlated to Hammett's substituent constants with good linearity ($\rho = -0.36$).

These acceleration effects due to DPTU are discussed on the basis of the results of the kinetic investigation and comparison with the effect of diphenyl urea.

EXPERIMENTAL

Materials

Di-*tert*-butyl peroxide was purified by distillation at a reduced pressure under nitrogen, b.p. 50°C./105 mm. Hg, $n_D^{20} = 1.3892$.

Dicumyl peroxide was purified by recrystallization from benzene, m.p. 39°C. The other peroxides were used without further purification. The preparation and purification of other reagents (MMA, benzene, DPTU, and its derivatives) and polymerization methods were similar to those in the previous paper.⁴

Polarography

Polarographic analysis of DPTU and its derivatives was carried out at room temperature with a Yanagimoto polarograph type PB-4 equipped with a rotating platinum electrode assembly. The conditions were as follows. A sample was dissolved in a solution containing dioxane (18 ml.), water (5 ml.), methanol (2 ml.) and 1*N* LiCl (3 ml.) as electrolyte. The platinum electrode rotated at 600 rpm, and the damping was zero.

Polymerization

Polymerizations were conducted in benzene at 50°C. in sealed tubes. The required amounts of reagents were placed into a clean tube, which was

then degassed by repeated freezing and thawing cycles and sealed. The conversions were kept to 2–10%.

Viscosity

The viscosities of polymers were measured by an Ubbelohde viscometer at 30°C. The number-average degree of polymerization was calculated from eq. (2).

$$\log \bar{P}_n = 3.420 + 1.13 \log [\eta] \quad (2)$$

RESULTS AND DISCUSSION

The effect of DPTU on the polymerization of MMA initiated by various organic peroxides has been studied. In striking contrast to the case of benzoyl peroxide–DPTU⁴-initiated polymerization, retardation effects were not observed for these systems on the addition of DPTU. The time–conversion curves of MMA polymerization initiated by the CHP–DPTU system are illustrated in Figure 1. The relation between the rates of polymerization initiated by peroxides (CHP, PMHP, tBPBz, DCP, and DBP) and DPTU concentrations are shown in Figure 2. As expected, DPTU had hardly any effect on the polymerization rate in the case of both DCP- and DBP-initiated polymerizations, since these initiators are known

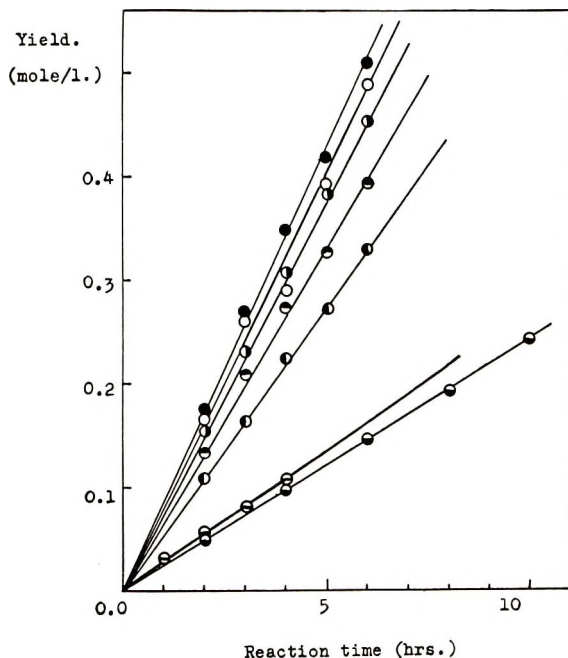


Fig. 1. The effect of DPTU on the CHP-initiated polymerization of MMA at 50°C., [CHP] = 12.0 mmole/l., [MMA] = 4.68 mole/l., and various DPTU concentrations: (○) 0.0; (●) 1.2 mmole/l.; (●) 2.4 mmole/l.; (●) 4.8 mmole/l.; (○) 7.2 mmole/l.; (●) 12.0 mmole/l.; (⊖) diphenyl urea, 11.0 mmole/l.

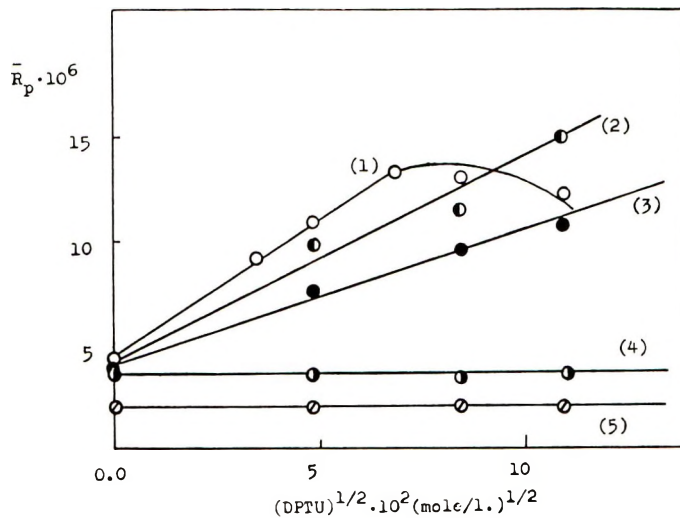


Fig. 2. Effect of DPTU on polymerization of MMA-initiated various peroxides at [peroxide] = 12.0 mmole/l., [MMA] = 4.68 mole/l.; (1) CHP; (2) PMHP; (3) tBPBz; (4) DCP; (5) DPB.

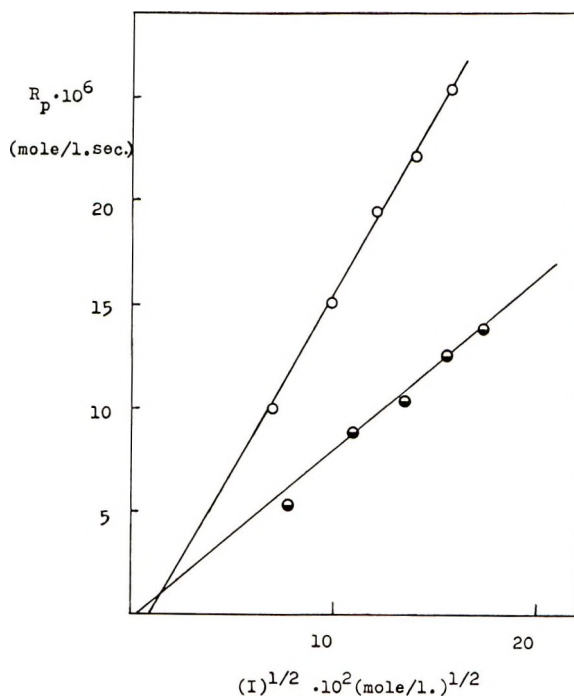


Fig. 3. Effect of CHP concentration on the rate of polymerization: (O) CHP-DPTU system, [MMA] = 4.68 mole/l., [DPTU] = 3.0 mmole/l.; (●) tBPBz-DPTU system, [MMA] = 4.68 mole/l., [DPTU] = 2.4 mmole/l.

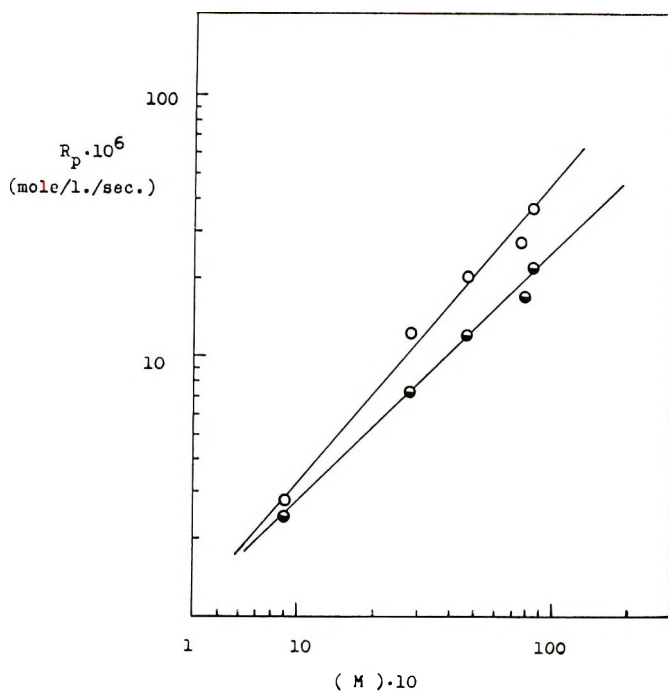


Fig. 4. Effect of monomer concentration on the rate of polymerization: (O) CHP-DPTU system, [CHP] = 12.0 mmole/l., [DPTU] = 3.0 mmole/l.; (●) tBPBz-DPTU system, [tBPBz] = 24.0 mmole/l., [DPTU] = 2.4 mmole/l.

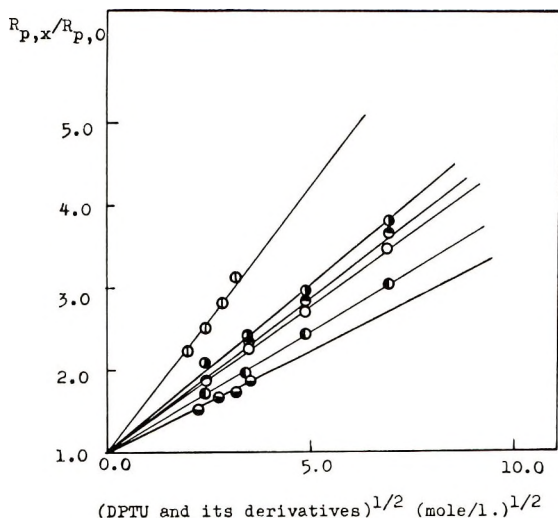


Fig. 5. Effect of substituents on phenyl of DPTU on polymerization rate at [MMA] = 4.68 mole/l., [CHP] = 12.0 mmole/l.: (⊕) *p*-N(CH₃)₂; (⦿) *p*-CH₃; (⊙) *m*-CH₃; (○) H; (⦿) *m*-OCH₃; (⊖) *m*-NO₂. $R_{p,x}$ and $R_{p,0}$ denote polymerization rates in the presence and absence of thiourea compounds, respectively.

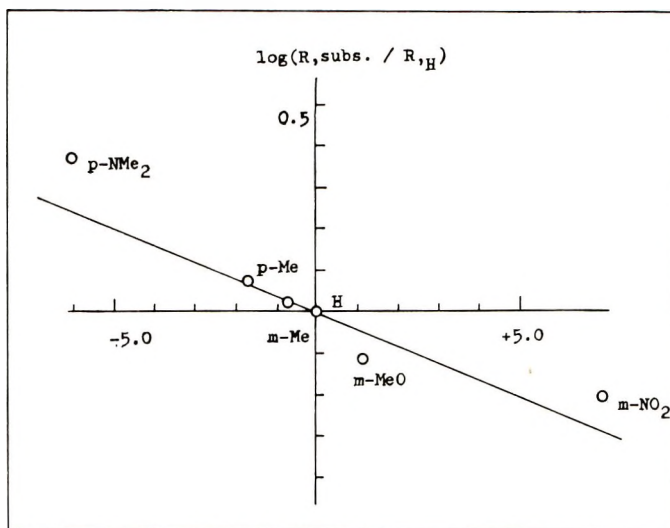


Fig. 6. Relation between rate ratio and Hammett's substituent constants.

The effect of diphenyl urea on the polymerization rate was found to be small compared to that of DPTU (Fig. 1); therefore it is unlikely that the acceleration effect is due to the interaction of peroxides and nitrogen atoms of DPTU molecule.

The dependence of polymerization rate on the monomer concentration differed depending on the type of peroxides as shown in eq. (1) and in Figure 4. These differences were probably due to the participation of monomer molecules in the initiation reaction. Tobolsky⁸ suggested that for the polymerization of styrene initiated by CHP in various solvents, the CHP-solvent initiation reaction was more important than the CHP-monomer initiation reaction for polar solvents, e.g., benzyl alcohol, dimethylaniline or pyridine, but that on the other hand, the CHP-monomer interaction was dominant and the CHP-solvent initiation reaction negligible for nonpolar solvents such as benzene, carbon tetrachloride, and cyclo-

TABLE I
Polarographic Characterization of DPTU and Its Derivatives^a

Substituents of DPTU	$E_{1/2}$, V.-scd
<i>p</i> -N(CH ₃) ₂	+0.48
<i>p</i> -CH ₃	+0.57
<i>m</i> -CH ₃	+0.57
H	+0.58
<i>m</i> -OCH ₃	+0.63
<i>p</i> -Cl	+0.91
<i>m</i> -NO ₂	—

^a Experimental conditions for measurements of half-wave potentials of DPTU and its derivatives: dioxane, 18 ml.; MeOH, 2 ml.; water, 5 ml.; 1*N* LiCl, 3 ml.; sample, ca. 1 mmole; temperature, ca. 17°C.

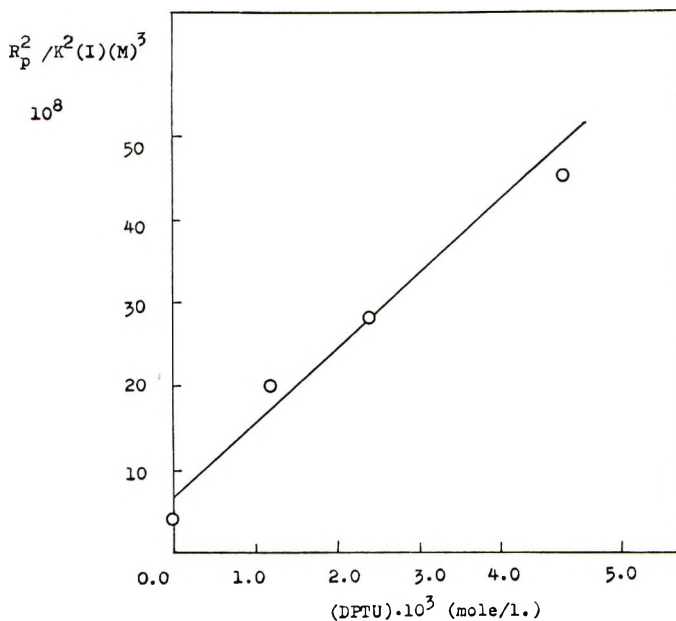


Fig. 7. Plot of $R_p^2/K[I][M]^3$ vs. [DPTU] [eq. (7b)].

hexane. In these latter solvents the polymerization rate depends on powers of M close to the predicted value of 1.5 or somewhat larger.

Hence, the rate of initiation R_i for the CHP-DPTU system is represented by eq. (5):

$$R_i = k_1[I][M] + k_2[I][S] + k_3[I][M][DPTU] + k_4[I][S][DPTU] \quad (5)$$

where $[I]$, $[M]$, and $[S]$ denote the concentrations of peroxide, monomer, and solvent, respectively. The chain-transfer reaction to form the oxidized product (disulfide) might not be a major reaction up to 5.0×10^{-3} mole/l. of DPTU. Since the rate of polymerization is represented by the equation:

$$R_p^2 = (k_p^2/k_t)[M]^2R_i \quad (6)$$

eqs. were derived from eqs. (5) and (6):

$$R_p^2/(k_p^2/k_t)[I][M]^3 = k_1 + k_2[S]/[M] + k_3[DPTU] + k_4[S][DPTU]/[M] \quad (7a)$$

$$= (k_1 + k_2[S]/[M]) + (k_3 + k_4[S]/[M])[DPTU] \quad (7b)$$

$$= (k_1 + k_3[DPTU]) + (k_2 + k_4[DPTU])[S]/[M] \quad (7c)$$

The plots of the left-hand side of eq. (7) against [DPTU] give values of $(k_1 + k_2[S]/[M])$ as an intercept and $(k_3 + k_4[S]/[M])$ as a slope. The results are shown in Figure 7, and the relation of eq. (7c) is illustrated in Figure 8.

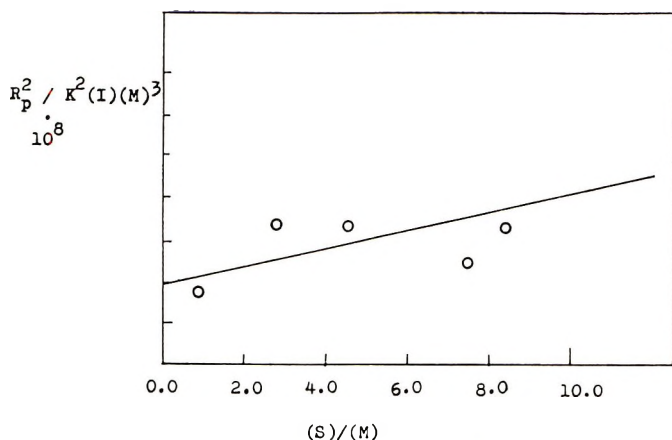
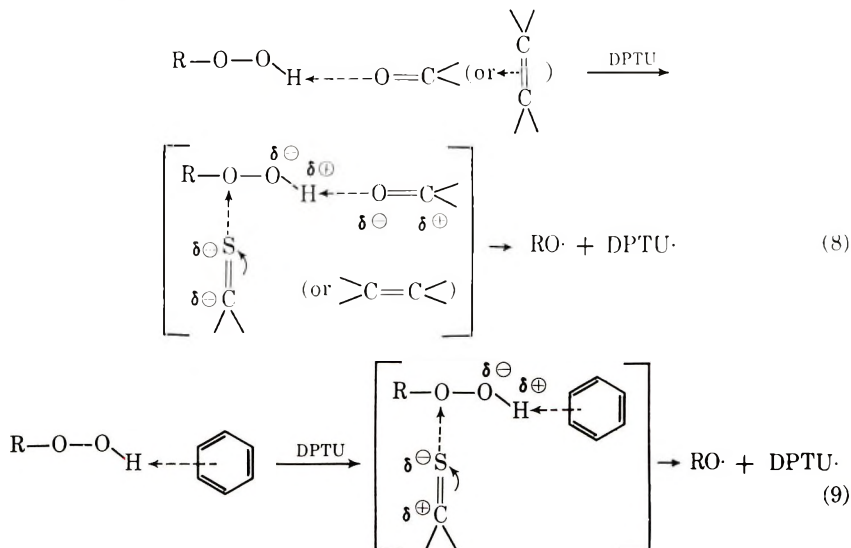


Fig. 8. Plot of $R_p^2/K^2[C][M]^3$ vs. $[S]/[M]$ [eq. (7c)].

From these data, rate constants of eq. (5) were found to be: $k_1 = 1.4 \times 10^{-8}$ sec.⁻¹, $k_3 = 5.4 \times 10^{-6}$ l.²/mole²-sec. and $k_4 = 6.2 \times 10^{-5}$ l./mole-sec. Therefore, it was considered that the major initiating radical-producing reactions probably include the following two: the reaction of a peroxide-monomer complex with DPTU and the reaction of a solvent-peroxide complex with DPTU, probably through a reaction intermediate, shown in eqs. (8) and (9).



It was thought that the reactivity of DPTU as a strong base would cause the order of monomer concentration to change from the value of 1.5.

On the other hand, R_i for tBPBz-initiated polymerization may be represented by eq. (10);

$$R_i = k'_1[I] + k'_2[I][\text{DPTU}] \quad (10)$$

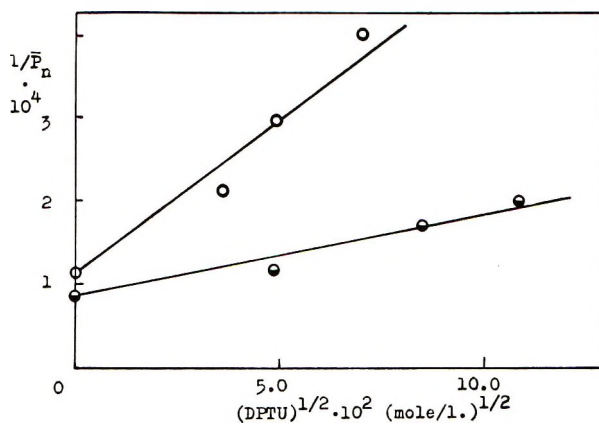


Fig. 9. Effect of DPTU on the degree of polymerization: (O) CHP-DPTU system, [CHP] = 12.0 mmole/l., [MMA] = 4.68 mole/l.; (●) tBPBz-DPTU system, [tBPBz] = 24.0 mmole/l., [MMA] = 4.68 mole/l.

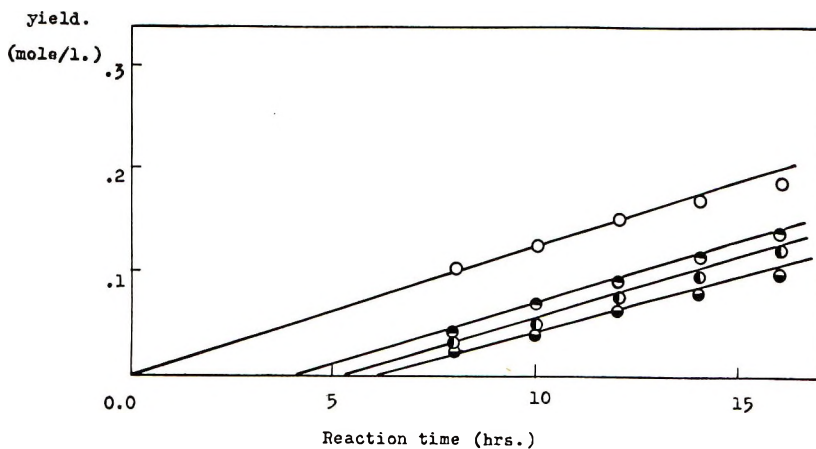


Fig. 10. Effect of DPTU on the DBP-initiated polymerization of MMA at [DPB] = 24.0 mmole/l., [MMA] = 4.68 mole/l., and various DPTU concentrations: (O) 0.0; (●) 2.4 mmole/l.; (◐) 7.2 mmole/l.; (◑) 12.0 mmole/l.

therefore,

$$R_p = K' [I]^{1/2} [M] (\beta + [\text{DPTU}])^{1/2} \quad (11)$$

where

$$K' = (k_p/k_t^{1/2})k'_2$$

$$\beta = k'_1/k'_2$$

The order with respect to monomer would be a value close to that from eq. (11).

The degree of polymerization (\bar{P}_n) decreased with increasing DPTU concentration. The relation between the reciprocal degree of polymeriza-

tion and the square root of DPTU concentration is linear, as shown in Figure 9.

The degree of polymerization (i.e., the ratio of propagation reaction rate to initiation reaction rate) was as shown in eq. (12) on the basis of eq. (5) or (11) and eq. (6).

$$1/\bar{P}_n \propto [\text{DPTU}]^{1/2} \quad (12)$$

The above kinetical treatments are also found to be suitable from these results.

On the other hand, the polymerizations initiated by DCP or DBP were found to proceed at the ordinary rates after the induction period, as shown in Figure 10. The induction period observed appears to be caused by the hydrogen abstraction of DPTU by initiating the radicals or by the radical deactivation reaction owing to electron transfer from DPTU to the polymer or the initiating radical, since the homolytic decomposition of DCP and DBP were not affected by DPTU and the transfer reactions for DPTU in the AIBN-initiated polymerization were found to be small as shown in the previous paper.⁴

From these results, it was concluded that the acceleration effect was caused by nucleophilic attack of DPTU by peroxides in which (CHP) forms a complex with monomer and solvents, followed by a one-electron transfer reaction concomitant with O—O bond cleavage.

The authors are indebted to Dr. S. Yamashita and co-workers of Kyoto University for supporting the research in measurements of polarographical analysis.

References

1. J. H. Baxendale, M. G. Evans, and G. S. Park, *Trans. Faraday Soc.*, **42**, 155 (1946).
2. L. Horner and E. Schwenk, *Ann.*, **556**, 69 (1950).
3. Y. Minoura, N. Yasumoto, and T. Sugimura, *J. Polymer Sci. A*, **3**, 2935 (1965).
4. Y. Minoura and T. Sugimura, *J. Polymer Sci. A-1*, **4**, 2721 (1966).
5. A. V. Tobolsky and B. Baysal, *J. Polymer Sci.*, **9**, 171 (1952).
6. N. Kharasch, *Organic Sulfur Compounds*, Pergamon Press, New York, 1961, p. 257.
7. C. G. Overberger and R. W. Cummins, *J. Am. Chem. Soc.*, **75**, 4250 (1953).
8. A. V. Tobolsky and L. R. Matlack, *J. Polymer Sci.*, **55**, 49 (1961).

Résumé

L'effet de la diphenyl-thiourée (DPTU) sur la polymérisation radicalaire du polyméthacrylate de méthyle (MNA) a été étudié en solution benzénique à 50°C utilisant l'hydroperoxyde de cumène (CHP), l'hydroperoxyde de menthyle (PMHP), le perbenzoate de *tert*-butyle (tBPBz), le peroxyde de di-*tert*-butyle (DBP) et le peroxyde de dicumyle (DCP) comme initiateurs. Dans la polymérisation initiée d'hydroperoxyde de cumène, la vitesse de polymérisation croît appréciablement par addition de DPTU avec une dépendance linéaire de la racine carrée de la concentration en DPTU jusqu'à un point maximum qui a été observé lorsque le rapport de la concentration d'hydroperoxyde de cumène sur DPTU était de 2.5. La vitesse décroît graduellement avec une augmentation de la concentration en DPTU dans un domaine où le rapport cite cidessus

est plus élevé. On a trouvé au départ des études cinétiques que la vitesse de polymérisation globale était exprimée par l'équation suivante: $R_p = K(\text{peroxyde})^{1/2} (\text{DPTU})^{1/2}$ (MMA), où K est la constante de vitesse, $\alpha = 1.2$ pour le CHP et $= 1$ pour le tBPBz. On peut considérer que l'effet accélérateur observé était dû à la réaction oxydoréductrice causée par l'interaction du peroxyde de monomère et par le complexe peroxyde-solvant et le DPTU, et que la diminution des vitesses de polymérisation qui étaient observées sur un certain domaine de concentrations en DPTU était due à l'action du produit d'oxydation du DPTU comme agent de transfert. L'effet des substituants a été étudié en utilisant des DPTU *para*- et *meta*-substitués et on a prouvé que la vitesse de polymérisation croissait en même temps que les propriétés électro-donneurs des substituants implantés dans le noyau aromatique de la DPTU avec une dépendance considérable suivant l'équation de Hammett ($\rho = -0.36$). L'effet accélérateur a également été observé au cours de polymérisations initiées à la fois par l'hydroperoxyde de *p*-menthyle et tBPBz, tandis que les systèmes initiés par le DCP et le DBP, il n'y a pas d'effet sur la vitesse de polymérisation.

Zusammenfassung

Der Einfluss von Diphenylthioharnstoff (DPTU) auf die durch Cumylhydroperoxyd (CHP), *p*-Menthanhydroperoxyd (PMPH), *tert*-Butylperbenzoat (tBPBz), Di-*tert*-butylperoxyd (DBP) und Dicumylperoxyd (DCP) in Benzollösung bei 50°C gestartete Polymerisation von Methylmethacrylat (MMA) wurde untersucht. Bei der CHP-gestarteten Polymerisation nahm die Polymerisationsgeschwindigkeit bei Zusatz von DPTU beträchtlich zu und zeigte eine lineare Abhängigkeit von der Wurzel aus der DPTU-Konzentration bis zu einem Maximalwert, der bei einem Konzentrationsverhältnis von CHP zu DPTU von 2,5 beobachtet wurde. Von hier nahm die Geschwindigkeit mit steigender DPTU-Konzentration gleichmässig wieder ab. Die Bruttopolymerisationsgeschwindigkeit (R_p) konnte durch folgende Gleichung dargestellt werden $R_p = K (\text{Peroxyd})^{1/2} (\text{DPTU})^{1/2} (\text{MMA})^\alpha$, wo K Geschwindigkeitskonstante und $\alpha = 1,2$ für CHP und 1,0 für tBPBz bei (DPTU) = $5 \cdot 10^{-2}$ Mol/lit. Es wird angenommen, dass der beobachtete Beschleunigungseffekt durch die durch Reaktion zwischen Peroxyd und Monomerkomplex oder Peroxyd und Lösungsmittel-komplex mit DPTU verursachte Redoxreaktion und die in einem bestimmten Konzentrationsbereich von DPTU beobachtete Abnahme der Polymerisationsgeschwindigkeit durch die Wirksamkeit des Oxydationsprodukts von DPTU als Überträger bedingt war. Der Substituenteneffekt wurde an *para*- und *meta*-substituiertem DPTU untersucht und eine Zunahme der Polymerisationsgeschwindigkeit bei elektronenliefernden Substituenten am Benzolring von DPTU entsprechend der Hammett Gleichung ($\rho = -0,36$) festgestellt. Der Beschleunigungseffekt wurde auch bei der PMPH- und tBPBz-gestarteten Polymerisation beobachtet, während bei DCP- und DBP-gestarteten Systemen kein Einfluss auf die Polymerisationsgeschwindigkeit besteht.

Received February 7, 1966

Revised March 9, 1966

Prod. No. 5118A

Effects of Polysulfides on the Polymerization of Methyl Methacrylate

TAKA AKI SUGIMURA, YAYOI OGATA, and YUJI MINOURA, *Department of Chemistry, Osaka City University, Kita-ku, Osaka, Japan*

Synopsis

The effect of organic sulfur compounds on the radical polymerization of methyl methacrylate initiated by azobisisobutyronitrile at 50°C. has been studied. The sulfur compounds used were benzene-type polysulfides ($C_6H_5CH_2-S_n-CH_2C_6H_5$; $n = 0-4$), benzyl mercaptan, and sulfur (S_8). All sulfur compounds studied, except dibenzyl, dibenzyl monosulfide, and dibenzyl disulfide, were found to behave as retarders under these experimental conditions. Chain-transfer constants of these compounds were determined from rate measurements and from the conventional method based on number-average degree of polymerization. Chain-transfer constants of benzyl-type polysulfides were less than those of mercaptan and sulfur and increased with increasing sulfur. The correlation of the reactivities of sulfur compounds as transfer agents and their molecular structures is discussed.

INTRODUCTION

Organic sulfur compounds, especially thiols and disulfides, have been used as transfer agent in the vinyl polymerization, since these compounds react readily with the macromolecular radicals at the position of weak bonds, e.g., S—H or S—S. These compounds have also been used in such major industrial applications as the vulcanization of rubber and as regulators or modifiers in polymerization. The chain-transfer constants of mercaptans and disulfides were reported by many workers, and reaction mechanisms and reactivities have been studied.¹

We have studied the effect of organic sulfur compounds in the radical polymerization to examine the various interesting redox-initiating systems. It was found that mercaptan,² sulfide,³ sulfoxide,³ and thiourea^{4,5} behave as accelerators in peroxides-catalyzed polymerization. Minoura has shown on the basis of ultraviolet and infrared spectra and molecular refraction measurements^{6,7} that the structures of polysulfides of the benzyl type are not branched but linear. He then proposed molecular structures from the results of dipole moment measurements.⁸ In this paper, the effect of the various sulfides on the polymerization of methyl methacrylate initiated by azobisisobutyronitrile at 50°C. in benzene was examined. The sulfur compounds used were as follows; dibenzyl, dibenzyl mono-, di-, tri-, and tetrasulfide, benzyl mercaptan, and sulfur. Using these sulfur compounds

the relation between the chain-transfer constants and the number of sulfurs was studied, since the previous investigations of sulfur compounds in vinyl polymerization dealt almost exclusively with thiol and disulfide. It was found that the polymerization rates were diminished by the addition of sulfur compounds, and comparatively large transfer constants were obtained except with addition of benzyl mono- and disulfide.

EXPERIMENTAL

Reagents

Methyl Methacrylate. Commercially available monomer was purified by steam distillation. It was carefully freed from inhibitor by successive washing with 10% alkaline solution and then with water. The monomer was dried with calcium chloride and distilled under nitrogen atmosphere at reduced pressure; the middle fraction was collected and kept in a dark place at 0°C. This fraction was freshly distilled prior to use at 45–47°C. under pressures of 100–110 mm. Hg.

Benzene. Analytical grade reagent was washed successively with concentrated sulfuric acid and with water. It was distilled twice over sodium wire after drying over calcium chloride.

Azobisisobutyronitrile. Commercially available product was recrystallized twice from ethanol, m.p. 102–103°C.

Dibenzyl. Benzyl chloride was reacted with sodium metal in benzene. The product was recrystallized from ethanol.

ANAL. Calcd. for $C_{14}N_{14}$: C, 92.26%; H, 7.74. Found: C, 92.21%, H, 7.58%.

Dibenzyl Monosulfide. An aqueous solution of sodium sulfide was dropped into an alcohol solution of benzyl chloride; on heating at 60°C. an oily product was separated. The reaction mixture was cooled to obtain the solid product which was recrystallized from alcohol, m.p. 48.5°C.

ANAL. Calcd. for $C_{14}H_{14}S$: C, 78.45%; H, 6.55%. Found: C, 78.43%; H, 6.55%.

Dibenzyl Disulfide.⁹ Calculated amounts of sulfur were added to aqueous solution of sodium sulfide to produce sodium disulfide; benzyl chloride was then added to the reaction mixture. The oily product obtained was recrystallized from alcohol, m.p. 70.5°C.

ANAL. Calcd. for $C_{14}H_{14}S_2$: C, 66.2%; H, 5.73%. Found: C, 66.60%; H, 5.72%.

Dibenzyl Trisulfide.¹⁰ The trisulfide was prepared from the reaction of benzyl mercaptan, which was obtained from the reaction of benzyl chloride with sodium hydrosulfide, with sulfur chloride (SCl_2) in ether. The product was recrystallized from carbon tetrachloride, m.p. 49°C.¹¹

ANAL. Calcd. for $C_{14}N_{14}S_3$: C, 60.38%; H, 5.07%. Found: C, 60.40%; H, 5.43%.

Dibenzyl Tetrasulfide. The reaction product of benzyl mercaptan with sulfur chloride (S_2Cl_2) in ether was recrystallized from ether, m.p. $54^\circ C$.

ANAL. Calcd. for $C_{14}H_{14}S_4$: C, 54.13%; H, 4.54%. Found: C, 54.14%; H, 4.14%.

Sulfur. Commercially available product was recrystallized from benzene, m.p. $119-120^\circ C$.

Polymerization

The polymerizations were conducted in benzene at $50^\circ C$. in sealed tubes. The thermostated bath was placed in dark to avoid photoinitiation by sulfur compounds. The reaction mixture was poured into a large excess of methanol after the desired length of time and filtered off. It was then dried at reduced pressure at $40^\circ C$. to constant weight.

Degree of Polymerization

The number-average degree of polymerization was calculated from eq. (1)¹² from the intrinsic viscosity in benzene solution at $30^\circ C$. as obtained by using an Ubbelohde viscometer.

$$\bar{P}_n = 2200[\eta]^{1.13} \quad (1)$$

Chain-Transfer Constant (C_{tr})

Chain-transfer constants were determined by the conventional method¹³ [Mayo equation, eq. (2)], and transfer constants for retarded systems were also determined by eqs. (3) and (4).¹⁴ The interpretation of eq. (3) will be described later in this paper.

$$1/\bar{P}_n = (1/\bar{P}_{n0}) + C_{tr}[S]/[M] \quad (2)$$

$$\frac{1}{\bar{P}_n} = C_{tr} \frac{[S]}{[M]} + \frac{R_0}{2R} \left(\frac{1}{\nu_0} \right) + \frac{k_t R}{2k_p^2 [M]^2} \quad (3)$$

$$\begin{aligned} \frac{R_0^2 [S]}{R^2 - R_0^2} \left[1 + \sqrt{1 + \frac{k_t k_z}{k_c^2} \left(\frac{R^2 - R_0^2}{R_0^2} \right)} \right] \\ = \frac{k_t R}{k_p k_{tr} [M]} \sqrt{1 + \frac{k_t k_z}{k_c^2} \left(\frac{R^2 - R_0^2}{R_0^2} \right)} + \frac{k_t k_i' [M]}{k_c k_{tr}} \quad (4) \end{aligned}$$

where [S] and [M] denote the concentration of sulfur compounds and of monomer, respectively; R and R_0 are the polymerization rate in the presence and absence of sulfur compounds, respectively; k_p and k_t are the rate constants for the propagation and the termination reaction, respectively; ν_0 is the kinetic chain length in the absence of sulfur compounds.

RESULTS

The polymerization of methyl methacrylate (MMA) initiated by azobisisobutyronitrile (AIBN) was carried out in benzene at $50^\circ C$. in the dark to examine the effect of sulfur compounds.

The sulfur compounds used were dibenzyl (DBS_0), dibenzyl monosulfide (DBS_1), dibenzyl disulfide (DBS_2), dibenzyl trisulfide (DBS_3), dibenzyl-tetrasulfide (DBS_4), benzyl mercaptan (BSH), and sulfur (S_8).

Effect on Polymerization Rate

It is known that the decomposition of AIBN is not induced by additives and its decomposition rate always remains constant. The use of these sulfur compounds as additives and determining their effect on polymerization rate may clarify whether these substances have the ability to initiate the polymerization or are reactive as transfer reagents. The relation between the ratio of the polymerization rate (R/R_0) in presence and absence of sulfur compounds and concentration of the added sulfur compound, is shown in Figure 1.

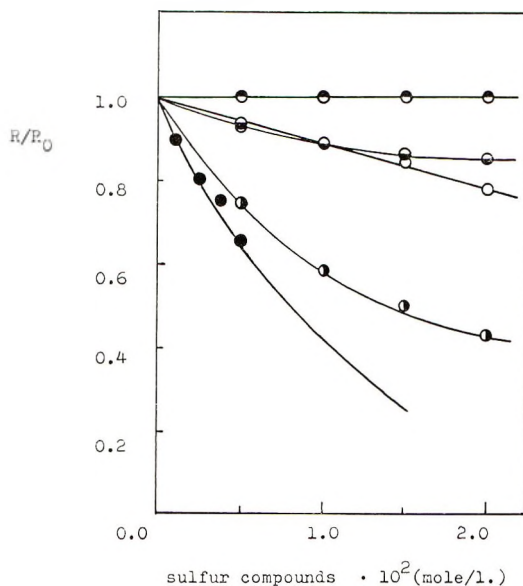


Fig. 1. Effect of sulfur compounds on rate of polymerization of MMA, $[\text{AIBN}] = 6.1 \times 10^{-3}$ mole/l., $[\text{MMA}] = 4.67$ mole/l.: (\bullet) no additive, DBS_0 , DBS_1 , and DBS_2 ; (\ominus) DBS_3 ; (\circ) BSH; (\odot) DBS_4 ; (\bullet) S_8 .

As shown in Figure 1, the polymerization rate was not affected by the addition of dibenzyl (DBS_0), dibenzyl monosulfide (DBS_1), and dibenzyl disulfide (DBS_2), but was retarded by dibenzyl trisulfide (DBS_3), dibenzyl tetrasulfide (DBS_4), BSH, and S_8 . These results indicate that the sulfur compounds act as either retarders or transfer agents under the experimental conditions. The effects as retarders decrease in the order: $\text{S}_8 > \text{DBS}_4 > \text{BSH} > \text{DBS}_3 \gg \text{DBS}_2 \approx \text{DBS}_1 \approx \text{DBS}_0$.

Transfer Reaction

Chain-transfer constants (C_{tr}) for these sulfur compounds were determined by the conventional method, i.e., plots of $1/\bar{P}_n$ versus $[S]/[M]$, and the results are summarized in Table I.

TABLE I
Chain-Transfer Constants of Polysulfides

Compound	$C_{tr} \times 10^2$ (calculated)		
	From eq. (2)	From eq. (3)	From eq. (4)
DBS ₀	ca. 0	—	—
DBS ₁	0.98	—	—
DBS ₂	1.6	—	—
DBS ₃	2.1	—	—
DBS ₄	8.4	5.3	10.3
BSH	2.7	—	—
S ₈	10.6	9.0	12.7

BSH reacts most readily with the polymer radical and C_{tr} increased with the increase in the number of sulfur atoms of the benzyl polysulfides. The C_{tr} values thus determined were plotted against the number of sulfur atoms (Fig. 2a).

For the retarded systems, values of C_{tr} were also calculated from eqs. (3) and (4) to compare with the results obtained from eq. (2). These results are shown in Figure 2 and Table I.

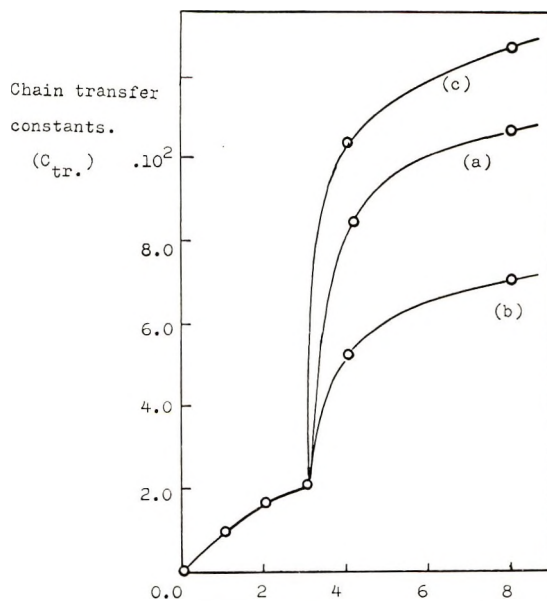


Fig. 2. Plots of number of sulfur atoms in DBS_n vs. chain-transfer constants: (a) C_{tr} calculated by eq. (2); (b) C_{tr} calculated by eq. (3); (c) C_{tr} calculated by eq. (4).

DISCUSSION

It is known¹⁵ that the bond dissociation energies of S—S (D_{S-S}) are generally low and are a little higher than that of peroxides (D_{O-O}), e.g., D_{S-S} of S_8 is 64 kcal./mole, D_{S-S} of disulfides are in the range of 40–75 kcal./mole. However, the values of D_{S-S} are variable due to the resonance stabilization of the radicals formed by homolytic cleavage. There are two types of homolytic scission: unimolecular scission by heat or light [eq. (5)] and bimolecular reaction by radical displacement [eq. (6)].



Although the reactivity of unimolecular decomposition is generally smaller than that of the bimolecular reaction, thermal homolyses of S—S bonds in S_8 occur in liquid sulfur and lead to the formation of polymers¹⁶ and some disulfides dissociate homolytically 80–160°C. to form radicals which are capable of initiating the polymerization of the certain monomers as shown by Tobolsky,^{17,18} Kern,¹⁹ and Otsu.²⁰ However, it is possible that the sulfur compounds used might react as transfer agents rather than as initiators under the experimental conditions, since neither induction period nor acceleration for the polymerization was observed.

It is known that disulfides, mercaptans, and S_8 are more reactive with nucleophiles than with electrophiles, but little is known of the relations between C_{tr} and the number of sulfur atoms in a polysulfide for their reaction with a certain radical. The values of C_{tr} for mercaptans are generally greater than that of disulfide, as shown in Table I. It is thought that in the transfer reaction for benzyl polysulfide, the hydrogen abstraction of methylene groups could be competitive in the radical substitution reaction (SH_2 reaction) for S—S bonds.

C_{tr} for DBS_1 , DBS_2 , DBS_3 , and DBS_4 is much greater than that for DBS_0 . This may be due to the electron-sharing conjugation by the shell expansion of sulfur by using vacant d orbitals [eq. (7)]. The C_{tr} value would increase with the number of sulfur by the conjugation shown in eq. (8).²¹



The reaction of the radical with the disulfide has been reported by Pryor in some detail,²² and he suggested that the most probable attacking direction of SH_2 is 3(a) (Fig. 3).

Minoura⁸ has shown that the molecular structure of benzyl polysulfides (Fig. 4) by the measurement of dipole moments. From these facts, it is considered that the SH_2 reaction of DBS_3 and DBS_4 would occur at arbitrary sulfur atoms without any steric hindrance. Therefore, the transi-

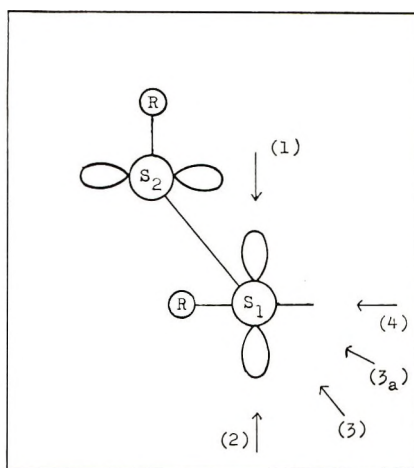


Fig. 3. Direction of radical attack on disulfide.

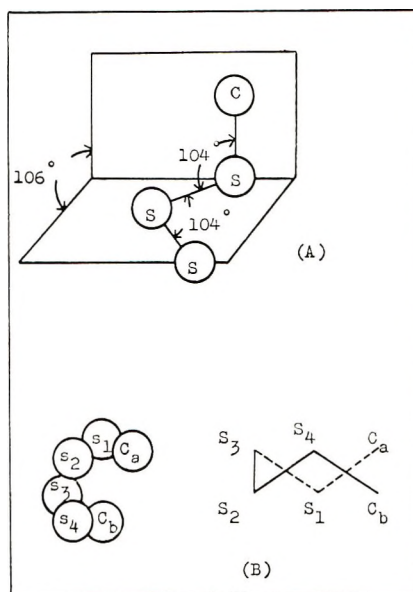
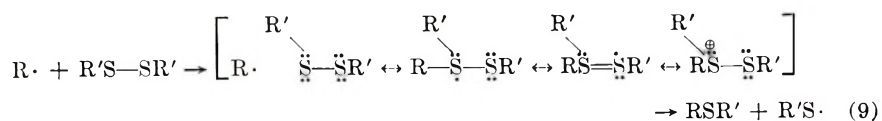
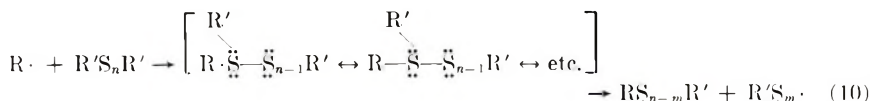


Fig. 4. Molecular structures of (A) DBS₃; (B) DBS₄.

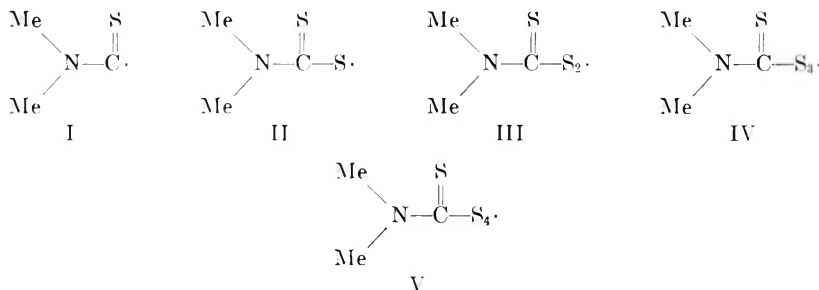
tion state of the SH₂ reaction of polysulfide may be written as shown in eqs. (9) and (10).





Therefore, the increase of C_{tr} with the increase in the number of sulfur atoms is probably due to the electron-sharing effect through conjugation of sulfur on a large number of reaction sites.

Tobolsky¹⁷ studied the polymerization of MMA using tetramethylthiuram monosulfide (TMTM), tetramethylthiuram disulfide (TMTD) and pentamethylenethiuram tetrasulfide (PMTT) and reported that TMTM is an effective initiator, TMTD is an initiator at the low concentrations but a retarder at high concentrations, and PMTT does not cause polymerization. He has explained the above differences by the hypothesis that radicals III-V derived from TMTD and PMTT would be less reactive than radicals I and II derived from TMTM and TMTD, and the former radicals would not initiate the polymerization of MMA.



The retardation effect observed for DBS_3 , DBS_4 , and S_8 may be attributable to the less reactive radicals formed by the transfer reaction, which would be stabilized by the resonance form shown in eq. (10) and these stable radicals would participate in the termination reaction.

TABLE II

Step	Equation	Rate
Initiation	$I \rightarrow R\cdot$	$k_{if}[I]$
Propagation	$R\cdot + M \rightarrow R\cdot$	$k_p[R\cdot][M]$
Transfer	$R\cdot + SX \rightarrow RX + S\cdot$	$k_{tr}[R\cdot][SX]$
Reinitiation	$S\cdot + M \rightarrow R\cdot$	$k_r'[S\cdot][M]$
Termination	$R\cdot + R\cdot \rightarrow$	$k_t[R\cdot]^2$
	$R\cdot + S\cdot \rightarrow$	
	$S\cdot + S\cdot \rightarrow$	
	$\left. \begin{array}{l} \\ \\ \end{array} \right\} \text{inert product}$	$k_c[R\cdot][S\cdot]$ $k_z[S\cdot]^2$

Then

$$\frac{1}{\bar{P}_n} = C_{tr} \frac{[S]}{[M]} + \frac{2R_0}{2R\nu_0} + \frac{k_t R}{2k_p^2 [M]^2} \times \left\{ 1 - \frac{1}{C} \left[\sqrt{1 + C \left(\frac{R_0^2 - R^2}{R^2} \right)} - 1 \right]^2 \right\} \quad (3')$$

The general relations are cumbersome and it suffices to discuss two limiting cases. In the first case $C = 1$; in this eq. (3') scarcely differs from eq. (2) for the unretarded cases. For the case where $C \ll 1$, eq. (3') could be rewritten as eq. (3).

Since the predominant termination is the disproportionation reaction for MMA, the degree of polymerization was used instead of the kinetic chain length (ν_0) for the calculation of C_{tr} using eq. (3).

It was found that the lower limit of C_{tr} for the retarded systems, could be obtained from eq. (3) as expected, but the upper limit of values of C_{tr} was obtained from eq. (4) with which C_{tr} was calculated from the polymerization rate rather than from eq. (2). These results are shown in Figure 2. However, the actual C_{tr} values would lie in the area between curves (b) and (c) of Figure 2.

References

1. A. V. Tobolsky and B. Baysal, *J. Am. Chem. Soc.*, **75**, 1757 (1953).
2. Y. Minoura, S. Higashimori, and T. Sugimura, *J. Polymer Sci. A*, in press.
3. Y. Minoura, T. Hirahara, and T. Sugimura, *J. Polymer Sci. A*, in press.
4. Y. Minoura, N. Yasumoto, and T. Sugimura, *J. Polymer Sci. A*, **3**, 2935 (1955).
5. Y. Minoura and T. Sugimura, *J. Polymer Sci. A-1*, **4**, 2721 (1966).
6. Y. Minoura, *Nippon Kagaku Zasshi*, **73**, 131, 224 (1952).
7. Y. Minoura, *J. Soc. Rubber Ind. Japan*, **74**, 263 (1951).
8. Y. Minoura, *Nippon Kagaku Zasshi*, **75**, 869 (1952).
9. C. Märcker, *Ann.*, **136**, 75 (1865).
10. J. O. Clayton and D. H. Etzler, *J. Am. Chem. Soc.*, **69**, 974 (1947).
11. J. T. Smythe and A. Ferster, *J. Chem. Soc.*, **1910**, 1195.
12. A. V. Tobolsky et al., *J. Polymer Sci.*, **9**, 171 (1952).
13. R. A. Gregg and E. R. Mayo, *Discussions Faraday Soc.*, **2**, 328 (1943).
14. J. L. Kice, *J. Am. Chem. Soc.*, **76**, 6274 (1954).
15. W. A. Pryor, *Mechanism of Sulfur Reactions*, McGraw-Hill, New York, 1962.
16. R. F. Bacon and R. Farelli, *J. Am. Chem. Soc.*, **65**, 639 (1943).
17. A. V. Tobolsky and T. E. Ferington, *J. Am. Chem. Soc.*, **77**, 4510 (1955).
18. A. V. Tobolsky and T. E. Ferington, *J. Am. Chem. Soc.*, **80**, 3215 (1958).
19. R. J. Kern, *J. Am. Chem. Soc.*, **77**, 1382 (1955).
20. T. Otsu, K. Naya et al., *Makromol. Chem.*, **27**, 142 (1958).
21. C. C. Price and S. Oae, *Sulfur Bonding*, Ronald Press, 1962, p. 44.
22. W. A. Pryor and H. Guard, *J. Am. Chem. Soc.*, **86**, 1150 (1964).
23. J. T. Smythe, *J. Chem. Soc.*, **1912**, 2076.

Résumé

L'effet de composés organiques sulfurés sur la polymérisation radicalaire du méthacrylate de méthyle, initiée par l'azo-bis-isobutyronitrile à 50°C a été examiné. Les composés suivants ont été utilisés: des polysulfures de type benzylique ($\text{PhCH}_2\text{S}_n\text{CH}_2\text{Ph}$; où n va de 0 à 4), le mercaptan benzylique et le soufre (S_8). Ces dérivés sulfurés, sauf le sulfure dibenzylique, le monosulfure de dibenzyle, les disulfures dibenzyliques agissent comme retardateurs dans nos conditions expérimentales. Les constantes de transfert de chaînes de ces dérivés ont été déterminées au départ de mesures de vitesse et par la méthode conventionnelle sur la base du degré de polymérisation moyen en nombre. Les constantes de transfert de chaîne des polysulfures du type benzylique sont inférieures à celles du mercaptan et du soufre; elles croissent avec une augmentation du nombre

d'atomes de soufre. Les réactivités des dérivés du soufre comme agents de transfert sont discutées en rapport avec les structures moléculaires.

Zusammenfassung

Der Einfluss organischer Schwefelverbindungen auf die radikalische, durch Azobisisobutyronitril bei 50°C gestartete Polymerisation von Methylmethacrylat wurde untersucht. Folgende Schwefelverbindungen wurden verwendet. Polysulfide vom Benzyltyp ($\text{PhCH}_2\text{-S}_n\text{-CH}_2\text{Ph}$; $n = 0-4$) Benzylmercaptan und Schwefel (S_8). Diese Schwefelverbindungen erwiesen sich unter den Versuchsbedingungen mit Ausnahme von Dibenzyl Dibenzylmonosulfid und Dibenzyl disulfid als Verzögerer. Die Übertragungskonstanten, dieser Verbindungen wurden aus Geschwindigkeitsmessungen nach der konventionellen Methode unter Verwendung eines Zahlenmittelpolymerisationsgrades bestimmt. Die Übertragungskonstanten von Polysulfiden vom Benzyltyp waren kleiner als diejenigen von Mercaptan und Schwefel und nahmen mit der Anzahl der Schwefelatome zu. Die Reaktionsfähigkeit von Schwefelverbindungen als Kettenüberträger wird in Beziehung zu ihrer Molekülstruktur diskutiert.

Received February 1, 1966

Revised April 6, 1966

Prod. No. 5138A

Copolymerization of Trialkylvinyltin Compounds

YUJI MINOURA, YASUYUKI SUZUKI, YASUHIRO
SAKANAKA, and HIROYUKI DOI, *Department of Chemistry,
Osaka City University, Kita-ku, Osaka, Japan*

Synopsis

The polymerizations of trimethylvinyltin (TMSnV) and tributylvinyltin (TBSnV) were carried out with the use of γ -ray, radical, or ionic initiators. These monomers did not undergo the polymerization by themselves, but they did copolymerize with styrene (St) or methyl methacrylate (MMA) when a radical initiator was used. From the results obtained by the copolymerization, monomer reactivity ratios and Q - e values were obtained as follows: for the system St(M_1)-TMSnV, $r_1 = 44.8$, $r_2 = 0.001$, $Q_2 = 0.005$, $e_2 = 0.962$; for the system MMA (M_1)-TMSnV, $r_1 = 25.1$, $r_2 = 0.03$, $Q_2 = 0.036$, $e_2 = 0.933$; for the system St(M_1)-TBSnV, $r_1 = 16.0$, $r_2 = 0.005$, $Q_2 = 0.017$, $e_2 = 0.822$; for the system MMA(M_1)-TBSnV, $r_1 = 27.9$, $r_2 = 0.03$, $Q_2 = 0.031$, $e_2 = 0.822$. The abilities of TMSnV and TBSnV to polymerize are discussed on the basis of the Q and e values obtained.

INTRODUCTION

Recently, a number of studies on the polymerization of vinylmetal compounds have been reported.¹⁻⁵ The majority of the works,^{1,2,4} dealt with silicon as the metal in the vinylmetal compounds. In some studies, germanium^{3,5} or tin³ have been used. Korshak and co-workers³ carried out the polymerization of trialkylvinyltin under a pressure of 6000 atm. at 120°C. for 6 hr. and obtained an oily, colorless product which was found to be the trimer.

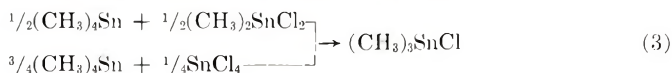
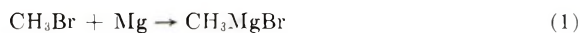
In this work the homopolymerization and copolymerization of trimethylvinyltin (TMSnV) and tributylvinyltin (TBSnV) were carried out, and the Q and e values were obtained from the results of the copolymerization. Moreover, the polymerizability of these monomers were discussed.

EXPERIMENTAL

Syntheses of Trialkylvinyltin Monomers

The method of synthesis of trialkylvinyltin reported by Seyferth and Stone⁶ was employed.

Preparation of TMSnV. TMSnV was prepared by a Grignard method,⁶ according to the reaction sequence shown in eqs. (1)-(5) (see following page).



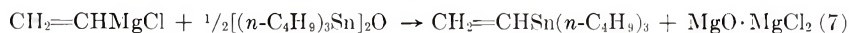
Methylmagnesium bromide was prepared by passing methyl bromide (47.4 mole) into ethyl ether (12 liters) containing magnesium ribbon (41 g.-atom). Tetrachlorotin (9.6 mole) was then added dropwise in a Grignard solution. The reaction mixture was refluxed for 5 hr., and tetramethyltin was obtained by distillation at atmospheric pressure on a steam bath. The fraction of boiling in the range 74–80°C. (lit.⁶ b.p. 76.8°C.) was collected; 620 g. of tetramethyltin was obtained (34%).

Trimethyltin chloride was prepared by dropwise addition of tetramethyltin (1.4 or 0.38 mole) to dimethyltin dichloride (1.4 mole) or tetrachlorotin (0.13 mole) at 100°C. The reaction mixture was distilled at 152–154°C. The yields of the trimethyltin chloride were 530 g. (94.6%) or 95 g. (94.3%), respectively.

Vinylmagnesium chloride was prepared from vinyl chloride (4.5 mole) and magnesium ribbon (4 g.-atom) in tetrahydrofuran (1 liter).

After the end of the Grignard reaction, TMSnV was obtained by the dropwise addition of trimethyltin chloride (3.2 mole) dissolved in 300 ml. of tetrahydrofuran and by distillation at 95–105°C. of the reaction mixture. The yield was 310 g. (50.8%).

Preparation of TBSnV. TBSnV was prepared by the same method as that for TMSnV, according to the reaction sequence shown in eqs. (6) and (7):



Vinylmagnesium chloride was first prepared by the same method as that for TMSnV, and bis(tri-*n*-butyltin) oxide (0.7 mole) was added. After the addition was completed, the reaction mixture was refluxed for 5 hr. It was subsequently cooled to room temperature and hydrolyzed by addition of 500 ml. of saturated aqueous solution of ammonium chloride. The organic layer was decanted and distilled under atmospheric pressure to remove the solvents. The residue was fractionally distilled under reduced pressure. In this manner, 354 g. (76%) of TBSnV was obtained.

The physical constants of these monomers are shown in Table I. The infrared spectra (Figs. 1 and 2) showed characteristic absorption bands at 1000 and 940 cm.⁻¹ (CH₂=CH—), 770 and 710 cm.⁻¹ (—Sn—) for TMSnV; 1000 and 940 cm.⁻¹ (CH₂=CH—), 770 and 740 cm.⁻¹ (—Sn—) for TBSnV.

TABLE I
Physical Constants of the Monomers Prepared

Monomer	b.p., °C.	d_4^{25}	n_D^{25}	Reference
TMSnV	95-105	1.268	1.4530	This work
	100	1.265	1.4544	Seyferth and Stone ⁶
TBSnV	110-121/ 3 mm. Hg	1.0869	1.4768	This work
	114/ 3 mm. Hg	1.0850	1.4761	Seyferth and Stone ⁶

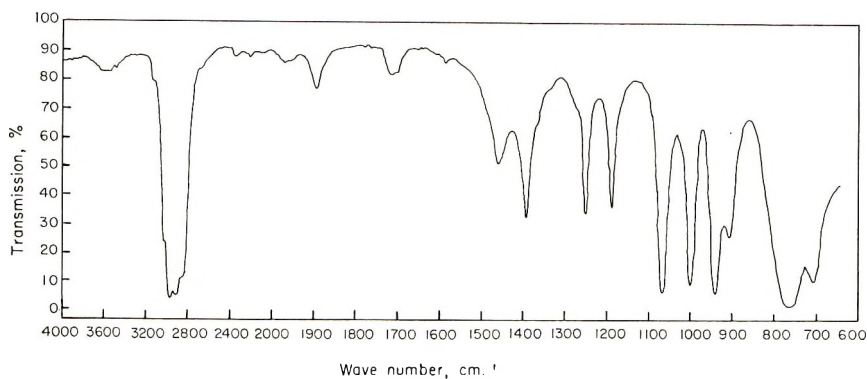


Fig. 1. Infrared spectrum of TMSnV monomer (NaCl).

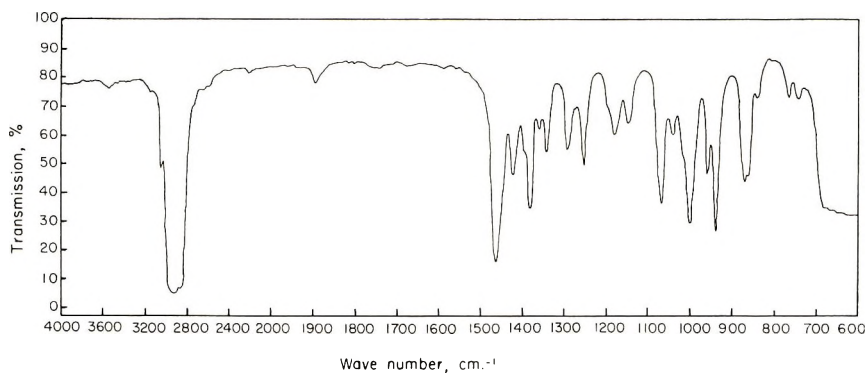


Fig. 2. Infrared spectrum of TBSnV monomer (NaCl).

Other Materials

Styrene and methyl methacrylate used as comonomers were purified by conventional methods.⁷ Azobisisobutyronitrile (AIBN) used as an initiator was recrystallized from ethanol. Boron trifluoride diethyl etherate was distilled before use. Butyllithium was used in the form of a hexane solution supplied by Foote Mineral Co. Benzene was distilled before use.

Homopolymerization

Homopolymerization was carried out with the use of γ -irradiation from a ^{60}Co source or radical or ionic initiators in sealed ampules of 20 ml. capacity containing 5 ml. of the monomer. The ampule was connected to a vacuum system, the monomer was degassed by repeated freeze-thaw cycles, and the ampule was sealed off. The homopolymerization was carried out under various conditions as shown in Table II. After the homopolymerization, the contents of the ampule were poured into a large amount of methanol to precipitate the product.

TABLE II
Results of the Polymerization of TMSnV and TBSnV

Monomer	Initiator	Temp., °C.	Time, hr.	Polymer formed
TMSnV or TBSnV	BPO	80	200	None
	AIBN	80	200	None
	$\text{BF}_3\text{O}(\text{C}_2\text{H}_5)_2$	-78	50	None
	BuLi	-78	50	None
	γ -ray ^a	ca. 20	50	None

^a From a ^{60}Co source, 10^4 – 10^6 r/hr.

Copolymerization

Copolymerization was carried out in a sealed ampule of 20 ml. capacity. The required amounts of both monomers, initiator (AIBN), and solvent (benzene) were placed in the ampule, and the ampule was connected to a vacuum system. After degassing, the ampule was sealed off.

The copolymerization was carried out in a constant temperature bath ($50 \pm 0.01^\circ\text{C}.$) until 10% conversion was reached. Then the contents of the ampule were poured into a large amount of methanol to precipitate the product, and the precipitate was washed thoroughly, filtered off, dried under vacuum at room temperature, and weighed.

Analysis of the Copolymer

The composition of the copolymer was determined by elementary analyses for C, H, and Sn.

Viscosity Measurement

Viscosity of the copolymer was measured in benzene solution at $30^\circ\text{C}.$ by using an Ubbelohde viscometer.

RESULTS AND DISCUSSION

Homopolymerization

The results of the homopolymerization of TMSnV and TBSnV monomers with γ -ray, radical, or ionic initiation are summarized in Table II.

TABLE III. Results of Copolymerization of S(-)-TMSnV System in Benzene at 50°C., [AIBN] = 5×10^{-2} mole/l.

Expt. no.	Monomer feed		TMSnV in comonomer, mole-%	Time, hr.	Conversion, %	$R_p \times 10$, %/hr.	C, %	Copolymer			
	St, g.	TMSnV, g.						Sn, %	TMSnV, %	Sn, mole-%	$[\eta]$, dl./g.
3-1	0	6.35	100	137	0	0	79.68	5.87	12.60	5.38	
2	0.46	7.37	83.8	137	1.59	0.11	85.87		5.91		0.10
3	0.91	6.37	80.2	64	3.10	0.49	88.66	2.67	3.20	2.39	
4	1.37	6.10	71.0	32	3.18	0.99	89.51		2.41		
5	1.82	5.08	60.3	19	3.18	1.67	90.02	1.65	1.93	1.47	
6	2.28	4.19	50.1	14.5	3.62	2.50	90.26	1.56	1.71		0.31
7	2.73	3.30	39.8	13.5	5.00	3.45	90.51	1.48	1.14	1.39	
8	3.19	2.54	30.3	10	5.62	5.06	90.88	1.02	0.99	0.89	0.42
9	3.64	1.65	19.8	8	4.85	6.06	91.04				
10	4.10	0.89	10.7	7	4.60	6.57					
11	4.55	0	0	2.5	3.48	9.94					0.51

 TABLE IV. Results of Copolymerization of MMA-TMSnV System in Benzene at 50°C., [AIBN] = 5×10^{-2} mole/l.

Expt. no.	Monomer feed		TMSnV in comonomer, mole-%	Time, hr.	Conversion, %	$R_p \times 10$, %/hr.	C, %	Copolymer			
	MMA, g.	TMSnV, g.						Sn, %	TMSnV, %	Sn, mole-%	$[\eta]$, dl./g.
4-1	0.38	6.22	89.1	137	0	0	56.83	5.71	6.04	5.78	
3	1.13	5.08	70.2	17	5.75	3.38	57.55		4.58		0.26
4	1.60	5.45	59.3	8	5.07	6.34	58.11	2.63	3.47	2.26	
5	2.07	3.94	49.9	5	4.92	9.84	58.69	1.40	2.35	1.19	0.49
6	2.54	3.18	39.7	3.5	5.10	14.57	58.79		2.16		
7	3.20	2.67	30.4	2.5	5.48	21.92	58.85	0.67	2.06	0.59	0.90
8	4.04	1.91	19.8	2	5.35	26.75			1.66		
9	5.45	1.14	9.9	1.5	5.27	35.13					
10	5.64	0	0	1	4.85	48.50					1.51

TABLE V. Results of Copolymerization of St-TBSnV System in Benzene at 50°C., [AIBN] = 5×10^{-2} mole/l.

Expt. no.	Monomer feed		TBSnV in comonomer, mole-%	Time, hr.	Conversion, %	$R_p \times 10$, %/hr.	C, %	Copolymer			
	St, g.	TBSnV, g.						Sn, %	TBSnV, %	Sn, mole-%	$[\eta]$, dl./g.
1-1	0	7.96	100.0	100	0	0					
2	0.27	7.19	89.7	100	0.05	0.005	73.20		21.46		
3	0.55	6.32	79.2	56	2.58	0.46	79.04		14.18		0.08
4	0.82	5.66	69.1	31	3.01	0.97	82.00	11.00	11.47	12.17	
5	1.09	4.80	59.2	18	2.09	1.61	79.79		13.14		0.13
6	1.27	3.92	50.3	13	2.70	2.08	74.71	6.22	20.85	6.15	
7	1.55	3.16	40.2	11.5	2.81	2.44	88.84		2.93		0.23
8	1.82	2.40	30.2	9	3.10	3.44	90.18	2.28	1.60	2.09	
9	2.09	1.65	20.4	6.5	3.00	4.62	90.68		1.26		0.29
10	2.37	0.76	9.5	5	3.20	6.40	90.70	1.80	1.23	1.66	
3-11	4.55	0	0	2.5	3.48	9.94					0.51

TABLE VI. Results of Copolymerization of MMA-TBSnV System in Benzene at 50°C., [AIBN] = 5×10^{-2} mole/l.

Expt. no.	Monomer feed		TBSnV in comonomer, mole-%	Time, hr.	Conversion, %	$R_p \times 10$, %/hr.	C, %	Copolymer			
	MMA, g.	TBSnV, g.						Sn, %	TBSnV, %	Sn, mole-%	$[\eta]$, dl./g.
2-1	0.28	7.19	88.5	100	3.10	0.31	56.67	14.98	21.86	17.40	
2	0.47	6.32	80.9	48	4.99	1.04	58.36		8.48		0.16
3	0.75	5.56	70.0	16.5	5.71	3.46	57.79	6.97	12.37	6.14	
4	1.03	4.80	59.4	7.5	3.30	4.40	59.03		4.53		0.33
5	1.32	3.92	48.5	5	3.50	7.00	58.98	3.37	4.81	3.03	
6	1.50	3.16	39.9	3.5	3.70	10.57	59.42		4.71		0.47
7	1.79	2.39	29.3	2.5	4.00	16.00	58.93	1.90	5.07	1.66	
8	1.97	1.64	20.7	2	4.20	21.00	58.74		6.17		0.60
9	2.26	0.76	9.7	1.5	4.70	31.33	58.98	1.58	4.81	1.37	
4-10	5.64	0	0	1	4.85	48.50					1.51

These monomers could not be homopolymerized under the experimental conditions, as shown in Table II.

Copolymerization

The results obtained by the copolymerizations of the St-TMSnV, MMA-TMSnV, St-TBSnV, and MMA-TBSnV systems are shown in Tables III-VI.

The effects of the monomer composition on the rate of copolymerization R_p are shown in Figures 3 and 4.

From the Figures 3 and 4, it was found that the rate of the copolymerization decreased with increasing molar ratio of the vinyltin compound to the comonomer for all systems.

Elementary analyses for C and H of the polymers, which were repeatedly purified by dissolving in benzene and precipitating with methanol, were carried out, and the fact that the composition did not vary after repeated purification suggested that the polymers were copolymers.

The viscosities of the product polymers were measured only for those polymers obtained in sufficiently large yields. Results are also shown in Tables III-VI. The intrinsic viscosity also decreased with increasing molar ratio of the vinyltin compound to the comonomer.

In the case of experiment 3-3, for example, as shown Table III where the intrinsic viscosity $[\eta]$ of the obtained polymer was 0.10, if the polymer consisted of only polystyrene, \bar{P}_n of this polymer would be 72 from the viscosity equation ($\log \bar{P}_n = 3.2480 + 1.4 \log [\eta]$) for polystyrene. The ratio of St to TMSnV in the copolymer, M_1/M_2 , was 7. Therefore, the results suggest that the copolymer chain having \bar{P}_n 72 contains about ten units of TMSnV. Similarly, in the case of experiment number 3-9, where

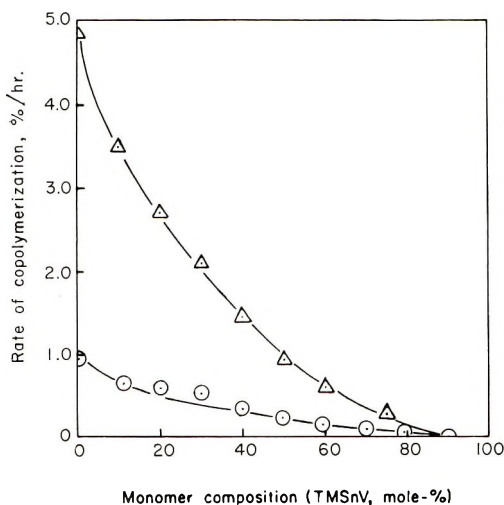


Fig. 3. Relationship between the rate of copolymerization and monomer composition: (○) St-TMSnV system; (△) MMA-TMSnV system.

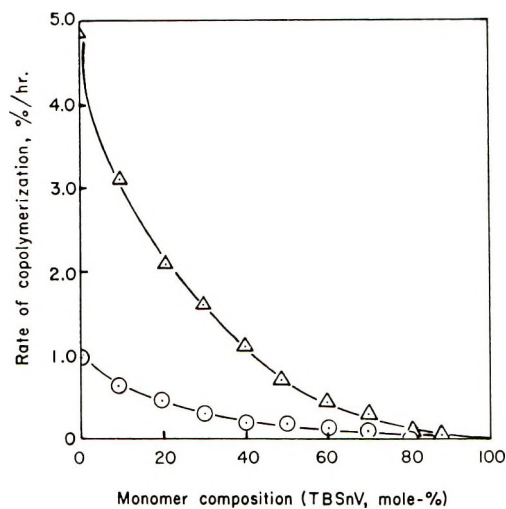


Fig. 4. Relationship between the rate of copolymerization and monomer composition; (○) St-TBSnV system; (△) MMA-TBSnV system.

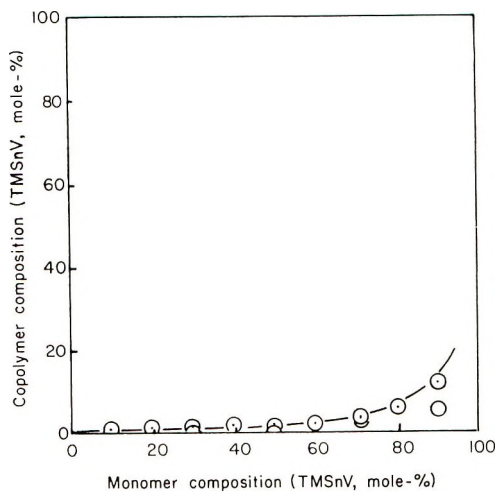


Fig. 5. Composition curve of St-TMSnV copolymer: (○) elementary analysis for Sn; (⊙) elementary analysis for C and H; (—) theoretical curve for $r_1(\text{St}) = 44.8$, $r_2 = 0.001$.

TABLE VII
 r_1 , r_2 and Q_2 , e_2 of TMSnV and TBSnV

M_1	M_2	r_1	r_2	Q_2	e_2
St	TMSnV	44.8	0.001	0.005	0.962
MMA	TMSnV	25.1	0.03	0.036	0.933
St	TBSnV	16.0	0.005	0.017	0.822
MMA	TBSnV	27.9	0.03	0.031	0.822

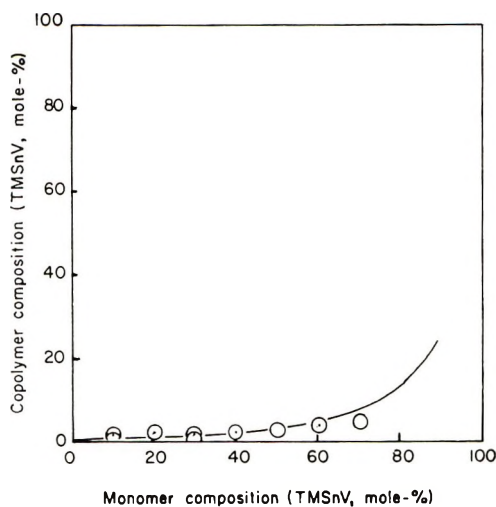


Fig. 6. Composition curve of MMA-TMSnV copolymer; (○) elementary analysis for Sn; (○) elementary analysis for C and H; (—) theoretical curve for r_1 (MMA) = 25.1, $r_2 = 0.03$.

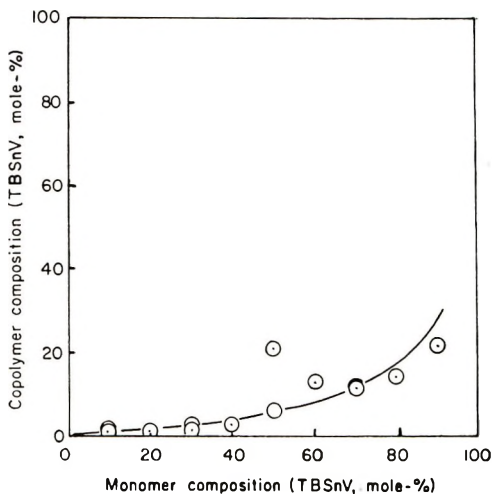


Fig. 7. Composition curve of St-TBSnV copolymer: (○) elementary analysis for Sn; (○) elementary analysis for C and H; (—) theoretical curve for r_1 (St) = 16.0, $r_2 = 0.005$.

$[\eta] = 0.42$ ($\bar{P}_n = 534$ for polystyrene), $M_1/M_2 = 87$. The copolymer chain having $\bar{P}_n = 534$ would contain about 6 TMSnV units.

The copolymerizations for all the systems followed almost the same trend as shown in Figures 5-8. The copolymerization composition curves based on the results are shown in Tables III-VI.

According to the Fineman-Ross method⁸ and to the curve-fitting method, the monomer reactivity ratios (r_1 and r_2) were calculated for these copoly-

merization systems (see Figs. 5-12). The results are summarized in Table VII. From the r_1 and r_2 values, Q and e values for the monomers were calculated by assuming the values: St ($Q_1 = 1.0$, $e_1 = -0.80$);⁹ MMA ($Q_1 = 0.74$, $e_1 = 0.40$).⁹

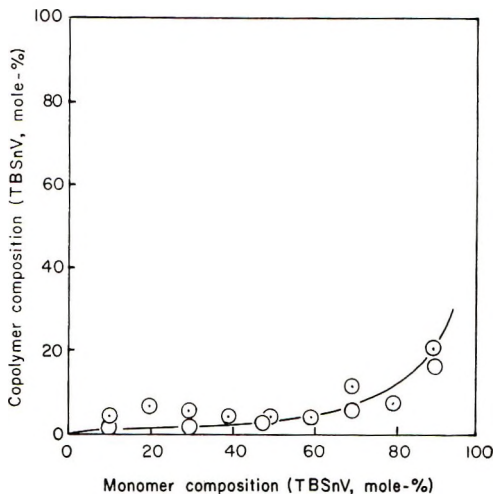


Fig. 8. Composition curve of MMA-TBSnV copolymer: (○) elementary analysis for Sn; (⊙) elementary analysis for C and H; (—) theoretical curve for r_1 (MMA) = 27.9, $r_2 = 0.03$.

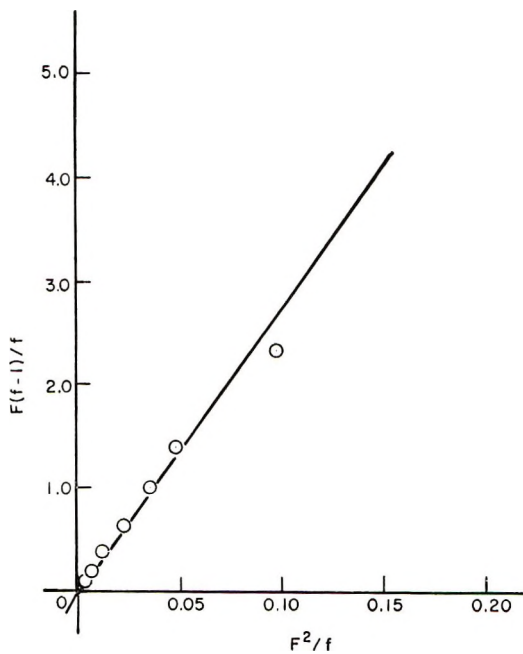


Fig. 9. Fineman-Ross plot of St-TMSnV system.

These results indicate that r_1 values are very much greater than r_2 values in all systems. Therefore, the rate of addition of styrene or methyl methacrylate monomer to its own radical is greater than that of the organo-metallic compound (TMSnV or TBSnV) monomer unit.

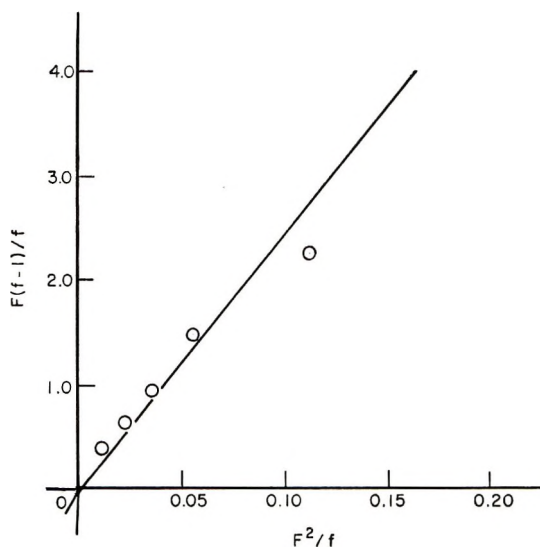


Fig. 10. Fineman-Ross plot of MMA-TMSnV system.

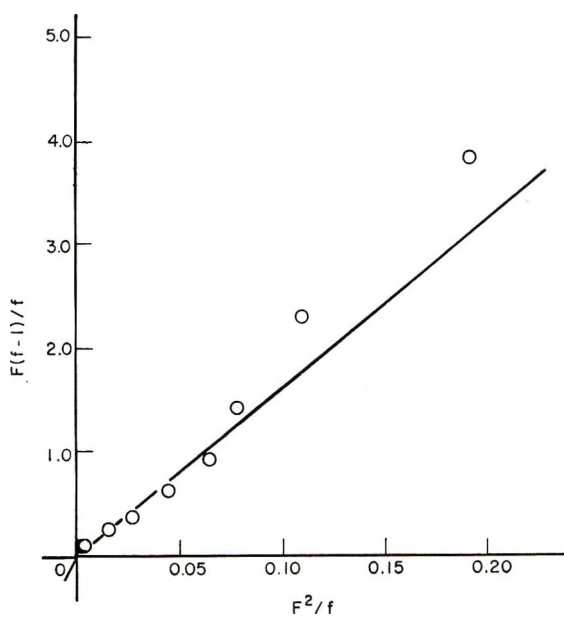


Fig. 11. Fineman-Ross plot of St-TBSnV system.

TABLE VIII
 $Q-e$ values and σ Constants for $\text{CH}_2=\text{CHR}$

R in $\text{CH}_2=\text{CHR}$	e	Q	Hammett constants	
			σ_m	σ_p
$\text{C}(\text{CH}_3)_3^a$	-0.63	0.007	-0.10 ± 0.03	-0.197 ± 0.02
$\text{Si}(\text{CH}_3)_3^a$	-0.14	0.035 ^b	-0.04 ± 0.1	-0.07 ± 0.1
	-0.10	0.031 ^c		
$\text{Sn}(\text{CH}_3)_3$	0.962	0.005 ^b		0.0 ± 0.1
	0.933	0.036 ^d		
$\text{Sn}(n\text{-C}_4\text{H}_9)_3$	0.822	0.017 ^b		
	0.822	0.031 ^d		

^a Data of Young.⁹

^b Copolymerization with styrene.

^c Copolymerization with acrylonitrile.

^d Copolymerization with methyl methacrylate.

The $Q-e$ values for *tert*-butylethylene⁹ and trimethylvinylsilane⁹ having structures similar to TMSnV and TBSnV respectively, are listed in Table VIII for comparison with those of TMSnV and TBSnV.

The second column in Table VIII shows that the e value changes from negative to positive as the atomic number in Group IV in the periodic table increases. This phenomenon may be explained as follows. The bond orbitals of carbon and silicon are $2s, 2p$ and $3s, 3p$, respectively, while those of tin are $5s, 5p$ with larger orbital radius than those of $2s, 2p$ and $3p, 3p$. Generally, in the case of silicon or tin, there is a contribution of d -orbital to bonding.

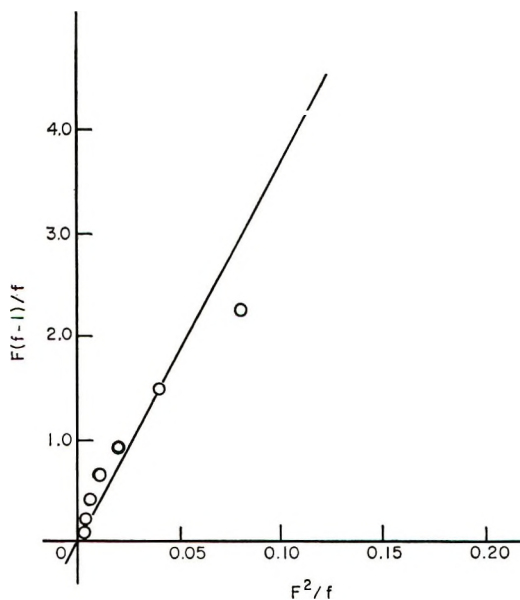


Fig. 12. Fineman-Ross plot of MMA-TBSnV system.

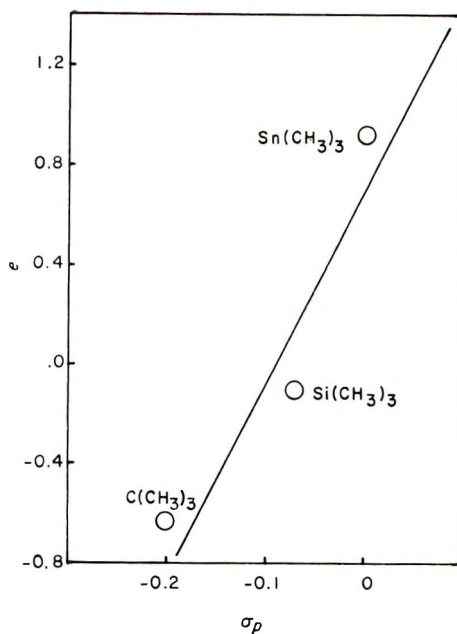


Fig. 13. Relationship between e values and σ_p constants for $CH_2=CHC(CH_3)_3$, $CH_2=CHSi(CH_3)_3$, and $CH_2=CHSn(CH_3)_3$.

Consequently, the mesomeric effect increases in the order: $C < Si < Ge < Sn$.

The e value for bonding of the butyl group to tin would be larger than that for bonding of the methyl group to tin, because the electron-releasing effect of the butyl group is larger than that of the methyl group.

In general, both the e value and Hammett's constant σ are terms which are related to the polarity. Furukawa and Tsuruta¹⁰ have found a linear relationship between them. In order to check this point, the e values were plotted against Hammett's constants (σ_p).¹¹

From the result shown in Figure 13, an approximate linear relationship was observed between the σ value and the e value, and the e values of TMSnV and TBSnV obtained in this work were therefore, thought to be appropriate.

References

1. C. E. Scott and C. C. Price, *J. Am. Chem. Soc.*, **81**, 2670 (1959).
2. B. R. Thompson, *J. Polymer Sci.*, **19**, 373 (1956).
3. V. V. Korshak and A. M. Palyalova et al., *Izv. Akad. Nauk SSSR, Otdel. Khim. Nauk*, **1959**, 179.
4. S. Murahashi, S. Nozakura, and M. Sumi, *Bull. Chem. Soc. Japan*, **32**, 670 (1959).
5. V. V. Korshak et al., *Dokl. Akad. Nauk SSSR*, **112**, 436 (1957).
6. D. Seyferth and F. G. A. Stone, *J. Am. Chem. Soc.*, **79**, 515 (1957).
7. E. R. Blout, W. P. Hohenstein, and H. Mark, *Monomer*, Interscience, New York, 1949.

8. M. Fineman and S. D. Ross, *J. Polymer Sci.*, **5**, 269 (1950).
9. L. J. Young, *J. Polymer Sci.*, **54**, 411 (1961).
10. J. Furukawa and T. Tsuruta, *J. Polymer Sci.*, **36**, 275 (1959).
11. D. H. McDaniel and H. C. Brown, *J. Org. Chem.*, **23**, 420 (1958).

Résumé

La polymérisation du triméthylvinyl-étain (TMSnV) et du tributylvinyl-étain (TBSnV) a été effectuée en utilisant les radiations γ , les polymérisations radicalaires et les initiateurs ioniques. Ces monomères ne subissent pas la polymérisation en eux-mêmes, mais ils copolymérisent avec le styrène ou le méthacrylate de méthyle, lorsqu'un initiateur radicalaire a été utilisé. Au départ de ces résultats obtenus en cours de copolymérisation, les rapports de réactivité des monomères et les valeurs Q et e , ont été obtenues, à savoir: St-TMSnV, $r_1 = 44.8$, $r_2 = 0.001$, $Q_2 = 0.005$, $e_2 = 0.962$; MMA-TMSnV, $r_1 = 25.1$, $r_2 = 0.03$, $Q_2 = 0.036$, $e_2 = 0.933$; St-TBSnV, $r_1 = 16.0$, $r_2 = 0.005$, $Q_2 = 0.017$, $e_2 = 0.822$; MMA-TBSnV, $r_1 = 27.9$, $r_2 = 0.03$, $Q_2 = 0.031$, $e_2 = 0.822$. La polymérisabilité du TMSnV et du TBSnV a été discutée sur la base des valeurs de Q et e obtenues.

Zusammenfassung

Die Polymerisation von Trimethylvinylzinn (TMSnV) wurde mit γ -Strahlen, sowie radikalischen oder ionischen Startern ausgeführt. Die Monomeren polymerisierten für sich selbst nicht, zeigten jedoch bei radikalischem Start Copolymerisation mit Styrol (St) und Methylmethacrylat (MMA). Die Ergebnisse führten zu folgenden Werten für die Monomerreaktivitätsverhältnisse, sowie für Q und e : St-TMSnV, $r_1 = 44.8$, $r_2 = 0.001$, $Q_2 = 0.005$, $e_2 = 0.962$; MMA-TMSnV, $r_1 = 25.1$, $r_2 = 0.03$, $Q_2 = 0.036$, $e_2 = 0.933$; St-TBSnV, $r_1 = 16.0$, $r_2 = 0.005$, $Q_2 = 0.017$, $e_2 = 0.822$; MMA-TBSnV $r_1 = 27.9$, $r_2 = 0.03$, $Q_2 = 0.031$, $e_2 = 0.822$. Anhand der erhaltenen Q - und e -Werte wurde die Polymerisationsfähigkeit von TMSnV und TBSnV diskutiert.

Received January 25, 1966

Revised April 15, 1966

Prod. No. 5141A

Studies on Polymers Containing Functional Groups. VI. Kinetics of the Polymerization and Copolymerization Behaviors of *o*-Hydroxystyrene

MASAO KATO and HIROYOSHI KAMOGAWA,
*Textile Research Institute of the Japanese Government,
Kanagawa, Yokohama, Japan*

Synopsis

Some kinetic studies were made of the homopolymerization of *o*-hydroxystyrene and its copolymerization behavior with styrene and methyl methacrylate in tetrahydrofuran using azobisisobutyronitrile as initiator were done. The rate of polymerization experimentally obtained is given by $R_p = K[M][I]^{0.72}$. Accordingly, it is likely that the growing chain radicals are terminated not only by mutual termination but also by a chain-transfer mechanism, the latter occupying a considerable portion. The latter is mostly attributed to the transfer to monomer, i.e., C_m for *o*-hydroxystyrene was 1.3×10^{-2} . Some transfer mechanisms were assumed, although it is difficult to elucidate the mechanism in detail, owing to its complexity. Effects of solvent on the rate of polymerization were examined, dioxane, methyl ethyl ketone, ethanol, and tetrahydrofuran being used. However, no differences were found among the solvents. The apparent activation energy of polymerization was found to be 21.5 kcal./mole. Monomer reactivity ratios and Alfrey-Price $Q-e$ values for *o*-hydroxystyrene were determined. The $Q-e$ values ($Q = 1.41$, $e = -1.13$) are rather similar to those of *p*-methoxystyrene. Thus, the e value for *o*-hydroxystyrene is more negative than that for styrene.

INTRODUCTION

It was reported in the previous paper¹ that *o*-hydroxystyrene (OHS) polymerizes by various mechanisms, depending on the method of polymerization. In the previous paper, it was emphasized that, in the case of polymerization with azobisisobutyronitrile (AIBN) as initiator, polymerization seems to proceed almost exclusively by the normal free-radical mechanism, although considerable chain transfer takes place.

The purpose of this study is to investigate the kinetics of the polymerization of OHS and its reactivity in the copolymerization with AIBN, in order to obtain detailed information on the mechanisms of polymerization of OHS with AIBN.

EXPERIMENTAL

Materials

o-Hydroxystyrene (OHS) was prepared from coumarin according to the method described in the previous paper¹ and was distilled under reduced pressure (ca. 1 mm.) before use.

Styrene (St) and methyl methacrylate (MMA) were all commercial products and were purified by distillation from stabilizers just before use.

Azobisisobutyronitrile (AIBN) as initiator was purified by recrystallization from methanol.

Tetrahydrofuran (THF), dioxane, methyl ethyl ketone, and ethanol used as solvents were purified in the usual manner.

Polymerization Procedures

Homopolymerization. Solutions of OHS in THF (3 ml.) and of AIBN in the same solvent (1 ml.) (each concentration was known) were put into a Pyrex glass tube. The tube was cooled with Dry Ice, evacuated, and filled with nitrogen. This operation was repeated twice, after which the tube was flushed with purified nitrogen gas, and then sealed.

Polymerizations were carried out in a thermostat kept at $50-80 \pm 0.1^\circ\text{C}$. The tubes were taken out at certain intervals from the thermostat, cooled, and opened. The contents of the tube were diluted with methanol containing a small amount of hydroquinone, then the solution was poured into ligroin. The mixture was subjected to centrifugation, and the sticky mass left in the centrifuge tube was dissolved in methanol. The solution thus produced was poured into a ca. 3% aqueous sodium sulfate solution to isolate polymer. It was then filtered with a glass filter (IG. No. 4) under suction, washed with water, and then dried over sodium hydroxide under reduced pressure at 50°C . The rates of polymerization were calculated from the polymer yields.

Copolymerizations. OHS, comonomer (St or MMA), and AIBN in THF were put into a tube. The tube was sealed accordingly as in the homopolymerization procedure. A typical reaction mixture consisted of 2 g. of each monomer, 20 mg. of AIBN, and 1 ml. of THF.

Polymerizations were carried out in a thermostat kept at $60 \pm 0.1^\circ\text{C}$. After polymerization (less than 10% conversion), the tubes were opened and the viscous solutions diluted with acetone containing a small amount of hydroquinone. In the case of the OHS-MMA system, copolymers were isolated by pouring their solutions into ligroin, except for the case in which the mole fraction of OHS in the mixture was 0.92. In this case the product was isolated by a procedure similar to that used in the homopolymerization. For the OHS-St system, copolymers produced from mixtures of 0.09-0.28 mole fraction of OHS were isolated by pouring their solutions into methanol containing 20% of water. The others were treated by a procedure similar to that used in the homopolymerizations.

Molecular Weight Determination

Molecular weight determinations were carried out with a Mechrolab vapor pressure osmometer. THF was used as solvent.

RESULTS AND DISCUSSION

Polymerization Kinetics of OHS in THF with AIBN as Initiator

The rates of homopolymerization of OHS, as depending on temperature and initiator concentration, are indicated in Figures 1-4. In each case the monomer concentration was fixed at 3.121 mole/l. As can be seen in the usual free-radical polymerizations, the rate of polymerization increases with increasing temperature and initiator concentration. In the case of polymerization at 50°C. (Fig. 1), inhibition effects (induction periods) seem to appear if monomer stored about 1 week at 0°C. after distillation is employed (*c'*, *d'*). However, this is not observed at temperatures above 70°C. Perhaps a small amount of oxidation products² of OHS was formed during storage, thereby inducing significant inhibitory effects at relatively lower temperatures.

An Arrhenius plot is given in Figure 5. From the plot, the apparent activation energy of polymerization was calculated to be 21.5 kcal./mole, a value which almost corresponds with that for styrene (23 kcal./mole).³

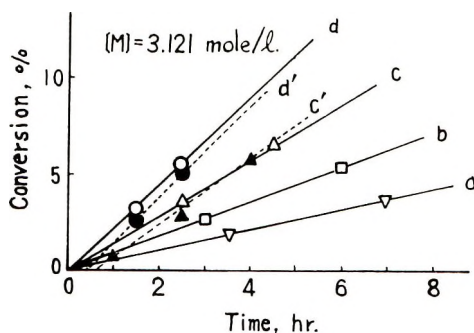


Fig. 1. Polymerizations of OHS in THF at 50°C. with AIBN at various AIBN concentrations: (a) 1.142×10^{-2} mole/l.; (b) 2.284×10^{-2} mole/l.; (c, c') 4.567×10^{-2} mole/l.; (d, d') 9.134×10^{-2} mole/l. For runs *a-d* monomer was used within 20 hr. after distillation; for runs *c'* and *d'* monomer was stored about 1 week at 0°C. after distillation.

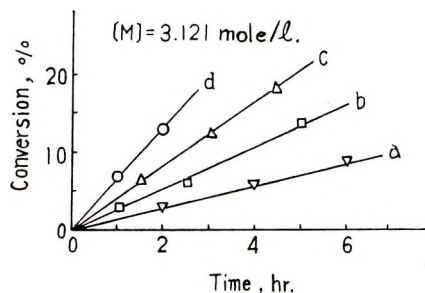


Fig. 2. Polymerization of OHS in THF at 60°C. at various AIBN concentrations: (a) 1.142×10^{-2} mole/l.; (b) 2.284×10^{-2} mole/l.; (c) 4.567×10^{-2} mole/l.; (d) 9.134×10^{-2} mole/l.

Logarithmic plots of the rate R_p against initiator concentration $[I]$ at 50, 60, 70, and 80°C. are shown in Figure 6. The plots give reasonably straight lines having slopes ranging from 0.65 to 0.75. Taking the experimental errors into account, it might be reasonable to assign a mean value of 0.72 for the slope. Therefore, the following relationship is obtained:

$$R_p \propto [I]^{0.72} \quad (1)$$

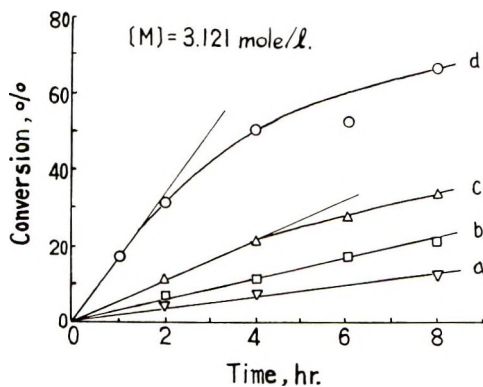


Fig. 3. Polymerization of OHS in THF at 70°C. at various AIBN concentrations: (a) 0.571×10^{-2} mole/l.; (b) 1.142×10^{-2} mole/l.; (c) 2.284×10^{-2} mole/l.; (d) 11.418×10^{-2} mole/l.

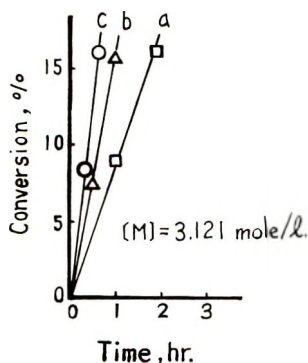


Fig. 4. Polymerization OHS in THF at 80°C. at various AIBN concentrations: (a) 1.142×10^{-2} mole/l.; (b) 2.284×10^{-2} mole/l.; (c) 4.567×10^{-2} mole/l.

Relationships between the rates of polymerization and monomer concentrations at 50, 70, and 80°C. were examined. Logarithmic plots of the rate against monomer concentration $[M]$ are indicated in Figure 7. The plots also give straight lines having a slope of 1.0. Thus, R_p is considered to be proportional to $[M]$:

$$R_p \propto [M] \quad (2)$$

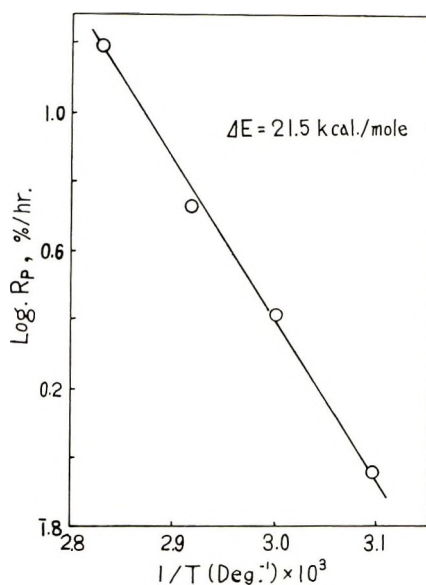


Fig. 5. Arrhenius plot for polymerization of OHS with the use of AIBN as initiator.

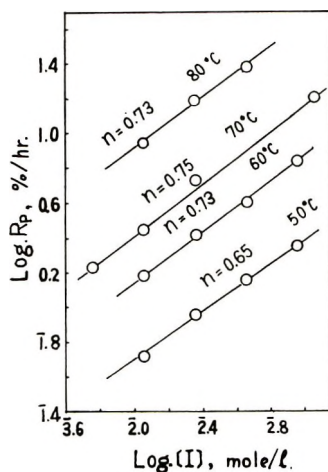


Fig. 6. Log-log plot of initial polymerization rates R_p of OHS in THF against initiator (AIBN) concentration at 50, 60, 70, and 80°C. Monomer concentration constant (3.121 mole/l.).

Consequently, the experimental equation for the rate of polymerization is given by

$$R_p = K[M][I]^{0.72} \quad (3)$$

This equation may suggest that the growing chain radicals are terminated not only by the mutual termination but also to a considerable extent by other mechanisms, since R_p is proportional to more than the 0.5 (between

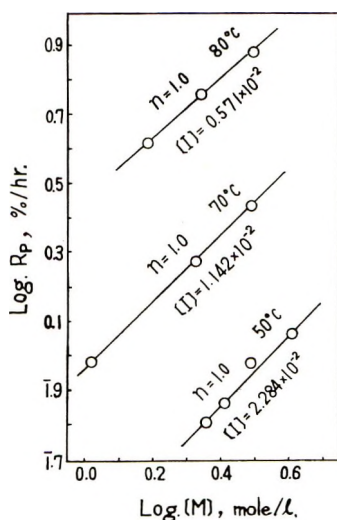


Fig. 7. Log-log plot of initial polymerization rate R_p of OHS in THF against monomer concentration at 50, 70, and 80°C.

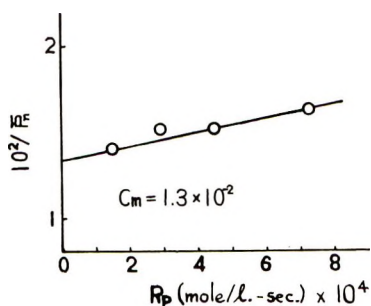


Fig. 8. Reciprocal average degree of polymerization vs. rate of polymerization at 70°C. for bulk OHS with AIBN initiator.

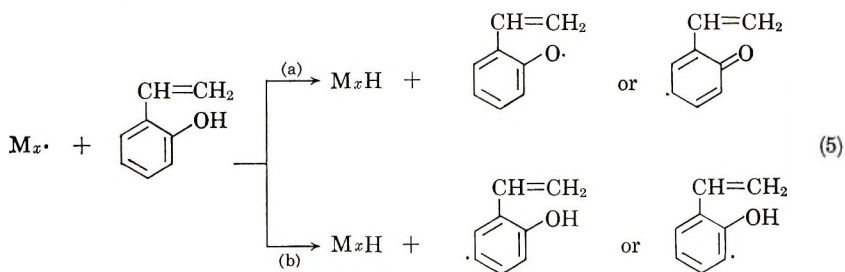
0.5 and 1.0) power of $[I]$. A plausible mechanism of termination other than the biradical one is chain transfer to monomer, as previously presumed.¹ In order to estimate the extent of the transfer, the reciprocal of the average degree of polymerization $1/\bar{P}_n$ is plotted against R_p at 70°C. for undiluted OHS in the presence of AIBN, according to the following relationship.

$$1/\bar{P}_n = C_m + C_i([I]/[M]) + AR_p \quad (4)$$

where A is a constant, and C_m and C_i represent chain-transfer constants to monomer and initiator, respectively. The plot has a comparatively good linearity, as shown in Figure 8. This may imply that C_i is almost zero and only chain transfer to monomer occurs in this case. The value of C_m is found to be 1.3×10^{-2} . It is considerably greater than that of styrene

(0.60×10^{-4}) ,⁴ indicating that OHS cannot produce polymers of such high molecular weights as styrene.

Minoura et al.⁵ investigated the effects of phenols on the polymerization of styrene. They established that, although phenols do not show any inhibition and retardation effects in the case of polymerization under oxygen-free conditions, chain transfer to phenols nevertheless takes place, i.e., the transfer constants are about 10^{-3} and in the decreasing order of *o*-cresol, *p*-cresol, *m*-cresol, and phenol. Assuming that the analogy exists in the case of hydroxystyrenes, it might be expected that C_m for OHS is smaller than that for *m*-hydroxystyrene. Bonsoll et al.⁶ found that R_p is proportional to $[M]^{0.63}$ for the polymerization of *m*-hydroxystyrene with AIBN. On comparing the relationship with the case of OHS, a similar tendency to that in the order of chain-transfer constants with phenols is discernible; the power of initiator concentration for OHS is somewhat larger than that for *m*-hydroxystyrene. It is difficult to elucidate conclusively the mechanisms of chain transfers in polymerization of OHS, because of their complexity. Some possible mechanisms, however, might be as illustrated in eqs. (5).



The growing radical $\text{M}_x \cdot$ attacks either the hydroxyl group or a phenolic nucleus of the monomer molecule to terminate by abstracting a hydrogen atom. Owing to resonance, the radicals thus produced should be relatively stable and reluctant to regenerate active chain radicals by adding monomers. If such radicals are incapable of carrying on the polymerization chains, they eventually disappear through combination with other growing

TABLE I
Effect of Solvents on the Rates of Polymerization of *o*-Hydroxystyrene with AIBN as Initiator^a

Solvent	Dielectric constant of solvent	Rate constant $K \times 10^{4b}$
Dioxane	2.21 (25°C.)	3.14
THF	7.58 (20°C.)	2.85
Methyl ethyl ketone	18.51 (20°C.)	2.85
Ethanol	24.30 (25°C.)	2.98

^a $[M] = 3.329$ mole/l., $[I] = 2.436 \times 10^{-2}$ mole/l., temp. = 70°C.

^b $K = R_p/[M][I]^{0.72}$ ($10^{0.72}$ mole^{-0.72}·sec.⁻¹).

free radicals or with each other. These mechanisms remind one of the autoinhibition occurring in polymerization of allyl compounds,⁷ although rational explanation for these has not yet been attained.

Effect of solvents on the rates of polymerization was also estimated, with the use of dioxane, THF, methyl ethyl ketone, and ethanol as solvents. There were observed, however, no differences among these solvents, as shown in Table I.

Copolymerization Behavior

Relationships between monomer and initial copolymer compositions are indicated in Figure 9. The copolymer compositions were calculated from the results of carbon-hydrogen analysis. It is well known that the product of reactivity ratios is a measure of the alternating tendency in copolymerization. The monomer reactivity ratios and Q - e values proposed by Alfrey and Price⁸ are shown in Table II. The alternating tendency is greater in

TABLE II
Monomer Reactivity Ratios (r_1r_2) and Q - e Values for *o*-Hydroxystyrene (M_1) at 60°C.

Comonomer (M_2)	r_1	r_2	r_1r_2	Q_1	e_1
Styrene	1.32 ± 0.25	0.72 ± 0.10	0.950	1.66	-1.03
Methyl methacrylate	0.21 ± 0.06	0.33 ± 0.08	0.069	1.15	-1.23
			Avg.	1.41	-1.13

MMA than in St as expected. There are obtained somewhat different values of Q_1 and e_1 for OHS between the OHS-St and OHS-MMA systems, so that the mean values were adopted. As regards Q_1 , i.e., the resonance term, its value is rather similar to that of *p*-methoxystyrene (1.36).⁹

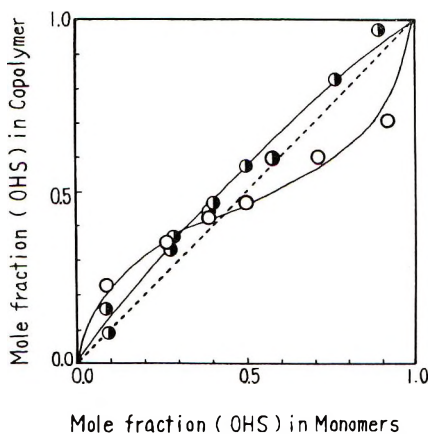


Fig. 9. Initial copolymer compositions in relation to monomer composition: (●) OHS-St; (○) OHS-MMA.

The polarity term e_1 , on the other hand, is more negative than for styrene, and also corresponds to that of *p*-methoxystyrene (-1.11). According to Bonsoll et al.⁶ Q_1 and e_1 values for *m*-hydroxystyrene obtained by the copolymerization with St are 1.10 and -0.80 , which are almost the same values as for styrene. It is generally accepted that styrene monomers substituted with an electron-donating group in the *para* position, such as *p*-methoxystyrene and *p*-methylstyrene, have a more negative e value than styrene itself.⁹ The effect of the substituent is transmitted to the vinyl group through the ring, and this can occur by conjugation only when it is in the *ortho* or *para* position. Hence, the hydroxyl group of *m*-hydroxystyrene can exert an influence only by the induction effect.

Thus, OHS is considered to be more reactive and more susceptible to cationic initiator than styrene, although its polymerization behavior is very complicated.¹

Grateful acknowledgment is made to Prof. S. Okajima of Tokyo Metropolitan University for kind advice.

References

1. M. Kato and H. Kamogawa, *J. Polymer Sci. A-1*, **4**, 1773 (1966).
2. B. B. Coroson, W. J. Heintzelman, L. H. Schwartzman, H. E. Tieffenthal, R. J. Lokken, J. E. Nickels, G. R. Atwood, and F. J. Parlik, *J. Org. Chem.*, **23**, 544 (1958).
3. P. J. Flory, *Principles of Polymer Chemistry*, Cornell Univ. Press, Ithaca, N. Y., 1953, p. 124.
4. F. R. Mayo, R. A. Gregg, and M. S. Matheson, *J. Am. Chem. Soc.*, **73**, 1691 (1951).
5. Y. Minoura, N. Yasumoto, and T. Ishii, *Makromol. Chem.*, **71**, 159 (1964).
6. E. P. Bonsoll, L. Vallentine, and H. W. Melville, *Trans. Faraday Soc.*, **48**, 763 (1952).
7. P. D. Bartlett and R. Altschul, *J. Am. Chem. Soc.*, **67**, 812, 816 (1945).
8. T. Alfrey, Jr. and C. C. Price, *J. Polymer Sci.*, **2**, 101 (1947).
9. L. J. Young, *J. Polymer Sci.*, **54**, 411 (1961).

Résumé

Quelques études cinétiques concernant l'homopolymérisation de l'*o*-hydroxystyrène et son comportement à la copolymérisation avec le styrène et le méthacrylate de méthyle dans le tétrahydrofurane en présence d'asobisisobutyronitrile comme initiateur ont été effectuées. La vitesse de polymérisation expérimentale est exprimée par $R_p = K[M][I]^{0.72}$. En accord avec ce résultat, il est probable que les chaînes en croissance se terminent non seulement par réaction de terminaison mutuelle, mais également par un mécanisme de transfert de chaînes, ce dernier ayant une importance considérable. Le mécanisme de transfert doit être principalement attribué au transfert sur monomère, c'est-à-dire, que C_m pour l'*o*-hydroxystyrène est égal à 1.3×10^{-2} . Quelques mécanismes de transfert sont également postulés, bien qu'il soit difficile d'élucider le mécanisme en détail, par suite de sa complexité. Les effets du solvant sur la vitesse de polymérisation ont été examinés utilisant le dioxane, la butanone et l'éthanol, aussi bien que le tétrahydrofurane; toutefois aucune différence n'a été trouvée entre ces différents solvants. L'énergie d'activation apparente de la polymérisation a été trouvée être égale à 21.5 Kcal/mole. Les rapports de réactivité des monomères et les valeurs de $Q-e$ (suivant Alfrey et Price), pour l'*o*-hydroxystyrène ont été déterminées. Des valeurs de $Q-e$, respectivement de 1.41 et de -1.13 , sont plutôt semblables à celles du méthoxystyrène. La valeur de e pour l'*o*-hydroxystyrène est donc plus négative que celle du styrène.

Zusammenfassung

Eine kinetische Untersuchung der Homopolymerisation von *o*-Hydroxystyrol und seines Kopolymerisationsverhaltens mit Styrol und Methylmethacrylat in Tetrahydrofuran mit Azobisisobutyronitril als Starter wurde durchgeführt. Die experimentell erhaltene Polymerisationsgeschwindigkeit beträgt $R_p = K[M][I]^{0.72}$. Wahrscheinlich werden die wachsenden Kettenradikale nicht nur durch gegenseitigen Abbruch, sondern auch in einem beträchtlichen Ausmass durch einen Kettenübertragungsmechanismus stabilisiert. Die grösste Rolle spielt die Übertragung zum Monomeren, C_m betrug für *o*-Hydroxystyrol $1,3 \cdot 10^{-2}$. Verschiedene Übertragungsmechanismen werden vorgeschlagen, doch ist wegen des komplexen Charakters eine Aufklärung des Mechanismus im Detail schwierig. Der Lösungsmiteleinfluss auf die Polymerisationsgeschwindigkeit wurde an Dioxan, Methyläthylketon, Äthanol und Tetrahydrofuran untersucht. Es traten jedoch keine Unterschiede zwischen den Lösungsmitteln auf. Die scheinbare Aktivierungsenergie der Polymerisation wurde zu 21,5 cal/Mol bestimmt. Monomerreaktivitätsverhältnisse und Q - e -Werte (Alfrey und Price) wurden für *o*-Hydroxystyrol bestimmt. Die Q - e -Werte ($Q = 1,41$, $e = 1,13$) sind denjenigen von *p*-Methoxystyrol recht ähnlich. Der e -Wert für *o*-Hydroxystyrol ist daher negativer als derjenige für Styrol.

Received February 1, 1966

Revised March 18, 1966

Prod. No. 5119A

Mechanism of Stereospecific Polymerization of Propylene with Titanium Trichloride— Aluminum Alkyl Catalysts

A. K. INGBERMAN, I. J. LEVINE, and R. J. TURBETT,
*Plastics Division, Union Carbide Corporation,
Bound Brook, New Jersey 08805*

Synopsis

The effect of various aluminum alkyls at varying concentrations on the rate and stereospecificity of propylene polymerizations with titanium trichloride was examined. It was concluded that dialkylaluminum halides were merely chemisorbed on the surface of the titanium trichloride while the trialkylaluminums reacted more extensively with the surface. In the case of diethylaluminum chloride standard chemisorption kinetics were observed. The rate of polymerization was also found to be a function of solvent, with certain aromatic solvents causing significant rate increases. With diethylaluminum chloride essentially no termination occurs; the polymers are "living polymers."

INTRODUCTION

In the past several years numerous publications and patents have appeared describing the stereospecific polymerization of propylene and of other vinyl monomers. Much conflicting information has appeared, and there is still considerable disagreement as to the precise nature of the polymerization process. To a certain extent this situation has arisen because of the experimental difficulties involved in studying these systems. Another contributing factor is that dissimilar systems are sometimes compared.

The most frequently used catalytic system for the stereoregular polymerization of propylene consists of one or another of the purple crystalline modifications of $TiCl_3$ in combination with a trialkylaluminum or a dialkylaluminum chloride. The α , γ , and δ forms of $TiCl_3$ are all layer lattice-type crystals which differ only in the nature of the close packing.¹ The β modification is a linear polymer and yields lower rates of polymerization and lower degrees of stereoregularity.

It seems quite clear from the work of Carrick et al.^{2,3} and Cossee⁴ that the active site from which the polymer chain propagates is a transition metal atom. In the case of $TiCl_3$, which is insoluble in most polymerization media, this active site must be near the surface of the crystal. The function of the aluminum alkyl is to alkylate the titanium atoms at the active

sites. These sites are probably chlorine vacancies, and stereoregularity is then a result of the spatial restrictions imposed by the crystal. The data reported here are wholly consistent with this general mechanism.

The effects of a variety of reaction variables on the rate of polymerization and on the nature of the polymer have been examined for the polymerization of propylene at moderate temperatures. The data obtained yield not only a self-consistent picture, but one which is in accord with the general principles of heterogeneous reactions.

RESULTS AND DISCUSSION

Nature and Concentration of the Aluminum Alkyl

When α/γ - TiCl_3 is used in a heptane diluent at 40°C. with diethylaluminum chloride, polypropylene of very high stereoregularity is produced. The atactic and, therefore, amorphous fraction represents less than 2% of the total polymer produced. In general, when triethylaluminum is used as a cocatalyst with α/γ - TiCl_3 about 25% of the polymer produced is amorphous. (It is important to note that in working up the polymerization mixture, it is possible to discard inadvertently the wholly amorphous fraction. Commonly, methanol is added to the reaction diluent in order to precipitate any polymer which may be in solution. However, because of the low solubility of methanol in aliphatic hydrocarbons, this procedure precipitates only a small portion of the amorphous fraction. As a result, claims in the literature of highly stereoregular polymerization cannot be accepted without examination of the polymer work-up procedure. The use of a volume of a 1:1 mixture of methanol and isopropanol equal to the volume of the polymerization solvent has been demonstrated to precipitate over 99% of the amorphous fraction. This fraction can then be separated from the crystalline fraction by extraction with diethyl ether. In addition, the crystalline fraction is not nearly as isotactic as when diethylaluminum chloride is used. The rate of polymerization is about an order of magnitude faster with triethylaluminum than with diethylaluminum chloride.

The differences between diethylaluminum chloride and triethylaluminum can be explained on the basis of their relative alkylating abilities. Diethylaluminum chloride, having only moderate alkylating ability, is incapable at moderate temperatures and under dilute condition, of reacting with a clean TiCl_3 surface. Instead, it is chemisorbed on TiCl_3 surface defects. These defects are most likely chlorine vacancies. Exchange of an ethyl moiety for a chlorine associated with this titanium atom then generates the active site for propylene polymerization. The result of site formation by chemisorption only, with no subsequent reactions, would be to make a relatively small number of active sites, equal in number to TiCl_3 surface defects, and to which the approach of propylene monomer is sterically restricted.

Triethylaluminum is a good alkylating agent and is postulated as capable of further alkylation (leading to reduction) of TiCl_3 . The first step is probably again chemisorption on defects. However, it is suggested that Et_3Al , both chemisorbed and in solution, is capable of further reaction with the TiCl_3 surface. This results in the generation of more potential titanium sites, of low steric hindrance, because removal of Cl by exchange with ethyl groups, and subsequent homolytic cleavage of the $\text{Ti}-\text{C}_2\text{H}_5$ bonds exposes titanium atoms. In effect, this amounts to a net removal of surface chlorine atoms.

The proposed model for the active site in essence asserts that a sterically hindered site makes highly stereoregular and crystalline polypropylene, while sterically unhindered sites produce not only moderately crystalline polypropylene, but also, when sufficiently exposed, the completely amorphous fraction typical of the $\text{Et}_3\text{Al}-\text{TiCl}_3$ catalyst system. This mechanism emphasizes the importance of the interaction of alkylating agent with TiCl_3 rather than the specific crystallography of the transition metal halide. The initial geometry of the transition metal halide surface need not, and with trialkylaluminums, probably does not correlate with the geometry of the surface after interaction with the cocatalyst.

TABLE I
Effect of Aluminum Alkyl Type and Concentration on Polymer Yield and Tacticity^a

Alkyl	Alkyl concn., $M \times 10^4$	Polymer yield, g./mmole Ti	Amorphous, %	Crystallinity, % ^b	$\bar{M}_r \times 10^{-5}$
Et_2AlCl	2.56	3.61	1.5	85	12.5
"	5.65	4.75	0	85	14.0
Et_3Al	2.60	3.02	6.1	85	17.2
"	4.42	8.88	7.0	70	13.6
"	7.00	13.0	13.2	65	

^a 2.0 ± 0.1 mmole TiCl_3 , 40°C ., *n*-heptane, 7.5 psig propylene pressure, 2.5 hr. polymerization time.

^b Refers to the crystallinity of polymer after removal of the wholly amorphous fraction based on the infrared method of Luongo.⁵

This mechanism predicts, in effect, that if Et_3Al were a less powerful alkylating agent, it should resemble Et_2AlCl in its interaction with TiCl_3 . In practice, one can test this prediction by using very low concentrations of Et_3Al . This would be expected to decrease its rate of reaction with the TiCl_3 surface. In fact, at very low concentrations, Et_3Al closely resembles Et_2AlCl not only in the rate of polymerization but in the nature of the polymer produced. (Table I.)

For a given sample of TiCl_3 , the dependence of polymerization rate on Et_2AlCl concentration should obey one or another of the chemisorption isotherms. Two common adsorption isotherms have been used frequently to correlate adsorption data. One of these, the Freundlich equation, lacks theoretical foundation but is a good empirical fit for much of the data

obtained for the adsorption of nonelectrolytes from solution.⁶ The Freundlich absorption isotherm translated into terms useful for this study is

$$\text{Wt. of Et}_2\text{AlCl adsorbed/mmole TiCl}_3 = k[\text{Et}_2\text{AlCl}]^n \quad (1)$$

where k and n are constants. The total polymerization rate is given by eq. (2).

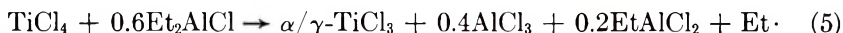
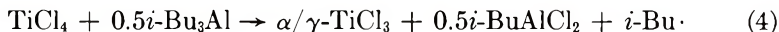
$$\text{Polymerization rate} = k'[\text{active sites}][\text{propylene}] \quad (2)$$

The polymerization rate remains essentially constant with time. Thus, if the number of active sites is proportional to the weight chemisorbed Et_2AlCl , eqs. (1) and (2) become:

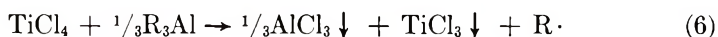
$$\text{Yield of polymer/mmole TiCl}_3 = k''[\text{Et}_2\text{AlCl}]^n \quad (3)$$

where k'' and n are constants.

When TiCl_4 is reduced with a moderate excess of aluminum alkyl over the stoichiometric equivalent required for the reduction of TiCl_4 to TiCl_3 , there is obtained along with the desired TiCl_3 an amount of RAlCl_2 corresponding to the excess aluminum alkyl. Two samples of TiCl_3 were prepared with excess aluminum alkyl, the precise stoichiometries being given by eqs. (4) and (5). The precise fate of the alkyl radicals was not determined but it is assumed that they were removed by standard paths.



The RAlCl_2 , where R is alkyl, is hydrocarbon-soluble but is not a catalyst for the polymerization. It can compete very strongly for sites; hence it can be a very effective poison as the data in Table II show. The experiments in Table II were carried out by adding each of the aluminum alkyls separately. The TiCl_3 was prepared according to eq. 6,



where R is isobutyl. Little or no aluminum alkyl would have been expected to be present with the TiCl_3 .

Invariably for TiCl_3 prepared with excess aluminum alkyl, active sites are formed in accordance with the Freundlich equation. The rate of

TABLE II
Effect of Ethylaluminum Dichloride on Polymer Yield^a

Et_2AlCl concn., $M \times 10^3$	EtAlCl_2 concn., $M \times 10^3$	Polymer yield, g./mmole Ti
7.20	0	6.00
6.74	0.33	4.64
7.06	0.71	3.71
7.13	1.35	2.24

^a 40°C., *n*-heptane, 8 psig, 2.0 mmole TiCl_3 , 2.5 hr. polymerization time.

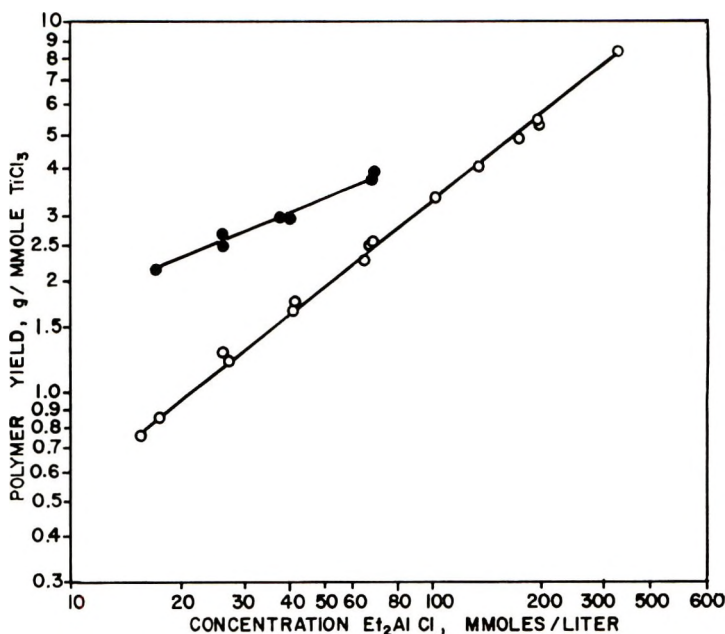


Fig. 1. Freundlich plot of log (polymer yield) vs. log $[\text{Et}_2\text{AlCl}]$: (O) TiCl_3 prepared according to eq. (5); (●) TiCl_3 prepared according to eq. (4). Yields are for 2.5-hr. polymerizations in *n*-heptane at 40°C . with 10 ± 0.2 mmole of TiCl_3 .

propylene polymerization increased monotonically according to eq. (3) (Fig. 1). Increasing polymerization rates were obtained with increasing Et_2AlCl concentrations even for very high concentrations of Et_2AlCl . This is in accord with the hypothesis that compounds of the type RAlCl_2 are preferentially chemisorbed by TiCl_3 and displaced only with difficulty by Et_2AlCl .

The second adsorption isotherm in common use is the Langmuir adsorption isotherm. This can be deduced from first principles, regardless of the kinetics of the process, provided that the molecules are adsorbed onto definite sites, do not interact with one another, and that the adsorbate molecules are in equilibrium with those in the fluid phase. The Langmuir equation⁷ translated into terms useful for our purposes is:

Number of active sites

Unit area of TiCl_3

$$= \frac{\frac{\text{Total potential active site}}{\text{Unit area of } \text{TiCl}_3} \times \text{concn. } (\text{Et}_4\text{Al}_2\text{Cl}_2)}{\beta \times \frac{\text{Total potential active sites}}{\text{Unit area of } \text{TiCl}_3} + \text{concn. } (\text{Et}_4\text{Al}_2\text{Cl}_2)} \quad (7)$$

where β is related to the partition function of the adsorbed phase. Making the assumptions: (a) that the same TiCl_3 preparation is used for a series of experiments and that it is of relatively uniform particle size, and that,

TABLE III
Effect of Diethylaluminum Chloride Concentration on Polymerization Rate with TiCl_3
Prepared According to Equation (6)

TiCl_3 , mmole	Et_2AlCl , mmole	Al/Ti	Polymer yield, g./mmole Ti	Ether solubles, %
2.10	0.153	0.070	0.22	—
2.08	0.384	0.160	3.61	1.5
2.06	0.538	0.262	4.26	2.0
2.04	0.940	0.461	4.75	0
2.12	1.09	0.515	4.97	0
1.85	1.90	1.03	5.70	1.8
1.98	11.0	5.52	6.70	1.0
2.12	24.5	11.6	6.90	0.7

therefore, the surface of the TiCl_3 is proportional to the weight used; (b) that the polymer yield is directly proportional to the number of active sites; (c) that a small amount of Et_2AlCl is destroyed by impurities which, as the data in Table III indicate, is for our experimental conditions about 0.08 mmole $\text{Et}_2\text{AlCl}/\text{l.}$, then:

Yield polymer
mmole TiCl_3

$$= \frac{\frac{\text{Total potential polymer yield}}{\text{mmole } \text{TiCl}_3} \times (\text{Et}_4\text{Al}_2\text{Cl}_2 - 0.04)}{\beta \times \frac{\text{Total potential polymer yield}}{\text{mmole } \text{TiCl}_3} + (\text{Et}_4\text{Al}_2\text{Cl}_2 - 0.04)} \quad (8)$$

The total potential polymer yield is obtained by covering all potential sites on the TiCl_3 surface with Et_2AlCl . Theoretically this obtains as $\text{Et}_2\text{AlCl}/\text{TiCl}_3$ approaches infinity, but as the data in Table III indicate, coverage is nearly complete at $\text{Et}_2\text{AlCl}/\text{TiCl}_3 = 10$. Therefore,

$$\frac{1}{\text{Yield of polymer}} = \frac{A}{(\text{Et}_4\text{Al}_2\text{Cl}_2 - 0.04)} + B \quad (9)$$

where A and B are new constants that incorporate all previous constants. Equation (9) assumes that the site-producing species adsorbed is the dimer, $\text{Et}_4\text{Al}_2\text{Cl}_2$. However, it is more likely that Et_2AlCl monomer is the effective adsorbate. Since



then

$$[\text{Et}_2\text{AlCl}] = K[\text{Et}_4\text{Al}_2\text{Cl}_2]^{1/2} \quad (11)$$

For monomeric Et_2AlCl as the active species, eq. (8) becomes

$$\frac{1}{\text{Yield polymer}} = \frac{A'}{(\text{Et}_4\text{Al}_2\text{Cl}_2 - 0.04)^{1/2}} + B \quad (12)$$

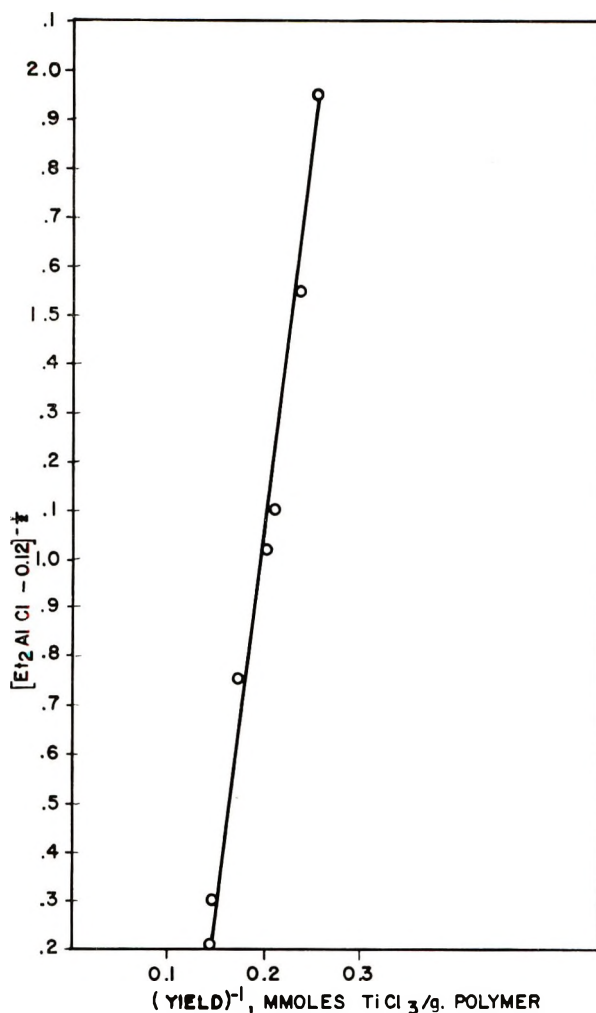


Fig. 2. Langmuir plot of $(\text{polymer yield})^{-1}$ vs. $[\text{Et}_2\text{AlCl} - 0.12]^{1/2}$, where the Et_2AlCl is the total amount used in 1.5 l. of solvent.

When TiCl_4 was reduced with a stoichiometric amount of R_3Al and the reaction [eq. (6)] driven to completion, no soluble aluminum compound should have remained. The resultant TiCl_3 preparation consisted essentially of co-crystallized TiCl_3 and AlCl_3 . The dependence of propylene polymerization rate on Et_2AlCl concentration with this sample of TiCl_3 is given in Table III. At low Et_2AlCl concentrations the polymerization rate increased monotonically with increasing Et_2AlCl . However, the rate became almost insensitive to increasing Et_2AlCl concentration at molar ratios of $\text{Et}_2\text{AlCl}/\text{TiCl}_3$ greater than 2.

In Figure 2 these data are plotted according to the predictions of the Langmuir treatment, eq. (12). The fit is very good for the assumption that the active adsorbate is Et_2AlCl monomer. Figure 3 is a similar plot of the

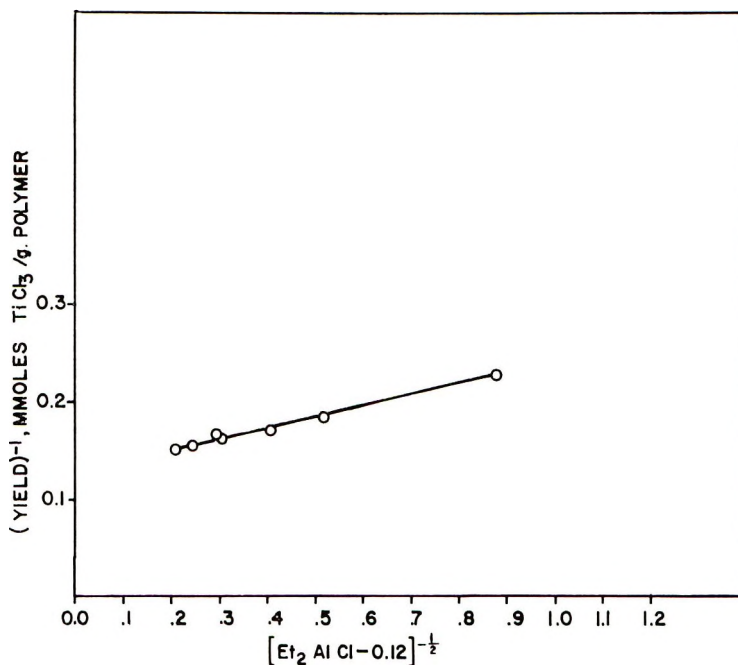


Fig. 3. Langmuir plot of $(\text{polymer yield})^{-1}$ vs. $(\text{Et}_2\text{AlCl} - 0.12)^{-1/2}$, where the Et_2AlCl is the total amount used in 1.5 l. of solvent.

data in Table IV for a different sample of TiCl_3 prepared in a similar manner.

Previous reports concerning the effect of aluminum alkyl concentration are confusing. Natta⁸ reported that the polymerization rate is independent of aluminum alkyl concentration and that it is proportional only to monomer pressure and the amount of TiCl_3 used. Similar results have been reported by other workers.⁹ Contrary results were reported by Ambröz et al.,¹⁰ who found a first-order dependence on alkyl concentration in the

TABLE IV
Effect of Diethylaluminum Chloride Concentration on Polymerization Rate with TiCl_3
Prepared According to Equation (6)^a

TiCl_3 , mmole	Et_2AlCl , mmole	Al/Ti	Polymer yield, g./mmole Ti	Ether solubles, %
2.02	0	0	0	0
2.07	1.41	0.681	4.39	0
2.06	3.82	1.86	5.34	1.4
1.90	6.06	3.20	5.77	0.1
2.02	6.30	3.12	5.95	0
1.86	11.0	5.90	6.08	0
2.07	11.2	5.40	5.88	0.8
1.92	11.4	5.96	5.96	0
2.02	17.0	8.42	6.30	0.8
1.84	22.5	12.2	6.60	1.6

^a 40°C., 7.5 psig propylene pressure, 2.5 hr. polymerization, 1.5 l. of *n*-heptane.

TiCl₃-Et₃Al catalyst system. Saltman¹¹ suggested a dependence on aluminum alkyl concentration expressed by the factor, θ_A , representing the fraction of the TiCl₃ surface covered by aluminum alkyl. He showed that θ_A should be proportional to the square root of the aluminum alkyl concentration. Natta's reported lack of dependence on aluminum alkyl was rationalized by assuming that under his conditions θ_A approached unity. For the TiCl₃-Et₃Al system, we did not observe a simple dependence on Et₃Al concentration. Further, the degree of stereoregularity of the polymer produced decreases with increasing Et₃Al concentration, as is evidenced by both the amount of wholly amorphous polymer produced and the isotacticity of the crystalline fraction (Table V). These observations are reasonable for a mechanism which envisions extensive reaction with the TiCl₃ surface.

TABLE V
Effect of Triethylaluminum Concentration on Polymer Yield and Tacticity^a

Et ₃ Al concn., $M \times 10^4$	Al/Ti	Polymer yield, g./mmole Ti	Ether solubles, %	$M \times 10^{-6b}$
2.60 ^c	0.175	3.02	6.1	17.2
2.96	0.218	4.96	4.7	—
2.96	0.212	5.26	6.1	17.0
4.42 ^d	0.400	8.88	7.0	13.6
4.42	0.332	9.00	5.9	15.5
7.00	0.511	13.0	13.2	—
12.3	1.05	16.5	16.6	—

^a *n*-Heptane, 40°C., 7.5 psig propylene pressure, 2.5 hr. polymerization.

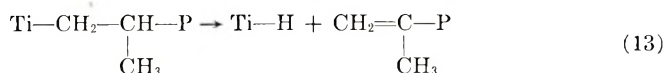
^b Refers to crystalline fraction only.

^c The infrared crystallinity of the ether-insoluble fraction was 85%.

^d The infrared crystallinity of the ether-insoluble fraction was 70%.

Termination

Several termination steps have been proposed in the literature. Natta¹² suggested that the principle chain-transfer mechanism is transfer to monomer. Saltman¹¹ argued for desorption of the growing chain from active sites and then readsorption on inactive sites. Pasquon¹³ has challenged this view. Bier¹⁴ suggested that the disproportionation reaction, eq. (13), was the major termination reaction. At lower temperatures



Bier reported that very little termination occurs. Since these workers probably prepared their catalysts in different ways, their results may not be directly comparable. Our data tend to be more in accord with those of Bier. Essentially no termination is observed at 40°C. Figure 4 is a plot of polymer molecular weight against polymer yield for a series of poly-

merizations carried out for varying lengths of time at 40°C., and 7.5 psig monomer pressure. The yield of polymer is, by definition, the product of the number of moles of polymer and its molecular weight. Thus, the linearity of the viscometric molecular weight, \bar{M}_v , with yield suggests that, in the region in which the relationship applies, the total number of polymer molecules remains constant. This assumes a constant \bar{M}_v/\bar{M}_n ratio where the \bar{M}_n is the number-average molecular weight. The simplest explanation of a constant number of polymer molecules which increase in molecular weight with time is that only one polymer molecule is formed per site, and

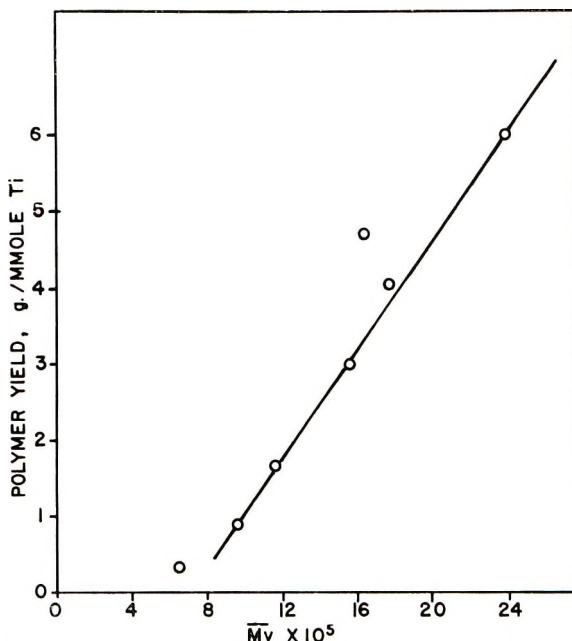


Fig. 4. Plot of \bar{M}_v vs. polymer yield for a series of polymerizations run under standard conditions for varying lengths of time.

it continues to propagate throughout the polymerization. If "living polymers" are indeed produced it should be possible to prepare block copolymers by the alternate introduction of two or more monomers. Bier¹⁵ has prepared this type of copolymer with his catalyst system. We have prepared block copolymers of ethylene and propylene which upon fractionation yielded no homopolymer fractions thus demonstrating that living polymers are produced with a catalyst system comprised of diethylaluminum chloride and TiCl_3 prepared from TiCl_4 by the stoichiometry given in eq. (6).

Since each site grows only one polymer molecule, the number of sites is equal to the number of molecules. This number is the slope of the line in the \bar{M}_v versus yield plot (Fig. 4) multiplied by the \bar{M}_v/\bar{M}_n ratio. If this ratio is assumed to be 2-5, then the percentage of active Ti atoms is cal-

culated to be between 0.7 and 1.8%. This is a reasonable order of magnitude based on the calculated surface area of the TiCl_3 particles.

Solvent Effects

A study was made of the influence of diethylaluminum chloride concentration in toluene, chlorobenzene, and *o*-dichlorobenzene. These solvents, together with *n*-heptane, range in dielectric constant from 1.9 to 9.3. The data for TiCl_3 prepared with excess aluminum alkyl [eq. (4)] are given in Table VI, and the data are plotted in Figure 5 according to the predictions of the Freundlich equation. From Figure 5 it is apparent that the polymer yield increased with aluminum alkyl concentration in each of the diluents studied. This variation is described by the Freundlich equation [eq. (3)]. The values of n and k'' are given in Table VII.

TABLE VI
Effect of Solvent on Polymerization Rate^a

Solvent	TiCl_3 , mmole	Et_2AlCl concn., mmole/l.	Polymer yield, g./mmole TiCl_3^b	Ether solubles, %
Toluene	6.22	9.7	4.97	1.3
"	9.80	21.7	4.04	1.7
"	6.60	24.4	5.35	2.4
"	6.10	28.3	6.85	1.8
"	6.22	40.2	5.90	4.1
"	6.5	54.7	6.63	4.7
"	6.00	69.0	6.55	5.2
Heptane	6.20	10.3	2.53	0.6
"	6.29	39.8	4.31	1.4
"	6.05	82.2	5.91	3.2
<i>o</i> -Dichlorobenzene	6.45	12.1	5.96	1.8
"	6.50	20.7	5.80	1.8
"	6.57	39.9	6.91	2.5
"	6.45	81.6	8.56	3.4
Chlorobenzene	6.61	12.7	5.05	1.4
"	6.46	21.3	5.61	1.7
"	6.48	40.2	6.77	2.1
"	6.62	81.2	8.07	2.4

^a 40°C., 7.5 psig propylene, 2.5 hr. polymerization, 1.5 l. of solvent.

^b Corrected to allow for the different solubilities of propylene in the various solvents.

TABLE VII
Solvent Properties

Solvent	Dielectric constant	n	k''
<i>n</i> -Heptane	1.9	0.41	2.5
Toluene	2.3	0.19	4.7
Chlorobenzene	5.4	0.27	4.6
<i>o</i> -Dichlorobenzene	9.3	0.28	4.8

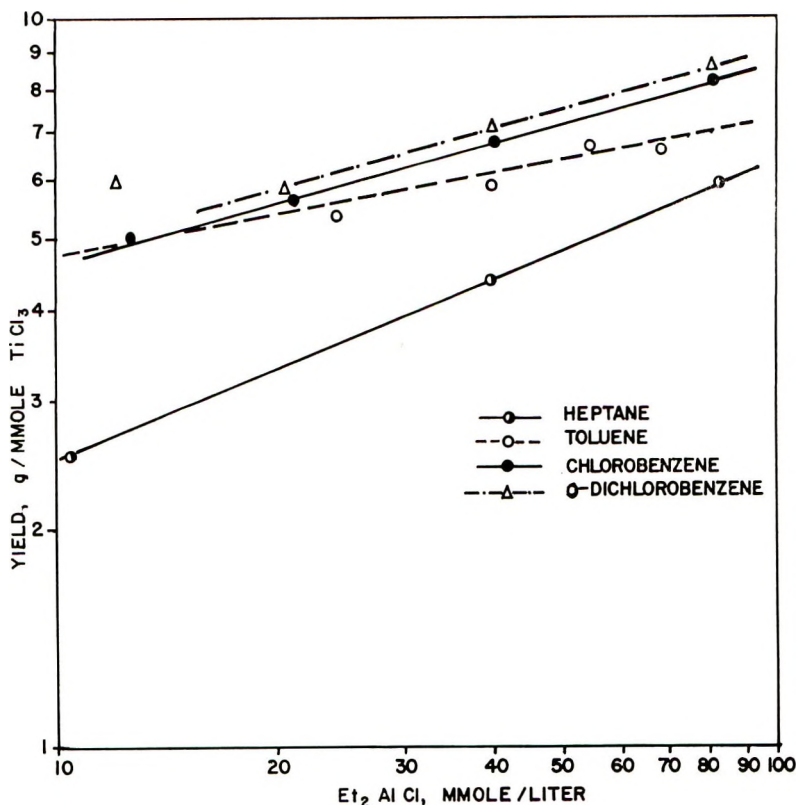


Fig. 5. Freundlich plot of \log (polymer yield) vs. $\log [Et_2AlCl]$ in various solvents. Yields are for 2.5-hr. polymerizations at $40^\circ C$. with 8 ± 0.3 mmole of $TiCl_3$.

The adsorbate, Et_2AlCl , is soluble in each of the solvents and competes with solvent for chemisorption onto sites on the $TiCl_3$ surface. In general, the value of n in the Freundlich equation is found to be less than unity, the precise value being a function of solvent. The second constant k is a measure of the number of active sites at unit Et_2AlCl concentration. The fact that all of the aromatic solvents exhibit the same k value regardless of their dielectric constant suggests that the $TiCl_3$ surface is contaminated by a displaceable impurity which is capable of distributing itself between the $TiCl_3$ surface and the solvent. A likely impurity for this sample of $TiCl_3$ is $i-BuAlCl_2$ or its thermal decomposition product $HAAlCl_2$, either being readily chemisorbed by $TiCl_3$ and favorably complexed by aromatic solvents. The aromatic solvents would, by favoring the desorption, expose more sites. Thus it seems likely that the rate increase produced by the aromatic solvents is due, not to their higher dielectric constants, but to their ability to cause desorption of poisons from the $TiCl_3$ surface. A large solvent effect would not be expected in any event for two reasons. First, the transition state probably involves only dipolar molecules rather than full charges. Second, the reaction is heterogeneous; therefore, solvation

of the transition state can only occur from one side. This reduces the total possible solvation energy.

TiCl₃ Concentration

Polymerization rates should be proportional to the number of polymerization sites. Thus, for a given sample of TiCl₃ the quantity of polymer produced per unit of TiCl₃ per unit time should be independent of the total concentration of TiCl₃. This is, in fact, observed at low concentrations of TiCl₃ (Table VIII, Fig. 6). At higher TiCl₃ concentrations, however, there is a decrease in polymer yield per unit of TiCl₃. This decrease is directly proportional to a decrease in the molecular weight of the polymer produced, thus indicating that some termination mechanism is becoming important. A very similar observation was made by Hoeg and Liebman.¹⁶ Similar results were also obtained in toluene both at constant Et₂AlCl concentration and at a constant Al/Ti ratio (Table IX).

In toluene as in heptane, the molecular weight decrease precisely correlated with the decrease in polymer yield. Figure 7, which is a plot of moles of polymer versus TiCl₃ concentration in toluene, demonstrates that the number of moles of polymer and the number of sites, is linear in TiCl₃.

TABLE VIII
Effect of TiCl₃ Concentration on Polymer Yield in *n*-Heptane^a

Et ₂ AlCl, mmole	TiCl ₃ , mmole	Yield, g.	Polymer yield, TiCl ₃ g./mmole	$\bar{M}_v \times 10^{-6}$
10.9	0.680	4.57	6.72	1.90
11.4	1.27	8.98	7.07	—
11.0	1.98	13.3	6.70	1.91
11.4	3.32	21.1	6.35	—
11.5	6.65	33.9	5.10	1.42

^a 40°C., 1.5 l. *n*-heptane, 7.5 psig C₃H₆, 2.5 hr. polymerization.

TABLE IX
Effect of TiCl₃ Concentration on Polymer Yield in Toluene^a

Et ₂ AlCl, mmole	TiCl ₃ , mmole	Yield, g.	Polymer yield, g./mmole TiCl ₃	$\bar{M}_v \times 10^{-6}$
1.25	0.95	9.45	9.95	2.19
1.96	1.95	20.45	10.50	2.04
4.56	3.96	39.0	9.85	2.19
8.46	8.18	64.7	7.92	1.62
8.38	0.99	10.8	10.9	2.46
8.30	1.96	20.46	10.46	2.04
8.47	4.16	43.8	10.5	2.46

^a 40°C., 1.5 l. toluene, 7.5 psig C₃H₆, 2.5 hr. polymerization.

The decrease in yield is directly proportional to the decrease in the molecular weight of the polymer.

At first appearance, it might be anticipated that if the TiCl_3 contains some chain-transfer agent, the quantity of this agent would be directly proportional to the amount of TiCl_3 used, and the molecular weight of the polymer should decrease linearly with increasing TiCl_3 . However, if the transfer agent distributes itself between the solvent and the TiCl_3 and then is slowly chemisorbed on active sites to poison them, a linear relationship would not necessarily be expected. Slow chemisorption usually follows

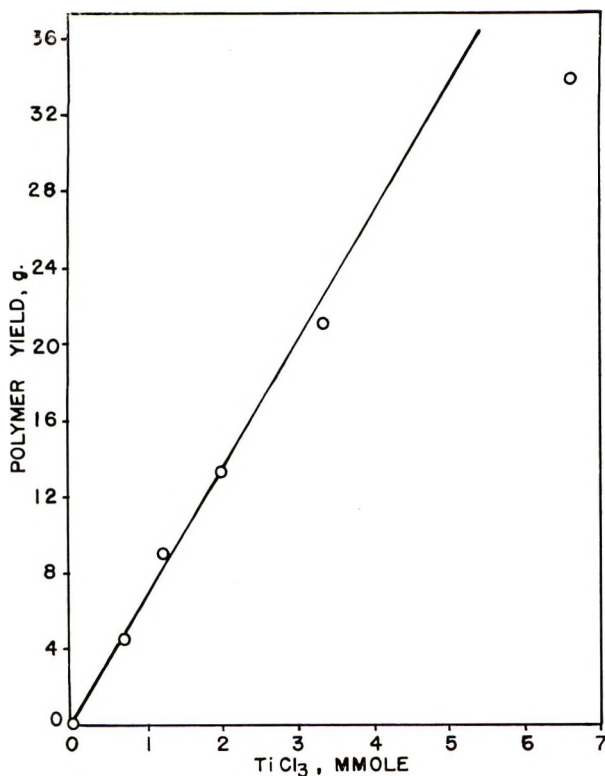


Fig. 6. Plot of polymer yield vs. TiCl_3 concentration in *n*-heptane.

Elovich kinetics¹⁷ in which the rate of chemisorption is not dependent in a simple manner on the concentration of the adsorbate. Also, as we have seen, the amount of chemisorption is not a simple function of adsorbate concentration even for fast chemisorption, but follows one or another of the chemisorption isotherms. Thus, the quantity of transfer agent might be linear in TiCl_3 , but the polymerization rate could fall off in a more complex manner. The data are unfortunately inadequate for fitting meaningfully to any of these equations, nor do they afford any basis for speculation as to the nature of the transfer agent.

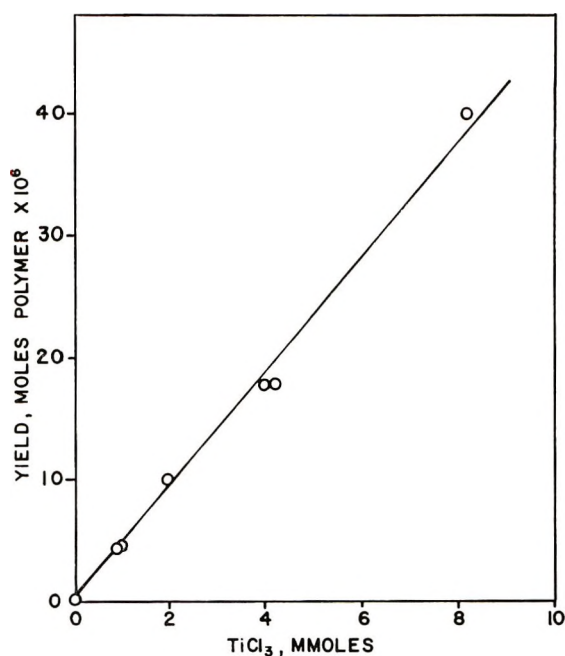


Fig. 7. Plot of polymer yield vs. TiCl_3 concentration in toluene.

Kinetic Order in Propylene

For the $\alpha/\gamma\text{-TiCl}_3\text{-Et}_2\text{AlCl}$ system there was observed an essentially linear increase in polymer yield with increasing propylene concentration (Table X). The polymerization is assumed to proceed by a two-step mechanism involving coordination of olefin with the transition metal site followed by insertion of the coordinated olefin between the transition metal

TABLE X
 TiCl_3 Prepared According to Eq. (6) (Heptane, 60°C.)

TiCl_3 , mmole	Et_2AlCl , mmole	Propylene, mole fraction	Polymer yield, g./mmole Ti/3 hr.
5.26	4.73	0.124	14.7
2.22	3.66	0.500	44.6
2.2	2.56	1.0	78.1

and the polymer chain. The coordination step would be expected to follow chemisorption kinetics. These seldom show any simple dependence on adsorbate concentration.¹⁷ If this step were rate-limiting, therefore, the polymerization rate would not be expected to be linear in propylene concentration. Thus the rate-limiting step would appear to be the insertion of coordinated propylene between the Ti atom and the polymer chain.

Activation Energy

Several polymerizations in liquid propylene at different temperatures yielded an activation energy of 12 kcal./mole. Considering the problems of accurately measuring rates in liquid propylene this value is in satisfactory agreement with Natta's value¹⁸ of 11–14 kcal./mole and Firsov's value¹⁹ of 13–14 kcal./mole.

EXPERIMENTAL

Materials

The *n*-heptane was Phillips Petroleum Company ASTM grade. Toluene, chlorobenzene, *o*-dichlorobenzene, and titanium tetrachloride were reagent-grade materials from Matheson, Coleman and Bell. High purity *n*-decane was obtained from the Humphrey-Wilkinson Company. All solvents were purged with N₂ before use until the effluent gas stream contained less than 10 ppm of water as measured by an electrolytic hygrometer. Aluminum alkyls were purchased from Ethyl Corporation and used without purification. The propylene used was Sinclair Refining Company 99.7% purity grade, and the N₂ used was Linde Company high purity grade. Both gases were passed through both an Ascarite column and a column packed with Linde 4A molecular sieves.

α/γ -TiCl₃

The preparation was carried out in a 1-liter creased resin kettle equipped with a gas inlet tube bearing a Teflon stopcock. The kettle was sealed to the head with a 4-in. Teflon envelope gasket. The head was fitted with a dropping funnel, jacketed coil condenser, and thermometer well. The agitator was mounted on a 1/2-in. stainless steel shaft and was fitted to the flask through a bushing designed to be blanketed with an inert gas. In a dry box 75.20 g. of TiCl₄ (0.396 mole) was added to about 500 g. of *n*-decane. The *n*-decane had been carefully fractionated, passed through alumina, and purged with N₂ before use. The solution was then transferred to the resin kettle by means of nitrogen pressure through stainless steel and polyethylene transfer lines. In a similar manner a solution of 39.51 g. of triisobutylaluminum (0.194 mole) in about 150 g. of decane was transferred to the dropping funnel. In both cases the flask and transfer lines were rinsed three times with 20-ml. portions of dry *n*-decane. The *i*-Bu₃Al solution was added dropwise over about 40 min. with constant agitation. The temperature rose during this period from 25 to 50°C. Stirring was continued at 50–55°C. for 20 min. after the addition was complete. The reaction mixture was then heated to reflux and refluxed for 90 min. After about 45 min. of this period the brown β -TiCl₃ was completely converted to the purple α/γ -TiCl₃. After cooling to room temperature, the TiCl₃ slurry was transferred under N₂ pressure to a tared flask. The weight of the slurry was 751 g. Assuming no loss of titanium compounds, the slurry

contained 0.397 mmole TiCl_3/g . In a wholly similar manner $\alpha/\gamma\text{-TiCl}_3$ was prepared at an $i\text{-Bu}_3\text{Al}/\text{TiCl}_4$ ratio of 0.35 and at a $\text{Et}_2\text{AlCl}/\text{TiCl}_4$ ratio of 0.60.

Polymerizations

Polymerizations were, for the most part, carried out in a modified 2-liter, heavy-walled, Erlenmeyer flask (Fig. 8). All pipe flange connections were made with Teflon envelope gaskets. Polyethylene tubing was used and was connected by means of Imperial compression fittings. The brass fittings were sealed to the glass polymerization vessel with epoxy resin. Solvent (1500 ml.) was placed in the flask and purged successively with dry N_2 and dry propylene until the effluent gas stream contained less than 10 ppm of water. The flask was allowed to come to temperature equilibrium in a water bath while maintaining the propylene purge. The requisite amount of aluminum alkyl was added through the serum stopper from a syringe which was weighed before and after the addition. A weighed amount of TiCl_3 was added in a similar manner. The propylene pressure,

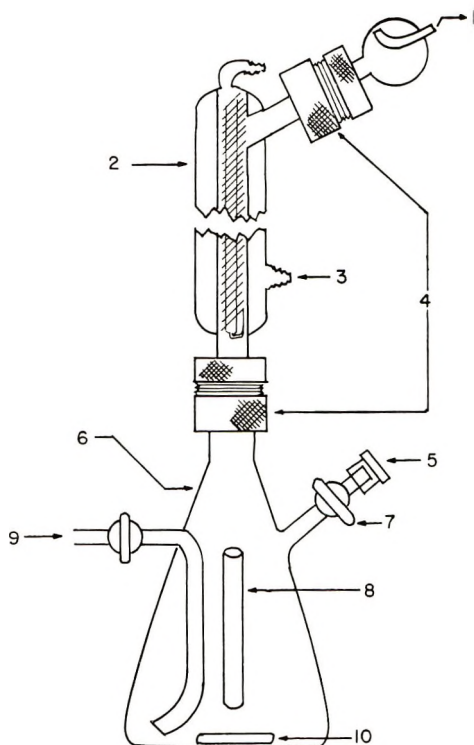


Fig. 8. Polymerization flask: (1) exit gas to pressure gage, throttling valve, and flow meter or water meter; (2) shell and coil condenser; (3) water; (4) threaded couplings for 1-in. Pyrex pipe flanges; (5) injection port; (6) modified 2-liter flask; (7) stopcocks, 6-mm. bore Teflon plug; (8) thermometer well, (9) gas inlet; (10) magnetic stirrer bar.

normally 7.5 psig, was maintained by adjusting inlet and outflow valves so that the pressure remained constant at a blowoff rate of 0.5–1 l./min. Agitation was by means of a magnetic stirrer. After 2.5 hr. the polymerization was stopped by the injection of 20 ml. of methanol through the serum stopper. The methanol reacted almost instantaneously to discharge the $TiCl_3$ color. The polymer slurry was then poured into a mixture of 750 ml. of methanol and 750 ml. of isopropanol. This served to precipitate all of the polymer which might have been in solution. The polymer was filtered and dried at 60°C. Catalyst residues were removed by refluxing the polymer with HCl in *n*-propanol.

Polymerizations in liquid propylene were carried out in a stainless steel autoclave by using essentially the same catalyst addition and polymer work-up procedures described above.

Extractions

Extractions with diethyl ether were carried out in a large vapor-jacketed Soxhlet extractor until no more weight loss was observed.

Molecular Weights

Molecular weights were computed from the reduced viscosities measured in decalin at 135°C. by using the relationships described by Kinsinger and Hughes.²⁰

References

1. G. Natta, P. Corradini, and G. Allegra, *J. Polymer Sci.*, **51**, 399 (1961).
2. W. L. Carrick, F. J. Karol, G. L. Karapinka, and J. J. Smith, *J. Am. Chem. Soc.*, **82**, 1502 (1960).
3. F. J. Karol and W. L. Carrick, *J. Am. Chem. Soc.*, **83**, 2654 (1961).
4. P. Cossee, *Trans. Faraday Soc.*, **58**, 1226 (1962).
5. J. P. Luongo, *Anal. Chem.*, **33**, 1816 (1961).
6. J. J. Kipping, *Quart. Rev.*, **5**, 60 (1951).
7. R. Fowler and E. A. Guggenheim, *Statistical Thermodynamics*, Cambridge Univ. Press, London, 1956, p. 427.
8. G. Natta, *J. Polymer Sci.*, **34**, 21 (1959).
9. E. Kohn, H. J. L. Schuurmans, J. V. Cavender, and R. A. Mendelson, *J. Polymer Sci.*, **58**, 681 (1961).
10. J. Ambróz, L. Ambróz, and K. Veselý, paper presented at Symposium on Macromolecules, Weisbaden, Germany, October, 1959, Sec. III A1.
11. W. M. Saltman, *J. Polymer Sci.*, **46**, 375 (1960).
12. G. Natta, I. Pasquon, and E. Giachetti, *Makromol. Chem.*, **24**, 258 (1957).
13. I. Pasquon, *J. Polymer Sci.*, **60**, S47 (1962).
14. G. Bier, *Kunststoffe*, **48**, 354 (1958).
15. G. Bier, G. Lehmann, and H. J. Leugering, *Makromol. Chem.*, **44–46**, 347 (1961).
16. D. F. Hoeg and S. Liebman, *Ind. Eng. Chem. Process Design Devel.*, **1**, 120 (1962).
17. M. J. D. Low, *Chem. Rev.*, **60**, 267 (1960).
18. G. Natta, I. Pasquon, E. Giachetti, and F. Selari, *Chim. Ind. (Milan)*, **40**, 103 (1958).
19. A. P. Firsov, V. I. Tsvetkova, and N. M. Chirkov, *Vysokomol. Soedin.*, **3**, 1161 (1961).
20. J. B. Kinsinger and R. E. Hughes, *J. Phys. Chem.*, **63**, 2002 (1959).

Résumé

Les effets de différents alcoylaluminiums à concentration différente sur la vitesse et la stéréospécificité de polymérisation de propylène en présence de trichlorure de titane ont été examinées. On a trouvé que les halogénures de dialcoylaluminium sont essentiellement chemisorbés sur la surface du trichlorure de titane tandis que les trialcoylaluminiums réagissent de façon plus importante avec la surface. Dans le cas du chlorure de diéthylaluminium, une cinétique de chemisorbtion typique a été observée. La vitesse de polymérisation est également fonction du solvant; en présence de certains solvants aromatiques une augmentation de vitesse significative a été observée. Avec le chlorure de diéthyl-aluminium on n'observe pratiquement pas de réaction de terminaison; les polymères sont considérés comme polymères vivants.

Zusammenfassung

Der Einfluss verschiedener Aluminiumalkyle bei variiertter Konzentration auf die Geschwindigkeit und Stereospezifität der Propylenpolymerisation mit Titantrichlorid wurde untersucht. Man kam zu dem Schluss, dass Dialkylaluminiumhalogenide an der Oberfläche von Titantrichlorid nur chemisorbiert wurden, während Trialkylaluminium eine weitergehende Reaktion mit der Oberfläche zeigte. Im Falle des Diäthylaluminiumchlorids wurde die Standardkinetik der Chemisorption beobachtet. Die Polymerisationsgeschwindigkeit erwies sich weiters als eine Funktion des Lösungsmittels, wobei gewisse aromatische Lösungsmittel eine signifikante Geschwindigkeitszunahme verursachen. Mit Diäthylaluminiumchlorid trat im wesentlichen keine Abbruchreaktion auf; die Polymeren sind "lebende Polymere."

Received December 2, 1965

Revised March 2, 1966

Prod. No. 5120A

Ionic Polymerization Under an Electric Field. III. Cationic Polymerizations of α -Methylstyrene and Styrene

ICHIRO SAKURADA, NORIO ISE, YOSHINOBU TANAKA, and
YUZURU HAYASHI, *Department of Polymer Chemistry, Kyoto University,
Kyoto, Japan*

Synopsis

Cationic polymerizations of α -methylstyrene and styrene were carried out in an electric field with iodine as a catalyst and ethylene dichloride as the solvent. The effects of the field on the rate of polymerization and the degree of polymerization were studied. It was found that the field increased the rate of polymerization of α -methylstyrene and, also slightly increased the degree of polymerization, whereas the field had no influence on these quantities in the case of styrene. The expressions for the rate of polymerization and the degree of polymerization, which were derived in a previous paper and refined in the present paper, show that these quantities are generally a function of the degree of dissociation of ion pairs at growing chain ends. For a comparatively large degree of dissociation, these expressions can account for the field effect as was observed on α -methylstyrene, if one assumes that the degree of dissociation in the presence of an electric field is larger than that in its absence, and that the free-ion propagation proceeds much faster than the ion-pair propagation. For a small degree of dissociation, however, these expressions become practically independent of the degree of dissociation so that a possible increase due to the presence of an electric field gives rise to no observable effect on the polymerization. This situation may be interpreted as corresponding to the case of styrene. In other words, the polymerization of α -methylstyrene has more free ionic character than that of styrene.

INTRODUCTION

In order to elucidate the polymerization mechanism, we have carried out various polymerizations under an electric field; the effects of the electric field on the rate of polymerization and on the degree of polymerization of polymers produced have been studied. For the catalytic cationic polymerization of *p*-methoxystyrene¹ and radiation-induced cationic polymerization of styrene,² the field has been found definitely to increase the rates of polymerization and the degrees of polymerization, whereas the field has not affected the radical polymerizations of styrene and methyl methacrylate.¹ In the present paper, the experimental data of polymerizations under an electric field of α -methylstyrene and styrene with iodine as a catalyst and ethylene dichloride as the solvent will be reported. According to the existing data,^{3,4} the polymerizations in these systems are believed to proceed by a cationic mechanism.

EXPERIMENTAL

Materials

α -Methylstyrene, a gift of the Kurashiki Rayon Company, Kurashiki, Japan, was distilled under reduced pressure in a nitrogen atmosphere after drying over Drierite for 20 hr. Styrene and ethylbenzene were purified by the usual methods. The purification of ethylene dichloride was described in the previous paper.¹ Special attention was paid to purification of these materials. The water level was always below 2 mmole/l. The quantity of ionic impurities was monitored by electric conductivity, which was determined from applied field strength (1 kv./cm.) and current strength (measured with an ammeter reading 25 μ a. for full-scale deflection). When the specific conductivity of ethylene dichloride was larger than 10^{-11} mho/cm., solvent was not used for the polymerizations. The conductivity of the monomers was too small to measure, and that of the monomer-solvent mixture was much smaller than that of the pure solvent. Our experience shows that the use of the "impure" materials gave irreproducible results and often a very low rate of polymerization.

Apparatus and Procedures

α -Methylstyrene. The polymerizations of α -methylstyrene were carried out in a glass vessel with platinum parallel plate electrodes (area about 11 cm.², about 1 cm. apart, with a cell constant of 0.083 cm.⁻¹) unless otherwise specified. Immediately after adding the monomer to an iodine solution of ethylene dichloride (catalyst solution), a high (d.c.) voltage was applied to the solution. After a definite time, the solution was poured into a large quantity of methanol; the precipitated polymer was washed with methanol, dried at 70°C., and weighed.

Polymerizations in the absence of electric field were carried out in the same way as in the presence of the field. All polymerizations were performed at -20°C. unless otherwise specified.

The average molecular weight of the polymer produced was determined by viscosity measurement in benzene at 30°C. by using the equation,

$$[\eta] = 0.0150 + 1.787 \times 10^{-5}M$$

which was obtained from cryoscopic measurements on unfractionated polymer samples by Worsfold and Bywater.⁵ Here $[\eta]$ is in units of deciliters per gram.

Styrene. The apparatus used and experimental procedures were the same as described previously.¹ Polymerizations of styrene initiated with iodine were carried out at 30°C. unless otherwise specified.

The average molecular weight of the polymer was determined by viscosity measurement in toluene at 30°C. by using the equation,⁶

$$[\eta] = 1.2 \times 10^{-4} \bar{M}_n^{0.70}$$

where \bar{M}_n is the number-average molecular weight.

RESULTS

 α -Methylstyrene

Time-Conversion Curve. Figure 1 shows the time-conversion curves at different catalyst concentrations obtained in the presence ($E = 1$ kv./cm.) and in the absence of an electric field. It is seen that the application of the electric field accelerates the polymerization. From the initial tangent of the curve, the initial rate of polymerization R_p was determined.

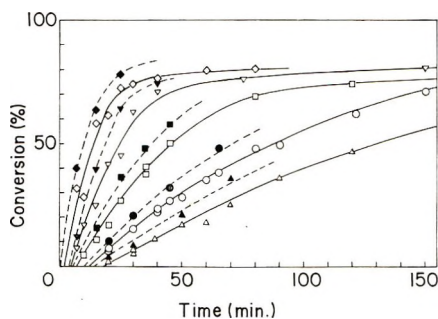


Fig. 1. Time-conversion curves of α -methylstyrene at -20°C ., $[M]_0 = 0.80$ mole/l. and varying $[I_2]_0$: (Δ, \blacktriangle) 1.5×10^{-3} mole/l.; (\circ, \bullet) 2.0×10^{-3} mole/l.; (\square, \blacksquare) 2.5×10^{-3} mole/l.; ($\nabla, \blacktriangledown$) 3.0×10^{-3} mole/l.; (\square, \blacklozenge) 4.0×10^{-3} mole/l. ($\Delta, \circ, \square, \nabla, \square$) $E = 0$; ($\blacktriangle, \bullet, \blacksquare, \blacktriangledown, \blacklozenge$) $E = 1.0$ kv./cm.

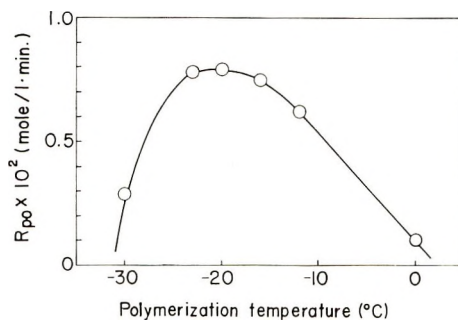


Fig. 2. Rate of polymerization of α -methylstyrene and polymerization temperature; $[M]_0 = 0.80$ mole/l., $[I_2]_0 = 2.0 \times 10^{-3}$ mole/l.

Initial Rate of Polymerization and Polymerization Temperature. In order to rule out the possibility that the observed acceleration of the polymerization is due to an increase in temperature of the polymerizing solution by Joule heat, the temperature dependence of the initial rate of polymerization in absence of electric field R_{p0} was measured. The results are given in Figure 2. It is seen that below -20°C . the initial rate of polymerization R_{p0} increases with increasing temperature, whereas above -20°C . R_{p0} decreases. This means that the apparent overall activation energy is positive below -20°C . and negative above this temperature. Thus we

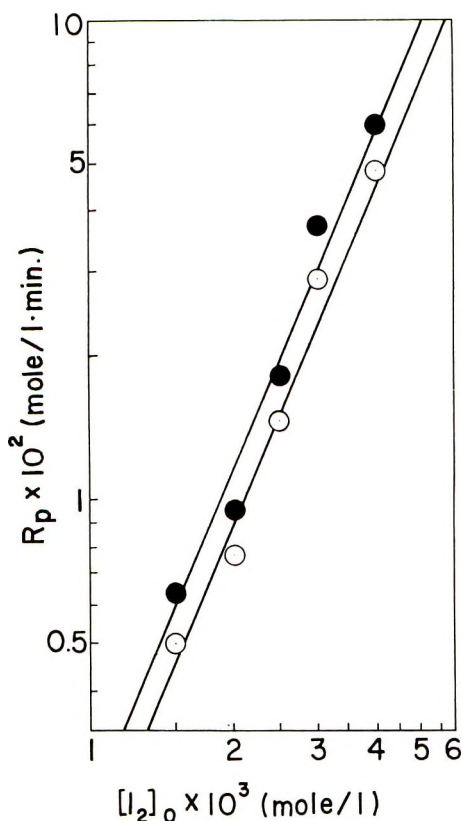


Fig. 3. Dependence of the initial rate of polymerization of α -methylstyrene on the catalyst concentration at $[M]_0 = 0.80$ mole/l.: (●) $E = 1.0$ kv./cm.; (○) $E = 0$.

may conclude that the Joule heat is not a factor in enhancement of the polymerization above -20°C .

Moreover the observed temperature rise by electrical heat was 2°C . at most. Therefore no temperature correction of the rate of polymerization was carried out unless otherwise described.

Dependence of Initial Rate of Polymerization on Initial Concentrations of Catalyst and α -Methylstyrene. The log-log plots of initial rate of polymerization R_p against initial concentrations of iodine $[I_2]_0$ and α -methylstyrene $[M]_0$ are shown in Figures 3 and 4, respectively. The results at $E = 1$ kv./cm. and $E = 0$ can be expressed as

$$R_{p0} = 4.2 \times 10^6 [M]_0^2 [I_2]_0^{2.4} \quad (1)$$

and

$$R_{pE} = 5.2 \times 10^6 [M]_0^2 [I_2]_0^{2.4} \quad (2)$$

where R_{p0} and R_{pE} are the initial rate of polymerization in the absence and the presence of electric field, respectively (in mole/liter-minute, the unit

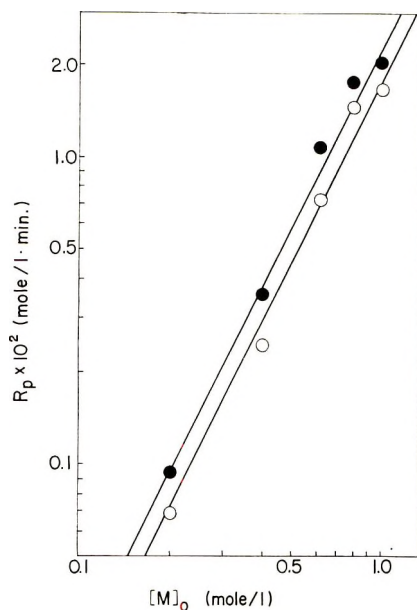


Fig. 4. Dependence of the initial rate of polymerization on α -methylstyrene concentration at $[I_2]_0 = 2.5 \times 10^{-3}$ mole/l.: (●) $E = 1.0$ kv./cm.; (○) $E = 0$.

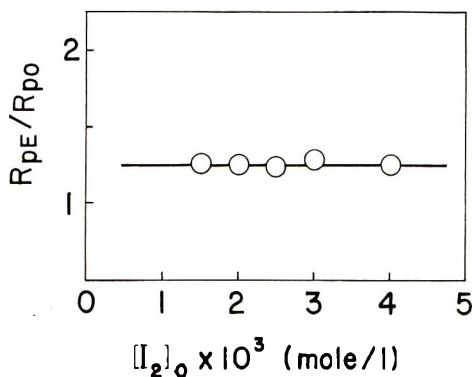


Fig. 5. Field effect on the rate of polymerization of α -methylstyrene and catalyst concentration at $[M]_0 = 0.80$ mole/l.

of $[M]_0$ and $[I_2]_0$ being mole/liter). It is seen that the electric field increased the rate constant, leaving the exponents unchanged.

Effect of Electric Field on Initial Rate of Polymerization, and Effect of Initial Concentrations of Catalyst and Monomer. The ratio R_{pE}/R_{p0} representing the relative effect of electric field on the initial rate of polymerization is plotted against concentrations of iodine and α -methylstyrene in Figures 5 and 6, respectively. The effect of electric field appears to be independent of the initial concentrations of iodine and α -methylstyrene. A similar independence has already been found in the polymerization of

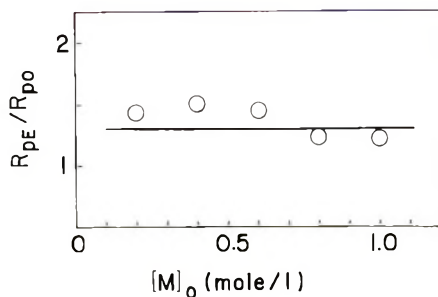


Fig. 6. Field effect on the rate of polymerization of α -methylstyrene and monomer concentration at $[I_2]_0 = 2.5 \times 10^{-3}$ mole/l.

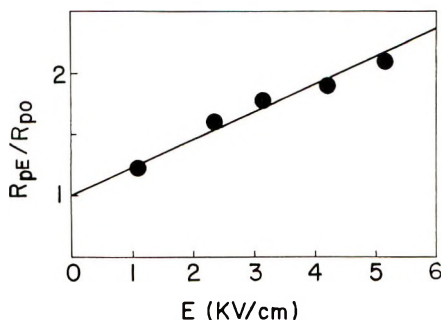


Fig. 7. Field effect on the rate of polymerization of α -methylstyrene and field strength at $[M]_0 = 0.80$ mole/l., $[I_2]_0 = 2.0 \times 10^{-3}$ mole/l.

p-methoxystyrene with iodine¹ and the radiation-induced polymerization of styrene.²

Field Strength and Effect of Electric Field on Initial Rate of Polymerization.* The R_{pE}/R_{p0} values plotted against field strength are shown in Figure 7. The filled circles indicate R_{pE}/R_{p0} values corrected for the temperature rise, which is not negligible at higher electric fields.† The R_{pE}/R_{p0} values increase linearly with field strength. This linearity was also found in the polymerizations of *p*-methoxystyrene with iodine¹ and of styrene by γ -irradiation.²

Degree of Polymerization. The reproducibility of the degree of polymerization was satisfactory when for a series of experiments materials purified at one time are used. The degree of polymerization \bar{P} thus found was constant with polymerization time below a conversion of 15%. The \bar{P} value given in this paper is this constant value. Figure 8 shows the dependence of the degree of polymerization on initial concentration of catalyst ($[I_2]_0$).

* In this series of experiments a reaction vessel with platinum parallel-plate electrodes (area about 2 cm.², about 3.7 cm. apart, cell constant 1.0 cm.⁻¹) was used, in order to obtain high field strengths with our d.c. generator which had a rather low output.

† The correction was carried out on the basis of the activation energy data obtained from the data shown in Figure 2 for an average temperature rise, which was determined graphically from the observed temperature-time diagram.

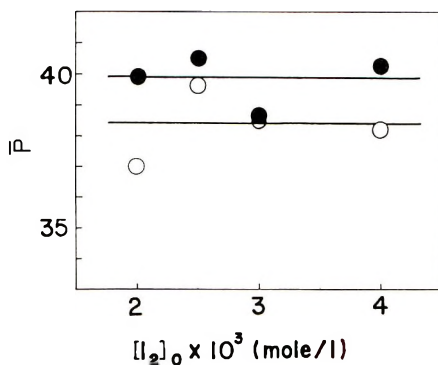


Fig. 8. Degree of polymerization of α -methylstyrene and catalyst concentration at $[M]_0 = 0.80$ mole/l.: (●) $E = 1.0$ kv./cm.; (○) $E = 0$.

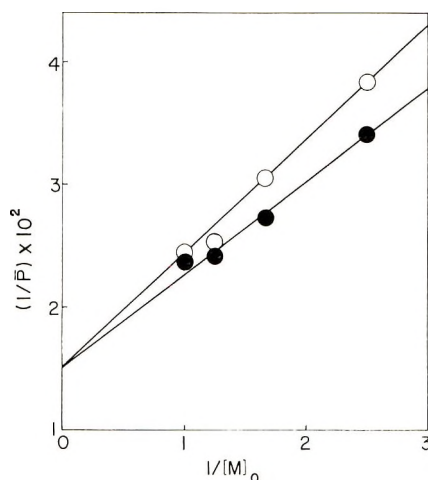


Fig. 9. Variation of degree of polymerization of α -methylstyrene with monomer concentration at $[I_2]_0 = 2.5 \times 10^{-3}$ mole/l.; (●) $E = 1.0$ kv./cm.; (○) $E = 0$.

\bar{P} values may be slightly increased by the electric field. Furthermore it may be seen that \bar{P} is likely to be independent of $[I_2]_0$. The degree of polymerization at different monomer concentrations is shown in Figure 9. The presence of an electric field (1.0 kv./cm.) also increases slightly the degree of polymerization, and $1/\bar{P}$ changes linearly with $1/[M]_0$. Therefore we have,

$$1/\bar{P} = a + b(1/[M]_0) \quad (3)$$

where $a_0 = 1.5 \times 10^{-2}$, $b_0 = 0.9_3 \times 10^{-2}$ mole/l., for $E = 0$; and $a_E = 1.5 \times 10^{-2}$, $b_E = 0.7_5 \times 10^{-2}$ mole/l., for $E = 1$ kv./cm.

Quantity of Electricity. The current strength passing through the polymerization system was measured with an ammeter reading $500 \mu\text{a.}$ for full-scale deflection. The quantity of electricity passed was obtained by a

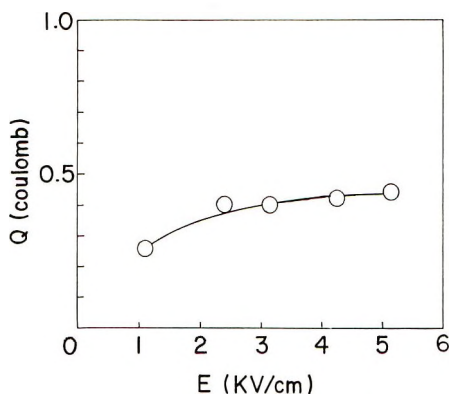


Fig. 10. Quantity of electricity (Q) and field strength (E) in the polymerization of α -methylstyrene.

graphical integration of current strength from 2 min. to 37 min. of polymerization time. Figure 10 shows that the quantity of electricity increases rather slowly with increasing field strength.

Infrared Analysis. The infrared spectra of polymers produced with and without an electric field were compared. No structural difference between these two was observed.

Styrene

Initial Rate of Polymerization and Initial Concentrations of Catalyst and Styrene. The initial rate of polymerization was determined from the initial slope of the time-conversion curve. Figure 11 shows log-log plots of R_p against the initial concentration of iodine ($[I_2]_0$) in the absence and the presence of an electric field (0.5 kv./cm.). This figure indicates that the electric field has no effect on R_p . The slope of the plots is nearly equal to 3. Figure 12 shows the log-log plots of R_p against the initial concentration of styrene ($[M]_0$) in the absence and the presence of an electric field (0.5 kv./cm.). These data also indicate no field effect. The slope of the plots is equal to 2. These results can be expressed by:

$$R_{p_E} = R_{p_0} \propto [M]_0^2 [I_2]_0^3 \quad (4)$$

Earlier Kanoh et al.⁴ reported the following relation for the present system:

$$R_{p_0} \propto [M]_0 [I_2]_0^3 \quad (5)$$

which is in disagreement with our results. In this respect, it should be mentioned that in our experiments, the dielectric constant was maintained constant in spite of varying styrene composition by the addition of ethylbenzene to the solution as a substitute for styrene. Since eq. (5) was derived from the data obtained in ethylene dichloride (without the adjustment of the dielectric constant), the discrepancy in the order with

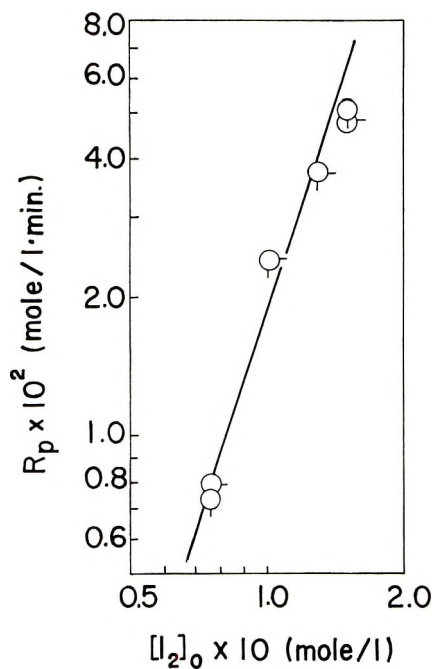


Fig. 11. Dependence of the initial rate of polymerization of styrene on catalyst concentration at $[M]_0 = 0.87$ mole/l.: (\circ) $E = 0.5$ kv./cm.; (\square) $E = 0$.

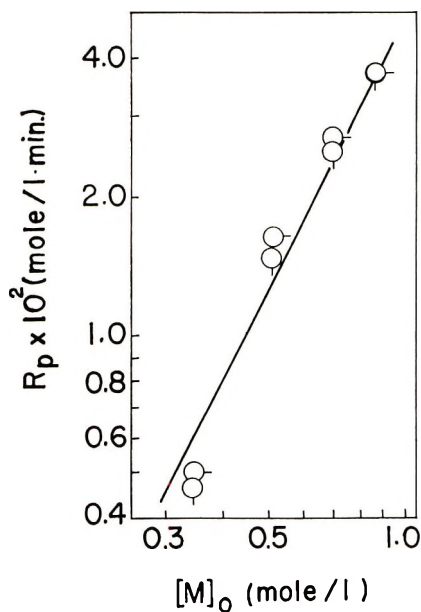


Fig. 12. Dependence of the initial rate of polymerization of styrene on monomer concentration at styrene + ethylbenzene = 10 vol.-%, $[I_2]_0 = 1.30 \times 10^{-1}$ mole/l.: (\circ) $E = 0.5$ kv./cm.; (\square) $E = 0$.

respect to $[M]_0$ is probably due to the effect of changing dielectric constant of polymerizing solution.

Degree of Polymerization. The degree of polymerization is plotted against initial concentrations of iodine and styrene in Figures 13 and 14. Figure 13 shows that the field has no effect on \bar{P} and that the degree of polymerization is likely to decrease with increasing $[I_2]_0$. Figure 14, also indicating no field effect, shows that the plot of $1/\bar{P}$ against $1/[M]_0$ is linear. The present system therefore also follows eq. (3). Under our experimental conditions, the value of a was $0.3_8 \times 10^{-2}$, and b was $0.3_5 \times 10^{-2}$ mole/l., irrespective of the electric field.

Field Strength and the Field Effect. The polymerization experiments were carried out at higher field strengths, up to 1.8 kv./cm. However, no field effects have been observed on the rate of polymerization and the degree of polymerization when the effect of Joule heat has been taken into consideration.

Infrared Analysis. The infrared spectra of polymers produced were taken. No difference was observed between the polymers obtained in the absence and the presence of electric fields.

DISCUSSION

In the foregoing sections, the high electric field was shown to accelerate the rate of polymerization of α -methylstyrene and increase the degree of polymerization of the polymers produced, though slightly, whereas it was demonstrated that the field had no effect on these quantities in the case of styrene. These experimental results on α -methylstyrene are in qualitative agreement with those previously found for *p*-methoxystyrene.¹

As was mentioned above, the possibility that the Joule heat is a factor responsible for the observed field effect could be definitely denied. Another possibility, that the observed effect is due to the so-called electroinitiated polymerization,⁷ can be ruled out more definitely than in the previous

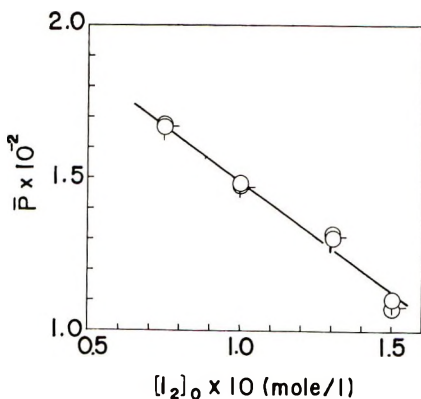


Fig. 13. Variation of degree of polymerization of styrene with catalyst concentration at $[M]_0 = 0.87$ mole/l.: (O) $E = 0.5$ kv./cm.; (□) $E = 0$.

paper,¹ as follows. If a polymerization of this sort intervenes, we may expect that the effect should increase with the quantity of electricity passing through polymerizing systems. According to Figure 10, the quantity of electricity is insensitive towards field strength above 2 kv./cm.* Nonetheless, the effect of electric field on the rate of polymerization of α -methylstyrene increases with increasing field strength as was shown in Figure 7. Thus, it can be concluded that the effect of electric field is not due to the so-called electroinitiated polymerization.

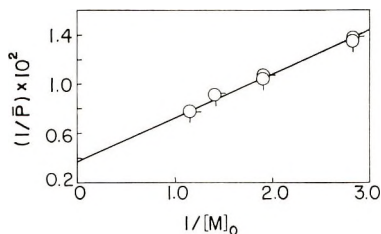


Fig. 14. Variation of degree of polymerization of styrene with monomer concentration at styrene + ethylbenzene = 10 vol.-%, $[I_2]_0 = 1.30 \times 10^{-1}$ mole/l.: (○) $E = 0.5$ kv./cm.; (◻) $E = 0$.

Thus we are again led to the consideration of the Wien effect, which was discussed in the previous paper.¹ We assume that the initiation reaction in our systems is composed of two steps: the first is the addition of catalyst to monomer M to form an ion pair M_1^\pm ,



and the second the dissociation of the ion pair into a free carbonium ion M_1^+ (where the subscript 1 denotes that the ion is monomeric) and a free anion† I^- to set up the equilibrium,



* This fact means that the current strength does not increase with increasing field strength, that is, the apparent specific resistance of the solution increases with increasing field strength. For this phenomenon we may immediately give two explanations: deposition of the polymer produced on the electrodes and removal of ionic species in the solution due to electrolysis by the electric field. Both explanations, however, are unreasonable in the light of the following facts. The same phenomenon was also found in applying the electric field to pure ethylene dichloride (containing no polymer). Moreover, in the case of the polymerizing systems, the current strength slightly increased with polymerization time, though the current strength ought to decrease as the polymerization proceeds, since the deposition of the polymer on the electrodes increases the resistance. Removal of ionic species by applying electric field is no explanation for the phenomenon either, because the current strength did not decrease with time in the polymerizing system in ethylene dichloride and in ethylene dichloride-iodine solution. Thus the reason for this observed independence of the quantity of electricity towards the field strength is not clear. Whatever the reason may be, the electroinitiated polymerization can be ruled out.

† The free anion I^- involves I^- , I_3^- , I_5^- , etc.

where K is an equilibrium constant; we thus have

$$K = [M^+][I^-]/[M^\pm] \quad (8)$$

where M^+ and M^\pm are free ion and ion pair of any chain length, respectively and the brackets denote concentrations. We assume that this equilibrium can be established instantaneously after M^\pm is formed. Then the initiation can be treated as the addition of the catalyst to a monomer to form not only an ion pair but also a free ion as growing chain end.

Formally, we may write with a single rate constant of initiation k_i as follows:

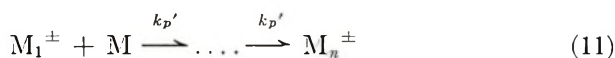


where M_1^* represents both free-ion end M_1^+ and ion-pair end M_1^\pm , and the concentrations of M^* , M^+ , and M^\pm (without suffix) are related by eq. (10):

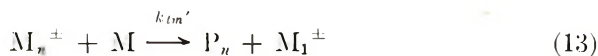
$$[M^*] = [M^+] + [M^\pm] \quad (10)$$

We further assume that propagation, transfer to monomer, and termination proceed through free-ion and ion-pair mechanisms at the same time, and that there also exists an equilibrium between growing chain ends of free-ion type and ion-pair type, which can also be characterized by K defined by eq. (8). Then we have:

Propagation:



Monomer transfer:



Termination:



Here k' and k'' are rate constants of the reactions of ion pairs and of free ions, respectively. The subscripts of k' and k'' , such as p , t_m , t , denote propagation, transfer to monomer, and termination, respectively, and P_n designates the polymer molecule produced.

The rates of elementary reactions may then be written in terms of the concentration of species involved and the rate constants, as follows. The rate of initiation is

$$R_i = k_i[I_2]^n[M] \quad (17)$$

The rates of propagation and transfer are

$$\begin{aligned} R_p &= k_p''[M^+][M] + k_p'[M^\pm][M] \\ &= \alpha k_p''[M^*][M] + (1 - \alpha)k_p'[M^*][M] \end{aligned} \quad (18)$$

and

$$\begin{aligned} R_{tm} &= k_{tm}''[M^+][M] + k_{tm}'[M^\pm][M] \\ &= \alpha k_{tm}''[M^*][M] + (1 - \alpha)k_{tm}'[M^*][M] \end{aligned} \quad (19)$$

respectively, where α is the degree of dissociation of ion pairs into free ions, that is,

$$\alpha = [M^+]/([M^+] + [M^\pm]) = [M^+]/[M^*] \quad (20)$$

The rate of termination is

$$\begin{aligned} R_t &= k_t''[M^+][I^-] + k_t'[M^\pm] \\ &= \alpha^2 k_t''[M^*]^2 + (1 - \alpha)k_t'[M^*] \\ &= (1 - \alpha)Kk_t''[M^*] + (1 - \alpha)k_t'[M^*] \end{aligned} \quad (21)$$

Now in the steady-state condition $R_i = R_t$, eqs. (17) and (21) may then be equated to solve for $[M^*]$. Then we have

$$[M^*] = [I/(1 - \alpha)][k_i/(Kk_t'' + k_t')] [I_2]^n [M] \quad (22)$$

Substitution of $[M^*]$ from eq. (22) into eq. (18) gives

$$R_p = \frac{k_i}{Kk_t'' + k_t'} \left[\left(\frac{\alpha}{1 - \alpha} \right) k_p'' + k_p' \right] [I_2]^n [M]^2 \quad (23)$$

For α -methylstyrene, the degree of dissociation α may be considered to be almost constant against concentration of iodine in the rather limited range of low concentrations studied, i.e., 1.5–4.0 mmole/l. Equation (23) with $n = 2.4$ is thus in agreement with our experimental results, since the rate constants and equilibrium constant are independent of iodine concentration. For styrene, on the other hand, α is probably dependent on iodine concentration, since a range of high concentrations of iodine was used, i.e., 75–150 mmole/l. Then it might be possible that $\{[\alpha/(1 - \alpha)]k_p'' + k_p'\} [I_2]^n$ on the right-hand side of eq. (23) is proportional to $[I_2]^3$, in agreement with our experimental results.

Furthermore, eq. (23) gives

$$\frac{R_{pE}}{R_m} = \frac{(K_0k_t'' + k_t')\{[\alpha_E/(1 - \alpha_E)]k_p'' + k_p'\}}{(K_Ek_t'' + k_t')\{[\alpha_0/(1 - \alpha_0)]k_p'' + k_p'\}} \quad (24)$$

From eqs. (18), (19), and (21) we obtain for the inverse degree of polymerization

$$\frac{1}{\bar{P}} = \frac{[\alpha/(1 - \alpha)]k_{tm}'' + k_{tm}'}{[\alpha/(1 - \alpha)]k_p'' + k_p'} + \frac{Kk_t'' + k_t'}{[\alpha/(1 - \alpha)]k_p'' + k_p'} \left(\frac{1}{[M]} \right) \quad (25)$$

It is interesting to point out that the observed field effect on the polymerizations of α -methylstyrene can be accounted for by eqs. (24) and (25), by assuming that the degree of dissociation increases with increasing field strength, i.e., $\alpha_E > \alpha_0$, that Kk_t'' is much smaller than k_t' , and that k_p'' is much larger than k_p' . The first assumption may be substantiated by the Wien effect that the dissociation of the ion pair becomes large with increasing high field strength.⁸ The second assumption appears to be reasonable, since the degree of dissociation, and hence K , would be small and k_t'' would probably not be larger than k_t' ; in other words, the termination reaction of the ion pair may more easily take place than that of free ion. Thus eq. (24) can be simplified to

$$\frac{R_{pE}}{R_{p_0}} = \frac{[\alpha_E/(1 - \alpha_E)]k_p'' + k_p'}{[\alpha_0/(1 - \alpha_0)]k_p'' + k_p'} \quad (24')$$

The third assumption has been verified independently by Hostalka et al.⁹ and Smid and Szwarc.¹⁰ From these three assumptions, we have for comparatively large α

$$R_{pE}/R_{p_0} > 1 \quad (26)$$

which is in agreement with the experimental fact on α -methylstyrene. For extremely small α , we obtain

$$[\alpha/(1 - \alpha)]k_p'' + k_p' \approx \alpha k_p'' + k_p' \approx k_p' \quad (27)$$

in spite of the inequality, $k_p'' \gg k_p'$. Equation (27) leads us to

$$R_{pE}/R_{p_0} = 1 \quad (28)$$

which agrees with the above-mentioned experimental data for styrene.

Equation (25) accounts for the field effect on the degree of polymerization. Since the rate constants and the equilibrium constant appearing on the right-hand side of eq. (25) are independent of the monomer concentration, eq. (25) tells us that $1/\bar{P}$ is a linear function of $1/[M]$, as was found experimentally at low conversions for α -methylstyrene and styrene, if α is taken to be practically constant with changing monomer concentration.

It was mentioned above that the α value depends on catalyst concentration in the case of styrene whereas this is not the case for α -methylstyrene. Equation (25) then suggests that $1/\bar{P}$ is independent of catalyst concentration in the case of α -methylstyrene, as was found experimentally, whereas it varies with catalyst concentration in the case of styrene. Since the information pertaining to the magnitudes of rate constants in eq. (25) is not available, no further meaningful discussion on styrene can be given at present.

Comparison of eq. (3) with eqs. (24) and (25) gives

$$R_{pE}/R_{p_0} = b_0/b_E \quad (29)$$

Equation (29) gives a correlation between field effects on the rate of polymerization and on the degree of polymerization. The experimental

results for α -methylstyrene shown in Figure 5 give $R_{p_E}/R_{p_0} = 1.2_5$, whereas those on the degree of polymerization shown in Figure 9 give $b_0/b_E = 1.2_4$. Therefore eq. (29) is satisfied and is consistent with the experimental results.

In the preceding explanation, it has been assumed that the degree of dissociation, and hence the equilibrium constant was affected by the application of the electric field: no effect on the various elementary rate constants, such as rate constant of initiation, was assumed. In this respect, it is important to mention the consistency of our treatment. From eqs. (3) and (25), we obtain

$$b = \frac{Kk_i'' + k_i'}{[\alpha/(1 - \alpha)]k_p'' + k_p'} \quad (30)$$

and then, from eqs. (23) and (30), we have

$$R_p = (k_i/b)[I_2]^n[M]^2 \quad (31)$$

On substituting experimental values for R_p , $[I_2]$, $[M]$, n , and b , we obtain for α -methylstyrene $k_i = 3.9 \times 10^4$ (mole^{-2.4}l.^{2.4} min.⁻¹) at $E = 1$ kv./cm.; $k_i = 3.9 \times 10^4$ (mole^{-2.4}l.^{2.4} min.⁻¹) at $E = 0$. The value of k_i thus found is independent of the electric field. In other words, our assumption, that electric field has no effect on an initiation reaction, is consistent with our kinetic treatment mentioned above.

The field effects upon some vinyl monomers are compared in Table I.

TABLE I
Comparison of Field Effects of Some Vinyl Monomers

Monomer	R_{p_E}/R_{p_0}	\bar{P}_E/\bar{P}_0	Relative reactivity ^a
Styrene	1.0 ₀	1.0 ₀	1
α -Methylstyrene ^b	1.2 ₅	1.0 ₅	5-8
Isobutyl vinyl ether ^c	1.2 ₈	1.0 ₄	40-60
<i>p</i> -Methoxystyrene	1.3 ₄	1.7 ₅	10-100

^a Data of Pepper.¹¹

^b Polymerizations of this monomer were performed at -20°C ., while polymerizations of other monomers at 30°C .

^c Data of Sakurada et al.¹²

R_{p_E}/R_{p_0} and \bar{P}_E/\bar{P}_0 in this table were obtained by extrapolation of the observed ratios to $[I_2]_0 = 1.0 \times 10^{-5}$ mole/l., $[M]_0 = 0.8$ mole/l., and $E = 1.0$ kv./cm. Table I also gives the reactivity of some monomers towards carbonium ions, relative to that of styrene, presented by Pepper.¹¹ Interestingly enough, there seems to exist a parallel between the field effect and the reactivity.

This situation may be understood if one recalls that the field effects become large as the degree of dissociation of ion-pair ends increases, and

that the high degree of dissociation gives rise to a larger polymerization rate, or reactivity.

One of us (N. I.) gratefully acknowledges the useful discussion received from Professors S. Okamura, T. Higashimura, and F. Williams.

References

1. I. Sakurada, N. Ise, and T. Ashida, *Makromol. Chem.*, **82**, 284 (1965); **95**, 1 (1966).
2. I. Sakurada, N. Ise, and S. Kawabata, *Makromol. Chem.*, in press.
3. K. Hirota, G. Meshitsuka, F. Takemura, and T. Tanaka, *Nippon Kagaku Zasshi*, **82**, 1103 (1961).
4. N. Kanoh, T. Higashimura, and S. Okamura, *Makromol. Chem.*, **56**, 65 (1962).
5. D. J. Worsfold and S. Bywater, *J. Am. Chem. Soc.*, **79**, 4917 (1957).
6. T. Alfrey, A. Bartovics, and H. Mark, *J. Am. Chem. Soc.*, **65**, 2319 (1943).
7. B. L. Funt and S. N. Bhadani, *Can. J. Chem.*, **42**, 2733 (1964).
8. L. Onsager, *J. Chem. Phys.*, **2**, 599 (1934).
9. H. Hostalka, R. V. Figini, and G. V. Schulz, *Makromol. Chem.*, **71**, 198 (1964).
10. J. Smid and M. Szwarc, *Polymer*, **5**, 54 (1964).
11. D. C. Pepper, *Quart. Rev.*, **8**, 88 (1954).
12. I. Sakurada, N. Ise, and S. Hori, to be published.

Résumé

Les polymérisations cationiques de l' α -méthylstyrène et du styrène ont été effectuées en présence d'un champ électrique utilisant l'iode comme catalyseur et le dichloroéthylène comme solvant. Les effets du champ sur la vitesse de polymérisation et le degré de polymérisation ont été étudiés. On a trouvé que le champ accroît les vitesses de polymérisation de l' α -méthylstyrène, et bien que faiblement, accroît également le degré de polymérisation tandis que le champ n'exerce pas d'influence sur ces quantités dans le cas du styrène. Les expressions pour la vitesse de polymérisation et le degré de polymérisation, qui ont été déduites dans une publication précédente, et améliorées dans l'article actuel, montrent que ces quantités sont généralement une fonction du degré de dissociation des paires d'ions aux extrémités de chaînes. Pour des degrés de dissociation relativement importants ces expressions peuvent rendre compte de l'effet du champ tel qu'il a été observé pour l' α -méthylstyrène si on admet que le degré de dissociation en présence d'un champ électrique est plus grand que celui en absence de celui-ci, et que la propagation de l'ion libre est beaucoup plus rapide que la propagation par paire d'ions. Pour de faibles degrés de dissociation, toutefois, ces expressions deviennent pratiquement indépendantes du degré de dissociation, de sorte qu'une augmentation éventuelle du degré de dissociation par suite de la présence d'un champ électrique ne donne pas d'effet pratiquement observable sur la polymérisation. Cette situation peut être interprétée comme correspondante au cas du styrène. En d'autres mots, la polymérisation de l' α -méthylstyrène a plus de caractère d'ions libres que celle du styrène.

Zusammenfassung

Kationische Polymerisation von α -Methylstyrol und Styrol mit Jod als Katalysator und Äthylendichlorid als Lösungsmittel wurde in einem elektrischen Feld ausgeführt. Der Einfluss des Feldes auf Polymerisationsgeschwindigkeit und Polymerisationsgrad wurde untersucht. Es wurde gefunden, dass das Feld die Polymerisationsgeschwindigkeit und in geringem Ausmass auch den Polymerisationsgrad von α -Methylstyrol erhöht, während es im Falle des Styrols auf diese Grössen keinen Einfluss hat. Die in einer früheren Mitteilung abgeleiteten und hier verfeinerten Ausdrücke für Polymerisationsgeschwindigkeit und Polymerisationsgrad zeigen, dass diese Grössen allgemein eine Funktion des Dissoziationsgrades der Ionenpaare am wachsenden Kettenende sind.

Bei vergleichsweise grossem Dissoziationsgrad können diese Ausdrücke den bei α -Methylstyrol beobachteten Feldeffekt unter der Annahme erklären, dass der Dissoziationsgrad in Anwesenheit eines elektrischen Feldes grösser ist als in dessen Abwesenheit und dass das Wachstum des freien Ions viel rascher verläuft als dasjenige des Ionenpaares. Bei kleinem Dissoziationsgrad werden dagegen die Ausdrücke vom Dissoziationsgrad praktisch unabhängig, sodass eine mögliche Zunahme des Dissoziationsgrades im elektrischen Feld zu keinem beobachtbaren Effekt bei der Polymerisation führt. Diese Sachlage könnte dem Falle des Styrols entsprechen. In anderen Worten, die Polymerisation von α -Methylstyrol verläuft in höherem Masse über freie Ionen als diejenige des Styrols.

Received January 25, 1966

Revised March 28, 1966

Prod. No. 5132A

Copolymerization of Styrene and Methyl Methacrylate. Reactivity Ratios from Conversion-Composition Data

VICTOR E. MEYER, *Plastics Fundamental Research, The Dow Chemical Company, Midland, Michigan 48640*

Synopsis

A method for the determination of reactivity ratios from conversion-composition data has been outlined. The conversion-composition changes during the copolymerization of styrene (M_1) and methyl methacrylate (M_2) have been studied at 60°C. By a method of graphical intersection, the integrated form of Skeist's equation has been used to determine the reactivity ratios ($r_1 = 0.54 \pm 0.02$ and $r_2 = 0.50 \pm 0.06$) in reasonably good agreement with values reported in the literature. The area of intersection was used as a measure of the precision of the data.

Introduction

The four chain growth steps and rate expressions for binary copolymerization are shown in Table I.

Despite the rather large volume change, 10-20%, which occurs during the polymerization of monomers to polymers, this effect appears to have been ignored by most authors. However, it may be shown that the volume terms cancel out of the relative instantaneous rate expressions. The rate of disappearance of M_1 per unit time and per unit volume is:¹

$$-\frac{1}{V} \frac{dM_1}{dt} = k_{11} \frac{m_1}{V} \left(\frac{M_1}{V} \right) + k_{21} \frac{[m_2]}{V_1} \left(\frac{M_1}{V} \right) \quad (1)$$

or, on multiplying through by V ,

$$-\frac{dM_1}{dt} = k_{11} m_1 [M_1] + k_{21} m_2^* [M_1] \quad (2)$$

TABLE I
Binary Copolymerization Chain Growth Steps and Rate Expressions

Growing chain	Adding monomer	Rate constant	Reaction product	Rate expression
$\sim m_1$	+ M_1	$\xrightarrow{k_{11}}$	$\sim m_1$	$R_{11} = k_{11} m_1 [M_1]$
$\sim m_1$	+ M_2	$\xrightarrow{k_{12}}$	$\sim m_2^*$	$R_{12} = k_{12} m_1 [M_2]$
$\sim m_2^*$	+ M_1	$\xrightarrow{k_{21}}$	$\sim m_1$	$R_{21} = k_{21} m_2^* [M_1]$
$\sim m_2^*$	+ M_2	$\xrightarrow{k_{22}}$	$\sim m_2^*$	$R_{22} = k_{22} m_2^* [M_2]$

Similarly, for M_2 ,

$$-\frac{dM_2}{dt} = k_{12} m_1[M_2] + k_{22} m_2[M_2] \quad (3)$$

The steady-state assumption then leads to,

$$m_2 = \frac{k_{12}}{k_{21}} \frac{M_2}{M_1} m_1 \quad (4)$$

The ratio of the rate of disappearance of M_1 and M_2 is then,

$$\frac{dM_1}{dM_2} = \frac{M_1}{M_2} \left(\frac{r_1 M_1 + M_2}{M_1 + r_2 M_2} \right) \quad (5)$$

or

$$F_1 = \frac{dM_1}{dM_1 + dM_2} = \frac{r_1 f_1^2 + f_1 f_2}{r_1 f_1^2 + 2f_1 f_2 + r_2 f_2^2} \quad (6)$$

where

$$r_1 = k_{11}/k_{12}; \quad r_2 = k_{22}/k_{21}; \quad f_1 = M_1/M = 1 - f_2; \quad \text{and } M = M_1 + M_2.$$

Thus, in this formulation of the problem, the volume cancels out. The instantaneous compositions and changes in composition during conversion depend only on the reactivity ratios and the relative number of moles of both species present. This is in contrast to the molar quantities occasionally given in the literature. Experimentally, moles, rather than the molar quantities which would require volume corrections with conversion, are used in the work reported here.

From the derivative of

$$f_1 = M_1/M \quad (7)$$

one obtains

$$\frac{df_1}{dM} = \frac{1}{M} \left(\frac{dM_1}{dM} - \frac{M_1}{M} \right) = \frac{1}{M} (F_1 - f_1) \quad (8)$$

The integration of eq. (8) gives Skeist's equation²

$$\ln \frac{M}{M_0} = \int_{f_1^0}^{f_1} \left(\frac{1}{(F_1 - f_1)} \right) df_1 \quad (9)$$

The right side of eq. (9) has recently been integrated to yield:³

$$\frac{M}{M_0} = \left(\frac{f_1}{f_1^0} \right)^\alpha \left(\frac{f_2}{f_2^0} \right)^\beta \left(\frac{f_1^0 - \delta}{f_1 - \delta} \right)^\gamma \quad (10)$$

where $\alpha = r_2/(1 - r_2)$; $\beta = r_1/(1 - r_1)$; $\gamma = (1 - r_1 r_2)/[(1 - r_1)(1 - r_2)]$; and $\delta = (1 - r_2)/(2 - r_1 - r_2)$. For given values of the reactivity ratios, eq. (10) may then be used to calculate the mole conversion, $1 - M/M_0$, as a function of change in monomer mixture composition.

Alternatively, if conversion-composition data are available, eq. (10) may be used to determine reactivity ratios. Since the styrene-methyl methacrylate system has been frequently studied, and also because this system remains clear, i.e., no phase separation appears to occur over a fairly wide conversion-composition range, these monomers appeared appropriate for an initial test of eq. (10). The method of graphical intersection, a technique frequently employed in the determination of reactivity ratios, will also be used on eq. (10).

Experimental

Freshly distilled center portions of styrene ($n_D^{20} = 1.5473$) and methyl methacrylate ($n_D^{20} = 1.4151$) and initiator were placed in $3/4$ -in. outside diameter thick-walled glass tubes which were sealed under vacuum at Dry Ice temperature. The tubes were then placed in a silicone oil bath at $60.0 \pm 0.1^\circ\text{C}$. Samples were removed at appropriate intervals and the per cent solids determined in the following manner. A small portion, approximately 1.0 g., was placed in a small aluminum weighing dish. The sample was then diluted with toluene containing a trace of benzoquinone, followed by precipitation with methanol and air drying at room temperature. The last trace of monomer and solvent was then removed by vacuum devolatilization at 210°C . for 15 min. Per cent weight conversion was then calculated from initial and final weights. Triplicate samples were run in all cases. The maximum deviation from the mean was normally less than 0.5%. These results were also in good agreement with variations of the method, such as room temperature vacuum devolatilization, or in the case of the low-conversion samples, leaving out the benzoquinone. The remaining portion of each copolymer sample was also diluted with toluene containing a trace of benzoquinone, followed by precipitation into methanol.

TABLE II
Conversion-Composition Data for the Mass Copolymerization of Styrene and Methyl Methacrylate at 60°C ., Experiment 19-30^a

Sample	Time, min.	Oxygen		f_1	Conversion, mole-%
		Conversion, wt.-%	in copolymer, wt.-%		
19-30	0	0.00	0.00	0.8000	0.00
1	235	9.01	8.12	0.8061	9.03
2	355	11.74	8.32	0.8091	11.77
3	475	15.61	8.24	0.8122	15.65
4	850	29.32	7.92	0.8229	29.38
5	1345	46.18	7.61	0.8391	46.26
6	1555	53.03	7.52	0.8481	53.12
7	1710	65.88	7.43	0.8769	65.98
8	1780	71.65	6.92	0.8586	71.72
9	1860	86.37	7.00	0.9648	86.46

^a Starting composition: styrene, 833.12 g.; methyl methacrylate, 200.22 g.; benzoyl peroxide, 5.00 g.

TABLE III
Conversion-Composition Data for the Solution Copolymerization of Styrene and Methyl Methacrylate in 25 Wt.-% Toluene at 60°C., Experiment 19-13-2^a

Sample	Time, min.	Oxygen		f_1	Conversion, mole-%
		Conversion, wt.-%	in copolymer, wt.-%		
19-13-2	0	0.00	0.00	0.2000	0.00
A	720	11.79	24.20	0.1952	11.77
B	1200	18.85	23.80	0.1889	18.81
C	1440	39.88	23.80	0.1683	39.80
D	1680	44.80	24.00	0.1661	44.73
E	1920	53.93	24.50	0.1690	53.87
F	2340	69.57	25.00	0.1743	69.54
G	2880	94.96	25.70	0.3929	95.00

^a Starting composition: styrene, 104.14 g.; methyl methacrylate, 400.44 g.; azobisisobutyronitrile, 0.1 g.; toluene, 168.22 g.

Final purification was by reprecipitation using pure solvents. The samples were then dried to essentially constant weight at 60°C. or less. Oxygen content of the copolymer samples was then determined by neutron activation analysis. From the copolymer composition and average weight conversion, mole conversion and monomer mixture composition were then calculated (Tables II and III). In Figure 1 the mole fraction of styrene in

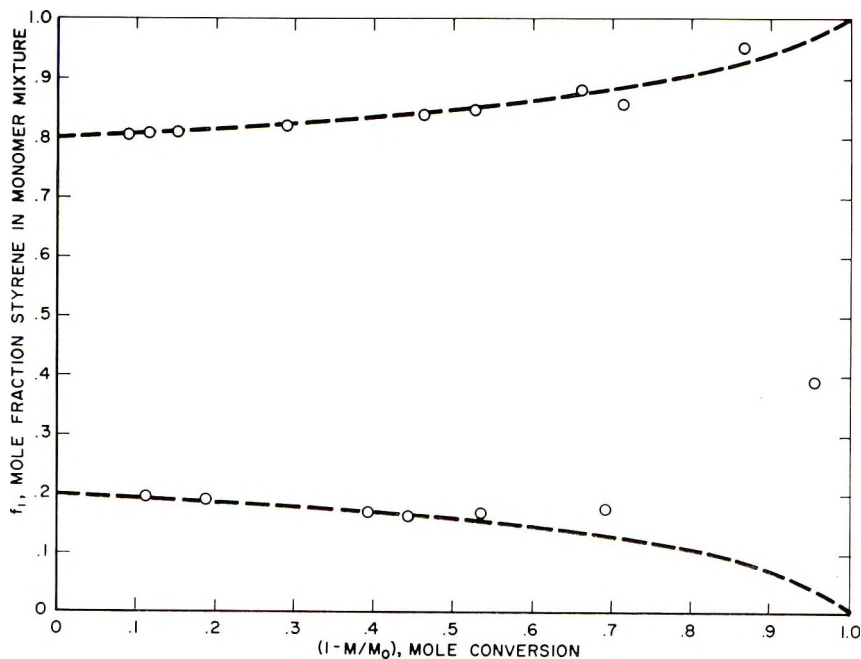


Fig. 1. Experimental points for the copolymerization of styrene and methyl methacrylate at 60°C. Curves calculated according to eq. (10) for $f_1^0 = 0.8$, $r_1 = 0.53$, $r_2 = 0.56$ and for $f_1^0 = 0.2$, $r_1 = 0.53$, $r_2 = 0.56$.

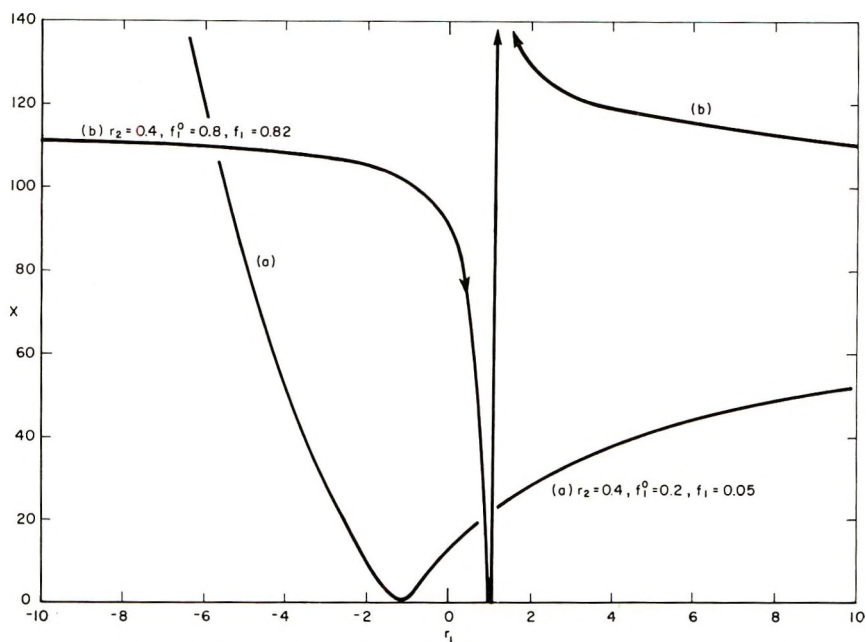


Fig. 2. Variation of X [eq. (11)] with r_1 at different fixed values of r_2 .

the monomer mixture is plotted as a function of mole conversion. The theoretical curve, eq. (10), for $r_1 = 0.53$, $r_2 = 0.56$, is also shown in Figure 1. These values for the reactivity ratios were determined from the experimental points in the following manner. First, an equation similar to eq. (10), is defined,

$$X \equiv \left(\frac{f_1}{f_1^0} \right)^\alpha \left(\frac{f_2}{f_2^0} \right)^\beta \left(\frac{f_1^0 - \delta}{f_1 - \delta} \right)^\gamma \quad (11)$$

where, α , β , γ , and δ are as previously defined.

Next, we consider the behavior of eq. (11) for a fixed value of r_2 (0.4), and for two different values of f_1^0 (0.8 and 0.2) corresponding to opposite sides of the crossover point. The values of X are then calculated for increments of r_1 between -10 and $+10$ (Fig. 2). The curve (Fig. 2a) for $f_1^0 = 0.2$ is reasonably well behaved, having only the known singularity³ at $r_1 = 1.0$, whereas the $f_1^0 = 0.8$ curve (Fig. 2b) shows a complete change in behavior at this point. (For $r_2 = 0.8$, both curves show essentially the same general behavior as for the $r_2 = 0.4$ curves.)

Next, for various assigned values of r_2 in the range of 0.4–0.8, it is desired to determine the corresponding value of r_1 which makes X , eq. (11), arbitrarily close to M/M_0 , i.e., that satisfies eq. (10).

The general procedure may be illustrated by the following example, for $r_2 = 0.4$, $f_1^0 = 0.8$. (1) Calculate values of X for increasing increments of r_1 from zero to 1.0. X is decreasing in this region. (2) When X becomes less than M/M_0 , then interpolate between the last and preceding value

TABLE IV
Interpolated Solutions of Equation (11)

f_1^0	f_1	M/M_0	X	r_1	r_2
0.80	0.8229	70.62	70.61	0.512	0.40
0.80	0.8229	70.62	71.19	0.521	0.50
0.80	0.8229	70.62	70.61	0.543	0.60
0.80	0.8229	70.62	70.58	0.559	0.70
0.80	0.8229	70.62	70.41	0.577	0.80

of X . The interpolation is repeated a number of times, or until the desired agreement between X and M/M_0 is obtained. Typical values obtained from such calculations are shown in Table IV. Plots of r_2 versus r_1 which are essentially straight lines may now be made from these calculations. For a given starting composition, e.g., $f_1^0 = 0.8$, a family of more or less parallel lines are obtained. Thus, in order to obtain suitably intersecting curves, different starting compositions are necessary. The starting composition, $f_1^0 = 0.2$ gives a family of curves (straight lines) perpendicularly intersecting the $f_1^0 = 0.8$ family of curves (straight lines), as shown in Figure 3. All calculations were carried out on a Burroughs B5500.

In order to obtain controllable rates of polymerization with the larger amounts of methyl methacrylate, the use of diluent was found necessary. However, even in the presence of the diluent, the results at higher conversions tend to show a scatter towards higher styrene content in the monomer mixture. This tendency becomes more critical at higher conversions (Fig. 1). For this reason, only experimental points below 50 mole-% conversion have been used to determine the reactivity ratios.

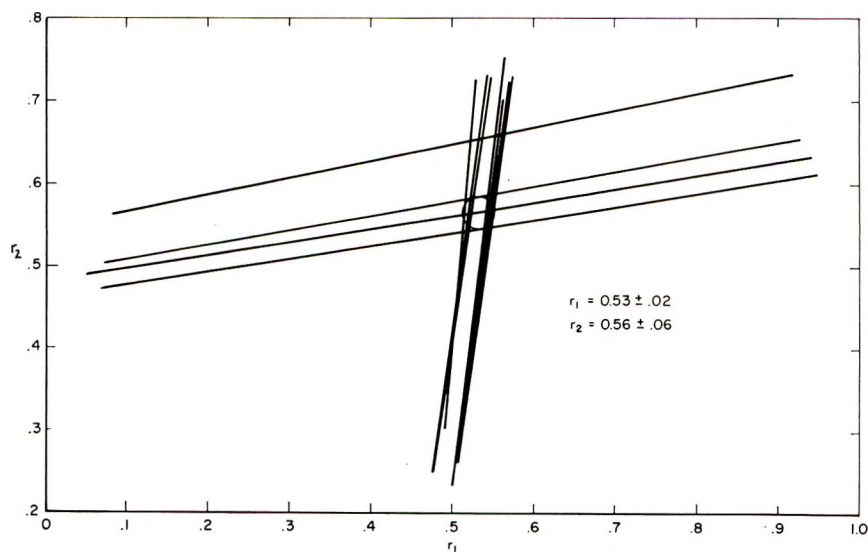


Fig. 3. Reactivity ratios from the intersection of r_2 vs. r_1 curves for experimental data fitted into eq. (10).

Because of the greater scatter encountered at the higher methyl methacrylate levels ($f_1^0 = 0.2$), these experiments were repeated at different diluent levels; however, little improvement in precision was experienced. These data are collected in Tables V–X.

The binary reactivity ratios, as determined from the conversion–composition data and the integrated form of Skeist's equation, are given in columns 3 and 4 of Table XI. In columns 1 and 2 are indicated the corresponding series of experiments from which the reactivity ratios were determined.

TABLE V
Conversion–Composition Data for the Solution Copolymerization of Styrene and Methyl Methacrylate in 25 Wt.-% Toluene at 60°C., Experiment 19-43^a

Sample	Time, min.	Oxygen		f_1	Conversion, mole-%
		Conversion, wt.-%	in copolymer, wt.-%		
19-43	0	0.00	0.00	0.8000	0.00
1	1410	13.83	7.90	0.8088	13.86
2	1890	17.55	8.26	0.8141	17.59
3	2850	23.04	7.96	0.8166	23.09
4	3330	24.96	7.90	0.8182	25.01
5	4290	29.81	7.83	0.8222	29.87
6	4770	31.61	7.85	0.8246	31.68
7	5730	34.59	7.70	0.8255	34.65
8	6210	36.13	7.78	0.8287	36.20
9	10050	44.27	7.63	0.8367	44.35
10	67860	60.47	7.37	0.8577	60.56

^a Starting composition: styrene, 416.56 g.; methyl methacrylate, 100.11 g.; azobisisobutyronitrile, 0.10 g.; toluene, 172.22 g.

TABLE VI
Conversion–Composition Data for the Solution Copolymerization of Styrene and Methyl Methacrylate in 50 Wt.-% Toluene at 60°C., Experiment 19-17-2^a

Sample	Time, min.	Oxygen		f_1	Conversion, mole-%
		Conversion, wt.-%	in copolymer, wt.-%		
19-17-2	0	0.00	0.00	0.2000	0.00
A	990	16.96	23.70	0.1896	16.93
B	1070	21.04	23.80	0.1872	21.00
C	1310	24.92	24.00	0.1861	24.89
D	2430	37.40	23.80	0.1714	37.33
E	2610	40.22	23.20	0.1555	40.11
F	2850	42.40	23.30	0.1536	42.29
G	3870	53.24	24.40	0.1664	53.18
H	4050	54.82	24.20	0.1568	54.74
I	4290	59.52	23.80	0.1298	59.41
J	5310	86.38	24.60	0.0521	86.30

^a Starting composition: styrene, 52.07 g.; methyl methacrylate, 200.22 g.; azobisisobutyronitrile, 0.1 g.; toluene, 252.29 g.

TABLE VII

Conversion-Composition Data for Solution Copolymerization of Styrene and Methyl Methacrylate in 50 Wt.-% Toluene at 60°C., Experiment 19-49-B^a

Sample	Time, min.	Conversion, wt.-%	Oxygen in copolymer, wt.-%	f_1	Conversion, mole-%
19-49-B	0	0.00	0.00	0.2000	0.00
1	1440	18.20	23.08	0.1844	18.15
2	2880	30.80	23.74	0.1779	30.74
3	3360	34.86	24.07	0.1789	34.81
4	4320	41.50	23.14	0.1517	41.39
5	4800	45.22	23.68	0.1576	45.13
6	5760	51.88	24.73	0.1789	51.84
7	6240	54.12	24.02	0.1515	54.03
8	10080	67.80	24.46	0.1415	67.73

^a Starting composition: styrene, 52.07 g.; methyl methacrylate, 200.22 g.; azobisisobutyronitrile, 0.05 g.; toluene, 252.29 g.

TABLE VIII

Conversion-Composition Data for Benzoyl Peroxide-Initiated Mass Copolymerization of Styrene and Methyl Methacrylate at 60°C., Experiment 19-34^a

Sample	Time, min.	Conversion, wt.-%	Oxygen in copolymer, wt.-%	f_1	Conversion, mole-%
19-34	0	0.00	0.00	0.2000	0.00
1	285	16.29	22.99	0.1859	16.24
2	405	24.37	22.76	0.1744	24.29
3	490	31.04	24.07	0.1822	30.99
4	630	70.40	25.35	0.1987	70.40

^a Starting composition: styrene, 208.28 g.; methyl methacrylate, 800.88 g.; benzoyl peroxide, 5.00 g.

For comparative purposes, by using the initial monomer mixture composition, $f_1^0 = 0.2$ and $f_1^0 = 0.8$, and average copolymer composition, F_1 , as determined from the analyses of the number of moles of each component found for the lowest conversion point for each of the respective runs, Ross-Fineman plots⁸ were used to determine the reactivity ratios in the usual manner. These results are shown in columns 3 and 4 of Table XII.

These values for the reactivity ratios are relatively high compared with the values determined from conversion-composition behavior (Table XI) or with literature values (Table XIII). Some improvement is obtained by using an averaged monomer mixture composition \bar{f}_1 , which is taken as the composition halfway between the initial value and the monomer mixture composition at the conversion corresponding to F_1 (Table XIV). Since these lowest conversion points used in the Ross-Fineman treatments still correspond to relatively high conversions (6.25-22.70%), it is suggested that the relatively high values for the reactivity ratios obtained from the Ross-Fineman plots simply reflect the fact that in using the "instantaneous"

TABLE IX
Conversion-Composition Data for Azobisisobutyronitrile-Initiated Mass Copolymerization of Styrene and Methyl Methacrylate at 60°C., Experiment 19-42*

Sample	Time, min.	Oxygen		f_1	Conversion, mole-%
		Conversion, wt.-%	in copolymer, wt.-%		
19-42	0	0.00	0.00	0.8000	0.00
1	450	6.23	8.33	0.8046	6.25
2	1410	16.97	7.81	0.8106	17.00
3	1890	22.20	7.78	0.8145	22.24
4	2950	31.54	7.63	0.8212	31.60
5	3430	35.56	7.90	0.8302	35.64
6	4390	44.39	7.72	0.8391	44.48
7	4870	50.37	7.70	0.8490	50.47
8	5830	59.75	7.37	0.8559	59.84
9	6310	64.11	7.12	0.8532	64.18
10	10150	91.03	6.54	0.9122	91.07

* Starting composition: styrene, 416.56 g.; methyl methacrylate, 100.10 g.; azobisisobutyronitrile, 0.10 g.

TABLE X
Conversion-Composition Data for the Solution Copolymerization of Styrene and Methyl Methacrylate in 25 wt.-% Toluene at 60°C., Experiment 19-45*

Sample	Time, min.	Oxygen		f_1	Conversion, mole-%
		Conversion, wt.-%	in copolymer, wt.-%		
19-45	0	0.00	0.00	0.2000	0.00
1	1410	22.72	24.61	0.1932	22.70
2	1890	31.67	23.16	0.1687	31.58
3	2850	59.84	23.29	0.1055	59.69
4	3330	68.05	23.91	0.1055	67.93

* Starting composition: styrene, 104.14 g.; methyl methacrylate, 400.44 g.; azobisisobutyronitrile, 0.10 g.; toluene, 168.20 g.

TABLE XI
Reactivity Ratios of Styrene (M_1) and Methyl Methacrylate (M_2) at 60°C. as Determined from Conversion-Composition Data

Experiment number		Reactivity ratios	
$f_1^0 = 0.8$	$f_1^0 = 0.2$	r_1	r_2
19-30	19-13	0.53 ± 0.02	0.56 ± 0.06
19-43	19-17	0.55 ± 0.02	0.53 ± 0.06
19-43	19-49	0.54 ± 0.02	0.53 ± 0.08
19-43	19-34	0.53 ± 0.02	0.46 ± 0.06
19-42	19-45	0.53 ± 0.03	0.42 ± 0.06
Avg.		0.536 ± 0.02	0.50 ± 0.06

TABLE XII

Reactivity Ratios of Styrene (M_1) and Methyl Methacrylate (M_2) at 60°C. as Determined from Ross-Fineman Plots Based on Initial Monomer Mixture Composition

Experiment number		Reactivity ratios	
$f_1^0 = 0.8$	$f_1^0 = 0.2$	r_1	r_2
19-30	19-13	0.58	0.68
19-43	19-17	0.59	0.61
19-43	19-49	0.58	0.52
19-43	19-34	0.58	0.51
19-42	19-45	0.56	0.74

TABLE XIII

Literature Values of r_1 and r_2 for Styrene and Methyl Methacrylate at 60°C.

Reference	r_1	r_2
Wiley and Davis ⁴	0.53	0.49
Lewis et al. ⁵	0.50 ± 0.02	0.50 ± 0.02
Lewis et al. ⁶	0.52 ± 0.03	0.46 ± 0.03
Wiley and Sale ⁷	0.48	0.46
This paper	0.54 ± 0.02	0.50 ± 0.06

TABLE XIV

Reactivity Ratios of Styrene (M_1) and Methyl Methacrylate (M_2) at 60°C. as Determined from Ross-Fineman Plots Based on Averaged Monomer Mixture Composition

Experiment and monomer mixture composition				Reactivity ratios	
Expt.	\bar{f}_1	Expt.	\bar{f}_1	r_1	r_2
19-30	0.80310	19-13	0.19760	0.56	0.66
19-43	0.80438	19-17	0.19480	0.57	0.58
19-43	0.80438	19-49	0.19222	0.55	0.49
19-43	0.80438	19-34	0.19294	0.55	0.48
19-42	0.80228	19-45	0.19660	0.54	0.72
Avg.				0.56	0.59

methods for the determination of reactivity ratios, experiments should be restricted to fairly low conversions.

Conclusions

Literature values for r_1 and r_2 are given in Table XIII. It is seen that the values of the reactivity ratios, as determined from conversion-composition data by the methods outlined in this paper are in reasonably good agreement with values reported in the literature.⁴⁻⁷ In these experiments, in particular, at the higher methyl methacrylate concentrations ($f_1^0 = 0.2$), a scatter towards higher styrene content in the monomer mixture was more or less consistently observed at the higher conversion levels (Fig. 1). It is suggested that more precise experimental data are necessary for a meaningful interpretation of this phenomenon.

The determination of reactivity ratios from any of the instantaneous copolymerization equations must inevitably involve copolymerizing the monomers to at least a few per cent conversion. Because of the drift (usually 1–2%) in copolymer composition which normally occurs in such copolymerizations, the values of the reactivity ratios determined from such an approach must reflect this approximation to instantaneous behavior. Unfortunately, certain phenomena which one might wish to study, such as the penultimate effect⁹ are apt to be of this same order of magnitude.

By way of contrast, no such approximation is involved in the determination of reactivity ratios from conversion–composition data. In this sense, the method outlined here is potentially more precise. Since eq. (10) can be rearranged to the equation of Lewis and Mayo,⁵ these considerations should likewise apply to eq. (12) of reference 5. The Lewis and Mayo treatment, although also utilizing conversion–composition data, is primarily concerned with the determination of the reactivity ratios from the change of each monomer relative to its initial value, i.e., from the ratios ($[M_1]/[M_1^0]$) and ($[M_2]/[M_2^0]$), whereas the treatment outlined here is primarily concerned with conversion behavior. Thus, although both methods are potentially equally precise, it is suggested that the conversion–composition approach should be more amenable to the detection and interpretation of deviations from “ideal” copolymerization behavior. However, such an approach will require more precise experimental data than are currently available.

Miss Mersina Karris, D. W. Briden, and O. A. Anders determined the per cent oxygen in the copolymer samples by neutron activation analyses. The simplified derivation of Skeist's equation, eqs. (7)–(9), is due to R. A. Wessling. Special thanks are also due J. A. Barber for his assistance in the experimental portion of this work.

References

1. S. M. Walas, *Reaction Kinetics for Chemical Engineers*, McGraw-Hill, New York, 1959, p. 5.
2. I. Skeist, *J. Am. Chem. Soc.*, **68**, 1781 (1946).
3. G. G. Lowry and V. E. Meyer, *J. Polymer Sci. A*, **3**, 2843 (1965).
4. R. H. Wiley and B. Davis, *J. Polymer Sci.*, **62**, S132 (1962).
5. F. M. Lewis and F. R. Mayo, *J. Am. Chem. Soc.*, **66**, 1594 (1944).
6. F. M. Lewis, F. R. Mayo, and W. F. Hulse, *J. Am. Chem. Soc.*, **67**, 1701 (1945).
7. R. H. Wiley and E. E. Sale, *J. Polymer Sci.*, **42**, 479 (1960).
8. M. Fineman and S. D. Ross, *J. Polymer Sci.*, **5**, 259 (1950).
9. G. E. Ham, *J. Polymer Sci. B*, **3**, 185 (1965).

Résumé

Une méthode de détermination des rapports de réactivité au départ de résultats de degré de conversion–composition a été soulignée. Les variations de la composition en fonction de la conversion en cours de la copolymérisation de styrène (M_1) et de méthacrylate de méthyle (M_2) ont été étudiées à 60°C. Par une méthode d'intersection graphique, une forme intégrée de l'équation de Skeist a été utilisée pour déterminer les rapports de réactivité ($r_1 = 0.54 \pm 0.02$ et $r_2 = 0.50 \pm 0.06$) en accord raisonnablement bon avec les valeurs rapportées dans la littérature. La surface intersectée était utilisée comme une mesure de la précision des résultats.

Zusammenfassung

Eine Methode zur Bestimmung der Reaktivitätsverhältnisse aus Umsatz-Zusammensetzungsdaten wurde angegeben. Die Umsatz-Zusammensetzungsänderungen während der Kopolymerisation von Styrol (M_1) und Methylmethacrylat (M_2) wurden bei 60°C untersucht. Mittels einer graphischen Schnittmethode wurde die integrierte Form der Gleichung von Skeist zur Bestimmung der Reaktivitätsverhältnisse $r_1 = 0,54 \pm 0,02$ und $r_2 = 0,50 \pm 0,06$ in guter Übereinstimmung mit Literaturwerten verwendet. Die Fläche bei der Schnittbildung wurde als Mass für die Genauigkeit der Daten verwendet.

Received January 20, 1966

Revised March 15, 1966

Prod. No. 5136A

Model Compounds and Polymers with Quinoxaline Units

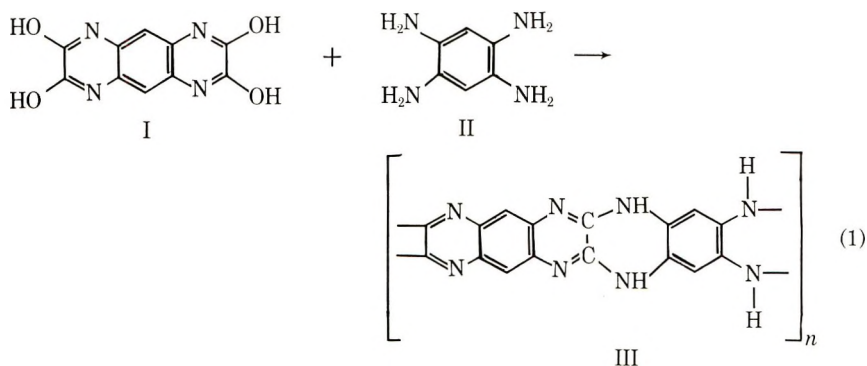
HANS JADAMUS, FRANZ DE SCHRYVER, WALTER DE WINTER, and C. S. MARVEL, *Department of Chemistry, University of Arizona, Tucson, Arizona*

Synopsis

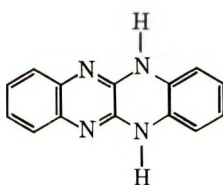
Tetra- and heptanuclear *N*-heterocycles, their dimers and their polymers have been prepared by condensation of *o*-phenylenediamine or 3,3'-diaminobenzidine with 2,3-dihydroxyquinoxaline, 2,3,2,3'-tetrahydroxy-6,6'-bisquinoxaline, or 2,3,7,8-tetrahydroxy-1,4,6,9-tetraazaanthracene in polyphosphoric acid, or with the *O*-phenyl derivatives of the latter three compounds in phenol. The condensation products are highly colored compounds with characteristic absorption spectra. The polymers show good thermal stability.

Introduction

Recent studies¹⁻³ have indicated that polyquinoxalines have unusually good thermal stability. Also, it has been established that aromatic ladder structures^{4,5} seem to offer further improvement in thermal properties than the other polyaromatic types. Accordingly, this work on model compounds was undertaken to learn how to prepare ladder structures such as might be obtained in reactions of the type shown in eq. (1).



Since that time, Fluorflavine (IV) has been made by (1) the condensation of (see following page)

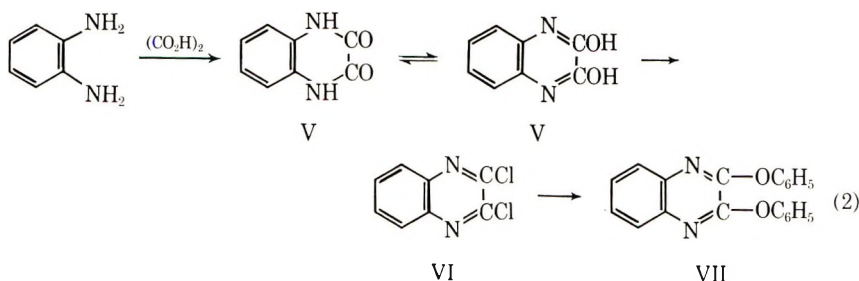


IV

2,3-dichloroquinoxaline with *o*-phenylenediamine;⁶ (2) by the melt condensation of 2,3-dihydroxyquinoxaline with *o*-phenylenediamine;⁵ (3) by the melt condensation of oxalic acid with *o*-phenylenediamine;⁶ by the condensation of 2,3-dihydroxyquinoxaline with *o*-phenylenediamine in polyphosphoric acid;⁷ and (5) by the condensation of *o*-phenylenediamine with 1,1,2,2-tetrachloro-1,2-di-*n*-butoxyethane.⁸ These seemed to be reactions which could potentially be extended to polymer formations. Examination indicated that methods 1, 2, and 4 would be the most useful polymer-forming reactions since by-products were encountered in the other methods. We, accordingly, set out to study these reactions with model compounds and then followed this study with some polymer syntheses.

Model Compounds

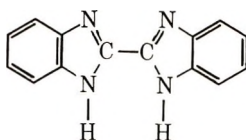
2,3-Dihydroxyquinoxaline (V) was prepared by the method of Phillips⁹ from *o*-phenylenediamine and oxalic acid. Although the material is usually called a dihydroxy derivative, the infrared spectrum indicates it is largely in the keto form. The dihydroxy derivative was transformed to



the dichloro compound (VI) by the method of Cheeseman.¹⁰ We have found that the diphenoxy compound (VII) which is readily prepared from the dichloro compound and phenol or sodium phenoxide is very useful in further condensation reactions. For example when the diphenoxy compound was heated with *o*-phenylenediamine, Fluoflavine was obtained which was identical with the product of Badger and Nelson.⁷

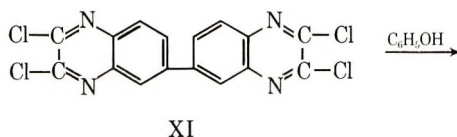
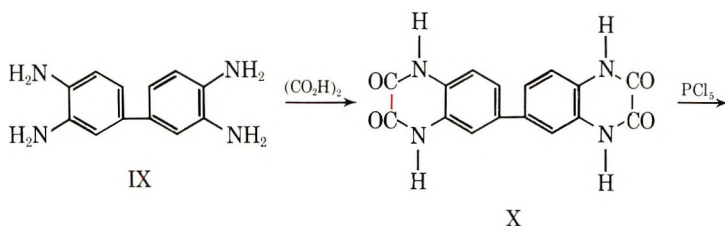
We also had occasion to repeat the condensation reaction of oxamide with *o*-phenylenediamine described by Lane¹¹ which is said to yield 2,2'-bisbenzimidazole (VIII) which he described as a yellow product. We have found that this reaction produces both the bisbenzimidazole (VIII)

and Fluoflavine. When they are completely separated, the bisbenzimidazole is a colorless compound.

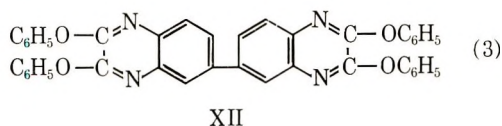


VIII

Using the general method of condensing oxalic acid with an *o*-diamine, we have prepared a series of tetrafunctional bisquinoxaline derivatives from 3,3'-diaminobenzidine (IX) as shown in eq. (3).

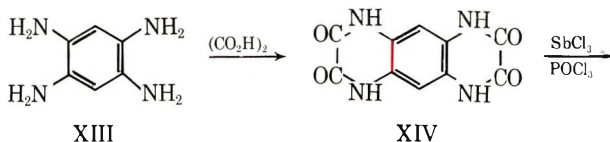


XI



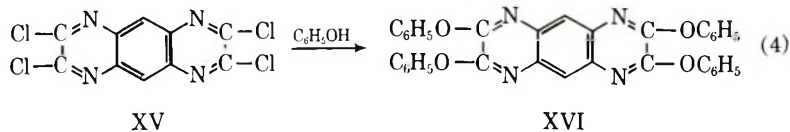
XII

In a similar manner 1,2,4,5-tetraaminobenzene (XIII) has been converted to a tetrafunctional series of derivatives of tetraazaanthracene.



XIII

XIV

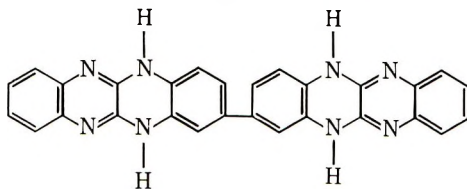


XV

XVI

In attempting to convert XIV to XV by the use of phosphorus pentachloride, we isolated a pentachloro and a hexachloro compound which presumably are the chlorination products of the benzene ring in one or two of the open *para* positions.

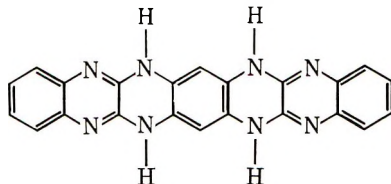
The tetraphenoxy compound XII from diaminobenzidine has been converted to 2,2'-bisfluorflavine (XVII) by heating with *o*-phenylenediamine. The same product has been obtained by heating 3,3'-diaminobenzidine



XVII

with 2,3-diphenoxyquinoxaline (VII) and by heating tetrahydroxybisquinoxaline (XII) with *o*-phenylenediamine in polyphosphoric acid. These reactions might be expected to give somewhat different products, but, apparently, they tautomerize to the same final product since all had ultraviolet absorption at 410, 433, and 459 $m\mu$.

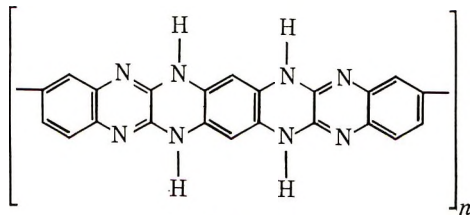
5,6,8,9,14,15,17,18-Octaaza-6,8,15,17-tetrahydroheptacene (XVIII) was prepared from tetraphenoxytetraazaanthracene (XVI) and *o*-phenylenediamine, from tetraaminobenzene and 2,3-diphenoxyquinoxaline (VII) and from tetrahydroxytetraazaanthracene (XIV) and *o*-phenylenediamine by treatment with polyphosphoric acid. Again isomers were not obtained.



XVIII

Polymers

A polymer was obtained by condensing compound XIV with diaminobenzidine in polyphosphoric acid. This polymer should have the structural unit XIX. One sample was soluble in concentrated sulfuric acid and had



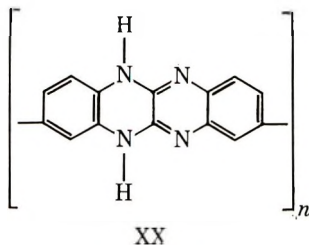
XIX

an inherent viscosity of 0.3 (0.5% in concentrated sulfuric acid). The product was a shiny copper-colored solid which gave a blue solution in sulfuric acid. The sulfuric acid solution showed λ_{\max} at 618 and 564 $m\mu$ with

a shoulder at $525 \text{ m}\mu$. The thermogravimetric analysis is shown in Figure 1 (curve 1).

Heating tetraphenoxytetraazaanthracene (XVI) with 3,3'-diaminobenzidine in phenol solution gave a polymer with an inherent viscosity of 0.135 (0.5% in concentrated sulfuric acid). It presumably also has the structure (XIX) and the thermogravimetric properties are given in Figure 1 (curve 4).

Polyfluorflavine (XX) has been obtained by heating 3,3'-diaminobenzidine with the tetraphenoxy compound (XII) in phenol to give a reddish solid which is soluble in sulfuric acid. This solution has λ_{max} at 508 and $548 \text{ m}\mu$. The sample (Fig. 1, curve 2) had an inherent viscosity of 0.3 (0.5% in concentrated sulfuric acid). Heating tetrahydroxyquinoxaline (X) and diaminobenzidine with polyphosphoric acid also gave this polymer. Such a sample had an inherent viscosity of 0.2 (0.5% in concentrated sulfuric acid). It is shown in Figure 1, curve 3.



Analytical results on these polymers have been unsatisfactory. Since usually the C/N ratio agrees with the expected value, it is believed that incomplete combustion is causing the difficulty.

Experimental

2,3-Dihydroxyquinoxaline (V). This was prepared by the method of Phillips⁹ from *o*-phenylenediamine and oxalic acid in 4*N* hydrochloric acid.

2,3-Dichloroquinoxaline (VI). This was prepared by the method of Cheeseman¹⁰ from (V), phosphorus oxychloride, and *N,N*-dimethylaniline.

2,3-Diphenoxyquinoxaline (VII). 2,3-Dichloroquinoxaline (19.9 g.) was boiled under reflux in phenol (40 g.) for 14 hr. After cooling, the mixture was triturated with methanol (50 ml.) and the white crystalline residue recrystallized from dioxane-methanol. The yield was 28 g. (89%), m.p. 164–165°C.

ANAL. Calcd. for $\text{C}_{20}\text{H}_{14}\text{O}_2\text{N}_2$: C, 76.3%; H, 4.5%; N, 8.9%. Found: C, 75.6%; H, 4.4%; N, 8.8%.

Alternate Method. 2,3-Dichloroquinoxaline (0.2 g.) and sodium phenoxide (4.6 g.) were heated under reflux in dimethylformamide (40 ml.) for $1/2$ hr. The reaction mixture was filtered and water was added to the

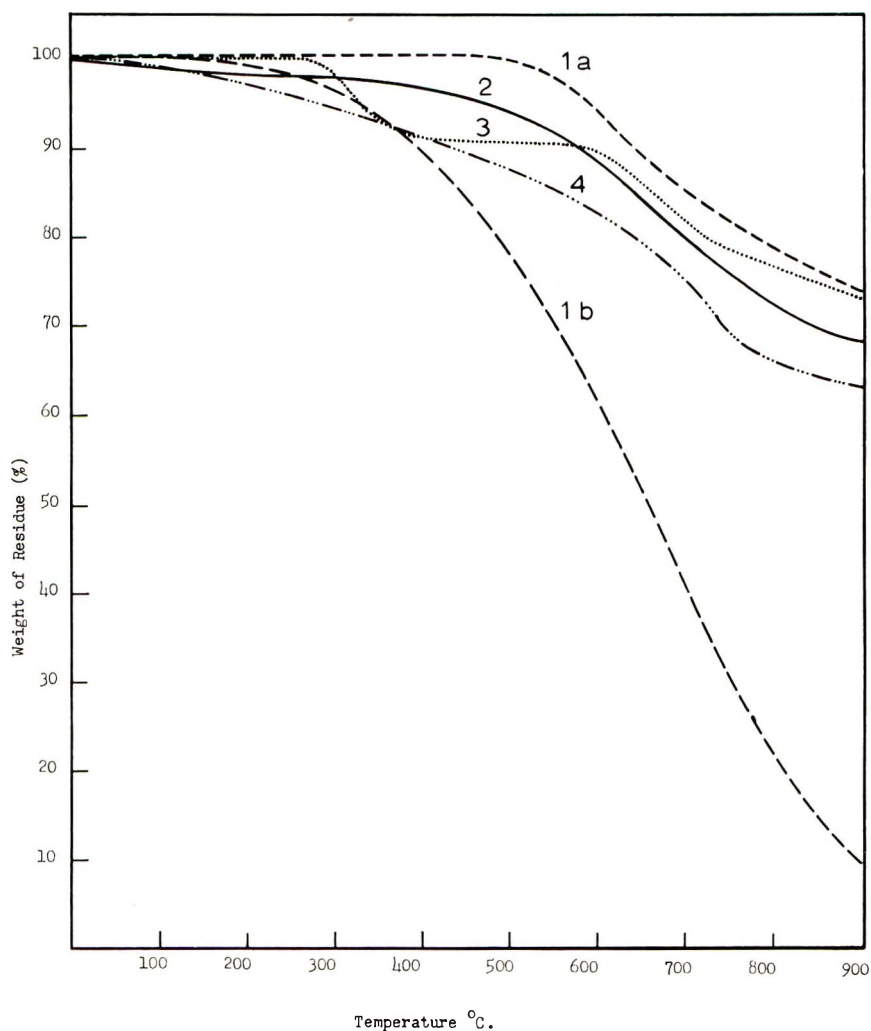


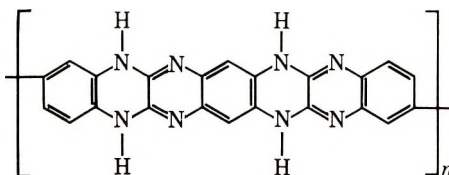
Figure 1. See caption, opposite page.

filtrate until a crystalline precipitate was formed. The yield after recrystallization from acetate-methanol was 2.7 g. (86%), m.p. 164–165°C.

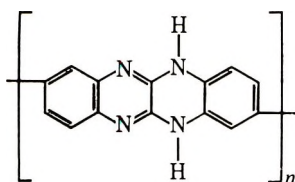
Fluoflavine (IV). 2,3-Diphenoxyquinoxaline (0.34 g.) and *o*-phenylenediamine (108 mg.) were heated under reflux in 4 g. of phenol for 2½ hr., during which time bright yellow needles precipitated. After cooling, the mixture was triturated with methanol (10 ml.) and the crystals were separated by filtration, washed with methanol, and dried. The yield was 207 mg. (88%). The ultraviolet spectrum showed λ_{\max} 435, 410, 390, 370 $m\mu$, dioxane. The spectrum of this material is identical with that of fluoflavine prepared by the method of Badger and Nelson.⁷

2,2'-Bisbenzimidazole (VIII). Crude 2,2'-bisbenzimidazole was prepared according to Lane¹¹ from oxamide and *o*-phenylenediamine. A

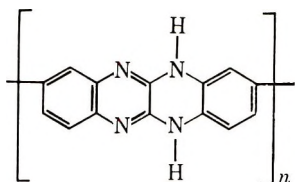
Fig. 1. TGA curves for (1)



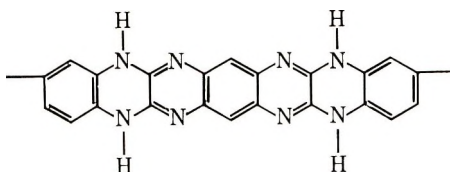
from tetrahydroxytetraazaanthracene with polyphosphoric acid (a) in nitrogen and (b) in air; (2)



from tetraphenoxybisquinoxaline and heat (in nitrogen); (3)



from tetrahydroxybisquinoxaline in polyphosphoric acid (in nitrogen); (4)



from tetraphenoxytetraazaanthracene (in nitrogen). Heating rate 150°C./hr.

7-g. portion of the crude product was extracted with 1 liter of 10% sodium hydroxide solution (charcoal used to decolorize) and reprecipitated with acetic acid. The colorless precipitate was recrystallized from glacial acetic acid. The yield was 3.1 g. of colorless needles. (2,2'-Bisbenzimidazole is usually described as yellow; the yellow color was due to the presence of Fluorflavine). The white product had λ_{max} in dioxane of 342, 325, 317 m μ . The residue from the alkaline extraction was mainly Fluorflavine.

2,2',3,3'-Tetrachloro-6,6'-bisquinoxaline (XI). A mixture of 2.2 g. of 3,3'-diaminobenzidine and 2.6 g. of oxalic acid dihydrate was dissolved in 20 ml. of 4*N* hydrochloric acid. The solution was heated at reflux temperature for 3 hr. A slightly brownish powder appeared during the heating. The mixture was cooled, the product was collected on a filter, washed with methanol, and dried.

A 5-g. portion of the crude product was placed in a 100-ml. flask with 15 ml. of phosphorus oxychloride and 5 ml. of *N,N*-dimethylaniline, the solution was heated at reflux temperature for 3 hr., cooled, and poured into 100 ml. of ice water. The precipitate was collected on a filter, dried and extracted with hot benzene. The benzene extract yielded 4.7 g. (80%) of compound XI. After recrystallization from benzene the product melted at 293–294°C., λ_{\max} at 418 $m\mu$, $\epsilon = 14,800$.

ANAL. Calcd. for $C_{16}H_6N_4Cl_4$: C, 49.0%; H, 1.6%; N, 14.1%; Cl, 35.9%. Found: C, 48.5%; H, 1.5%; Cl, 35.8%.

2,3,2',3'-Tetraphenoxy-6,6'-bisquinoxaline (XII). 2,3,2',3'-Tetrachloro-6,6'-bisquinoxaline (3.96 g.) was heated under reflux in phenol (7.5 g.) for 14 hr. After cooling, the solid mass was extracted with hot methanol until the washing liquid was colorless. The yield was 4.85 g. (77.5%), m.p. 247–249°C. (after recrystallization from dioxane-methanol). λ_{\max} in sulfuric acid: 415 $m\mu$, $\epsilon = 25,300$.

ANAL. Calcd. for $C_{40}H_{26}N_4O_4$: C, 75.6%; H, 4.4%; N, 9.6%. Found: C, 76.2%; H, 4.4%; N, 9.2%.

2,3,7,8-Tetrahydroxy-1,4,6,9-tetraazaanthracene (XIV). 1,5-Diamino-2,4-dinitrobenzene¹² (10 g.) was hydrogenated in dioxane (50 ml.) containing 1 g. palladium black (5% palladium on charcoal) at 60°C. When the absorption of hydrogen had stopped, the reaction mixture was cooled and the solvent was poured off under nitrogen and discarded. The tetraamine was separated from the catalyst by dissolving it in 100 ml. of degassed 2*N* hydrochloric acid and filtering into 200 ml. of concentrated hydrochloric acid. It was then heated under reflux for 3 hr. with 20 g. oxalic acid. A light brown material precipitated which weighed 12 g. after drying (97.5%), m.p. >360°C.

ANAL. Calcd. for $C_{10}H_6N_4O_4$: C, 48.8%; H, 2.5%; N, 22.8%. Found: C, 47.6%; H, 3.00%; N, 22.2%.

2,3,7,8-Tetrachloro-1,4,6,9-tetraazaanthracene (XV). Product XIV (12.3 g.), phosphorus oxychloride (62 g.), and antimony trichloride (123 g.) were heated to reflux temperature for 7 hr. After cooling, the reaction mixture was poured on ice-concentrated hydrochloric acid (3:1) and the residue was separated by centrifugation, washed with diluted hydrochloric acid, water, and methanol, dried, and extracted with benzene in a Soxhlet apparatus. The yield was 5.2 g. (32%) of pale yellow needles, m.p. 330°C. The infrared spectrum showed bands at 1240, 1100, 1000, and 900 $cm.^{-1}$, λ_{\max} in sulfuric acid 398 $m\mu$, $\epsilon = 22,000$.

ANAL. Calcd. for $C_{10}H_2N_4Cl_4$: C, 37.6%; H, 0.6%; N, 17.5%; Cl, 44.3%. Found: C, 37.6%; H, 0.8%; N, 17.8%; Cl, 43.3%.

When product XIV (1.23 g.), phosphorus pentachloride (4.16 g.), and antimony trichloride (10 g.) were heated under reflux for 3 hr. and the reaction product was worked up as described above, the extract in benzene

was dark and strongly fluorescent. Most of the soluble impurities were removed by a single extraction with 100 ml. of benzene. The residue was extracted in a Soxhlet apparatus (benzene) to give a yield of 0.60 g. The mother liquors were passed through a short alumina column to remove the dark impurities. By fractional crystallization of the eluate, 75 mg. of the main product could be recovered. The yield was 0.675 (42%). In another fraction 55 mg. of a lemon yellow substance, m.p. 284–285°C., crystallized out. The infrared spectrum had bands at 1260, 1250, 1240, 1160, and 1015 cm.^{-1} .

ANAL. Calcd. for $\text{C}_{10}\text{HN}_4\text{Cl}_5$: C, 33.9%; H, 0.3%; N, 15.8%; Cl, 50.0%. Found: C, 33.4%; H, 0.4%; N, 15.9%; Cl, 51.4%.

A second by-product (XII) was obtained in a few milligrams yield with a m.p. of 350°C. and infrared bands at 1260, 1175, and 1020 cm.^{-1} .

2,3,5,7,8,10-Hexachloro-1,4,6,9-tetraazaanthracene. 2,3,7,8-Tetrachloro-1,4,6,9-tetraazaanthracene (100 mg.), phosphorus pentachloride (1 g.), and antimony trichloride (1 g.) were heated for 1 hr. from 150 to 300°C. (oil bath). After cooling, water was added, the yellow residue was separated by centrifugation, washed with dilute hydrochloric acid, water, and methanol, and dried. The yield was 78 mg. A recrystallized sample was identical in melting point (350°C.) and infrared and ultraviolet spectra with the second by-product described in the preceding experiment.

ANAL. Calcd. for $\text{C}_{10}\text{N}_4\text{Cl}_6$: C, 30.9%; H, 0.0%; N, 14.4%; Cl, 54.4%. Found: C, 28.8%; H, 1.03%; Cl, 53.7%.

2,3,7,8-Tetraphenoxy-1,4,6,9-tetraazaanthracene (XVI). 2,3,7,8-Tetrachloro-1,4,6,9-tetraazaanthracene (IX, 320 mg.) and sodium phenoxide (930 mg.) were heated under reflux in dimethylformamide (15 ml.). After cooling, the precipitate was separated by filtration and washed with hot water. After drying, the nearly colorless residue weighed 428 mg. (yield, 82%). The recrystallized product (dioxane) had infrared bands at 1440, 1350, and 1210 cm.^{-1} , m.p. 360°C. λ_{max} in sulfuric acid 394 $\text{m}\mu$, $\epsilon = 27,600$.

ANAL. Calcd. for $\text{C}_{22}\text{N}_4\text{O}_4$: C, 74.2%; H, 4.0%; N, 10.2%. Found: C, 73.8%; H, 4.2%; N, 10.2%.

In an alternate method, 2,3,7,8-tetrachloro-1,4,6,9-tetraazaanthracene (XV) (6.4 g.) was heated under reflux in phenol (15 g.) for 14 hr. After 1 hr., nearly colorless crystals started to separate. After cooling, the solid mass was extracted with hot methanol until the methanol was colorless. The yield was 9.7 g. (88%).

2,2'-Bisfluorflavine (XVII). (a) 2,3,2',3'-Tetraphenoxy-6,6'-bisquinoxaline (63 mg.) and *o*-phenylenediamine (43 mg.), were heated under reflux in phenol (4 g.) for 1 hr. Light red crystals started to separate after about 10 minutes. After cooling, dioxane (10 ml.) was added and the precipitate was separated by filtration, washed with dioxane, and dried. The yield was 39 mg. (84%) of orange crystals, λ_{max} in dimethylformamide

at 459, 433, 410 $m\mu$, λ_{\max} sulfuric acid at 479, 515 $m\mu$, $\epsilon = 48,000$; 479 $m\mu$, $\epsilon = 54,000$.

ANAL. Calcd. for $C_{28}H_{18}N_8$: C, 72.1%; H, 3.8%; N, 24.0%. Found: C, 72.0%; H, 3.9%; N, 23.9%.

(b) 3,3'-Diaminobenzidine (107 mg.) and 2,3-diphenoxyquinoxaline (628 mg.) were heated under reflux for 1 hr. in phenol (4 g.). After 5 minutes, light red crystals started to precipitate. After cooling, dioxane (10 ml.) was added, the orange crystals were filtered, washed with dioxane and dried. The yield was 205 mg. (88%). The spectrum was identical with that of the material obtained below.

(c) Tetrahydroxybisquinoxaline (3.22 g.) and *o*-phenylenediamine (2.16 g.) were heated in polyphosphoric acid (50 g.) for 2 hr. at 250°C. The resulting red solution was poured into 1 liter of water with stirring. After washing with hot water and drying, the precipitate weighed 7.17 g. and was hygroscopic. Part of it was extracted in a Soxhlet apparatus with 88% formic acid to give a partly crystalline brown-orange fluofflavine with λ_{\max} in dimethylformamide at 458, 433, and 411 $m\mu$.

5,6,8,9,14,15,17,18-Octaza-6,8,15,17-tetrahydroheptacene (XVIII). (a) Tetraazatetraphenoxanthracene (XVI; 50.2 mg.) and *o*-phenylenediamine (50 mg.) were heated under reflux in phenol (10 g.) for 4 hr. The hot solution was filtered through a glass filter and the residue was washed with dioxane and dried. The yield was 32 mg. (82%), m.p. >360°C. λ_{\max} in sulfuric acid: 568, 524, 489, 458 $m\mu$.

ANAL. Calcd. for $C_{22}H_{14}N_8$: C, 67.7%; N, 28.8%; H, 3.6%. Found: C, 67.4%; N, 28.5%; H, 3.5%.

(b) 1,2,4,5-Tetraaminobenzenetetrahydrochloride (28 mg.) and 2,3-diphenoxyquinoxaline (100 mg.) were heated under reflux in phenol (4 g.) for 2 hr. Then the liquid was filtered off and the residue washed with dioxane and dried. The yield was 24 mg. (61%), λ_{\max} in sulfuric acid 567, 524, 489, 458 $m\mu$.

(c) The condensation product XIV (1.23 g.) and *o*-phenylenediamine (1.08 g.) were heated in polyphosphoric acid (50 g.) within 45 min. to 300°C. and kept at that temperature 1½ hr. After cooling to 100°C., the deep violet solution was poured into ice water with stirring. The red precipitate was separated by centrifugation, washed five times with 400 ml. of water and dried under reduced pressure at 120°C. The yield was 2.79 g. of a green, metallike material. It is only sparingly soluble in dimethylacetamide, glacial acetic acid, and nitrobenzene and soluble in dimethyl sulfide, formic acid, and sulfuric acid; λ_{\max} in sulfuric acid at 567, 524, 489, 458 $m\mu$.

Polyfluofflavine (XX). (a) 3,3'-Diaminobenzidine (0.5357 g.) and 2,3,2',3'-tetraphenoxyl-6,6'-bisquinoxaline (1.5667 g.) were heated under reflux in phenol (60 g.) for 20 hr. (nitrogen atmosphere). The solution turned red, and became turbid after 20 minutes. After cooling to 100°C.,

dioxane (60 ml.) was added to the suspension, and the red solid was separated by centrifugation, washed with dioxane and methanol, and dried. The yield was 1.15 g. The visible spectrum had maxima at 508 and 548 $m\mu$. (sulfuric acid). The inherent viscosity was 0.3 in sulfuric acid (0.5%), m.p. $>360^\circ\text{C}$.

ANAL. Calcd. for $\text{C}_{14}\text{H}_8\text{N}_4$: C, 72.2%; H, 3.5%; N, 24.3%. Found: C, 65.7%; H, 3.9%; N, 18.7%, Residue 4.2%. This sample was particularly hard to form.

(b) 3,3'-Diaminobenzidine (2.143 g.) and 2,3,2',3'-tetrahydroxy-6,6'-bisquinoxaline (3.223 g.) were heated in polyphosphoric acid (100 g.) within 30 min. to 300°C . and kept for 3 hr. at this temperature. After cooling to 100°C ., the red solution was poured into 1 liter of water with vigorous stirring. The precipitate was separated by centrifugation, washed with 3 liters of hot water, and dried under reduced pressure at 120°C . The product weighed 6.1 g. For purification, it was redissolved in 250 ml. of sulfuric acid, filtered, and poured slowly and with vigorous stirring into 2 liters of water. The precipitate was washed five times with 1 liter of hot water until the filtrate was free of SO_4^- ions. The product had an inherent viscosity of 0.2 (0.5% in concentrated sulfuric acid), λ_{max} at 508 $m\mu$ and a shoulder at 537 $m\mu$ (sulfuric acid). It did not melt below 360°C .

ANAL. Calcd. for $(\text{C}_{14}\text{H}_8\text{N}_4)_n$: C, 72.2%; H, 3.5%; N, 24.3%. Found: C, 58.8%; H, 3.7%; N, 16.6%, Residue 12.1%.

Polyoctazatetrahydroheptacene (XIX). (a) 3,3'-Diaminobenzidine (0.4285 g.) and tetraphenoxy compound (XIV) (1.1014 g.) were heated under reflux for 16 hr. in phenol (40 g.) (nitrogen atmosphere). After cooling to 100°C ., dioxane (40 ml.) was added, and the precipitate was separated by centrifugation, washed with dioxane and methanol, and dried. The yield was 0.55 g. The material dissolved in sulfuric acid with formation of violet color and had λ_{max} at 589, 545 $m\mu$ and a shoulder at 507 $m\mu$. The inherent viscosity in sulfuric acid was 0.135 (0.5%), m.p. $>360^\circ\text{C}$.

(b) The tetrahydroxy compound (X) (1.23 g.) and 3,3'-diaminobenzidine (1.07 g.) were heated in polyphosphoric acid (50 g.) within 30 min. to 300°C . and kept at this temperature for 3 hr. After cooling to 100°C ., the blue solution was poured into 2 liters of water with vigorous stirring. The precipitate was washed with 4 liters of hot water and dried. The yield was 2.10 g. of a copperlike, shiny material. The inherent viscosity in sulfuric acid (0.5%, 30°C .) was 0.3. The polymer dissolved with blue color in sulfuric acid and had λ_{max} at 618 and 564 $m\mu$ and a shoulder at 525 $m\mu$, m.p. $>360^\circ\text{C}$.

ANAL. Calcd. for $(\text{C}_{22}\text{H}_{12}\text{N}_8)_n$: C, 67.8%; H, 3.2%; N, 29.0%. Found: C, 63.2%; H, 3.3%; N, 20.4%, Residue 3.2%.

This work was supported by the Air Force Materials Laboratory, Research and Technology Division, Air Force Systems Command, Wright-Patterson Air Force Base, Ohio.

References

1. J. K. Stille and J. R. Williamson, *J. Polymer Sci. A*, **2**, 3867 (1964).
2. G. P. de Gaudemaris and B. J. Sillon, *J. Polymer Sci., B*, **2**, 203 (1964).
3. G. P. de Gaudemaris, B. J. Sillon, and J. Preve, *Bull. Soc. Chim., France*, **1964**, 1793.
4. J. F. Brown, in *First Biannual American Chemical Society Polymer Symposium (J. Polymer Sci. C, 1)*, H. W. Starkweather, Jr., Ed., Interscience, New York, 1963, p. 83.
5. W. De Winter and C. S. Marvel, *J. Polymer Sci. A*, **2**, 5123 (1964).
6. O. Hansberg and J. Pollak, *Ber.*, **29**, 784 (1896).
7. G. M. Badger and P. J. Nelson, *Australian J. Chem.*, **16**, 445 (1963).
8. H. Baganz and K. Krüger, *Ber.*, **91**, 806 (1958).
9. M. A. Phillips, *J. Chem. Soc.*, **1928**, 2393.
10. G. W. H. Cheeseman, *J. Chem. Soc.*, **1955**, 1804.
11. E. S. Lane, *J. Chem. Soc.*, **1953**, 2238.
12. R. Nietzki and A. Schedler, *Ber.*, **30**, 1666 (1892).

Résumé

On a préparé des *N*-hétérocycles, tétra- et heptanucléaires, leurs dimères et polymères par condensation de *o*-phénylènediamine ou 3,3'-diaminobenzidine avec le 2,3-dihydroxyquinoxaline, de 2,3,2',3'-tétrahydroxy-6,6'-bisquinoxaline ou le 2,3,7,8-tétrahydroxy-1,4,6,9-tétra-aza-anthracène dans l'acide polyphosphorique ou avec des dérivés *O*-phénylés de ces trois derniers composés dans le phénol. Les produits de condensation sont des composés fortement colorés avec des spectres d'absorption caractéristiques. Les polymères montrent une bonne stabilité thermique.

Zusammenfassung

Tetra- und heptanukleare *N*-Heterozyklen, ihre Dimeren und Polymeren wurden durch Kondensation von *o*-Phenylendiamin oder 3,3'-Diaminobenzidin mit 2,3-Dihydroxychinolin, 2,3,2',3'-Tetrahydroxy-6,6'-bis-chinolin oder 2,3,7,8-Tetrahydroxy-1,4,6,9-Tetraazaanthracen in Polyphosphorsäure oder mit den *O*-Phenyl-derivaten letzterer drei Verbindungen in Phenol dargestellt. Die Kondensationsprodukte sind stark gefärbte Verbindungen mit charakteristischen Absorptionsspektren. Die Polymeren zeigen eine gute thermische Beständigkeit.

Received March 1, 1966

Prod. No. 5137A

Influence of Catalyst Depletion or Deactivation on Polymerization Kinetics. II. Nonsteady-State Polymerization

R. CHIANG and J. J. HERMANS,
*Chemstrand Research Center, Inc., Research Triangle Park,
Durham, North Carolina 27702*

Synopsis

The number-average and weight-average degrees of polymerization at the end of the polymerization process have been calculated in terms of the initial monomer concentration, initial catalyst concentration, and rate constants for various polymerization processes, all of which assume instantaneous initiation. The mechanisms differ among themselves in that there is either first-order catalyst deactivation, or transfer to monomer, or both. The calculation is greatly simplified if only the molecular weights at the end of polymerization are considered. The method given is particularly useful for systems where the calculation of the distribution function as a function of time is complicated. The fact that the monomer concentration and catalyst concentration have a marked effect on the molecular weight provides a good test of the validity of the mechanism under consideration. A comparison of the calculated and observed molecular weights obtained for the homogeneous polymerization of acrylonitrile with an organometallic catalyst will be given in a later communication.

I. INTRODUCTION

The study of the polymerization mechanism by comparing the calculated and observed molecular weights is of considerable interest. If the reaction mechanism is known, the molecular weight distribution can, in principle, be calculated. Conversely, a comparison of the calculated and observed molecular weight and molecular weight distribution provides a test of the validity of the mechanism of polymerization.

However, the calculation of the molecular weight distribution is difficult when the concentrations of the monomer, catalyst, and transfer agent are changing with time or degree of polymerization; in some cases analytic solutions cannot be obtained in closed form. It is customary to calculate the molecular weight distribution by introducing simplifying assumptions. Examples of such simplifying assumptions are: (a) instantaneous initiation of polymerization; (b) no termination;¹ (c) all initiation, propagation, and termination rates are first-order with respect to monomer, so that the rate equations can be linearized by a simple transformation of the independent variable t to another variable;^{2,3} (d) the concentration of the monomer, catalyst, or solvent is kept constant.

This investigation deals with the calculation of the number- and weight-average molecular weights of polymers prepared by nonsteady-state polymerization. The calculation is greatly simplified if we are concerned only with the molecular weight averages at the end of the process. A direct comparison of the calculated and observed averages for the homogeneous polymerization of acrylonitrile with an organometallic catalyst will be given in a subsequent paper.⁴

Method of Moments

The kinetic equations may be used to derive equations for the moments.⁵⁻⁷ The n th moment of the molecular weight distribution is defined by

$$\sum_n = \sum_{k=1}^{\infty} k^n \mu_k \quad (1a)$$

where μ_k is the concentration of polymer molecules of degree of polymerization k . If both active and inactive polymers are present,

$$\sum_n = \sum_{k=1}^{\infty} k^n (n_k + \nu_k) \quad (1b)$$

where n_k is the concentration of the growing polymer and ν_k is the concentration of the inactive polymer, both with DP equal to k . The moments of distribution for the active and inactive polymers are, respectively:

$$L_n = \sum_{k=1}^{\infty} k^n n_k \quad (2a)$$

$$\Lambda_n = \sum_{k=1}^{\infty} k^n \nu_k \quad (2b)$$

For our present purpose it is sufficient to consider the values $n = 0, 1$, and 2. The number- and weight-average degrees of polymerization, including both active and inactive species are

$$\begin{aligned} \bar{P}_n &= \sum_1 / \sum_0 \\ \bar{P}_w &= \sum_2 / \sum_1 \end{aligned} \quad (3)$$

Generating Function

In many cases the complete molecular weight distribution can be derived from the kinetic equations by means of generating functions.⁸⁻¹¹ We define

$$X(z,t) = \sum_{k=1}^{\infty} n_k(t) z^k \quad (4)$$

$$Y(z,t) = \sum_{k=1}^{\infty} \nu_k(t) z^k \quad (5)$$

Differential equations for X and Y may be derived from the kinetic equations. If these differential equations can be solved, a series expansion of X and Y in powers of z yields the concentrations n_k and ν_k . Furthermore, the moments of the distribution can be derived from the generating function by differentiating with respect to $\ln z$:

$$\begin{aligned} L_n &= [\partial^n X / \partial (\ln z)^n]_{z=1} \\ \Lambda_n &= [\partial^n Y / \partial (\ln z)^n]_{z=1} \end{aligned} \quad (6)$$

Both the method of moments and the generating function have been applied by us to the problems discussed by Gold¹ and by Chien,¹² and proved to shorten the calculation to a considerable extent. Gold considered the molecular weight distribution for different ratios of propagation rate constant k_p to initiation rate constant k_i , keeping the number of propagating chains constant (no termination). The case treated by Chien is the polymerization of propylene in the presence of a Ziegler type catalyst on the assumption that the growing chain terminates by producing a dead polymer and a new active site. These calculations will not be repeated here, because the results can be found in the papers quoted. Instead, we consider three reaction schemes which to our knowledge have not been treated before.

There is good evidence that in a number of systems the growing polymer undergoes first-order deactivation (part I in this series),¹³ forming dead polymer without change in degree of polymerization. In addition, experimental evidence will be reported in a later paper⁴ which indicates that the growing polymer in our acrylonitrile polymerization undergoes not only first-order deactivation but also transfer to monomer. Finally, to establish the influence of the deactivation on \bar{P}_n and \bar{P}_w , results are given also for a mechanism in which there is transfer to monomer but no deactivation.

The processes studied here differ in many respects from those considered by Tobolsky¹⁴⁻¹⁶ and by Bamford,¹⁷ who discussed radical-induced polymerization when there is decay of initiator. Tobolsky has called this "dead-end polymerization" and has treated first-order decay with and without chain transfer to monomer. Bamford gave a more detailed treatment and included the case of second-order decay of initiator, but assumed the monomer concentration to be constant.

II. FIRST-ORDER DEACTIVATION

Assuming the initiation to be instantaneous, the reactions to be considered are propagation



and deactivation



where M represents the monomer, C the catalyst, and P_k the dead polymer with degree of polymerization k , ($k = 1, 2, \dots$). If m is the monomer concentration, the rate equations are

$$\dot{n}_k = -k_p m n_k + k_p m n_{k-1} - k_d n_k \quad (7)$$

$$\dot{m} = -k_p m L_0 \quad (8)$$

$$\dot{\nu}_k = k_d n_k \quad (9)$$

where the dot represents differentiation with respect to time t and where n_0 is taken to be zero. If a is the concentration of catalyst and b the initial concentration of monomer, the concentrations at $t = 0$ are $m(0) = b$; $\nu_1(0) = a$; $n_k(0) = 0$ when $k > 1$; $\nu_k(0) = 0$. To avoid confusion it is noted that $b = m_0^0 - a$, where m_0^0 is the monomer concentration before the (instantaneous) reaction of the monomer with the catalyst. By straightforward summation procedures one derives from eqs. (7)–(9) that

$$\begin{aligned} \dot{L}_0 &= -k_d L_0 \\ \dot{L}_1 &= -k_d L_1 + k_p m L_0 \end{aligned} \quad (10)$$

$$\begin{aligned} \dot{L}_2 &= -k_d L_2 + 2k_p m L_1 + k_p m L_0 \\ \dot{\Lambda}_0 &= k_d L_0 \\ \dot{\Lambda}_1 &= k_d L_1 \end{aligned} \quad (11)$$

$$\dot{\Lambda}_2 = k_d L_2$$

The initial values of L_n and Λ_n for all n are

$$L_n(0) = a$$

and

$$\Lambda_n(0) = 0 \quad (12)$$

Integration yields

$$L_0 = a \exp \{-k_d t\} \quad (13)$$

$$\Lambda_0 = a - L_0 = a(1 - \exp \{-k_d t\}) \quad (14)$$

Furthermore, it is seen from eqs. (7)–(11) that $dm/dL_0 = \beta m$ and $dL_1/dL_0 = L_1/L_0 - \beta m$, where

$$\beta = k_p/k_d \quad (15)$$

These results may be integrated:

$$m = b \exp \{\beta L_0 - \beta a\} \quad (16)$$

$$L_1 = L_0 + \beta b L_0 \int_{L_0}^a (dx/x) \exp \{\beta x - \beta a\} \quad (17)$$

We observe, further, that

$$\sum_1 \dot{\nu}_1 = \dot{L}_1 + \dot{\Lambda}_1 = k_p m L_0 = -\dot{m} \quad (18)$$

which is nothing but the condition of conservation of monomer. Consequently, with the use of eqs. (10), (11), and (16)

$$d\sum_1/dL_0 = -\beta m = \beta b \exp \{ \beta L_0 - \beta a \} \quad (19)$$

which integrates to

$$\sum_1 = a + b(1 - \exp \{ \beta L_0 - \beta a \}) \quad (20)$$

However, since $\sum_0 = L_0 + \Lambda_0 = a$, it follows that

$$\bar{P}_n = \sum_1/\sum_0 = 1 + (b/a)(1 - \exp \{ \beta L_0 - \beta a \}) \quad (21)$$

In particular, if we add a subscript f to denote final concentration, and remember that at the end of the reaction no active polymer is left:

$$\bar{P}_{n,f} = 1 + (b/a)(1 - \exp \{ -\beta a \}) \quad (22)$$

Likewise, the weight-average molecular weight at the end of the reaction can be evaluated as follows. From eqs. (10) and (11) we derive that

$$d\sum_2/dL_0 = -2\beta m L_1/L_0 - \beta m \quad (23)$$

TABLE I
Polymerization with Instantaneous Initiation and First-Order Deactivation^a

βa	$10^3 a$	b/a	$\Lambda_{1,f}/a$	$\Lambda_{2,f}/a$	$\bar{P}_{n,f}$	$\bar{P}_{w,f}$	Ratio
0.1	0.03690	40,730	3,878	29,250,000	3,878	7,542	1.945
0.2	0.07380	20,365	3,692	25,910,000	3,692	7,018	1.900
0.3	0.1107	13,580	3,521	23,020,000	3,521	6,538	1.856
0.4	0.1476	10,180	3,357	20,460,000	3,357	6,095	1.815
0.5	0.1845	8,146	3,206	18,270,000	3,206	5,699	1.777
0.6	0.2214	6,788	3,063	16,310,000	3,063	5,325	1.738
0.7	0.2583	5,818	2,929	14,610,000	2,929	4,988	1.702
0.8	0.2952	5,091	2,804	13,110,000	2,804	4,675	1.667
0.9	0.3321	4,525	2,685	11,790,000	2,685	4,391	1.635
1.0	0.3690	4,073	2,576	10,630,000	2,576	4,127	1.602
1.5	0.5535	2,715	2,110	6,596,000	2,110	3,102	1.470
2.0	0.7380	2,036	1,762	4,253,000	1,762	2,414	1.370
2.5	0.9225	1,629	1,496	2,903,000	1,496	1,940	1.296
3.0	1.107	1,358	1,291	2,143,000	1,291	1,659	1.285
3.5	1.292	1,163	1,129	1,529,000	1,129	1,354	1.199
4.0	1.476	1,018	1,000	1,170,000	1,000	1,170	1.170
4.5	1.661	904.8	896	920,000	896	1,026	1.145
5.0	1.845	814.6	811	740,000	811	912	1.124
6.0	2.214	678.8	678	506,000	678	746	1.100
7.0	2.583	581.8	582	369,000	582	634	1.089
10.0	3.690	407.3	408	172,700	408	423	1.036
20.0	7.380	203.6	205	43,060	205	210	1.024
40.0	14.76	101.8	103	10,760	103	104	1.009

^a Initial monomer concentration $b = 1.504$ mole/1000 g.; $\beta = k_p/k_d = 2710$ (mole/1000 g.)⁻¹; catalyst concentration a changes.

TABLE II
Polymerization with Instantaneous Initiation and First-Order Deactivation^a

βa	β	$\bar{P}_{n,f}$	$P_{w,f}$	Ratio
0.1	66.5	96	187	1.948
0.2	133.0	182	347	1.910
0.3	199.6	260	483	1.857
0.4	266.1	331	598	1.809
0.5	332.6	396	698	1.763
0.6	399.2	452	786	1.739
0.7	465.7	504	859	1.704
0.8	532.2	552	919	1.665
0.9	598.8	594	972	1.636
1.0	665	633	1,014	1.601
1.5	998	778	1,143	1.469
2.0	1,330	866	1,186	1.370
2.5	1,663	919	1,192	1.297
3.0	1,996	951	1,181	1.242
3.5	2,328	971	1,165	1.199
4.0	2,661	983	1,149	1.169
4.5	2,994	990	1,134	1.145
5.0	3,326	994	1,123	1.130
6.0	3,992	999	1,098	1.099
7.0	4,657	1,000	1,086	1.086
10.0	6,650	1,001	1,037	1.036
20.0	13,300	1,001	1,027	1.026
40.0	26,610	1,001	1,012	1.011

^a $b/a = 1000$ (fixed); $a = 1.504 \times 10^{-3}$ mole/1000 g.; β changes.

where m and L_1 may be considered as functions of L_0 [eqs. (16) and (17)] Now, initially, L_0 and \sum_2 are both equal to a . At the end of the reaction L_0 is zero, and it follows therefore that the final value of \sum_2 is

$$\sum_{2,f} = \Lambda_{2,f} = a + \int_a^0 dL_0 d\sum_2/dL_0 \quad (24)$$

On account of eqs. (16), (17), and (23), this becomes

$$\sum_{2,f} = a + 3b(1 - e^{-\beta a}) - 2\beta^2 b^2 \int_a^0 dx e^{\beta(x-a)} \int_x^a (dy/y) e^{\beta(y-a)} \quad (25)$$

Changing the order of integration:

$$\sum_{2,f} = a + 3b(1 - e^{-\beta a}) + 2\beta b^2 e^{-2\beta a} \int_0^a (dy/y) (e^{2\beta y} - e^{\beta y}) \quad (26)$$

The last term may be given a recognizable form if it is considered as

$$\begin{aligned} \lim_{\epsilon=0} \left[\int_{\epsilon}^{\beta a} (dy/y) e^{2y} - \int_{\epsilon}^{\beta a} (dy/y) e^y \right] \\ = \lim_{\epsilon=0} \left[\int_{\beta a}^{2\beta a} (dy/y) e^y - \int_{\epsilon}^{2\epsilon} (dy/y) e^y \right] \quad (27) \end{aligned}$$

which may be written as $V(\beta a) - \ln 2$, where

$$V(u) = \int_u^{2u} (dy/y) \exp \{y\} = (Ei[2u] - Ei[u]) \tag{28}$$

$Ei[u]$ is the exponential integral

$$Ei[u] = \int_{-\infty}^u (dy/y) \exp \{y\} \tag{29}$$

for which tables can be found in the literature.^{18,19} One obtains, therefore,

$$\begin{aligned} \frac{\sum_{2,f}}{a} = 1 + 3 \frac{b}{a} (1 - e^{-\beta a}) \\ + 2 \left(\frac{b}{a}\right)^2 \beta a e^{-2\beta a} (Ei[2\beta a] - Ei[\beta a] - \ln 2) \end{aligned} \tag{30}$$

On the other hand, it is seen from eq. (20) that

$$\sum_{1,f}/a = 1 + (b/a)(1 - \exp \{-\beta a\}) \tag{31}$$

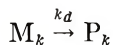
so that the ratio $\bar{P}_{w,f} = \sum_{2,f}/\sum_{1,f}$ may be calculated when b/a and βa are known. Some results are shown in Tables I and II.

III. DEACTIVATION ACCOMPANIED BY TRANSFER TO MONOMER

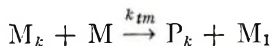
For instantaneous initiation the reactions to be considered are propagation:



deactivation:



and transfer:



Then

$$\dot{n}_1 = -k_p m n_1 - k_d n_1 + k_{tm} m \sum_{k=2}^{\infty} n_k \tag{32}$$

$$\dot{n}_k = -k_p m n_k + k_p m n_{k-1} - k_d n_k - k_{tm} m n_k \quad k \geq 2 \tag{33}$$

$$\dot{\nu}_k = (k_d + k_{tm} m) n_k \tag{34}$$

$$\dot{m} = -(k_p + k_{tm}) m L_0 \tag{35}$$

subject to the following initial conditions: $m(0) = b$; $n_1(0) = a$; all other $n_k(0) = 0$; $\nu_k(0) = 0$.

Note that in this scheme P_1 and M are not considered as identical species. P_1 contains a catalyst fragment and is supposed not to participate in polymerization.

Summation gives $\dot{L}_0 = -k_d L_0$; hence $L_0 = a \exp \{-k_d t\}$ so that eq. (35) may be integrated to give

$$\begin{aligned} \ln (m/b) &= -[(k_p + k_{tm})/k_d]a(1 - \exp \{-k_d t\}) \\ m_f &= b \exp \{-(k_p + k_{tm})a/k_d\} \end{aligned}$$

For the sake of convenience, the following abbreviations are used:

$$r = k_p/k_d \quad (36)$$

$$s = k_{tm}/k_d$$

$$q = r + s \quad (37)$$

$$r/q = \gamma$$

so that we have

$$m_f = b \exp \{-qa\} \quad (38)$$

$$m = b \exp \{qL_0 - qa\} \quad (39a)$$

or

$$\ln (1 - \xi) = q(L_0 - a) \quad (39b)$$

where ξ is the degree of conversion. At $t = \infty$:

$$\ln (1 - \xi_f) = -qa \quad (40)$$

which is the relation derived previously.¹³ It shows that if the mechanism postulated is correct, a straight line is obtained when plotting $\ln (1 - \xi_f)$ against the initial catalyst concentration a . This straight line will go through the origin and have a slope equal to $-(k_p + k_{tm})/k_d$. The converse of this is, of course, not necessarily true. In fact, it was found in Section II that a linear relation between $\ln (1 - \xi_f)$ and a exists also when there is no transfer to monomer, but the slope of the line equals $-k_p/k_d$ [see eq. (16) in which $L_0 = 0$].

On summing the eq. (34) and dividing the sum by eq. (35), it follows that

$$qd\Lambda_0/dm = s - 1/m$$

Hence

$$q\Lambda_0 = s(b - m) + \ln (b/m) \quad (41)$$

$$q\Lambda_{0,f} = qa + sb(1 - \exp \{-qa\}) \quad (42)$$

The number-average degree of polymerization at the end of the reaction, when unreacted monomer is not removed is

$$\bar{P}_{n,f} = \frac{a + b}{\Lambda_{0,f} + m_f} \quad (43a)$$

where

$$\Lambda_{0,f} + m_f = a + (b/q)(s + re^{-qa})$$

Of the $\Lambda_{0,f} + m_f$ molecules at the end of the reaction, only a molecules carry a catalyst fragment at the end. The number-average when all (and nothing but) unreacted monomer is removed is

$$\bar{P}_{n,f} = \frac{a + b - m_f}{\Lambda_{0,f}} = \frac{a + bH}{a + sbH/q} \quad (43b)$$

where

$$H = 1 - e^{-qa}$$

Here again, only a of the $\Lambda_{0,f}$ molecules carry a catalyst fragment as end-group. In either case it will often be a good approximation to set $\bar{P}_{n,f} = q/s = (k_p + k_{tm})/k_{tm}$ because with high degrees of polymerization $a \ll b$ and qa is large when the degree of conversion is high.

It may be noted that eq. (43b) can be obtained also from eqs. (32) and (33) by summing $k\dot{n}_k$, which gives

$$\dot{L}_1 = (k_p + k_{tm})mL_0 - (k_d + mk_{tm})L_1 \quad (44a)$$

Also

$$\dot{\Lambda}_1 = (k_d + k_{tm})L_1 \quad (44b)$$

so that

$$\dot{L}_1 + \dot{\Lambda}_1 = (k_p + k_{tm})mL_0 = -\dot{m} \quad (45)$$

This expresses the conservation of monomer and may be integrated immediately to give the result already shown.

After multiplying the rate equations by k^2 and summing over k one obtains

$$\dot{L}_2 = 2k_p mL_1 + (k_p + k_{tm})mL_0 - (k_d + k_{tm}m)L_2 \quad (46)$$

$$\dot{\Lambda}_2 = (k_d + k_{tm}m)L_2 \quad (47)$$

Consequently,

$$\dot{\Sigma}_2 = 2k_p mL_1 + (k_p + k_{tm})mL_0 \quad (48)$$

Now define the function

$$\psi = d\Sigma_2/dm \quad (49)$$

If eq. (48) is divided by eq. (35) it is found that

$$L_0\psi = -L_0 - 2\gamma L_1 \quad (50)$$

where γ is the quantity defined by eq. (37). Differentiating eq. (50) with respect to L_0 yields

$$\psi + L_0 d\psi/dL_0 = -1 - 2\gamma dL_1/dL_0 \quad (51)$$

On the other hand, if eq. (44a) is divided by $\dot{L}_0 = -k_d L_0$ one finds

$$dL_1/dL_0 = -qm + (1 + sm)L_1/L_0 \quad (52)$$

so that eq. (51) may be written

$$\psi + L_0 d\psi/dL_0 = -1 + 2rm + (1 + sm)(\psi + 1) \quad (53)$$

where use has been made of eq. (50) to express L_1/L_0 in terms of ψ . It is clear that eq. (53) is a differential equation for ψ in terms of L_0 if it is remembered that m is a function of L_0 [see eq. (39a)]. The integration of eq. (53) gives

$$\ln(2r + s + s\psi) = K + sbe^{-qa} \int_a^{L_0} (dx/x)e^{qx} \quad (54)$$

where K is an integration constant. At the beginning of the process, $L_1 = L_0 = a$, from which it follows on account of eq. (50) that

$$\psi(0) = -(3r + s)/q \quad (55)$$

Hence

$$K = \ln(2r^2/q) \quad (56)$$

and eq. (54) becomes

$$\ln[(2r + s + s\psi)q/2r^2] = \lambda\Phi(L_0) \quad (57)$$

$$\lambda = sb \exp\{-qa\} \quad (58)$$

$$\Phi(L_0) = Ei[qL_0] - Ei[qa] \quad (59)$$

If we rewrite eq. (49) as follows:

$$d\sum_2/dm = \psi = -1 - 2r/s + (2r^2/qs) \exp\{\lambda\Phi\} \quad (60)$$

and remember that initially $\sum_2 = a$ and $m = b$, it is found that

$$\sum_2 = a + (1 + 2r/s)(b - m) + (2r^2/qs) \int_b^m dm \exp\{\lambda\Phi\} \quad (61)$$

The integral in this expression may be replaced by an integral over the variable Φ if we make use of the fact that on account of eq. (39a):

$$dm/dL_0 = qb \exp\{qL_0 - qa\} \quad (62)$$

and because of eq. (59):

$$dL_0/d\Phi = L_0 \exp\{-qL_0\} \quad (63)$$

This leads to

$$\Sigma_2 = a + (1 + 2r/s)(b - m) + (2r^2/s)be^{-qa} \int_0^\Phi d\Phi L_0 e^{\lambda\Phi} \quad (64)$$

At the end of the process $L_2 = 0$, $m = m_f$ and $\Phi = -\infty$ (because $L_0 \rightarrow 0$). Hence

$$\Sigma_{2,f} = a + (1 + 2r/s)(b - m_f) - (2r^2/s)be^{-qa} \int_{-\infty}^0 d\Phi L_0 e^{\lambda\Phi} \quad (65)$$

where m_f is determined by eq. (39a). To evaluate $\Sigma_{2,f}$, the quantity L_0 is plotted versus Φ , by use of eq. (59) for the relation between L_0 and Φ . Then $L_0 \exp\{\lambda\Phi\}$ is plotted versus Φ and the integral, eq. (65) is determined graphically.

For the case of the polymerization of acrylonitrile with $\text{NaAlEt}_2\text{S}(i\text{-Pr})$ in DMF at -30°C . as an example,⁴ the experimental conditions and the rate constants are as follows:

$$q = r + s = (k_p + k_{tm})/k_d = 2710 \text{ (mole/1000 g.)}^{-1}$$

$$k_d = 0.0628 \text{ min.}^{-1}$$

$$k_p + k_{tm} = 170 \text{ (mole/1000 g.)}^{-1} \text{ min.}^{-1}$$

$$b = m(0) = 1.504 \text{ mole/1000 g.}$$

Thus, $\lambda = (k_{tm}/k_d)b \exp\{-(k_p + k_{tm})a/k_d\} = 0.142$ by eq. (58). The values of $L_0 \exp\{\lambda\Phi\}$ are given in Table III, and a plot versus Φ is shown in Figure 1. The integral is calculated from the area under the curve and is found to be 4.24×10^{-3} mole/1000 g. The final results are: $\Lambda_{0,f} = 2.16 \times 10^{-3}$, $\Lambda_{1,f} = 1.432$, $\Lambda_{2,f} = 1665$ mole/1000 g.; $\bar{P}_{n,f} = 660$, $\bar{P}_{w,f} = 1160$.

The results obtained in this section can also be derived by means of the generating functions X and Y defined by eqs. (4) and (5). In fact, it is easy to derive the differential equations for X and Y from the kinetic equa-

TABLE III
Evaluation of the Integral $\int_{-\infty}^0 d\Phi L_0 e^{\lambda\Phi}$ in Eq. (65)

$L_0 \times 10^3$	pL_0	$Ei[qL_0]$	Φ	$\lambda\Phi$	$e^{\Phi\lambda}$	$L_0 e^{\lambda\Phi} \times 10^3$
0	0	$-\infty$	$-\infty$	$-\infty$	0	0
0.0369	0.1	-1.623	-11.78	-1.673	0.188	0.00693
0.185	0.5	0.454	-9.69	-1.376	0.252	0.0466
0.369	1.0	1.895	-8.24	-1.170	0.310	0.114
0.553	1.5	3.301	-6.84	-0.970	0.379	0.210
0.738	2.0	4.954	-5.19	-0.737	0.477	0.352
0.923	2.5	7.074	-3.07	-0.436	0.644	0.594
1.033	2.8	8.679	-1.46	-0.207	0.810	0.837
1.108	3.0	9.934	-0.21	-0.030	0.970	1.075
1.12	3.03	10.14	0	0	1.000	1.12

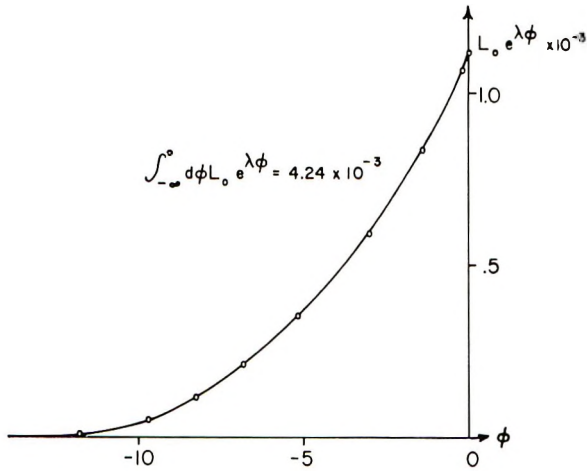


Fig. 1. Evaluation of integral $\int_{-\infty}^0 d\Phi L_0 e^{\lambda \Phi}$ for $b = 1.504$ and $a = 1.12 \times 10^{-3}$.

tions, eqs. (32)–(35). The solution of these differential equations is comparatively simple, and the zeroth, first, and second moments have been obtained by means of eq. (6). However, a series expansion of the generating functions leads to molecular weight distributions that are so complicated as to have little practical value. For this reason the calculation is not presented here.

IV. TRANSFER TO MONOMER BUT NO DEACTIVATION

We can get all the results for this case from Section III by letting k_d become zero, but in the expressions that lead to \bar{P}_w this procedure is sometimes so complicated that it is simpler to repeat part of the calculation. From the result $L_0 = a \exp \{-k_d t\}$ obtained in the previous section we conclude that in the present case $L_0 = a$ so that eq. (35) now leads to

$$m = b \exp \{-(k_p + k_{tm})at\} \quad (66)$$

As r , s , and q defined by eqs. (36) and (37) become infinite, eq. (41) reduces to

$$\begin{aligned} \Lambda_0 &= (b - m)k_{tm}/(k_p + k_{tm}) \\ \Lambda_{0,f} &= k_{tm}b/(k_p + k_{tm}) \end{aligned} \quad (67)$$

since m_f is now zero [see eq. (38)]. Both eqs. (43a) and (43b) must therefore be replaced by

$$\bar{P}_{n,f} = \frac{a + b}{L_{0,f} + \Lambda_{0,f}} = \frac{(k_p + k_{tm})(a + b)}{(k_p + k_{tm})a + k_{tm}b} \quad (68)$$

which could also have been found directly from eq. (43b) by inserting $k_a = 0$. Equation (48) remains valid, with $L_0 = a$, and this equation may now be solved by introducing a new variable σ such that

$$\begin{aligned} d\sigma &= mdt \\ \sigma(0) &= 0 \end{aligned} \quad (69)$$

It follows from eq. (66) that at $t = \infty$:

$$\sigma = \sigma_f = b/(k_p + k_{tm})a \quad (70)$$

In terms of the variable σ , eqs. (44a) and (48) become

$$dL_1 + k_{tm}L_1d\sigma = (k_p + k_{tm})ad\sigma, \quad (71)$$

$$d\Sigma_2 = [2k_pL_1 + (k_p + k_{tm})a]d\sigma \quad (72)$$

or, after integration

$$L_1/a = 1 + (k_p/k_{tm})[1 - \{\exp -k_{tm}\sigma\}] \quad (73)$$

$$\begin{aligned} \Sigma_2/a &= 1 + (k_p + k_{tm})(2k_p + k_{tm})\sigma/k_{tm} \\ &\quad - 2(k_p/k_{tm})^2[1 - \exp\{-k_{tm}\sigma\}] \end{aligned} \quad (74)$$

Inserting the value of eq. (70) for σ_f gives

$$\frac{\Sigma_{2,f}}{a} = 1 + \frac{2k_p + k_{tm}}{k_{tm}} \frac{b}{a} - 2\left(\frac{k_p}{k_{tm}}\right)^2 \left(1 - \exp\left\{-\frac{k_{tm}}{k_p + k_{tm}} \frac{b}{a}\right\}\right) \quad (75)$$

The value of $\bar{P}_{w,f}$ follows immediately when we remember that the conservation of monomer requires $\Sigma_{1,f}$ to be equal to $(a + b)$.

References

1. L. Gold, *J. Chem. Phys.*, **28**, 91 (1958).
2. R. Ginell and R. Simha, *J. Am. Chem. Soc.*, **65**, 706 (1943).
3. W. T. Kyner, J. R. M. Radok, and M. Wales, *J. Chem. Phys.*, **30**, 363 (1959).
4. R. Chiang and H. N. Friedlander, *J. Polymer Sci. A-1*, **4**, 2857 (1966).
5. G. Beall, *J. Polymer Sci.*, **4**, 483 (1949).
6. G. Herdan, *J. Polymer Sci.*, **10**, 1 (1953).
7. C. H. Bamford, W. G. Barb, A. D. Jenkins, and P. F. Onyon, *The Kinetics of Vinyl Polymerization by Radical Mechanisms*, Academic Press, New York, 1958.
8. C. H. Bamford and A. D. Jenkins, *Trans. Faraday Soc.*, **56**, 907 (1960).
9. W. H. Abraham, *Ind. Eng. Chem. Fundamentals*, **2**, 221 (1963).
10. H. Kilkson, *Ind. Eng. Chem. Fundamentals*, **3**, 281 (1964).
11. J. J. Hermans, in *Perspectives in Polymer Science (J. Polymer Sci. C, 12)*, E. S. Proskauer, E. H. Immergut, and C. G. Overberger, Eds., Interscience, New York, 1966, p. 345.
12. J. C. W. Chien, *J. Polymer Sci. A*, **1**, 425 (1963).
13. H. N. Friedlander, *J. Polymer Sci. A*, **2**, 3885 (1964).
14. A. V. Tobolsky, *J. Am. Chem. Soc.*, **80**, 5927 (1958).
15. R. H. Gobran, M. B. Berenbaum, and A. V. Tobolsky, *J. Polymer Sci.*, **46**, 431 (1960).
16. A. V. Tobolsky, R. H. Gobran, R. Bohme, and R. Schaffhauser, *J. Phys. Chem.*, **67**, 2336 (1963).

17. C. H. Bamford, *Polymer*, **6**, 63 (1965).
18. E. Jahnke and F. Emde, *Tables of Functions with Formulae and Curves*, 4th Ed., Dover Publications, New York, 1945.
19. S. M. Selby, R. C. Weast, R. S. Shankland, and C. D. Hodgman, Eds., *Handbook of Mathematical Tables*, Chemical Rubber Publ. Co., Cleveland, Ohio, 1962, p. 349.

Résumé

Les degrés de polymérisation moyens en nombre et en poids en fin de polymérisation ont été calculés sur la base de la concentration initiale en monomère et la concentration initiale en catalyseur, et les constantes de vitesses pour les différents processus de polymérisation, tous supposant une initiation instantanée. Les mécanismes diffèrent entre eux en ce sens qu'il y a soit une désactivation en catalyseur de premier-ordre, soit un transfert sur monomère, soit les deux. Le calcul est grandement simplifié si on considère uniquement les poids moléculaire en fin de polymérisation. La méthode est particulièrement utile pour les systèmes où le calcul de la fonction de distribution comme fonction du temps est compliquée. Le fait que la concentration en monomère et la concentration en catalyseur ont un effet marqué sur le poids moléculaire fournit un excellent test pour contrôler la validité du mécanisme considéré. Une comparaison des poids moléculaires calculés et obtenus en cours de polymérisation homogène de l'acrylonitrile avec un catalyseur organométallique sera donnée dans une communication ultérieure.

Zusammenfassung

Der Zahlenmittelwert und der Gewichtsmittelwert des Polymerisationsgrades am Ende der Polymerisation wurde aus der Anfangsmonomerkonzentration, der Anfangskatalysatorkonzentration und den Geschwindigkeitskonstanten für verschiedene Polymerisationsprozesse, bei welchen allen momentaner Start angenommen wird, berechnet. Die Mechanismen unterscheiden sich dadurch, dass entweder eine Katalysatordesaktivierung erster Ordnung oder Übertragung zum Monomeren oder beides angenommen wird. Die Berechnung wird stark vereinfacht, wenn nur die Molekulargewichte am Ende der Polymerisation betrachtet werden. Die angegebene Methode ist besonders bei solchen Systemen wertvoll, bei welchen die Berechnung der Verteilungsfunktion als Funktion der Zeit kompliziert ist. Die Tatsache, dass Monomer- und Katalysatorkonzentration einen merklichen Einfluss auf das Molekulargewicht besitzen, liefert einem Test für die Gültigkeit des betrachteten Mechanismus. Ein Vergleich der berechneten und der beobachteten, bei der homogenen Polymerisation von Acrylnitril mit einem metallorganischen Katalysator erhaltenen Molekulargewichte wird in einer späteren Mitteilung durchgeführt werden.

Received March 6, 1966

Revised March 23, 1966

Prod. No. 5143A

Influence of Catalyst Depletion or Deactivation on Polymerization Kinetics. III. Solution Polymerization of Acrylonitrile in *N,N*-Dimethylformamide at -30°C .

R. CHIANG and H. N. FRIEDLANDER,
*Chemstrand Research Center, Inc., Research Triangle Park,
Durham, North Carolina 27702*

Synopsis

The experimental results on homogeneous polymerization of acrylonitrile initiated with the sodium triethylthioisopropoxyaluminate, $\text{NaAlEt}_3\text{S}(i\text{-Pr})$, catalyst in DMF at -30°C . are compared with the prediction of equations based on a postulated mechanism. The agreement between the calculated and observed number-average molecular weight combined with the kinetic data and the relationship between the conversion and the initial catalyst concentration provides a rigorous test concerning the validity of the equations and the mechanism of the polymerization. A plausible mechanism is postulated as follows: The initiation must be relatively fast in accordance with the rate equations and the growing polymer undergoes propagation, transfer (to monomer), and deactivation simultaneously. The infrared spectrum of the low molecular weight polymer prepared at a high catalyst concentration showed strong absorption at 2337, 2205, and 1620 cm^{-1} but no absorption at 900 cm^{-1} , indicating that there are two nitriles in the polymer, one of which is conjugated. The possibility of having $-\text{CH}=\text{CH}_2$ groups in the polymer is ruled out by the absence of the band at 900 cm^{-1} . In view of these facts, it is concluded that the polymer has a $-\text{CH}=\text{CHCN}$ endgroup resulting from the transfer reaction.

I. INTRODUCTION

This is Part III of a series of reports dealing with the influence of catalyst depletion or deactivation on polymerization kinetics. Part I deals with the integrated kinetic expressions obtained on the basis of catalyst depletion but no termination.¹ In Part II, a set of equations has been derived by Chiang and Hermans² which enables us to calculate the weight-average and number-average molecular weights on the basis of the mechanism postulated. Among various cases considered, the one of particular interest to us involved a scheme in which the initiation is assumed to be instantaneous and the active polymer undergoes propagation, first-order deactivation, and transfer to monomer simultaneously. Although the instantaneous molecular weight distribution of such a system cannot be calculated by simple methods, the weight-average and number-average molecular

weights at the end of polymerization can be calculated in terms of the monomer concentration, catalyst concentration, and various rate constants.

In order to demonstrate the usefulness of these equations, the polymerization of acrylonitrile initiated with the $\text{NaAlEt}_2\text{S}(i\text{-Pr})$ catalyst in DMF at -30°C .³ was studied. The comparison of the calculated and observed molecular weights and the fit to the kinetic expressions put these equations to a critical test and give information on the mechanism of polymerization.

II. REVIEW OF EQUATIONS

If the reaction occurs under the above specified conditions, then we have:

$$-\ln(1 - \xi) = (r + s)a(1 - \exp\{-k_d t\}) \quad (1)$$

where

$$r = k_p/k_d$$

$$s = k_{tm}/k_d$$

where ξ is the conversion at any time t , a is the initial catalyst concentration, and k_p , k_{tm} , and k_d are the rate constants of propagation, transfer, and deactivation, respectively.

At $t = \infty$, eq. (1) is reduced to:

$$-\ln(1 - \xi_\infty) = (r + s)a \quad (2)$$

It can be shown readily from eqs. (1) and (2) that

$$\ln\left(\ln\frac{1 - \xi}{1 - \xi_\infty}\right) = \ln\left(\ln\frac{1}{1 - \xi_\infty}\right) - k_d t \quad (3)$$

where ξ_∞ is the conversion at $t = \infty$. According to eq. (2), a straight line can be obtained by plotting $\log(1 - \xi_\infty)$ against a , irrespective of the monomer concentration.

The second, first, and zeroth moment, from which the weight- and number-average molecular weights are obtained, can be represented, respectively, by:

$$\Lambda_{2,\infty} = a + (1 + 2r/s)(b - m_\infty) - (2r^2/s)b \exp\{-(r + s)a\} \int_{-\infty}^0 d\Phi L_0 \exp\{\lambda\Phi\} \quad (4)$$

$$\Lambda_{1,\infty} = a + b - m_\infty = a + bH \quad (5)$$

where

$$H = 1 - \exp\{-(r + s)a\}$$

and

$$\Lambda_{0,\infty} = a + s bH/(r + s) \quad (6)$$

where b is the monomer concentration at $t = 0$, m_∞ is the monomer concentration at $t = \infty$, $m_\infty = b \exp \{-(r + s)a\}$, $\Phi = \int_a^{L_0} (dx/x) \exp \{(r + s)x\} = Ei[(r + s)L_0] - Ei[(r + s)a]$. Ei denotes the exponential integral, and

$$\lambda = sb \exp \{-(r + s)a\}$$

$$L_0 = a \exp \{-k_d t\}$$

The weight- and number-average degree of polymerization at $t = \infty$ can then be calculated directly from the second, first, and zeroth moments:

$$\bar{P}_w = \Lambda_{2,\infty} / \Lambda_{1,\infty}$$

and (7)

$$\bar{P}_n = \Lambda_{1,\infty} / \Lambda_{1,\infty}$$

According to eq. (2), the value of $(k_p + k_{tm})/k_d$ can be calculated from the slope of the plot of $\log(1 - \xi_\infty)$ versus a , and the value of k_d can be obtained separately from the rate of conversion with time according to eq. (3). Finally, the weight-average and number-average molecular weights can be measured and compared with the value calculated from eq. (7). In our treatment of the data the value k_d is adjusted to fit the weight-average molecular weight, and the best value of k_{tm} obtained is used to calculate the number-average molecular weight. The agreement between the calculated and observed \bar{P}_n and the constancy of the value of k_{tm} provide additional evidence concerning the validity of the calculation and throw some insight into the mechanism of polymerization.

III. EXPERIMENTAL

Polymerizations were carried out in dimethylformamide (DMF) at -30°C . with special precautions for drying and exclusion of moisture and air. Acrylonitrile was distilled under nitrogen directly into a storage flask. Matheson spectrograde DMF was purified by the procedure of Thomas and Rochow⁴ and transferred into the reaction vessel which had been degassed while flaming under high vacuum.

Measurement of ξ_∞

The final conversion ξ_∞ was determined in a reaction vessel shown in Figure 1, where acrylonitrile and the catalyst solution were kept separate in flask A and tube B, respectively. After standing in a constant temperature bath at -30°C . for about 20 min. to reach constant temperature, the catalyst and acrylonitrile were allowed to mix through the side arm C. The reaction was usually complete in 45 min. (see below) and was allowed to take place for 2 hr., at the end of which time the reaction was stopped by adding a few milliliters of 3% HCl (diluted with DMF) and the polymer was recovered by precipitation in a large excess of methanol. The total

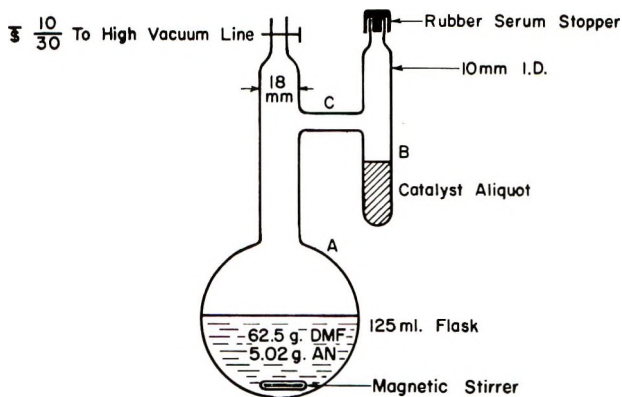


Fig. 1. Polymerization vessel.

conversion was calculated on the basis of the amount of the polymer recovered and the weight of the monomer used.

The experiment was repeated at different catalyst concentrations.

Determination of k_d

The rate of conversion, which is required for the calculation of k_d , was determined in a vessel as shown in Figure 2.

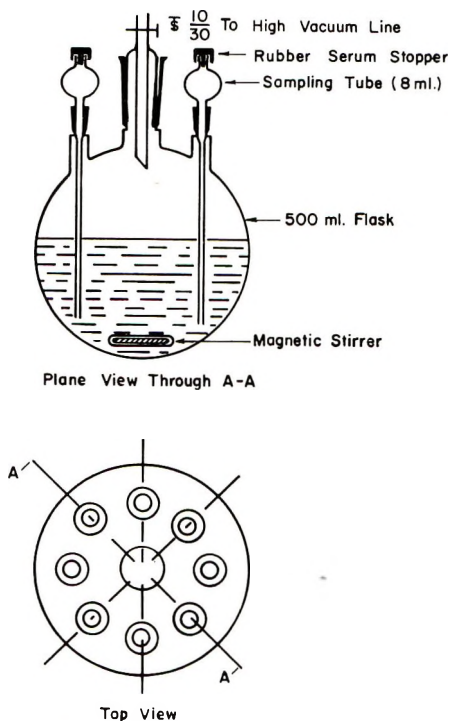


Fig. 2. Polymerization vessel for studying the rate of polymerization.

Sampling from a viscous solution without contamination is extremely difficult but the difficulty is overcome by the following technique. All sampling tubes were installed at the beginning of the experiment. At different time intervals, aliquots were taken from the mixture by applying a slight vacuum by means of a hypodermic needle through the rubber serum stopper. The sampling tube was removed from the flask while the content was protected with a small stream of argon. With this sampling technique, we found no difficulties in obtaining consistent data. Under favorable conditions, it was possible to take the first reading in 2 min. This procedure was repeated at different time intervals until no further change in conversion was observed. The value of ξ_∞ thus determined was in good accord with the value obtained by the previous method during which there was no interruption for sampling.

Weight-Average and Number-Average Molecular Weight

The weight-average molecular weight was calculated from the intrinsic viscosity determined in DMF at 25°C. by using the Cleland and Stockmayer equation:⁵

$$[\eta] = 2.33 \times 10^{-4} \bar{M}_w^{0.75}$$

The effect of polydispersity on the molecular weight is insignificant and is ignored. The number-average molecular weight was determined with a Mechrolab membrane osmometer. Although some diffusion of low molecular weight materials was encountered, the molecular weights obtained are within the limits of error for the present investigation.

IV. RESULTS AND DISCUSSION

The Value of $(k_p + k_{tm})/k_d$

The final conversion ξ_∞ is given in Table I as a function of the catalyst concentration, a . When $-\log(1 - \xi_\infty)$ is plotted against a , a very good

TABLE I
Polymerization of Acrylonitrile in DMF at -30°C .

$a \times 10^3$, mole/ 1000 g.	b , mole/ 1000 g.	ξ_∞	\bar{M}_w (meas- ured)	\bar{M}_n (meas- ured)	S, %	S, % (based on \bar{M}_n)
0.168	1.504	0.2617, 0.2932	74,200	^a	0.0104	—
0.280	1.504	0.5698	125,300	49,000	0.0104	0.065
0.560	1.504	0.7908	107,500	50,400	0.020	0.064
0.840	1.504	0.8817	72,100	46,000	0.025	0.077
1.12	1.504	0.954	61,400	36,500	0.028	0.091

^a No value was obtained on this sample because of diffusion of low molecular weight materials through the membrane.

TABLE II
Effect of Monomer Concentration and Catalyst
Concentration on Total Conversion

$a \times 10^3$, mole/1000 g.	b , mole/1000 g.	Conversion ξ_{∞}
1.12	0.271	0.952
1.12	0.503	~ 1.0
1.12	0.656	~ 1.0
1.12	0.867	0.964
1.12	1.043	0.952
1.12	1.286	0.924
0.84	0.556	0.904
0.84	0.673	0.739
0.84	1.101	0.775
0.84	1.354	0.883
—	0.240	0.388
—	0.653	0.446
—	0.910	0.372
—	1.108	0.435

straight line is obtained (Fig. 3). The slope of the line gives a value of $2710 \text{ (mole/1000 g.)}^{-1}$ for $(k_p + k_{tm})/k_d$.

The linear relationship between $-\ln(1 - \xi_{\infty})$ and a remains true throughout a wide range of monomer concentration (Table II), showing that eq. (2) is independent of the monomer concentration.

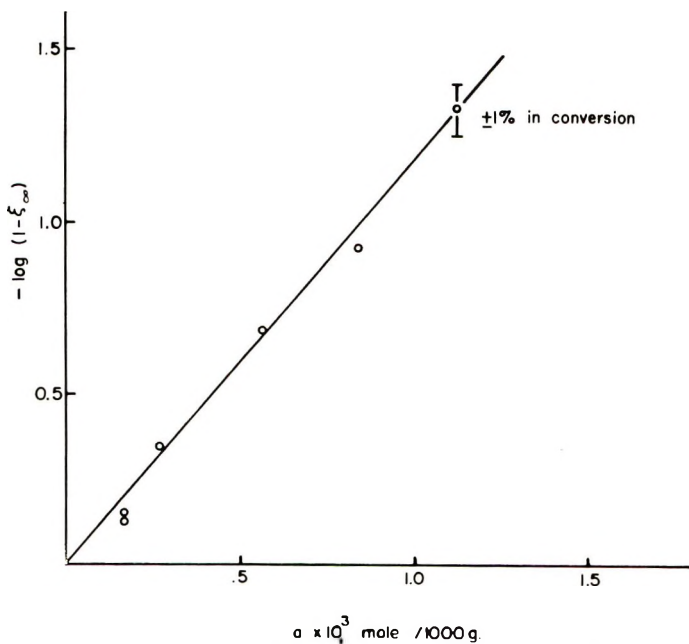


Fig. 3. Polymerization of acrylonitrile in DMF at -30°C . with the $\text{NaAlEt}_2\text{S}(i\text{-Pr})$ catalyst, $b = 1.504 \text{ mole/1000 g.}$

The essence of eq. (2), as discussed in the previous report,² is the fact that the rate of disappearance of the monomer is proportional to the monomer concentration and the deactivation of the growing polymer is proportional to the concentration of the active polymer taking part in the reaction, the deactivation being independent of the monomer concentration. Whether there is a transfer reaction (to monomer) or not has no bearing on the shape of the plot, since, in both cases, a linear relationship between $\ln(1 - \xi_\infty)$ and a exists; namely, with no transfer, $-\ln(1 - \xi_\infty) = (k_p/k_d)a_f$; while with transfer to monomer, $-\ln(1 - \xi_\infty) = [(k_p + k_{tm})/k_d]a$. The slope of the straight line has different physical meaning however; it gives a value for k_p/k_d if there is no transfer and a value for $(k_p + k_{tm})/k_d$ if transfer occurs. The study of the total conversion as a function of a yields no further information concerning the transfer reaction in question.

Molecular Weight and Sulfur Content

However, the nature of the transfer reaction can be inferred from the molecular weight and molecular weight distribution and the sulfur content of the polymer. The initiation in our polymerization involves the reaction



the sulfur being incorporated in the polymer in the initiation step. If there were no transfer reaction, each polymer molecule would contain one sulfur atom, and the sulfur content calculated on this basis would have been much higher than that observed (Table I, columns 6 and 7). Furthermore, the molecular weight distribution would have been narrower if there were no transfer reaction.² Thus, the transfer reaction as a whole does not affect the rate of formation of the polymer but reduces the molecular weight significantly and changes the sulfur content of the polymer.

The possibility of transfer to solvent is also ruled out on the basis of the same reasoning. The possibility of transfer to impurities is still under investigation.

The evidence indicates that the transfer to monomer reaction is the preferred explanation. This conclusion is also in agreement with the result obtained by Ottolenghi and Zilkha, who concluded that in the homogeneous polymerization of acrylonitrile in DMF with BuLi bimolecular chain transfer to monomer occurs.⁶

The Value of k_d

Only the value of $(k_p + k_{tm})/k_d$ was obtained from the total conversion measurement. The value of k_d has to be determined separately and can be estimated by plotting $\ln[\ln(1 - \xi)/(1 - \xi_\infty)]$ against t , according to eq. (3). Figures 4 and 5 give such a plot for different catalyst concentrations, Figure 4, for a catalyst concentration of 0.28×10^{-3} mole/1000 g., and

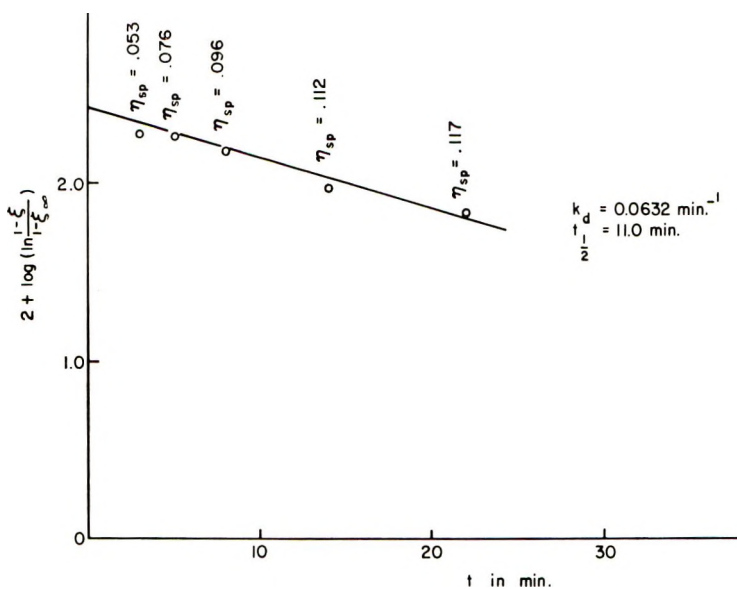


Fig. 4. Plot of $\ln [(1 - \xi)/(1 - \xi_\infty)]$ vs. t . Polymerization conditions: -30°C ., $b = 0.752$ mole/1000 g., $a = 0.28 \times 10^{-3}$ mole/1000 g.

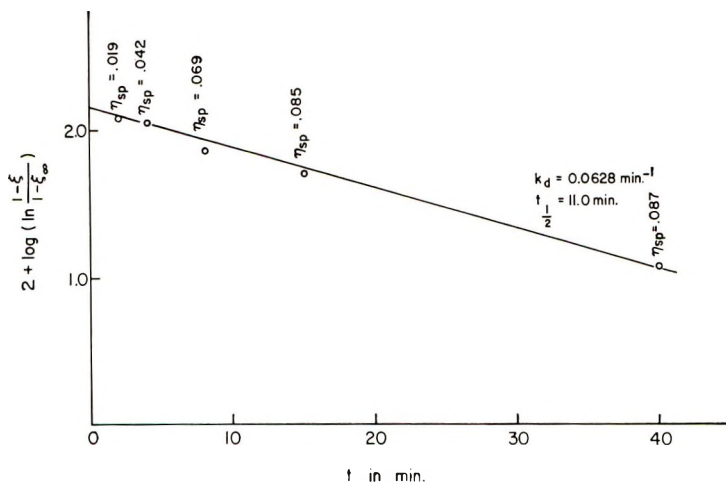


Fig. 5. Plot of $\ln [(1 - \xi)/(1 - \xi_\infty)]$ vs. t . Polymerization conditions: -30°C ., $b = 0.752$ mole/1000 g., $a = 0.56 \times 10^{-3}$ mole/1000 g.

Figure 5, for a concentration of 0.56×10^{-3} mole/1000 g. The same monomer concentration, 0.752 mole/1000 g., was used in both cases.

The value of k_d was 0.0632 and 0.0628 min^{-1} from Figures 4 and 5, respectively. The average, 0.0630, was taken as the value of k_d , and corresponds to an average half-life of 11.0 min. From k_d and $(k_p + k_{tm})/k_d$, the value of $k_p + k_{tm}$ is 170 (mole/1000 g.) $^{-1}$.

The numbers given on the plot are the specific viscosities of the samples which show the change in molecular weight with time and therefore with the degree of conversion.

Comparison of the Molecular Weights

The calculation of the weight- and number-average molecular weights according to eq. (4) is straightforward. The integral in eq. (4) was obtained graphically. The value of k_{tm} was obtained by the method of successive approximation, and the value which gives the corrected value of \bar{P}_w is used to calculate the number-average molecular weight.

The data required for the graphic integration are given, as an example,

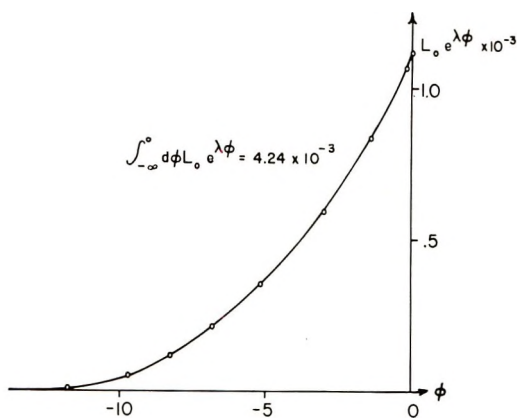


Fig. 6. Evaluation of the integral $\int_{-\infty}^0 d\Phi L_0 e^{\lambda\Phi}$ for $b = 1.50$ mole/1000 g., $a = 1.12 \times 10^{-3}$ mole/1000 g.

TABLE III

Evaluation of the Integral $\int_{-\infty}^0 d\Phi L_0 e^{\lambda\Phi}$ in Equation (7)

$(r + s)L_0$	$Ei[(r + s)L_0]$	Φ	$L_0 \times 10^3$	$\lambda\Phi$	$e^{\lambda\Phi}$	$L_0 e^{\lambda\Phi} \times 10^3$
0	$-\infty$	$-\infty$	0	$-\infty$	0	0
0.1	-1.623	-11.78	0.0369	-1.673	0.188	0.00693
0.5	0.454	-9.69	0.185	-1.376	0.252	0.0466
1.0	1.895	-8.24	0.369	-1.170	0.310	0.114
1.5	3.301	-6.84	0.553	-0.971	0.379	0.210
2.0	4.954	-5.19	0.738	-0.737	0.477	0.352
2.5	7.074	-3.07	0.923	-0.436	0.644	0.594
2.8	8.679	-1.46	1.033	-0.207	0.810	0.837
3.0	9.934	-0.21	1.108	-0.0298	0.970	1.075
3.03	10.14	0	1.112	0	1.000	1.12

TABLE IV
Comparison of the Calculated and Observed
Number-Average Degree of Polymerization

$a \times 10^3$, mole/ 1000 g.	b , mole/ 1000 g.	b/a	$\int_{-\infty}^0 d\Phi L_0 e^{\lambda\Phi}$ $\times 10^3$	\bar{P}_w	k_{tm}	\bar{P}_n	
						Calcd.	Obsd.
0.168	1.504	8930	0.043	1400	0.195	690	—
0.280	1.504	5360	0.183	2370	0.085	1210	925
0.560	1.504	2680	0.731	2030	0.075	1090	945
0.840	1.504	1790	1.73	1360	0.113	795	775
1.12	1.504	1340	4.24	1160	0.124	660	665
				Avg.	0.117		

for which $b = 1.504$, $a = 1.12 \times 10^{-3}$, $\bar{P}_w = 1160$ in Table III. The value of $L_0 e^{\lambda\Phi}$ is plotted against Φ , and the integral,

$$\int_{-\infty}^0 d\Phi L_0 e^{\lambda\Phi}$$

is equal to the area under the curve between $-\infty$ and 0 (Fig. 6). The final value of k_{tm} together with \bar{P}_w and \bar{P}_n are summarized in Table IV. The agreement between the calculated and observed \bar{P}_n is satisfactory.

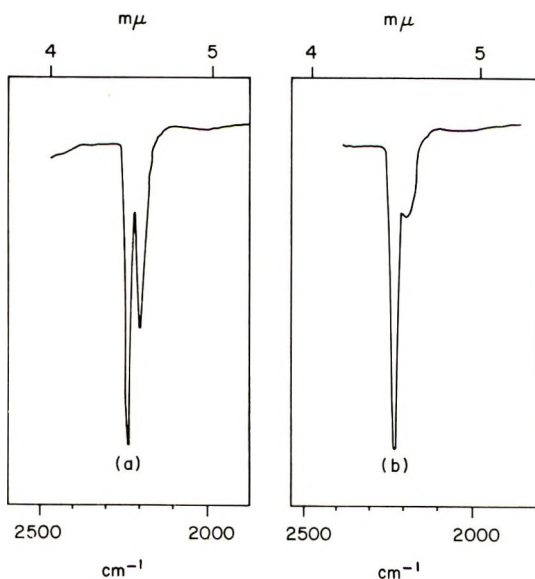


Fig. 7. Infrared spectra of the low molecular weight PAN, showing peaks at 2205 and 2237 cm^{-1} : (a) before reaction and (b) after reaction with Na_2SO_3 .

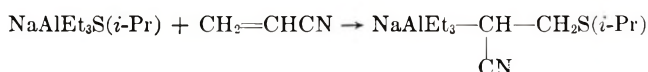
Infrared Spectra

The infrared spectrum of a low molecular weight polymer prepared at a high catalyst concentration showed peaks at 2237 and 2205 cm^{-1} and also a strong peak at 1620 cm^{-1} , but no absorption at 900 cm^{-1} . The 2205 cm^{-1} peak was removed by treating the sample in DMF with Na_2SO_3 acidified with H_2SO_4 , a procedure used by Critchfield and Johnson⁷ for the determination of α,β -unsaturated compounds. Figure 7 shows the infrared spectra of the polymer before and after reaction with Na_2SO_3 . Thus, it is clear that there are two nitriles in the polymer, only one of which is conjugated.⁸ The conjugation of the nitrile causes the shift of absorption from 2237 to 2205 cm^{-1} . The absorption at 1620 cm^{-1} is attributed to the $-\text{C}=\text{C}-$ bond. The absence of 900 cm^{-1} absorption suggests that terminal $-\text{CH}=\text{CH}_2$ is absent.⁹

V. CONCLUSION

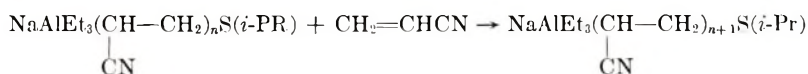
The present study of the homogeneous polymerization of acrylonitrile in DMF at -30°C . initiated with the $\text{NaAlEt}_3\text{S}(i\text{-Pr})$ catalyst shows that the initiation must be relatively fast and the active polymer undergoes propagation, transfer (to monomer), and deactivation at the same time, in accordance with the rate equations and the experimental data. The agreement between the calculated and observed results—the linear relationship between $-\ln(1 - \xi_\infty)$ and a (independent of the monomer concentration), the constancy of the transfer constant, and the agreement between the calculated and observed \bar{P}_n —provides a rigorous test concerning the validity of the equations and the mechanism of the polymerization.

A plausible mechanism involves initiation brought about by

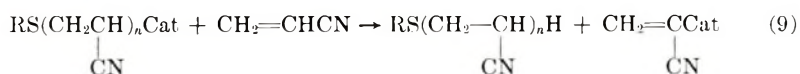
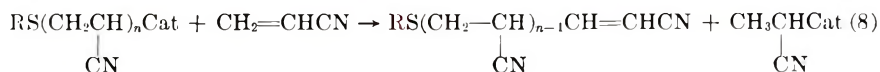


The latter product has been isolated and identified by infrared spectra.¹⁰

The propagation involves the successive addition of the monomer near the aluminum center:



Chain transfer with monomer occurs either by reaction (8) or (9).



Equation (8) is, in a sense, analogous to the hydride transfer reaction as discussed by Cundall et al.,¹¹ while eq. (9) is analogous to the proton transfer

process preferred by Zilkha et al.⁶ The infrared spectrum of low molecular weight PAN does not contain evidence for $-\text{CH}=\text{CH}_2$ groups, therefore eq. (8) is to be preferred to eq. (9).

The authors wish to express their thanks to Dr. L. H. Peebles, who developed an osmotic pressure procedure for measuring the number-average molecular weight, and to Mr. J. H. Rhodes for some of the measurements reported here.

References

1. H. N. Friedlander, *J. Polymer Sci. A*, **2**, 3885 (1964).
2. R. Chiang and J. J. Hermans, *J. Polymer Sci. A-1*, **4**, 2843 (1966).
3. R. Chiang, J. H. Rhodes, and R. A. Evans, *J. Polymer Sci. A-1*, in press.
4. A. B. Thomas and E. G. Rochow, *J. Am. Chem. Soc.*, **79**, 1843 (1957).
5. R. L. Cleland and W. H. Stockmayer, *J. Polymer Sci.*, **17**, 473 (1955).
6. A. Ottolenghi and A. Zilkha, *J. Polymer Sci. A*, **1**, 687 (1963).
7. F. E. Critchfield and J. B. Johnson, *Anal. Chem.*, **28**, 73 (1956).
8. L. J. Bellamy, *The Infra-Red Spectra of Complex Molecules*, Wiley, New York, 1962, pp. 263-264.
9. F. S. Dainton and G. B. B. M. Sutherland, *J. Polymer Sci.*, **4**, 37 (1949).
10. R. A. Evans, private communication.
11. R. B. Cundall, D. D. Eley, and J. Worrall, *J. Polymer Sci.*, **58**, 869 (1962).

Résumé

Les résultats expérimentaux de la polymérisation homogène de l'acrylonitrile initié avec le triéthylthioisopropoxyaluminate de sodium, $\text{NaAlEt}_3\text{S}(i\text{-Pr})$, comme catalyseur dans le DMF à -30°C sont comparés avec les prévisions basées sur les équations d'un mécanisme admis. L'accord entre le poids moléculaire moyen en nombre calculé et observé combiné avec les résultats cinétiques et le rapport entre le degré de conversion et la concentration initiale en catalyseur fournit un test rigoureux concernant la validité des équations et le mécanisme de polymérisation. Un mécanisme plausible est postulé suivant lequel l'initiation doit être relativement rapide en accord avec les équations de vitesse; et le polymère en croissance subit la propagation le transfert avec le monomère et la désactivation simultanément. Les spectres infra-rouges de polymères de bas poids moléculaires, préparés avec un concentration élevée en catalyseur, manifestaient une forte absorption à 2237, 2205 et 1620 cm^{-1} mais pas d'absorption à 900 cm^{-1} , ce qui indique qu'il y a deux fonctions nitriles dans le polymère, une qui est conjuguée et l'autre qui ne l'est pas. La possibilité d'avoir des groupes $-\text{CH}=\text{CH}_2$ dans le polymère est exclue par l'absence d'une bande à 900 cm^{-1} . Sur la base de ces faits, on conclut que le polymère a un groupe terminal $-\text{CH}=\text{CHCN}$ résultant de la réaction de transfert.

Zusammenfassung

Die Versuchsergebnisse bei der homogenen, mit Natriumtriäthylthioisopropoxyaluminat $\text{NaAlEt}_3\text{S}(i\text{-Pr})$ als Katalysator gestarteten Acrylnitrilpolymerisation in DMF bei -30°C werden mit den nach den auf dem aufgestellten Mechanismus beruhenden Beziehungen zu erwartenden verglichen. Die Übereinstimmung zwischen den berechneten und den beobachteten Zahlenmittelwerten des Molekulargewichts liefert zusammen mit den kinetischen Daten und der Beziehung zwischen Umsatz und Anfangskonzentration des Katalysators einen strengen Test für die Gültigkeit der aufgestellten Gleichungen und des Polymerisationsmechanismus. Ein plausibler Mechanismus mit verhältnismässig raschem Start in Übereinstimmung mit den Geschwindigkeitsgleichungen und gleichzeitigem Wachstum, Übertragung (zum Monomeren) und Desaktivierung des

wachsenden Polymeren wird aufgestellt. Das Infrarotspektrum des niedermolekularen, mit hoher Katalysatorkonzentration hergestellten Polymeren zeigte starke Absorption bei 2237, 2205 und 1620 cm^{-1} , jedoch keine Absorption bei 900 cm^{-1} , was dafür spricht, dass zwei Arten Nitril, ein konjugiertes und ein nichtkonjugiertes im Polymeren vorhanden sind. Die Möglichkeit der Anwesenheit von $-\text{CH}=\text{CH}_2$ -Gruppen im Polymeren wird durch das Fehlen der Bande bei 900 cm^{-1} ausgeschlossen. Es wird daher geschlossen, dass das Polymere eine aus der Übertragungsreaktion stammende $-\text{CH}=\text{CHCN}$ -Endgruppe besitzt.

Received March 8, 1966

Prod. No. 5142A

Electrolytic Formation and Destruction of Living Anions

B. L. FUNT, S. N. BHADANI, and D. RICHARDSON, *Department of
Chemistry, University of Manitoba, Winnipeg, Canada*

Synopsis

Electrolysis of solutions of α -methylstyrene in THF resulted in the formation of the characteristic spectra of the living anions in the cathode compartment. The increase in absorbance of the solution was strictly proportional to the charge transferred at the electrode, and was independent of the electrolyte for $\text{NaAl}(\text{C}_2\text{H}_5)_4$, $\text{NaB}(\text{C}_6\text{H}_5)_4$, and $\text{KB}(\text{C}_6\text{H}_5)_4$. For solutions of $\text{LiB}(\text{C}_6\text{H}_5)_4$ the color decreased spontaneously on standing, and a linear relationship between absorbance and charge transferred was not obtained. Mixing of the anode and cathode solutions resulted in a destruction of the living ends and a disappearance of the color, which could be regenerated by further electrolysis. Reversal of the polarity of the electrodes produced a stoichiometric destruction of the living ends and a decrease in absorbance directly dependent on the charge transferred. The exact stoichiometric dependence furnished means of estimating impurity levels, living anion concentrations, and optical extinction coefficients based on the number of faradays passed through the solution. The control of molecular weight distribution and rate of reaction by these methods is indicated.

Introduction

This work is concerned with the generation and control of the population of living anions. The kinetics of anionic polymerization are directly influenced by the concentration of living ends. Furthermore, the molecular weight and the molecular weight distribution can be controlled by suitable programming of the concentration of living anions throughout the course of the reaction. The electrically initiated anionic polymerizations of several monomers have been studied, but evidence for living anions was not obtained.¹⁻⁴

The first reported electrolytic production of living anions was that described by Yamazaki and co-workers for α -methylstyrene.⁵ Subsequent work in our laboratories reported the generation of living polystyryl anions and the control of polystyrene polymerization through electrolysis.⁶

In this paper we report a detailed study of the production and destruction of α -methylstyrene anions in solutions of several salts in tetrahydrofuran (THF).

Experimental

Electrolyses were performed at constant current in an apparatus shown in Figure 1. Two platinum electrodes (1×1 in.) were housed in a divided

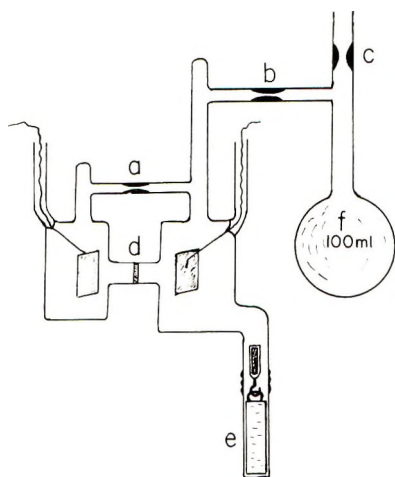


Fig. 1. Electrolysis cell: (a, b, c) constrictions for seal-off; (d) sintered disk; (e) 10-mm. quartz optical absorption cell for double-beam spectrophotometer and movable 9-mm. quartz spacer.

cell whose compartments were separated by a fine fritted glass disk, 1 cm. in diameter. All transfers were made under vacuum line techniques and the apparatus could be sealed and isolated after charging with reactants. The salts employed were prepared as described by Szwarc⁷ and were of the general formula $MB(C_6H_5)_4$, where M is Li, Na, K, or C_4H_9N . In practice a known amount of salt (ca. 0.5 g.) was dissolved in 10 ml. pure THF and introduced in the filling bulb. The bulb was attached to the vacuum line, the contents frozen in liquid N_2 and evacuated. The THF was distilled off and the salt dried *in vacuo* at $50^\circ C$. for 24 hr. The basic procedure was modified slightly to handle the pyrophoric $NaAl(C_2H_5)_4$ and the sparingly soluble $KB(C_6H_5)_4$. For the former, sealed ampules of the salt were prepared in a dry box, and the ampule was crushed and its contents mixed with the solution after the latter had been under high vacuum for 24 hr.

The monomer and THF were purified rigorously by established methods^{8,9} and were degassed by four to five freeze-thaw cycles. A known amount of freshly distilled monomer was transferred into the filling bulb under vacuum. THF was distilled from a Na film into a measuring tube and then into the apparatus. The apparatus was sealed at C at 10^{-6} mm. Hg pressure. The contents were brought to room temperature and transferred to the electrolysis cell. The total volume of solution was 84.8 ml. at $25^\circ C$. The cathode compartment volume was 55.2 ± 0.5 ml. and the monomer concentration in THF was $0.43M$.

The appendage to the cathode compartment of the cell was a 1×1 cm. quartz optical absorption cell coupled to the apparatus by a graded seal. A 9-mm. spacer could be inserted into the cell and could be moved with a magnet to provide a mixing of the contents.

If additional polymerization was desired the constriction a was sealed, the contents were transferred to the bulb f, the constriction b was sealed,

and the detached bulb immersed in a cold bath at -78°C . The living polymer was killed with a few drops of methanol.

Electrolysis of Solutions of Sodium Tetrphenylboron

The formation of living anions of α -methylstyrene was observed on the electrolysis of solutions of $\text{NaB}(\text{C}_6\text{H}_5)_4$ in THF. An absorption maximum was found at $340\text{ m}\mu$.¹⁰ With increase in time of electrolysis the absorbance of the solutions increased, but the peak remained at essentially the same position. The data are shown in Figure 2.

If the solutions from the anode and cathode compartments were mixed the color, due to the living anions, was destroyed and the resulting spectrum is shown in the bottom curve of Figure 3. When the mixed solution was again electrolyzed by a current of 5 ma. for 16 min. the original color reappeared in the cathode compartment, and this is shown in the top curve of Figure 3. The differential spectrum of the resulting solution is also plotted. Similar results were obtained with the other salts.

These results indicated that a species formed in the anode compartment interacted with the living anions. However, passage of sufficient current

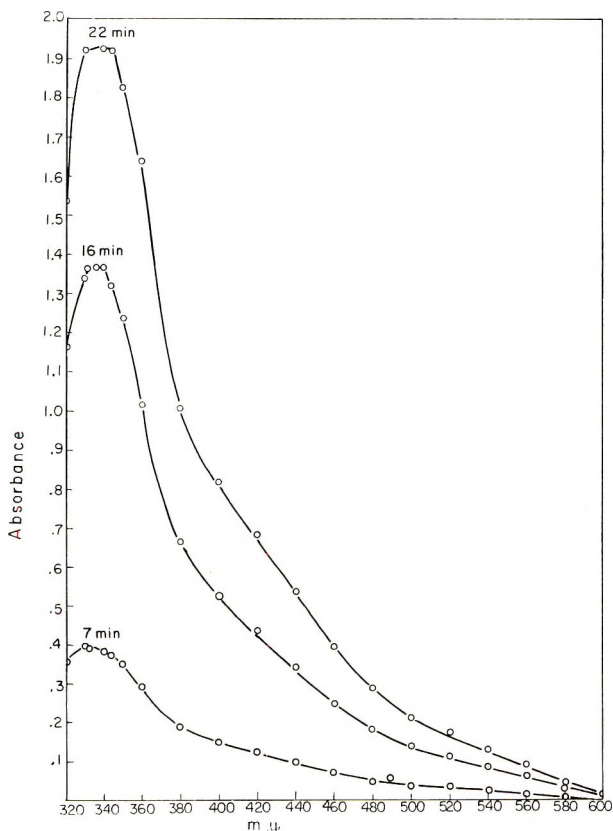


Fig. 2. Absorption spectra after 7, 16, and 22 min. electrolysis at a current of 5 ma. in a solution of $\text{NaB}(\text{C}_6\text{H}_5)_4$.

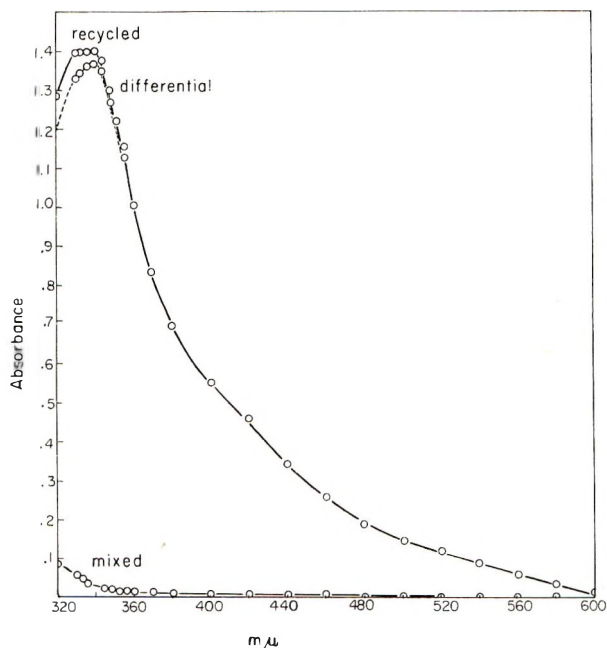


Fig. 3. Spectra of solution after mixing of anode and cathode solutions of Fig. 2 followed by further electrolysis for 16 min.

could, in turn, remove the interfering substance and allow the further formation of living anions.

Effects of Diffusion through the Fritted Disk

It was essential to determine whether diffusion through the fritted disk would be sufficiently rapid to vitiate kinetic measurements. A solution of sodium tetraphenylboron was electrolyzed and its absorbance measured as a function of time. The data are given in Table I, and it can be seen that there is negligible change in absorbance for the first 4 hr. and that

TABLE I
Change in Absorbance of Solutions after Electrolysis

Time, hr.	Absorbance
0	1.456
1	1.456
2	1.456
3	1.456
4	1.420
5	1.398
6	1.398
7	1.377
8	1.367
9	1.367
50	1.249

even after 50 hr. there is only a 14% change in the absorbance of the solution. Not all of this change can be attributed to diffusion, and this must be considered an upper limit to the effects of diffusion in the solution.

The constancy of the absorbance after electrolysis was also noted for solutions of the $\text{KB}(\text{C}_6\text{H}_5)_4$ and $\text{NaAl}(\text{C}_2\text{H}_5)_4$. However, for the $\text{LiB}(\text{C}_6\text{H}_5)_4$ a rapid decrease in color intensity was observed. This was not due to diffusion and reference to this phenomenon will be made at a later point. The results were encouraging in that they showed that diffusion need not be a major factor influencing the kinetics in these electrolytic reactions.

Quantitative Relationships between Charge Transferred and the Population of Living Anions

The absorbance of solutions of $\text{NaB}(\text{C}_6\text{H}_5)_4$ and $\text{KB}(\text{C}_6\text{H}_5)_4$ and of $\text{NaAl}(\text{C}_2\text{H}_5)_4$ were found to be strictly proportional to the number of electrons transferred at the electrode.

An examination of Figure 4 is instructive. It shows that 2-10 μF was required to achieve the first change in absorbance. Presumably this represented the removal of 2-10 μmole of impurity in the reaction volume. This is approximately $4 \times 10^{-5} M$ in impurity at the lower limit and is in reasonable agreement with other estimates of impurity levels.¹¹

After the first appearance of color the increase of absorbance is strictly

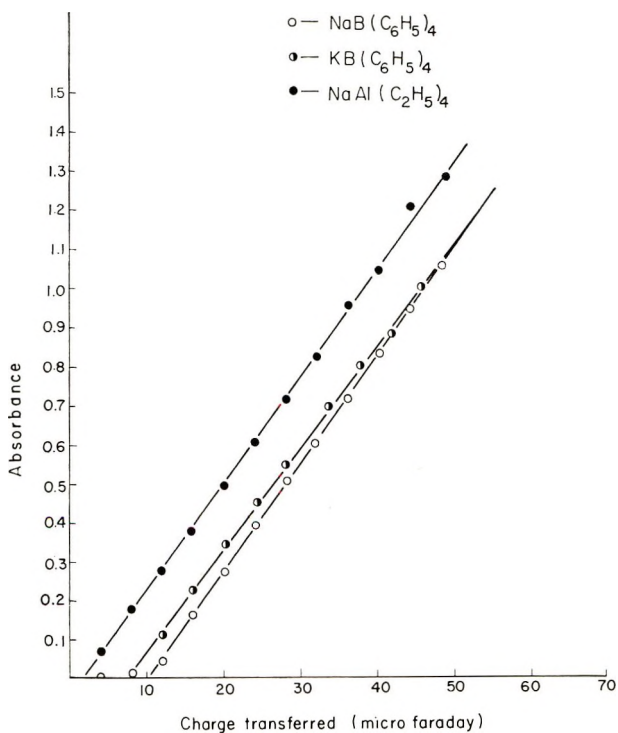


Fig. 4. Electrolysis of α -methylstyrene solutions with various salts.

proportional to the charge transferred at the electrode. Experimentally this is equivalent to time of electrolysis at constant current.

The $\text{KB}(\text{C}_6\text{H}_5)_4$ data in Figure 4 have a slightly different slope from the other results. We believe this is due to the relative insolubility of this salt and the correspondingly increased voltages which had to be applied to achieve constant current. The slight deviation from the other data is probably due to resultant electrodiffusion effects.

Destruction of Living Ends by a Reversal of the Polarity of the Electrodes

The effects of mixing the contents of the anode and cathode compartments suggested that the living end concentration could be decreased as well as increased electrolytically. Thus the polarity of the electrodes was reversed after a maximum color was obtained and the absorbance measured. It was found that exactly the same quantity of charge was required to decolorize the solution as was required to form the color initially. Furthermore, at the very instant that the cathode compartment became decolorized, the anode compartment developed its first trace of color. The data are shown graphically in Figure 5.

All the data for the electrolysis of the three salts fall accurately on a single straight line, if the effects of the varying induction periods of Figure

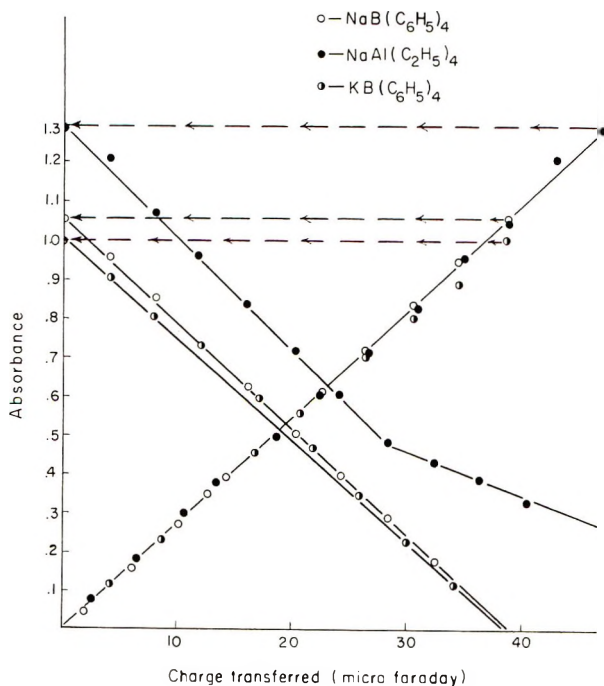


Fig. 5. Formation of living ends by electrolysis followed by their destruction on reversal of polarity. Net charge transferred from development of first color.

4 are subtracted from the total charge transferred. If, at the maximum color formation for a given salt the current is reversed, and the absorbance measured as a function of time, the falling curves of Figure 5 are obtained. It should be noted that the amount of electricity necessary to decolorize the solution is identical to that required to form a given intensity of color. The last three points for $\text{NaAl}(\text{C}_2\text{H}_5)_4$ are anomalous, and color formed in the cathode compartment past the dotted portion of this particular curve.

In all other instances the formation of color in the anode compartment and the disappearance of color at the cathode coincided with the passage of an equivalent amount of current to that initially employed to generate the color.

This ability to destroy as well as to generate living anions suggested a novel method for the estimation of the extinction coefficient of these solutions. Indeed, the extinction coefficient can be calculated directly from the slope of curves such as those given in Figure 4. The charge transferred is by Faraday's laws equivalent to the living end concentration and the slope of absorbance versus concentration gives the extinction coefficient directly. The molar extinction coefficient thus obtained was 1.53×10^4 .

Experiments with Lithium Tetraphenylboron

When a current of 3 ma. was passed through a solution of $\text{LiB}(\text{C}_6\text{H}_5)_4$ in α -methylstyrene dissolved in THF, the plot of absorbance versus charge transferred deviated from linearity, as shown in Figure 6. After the cur-

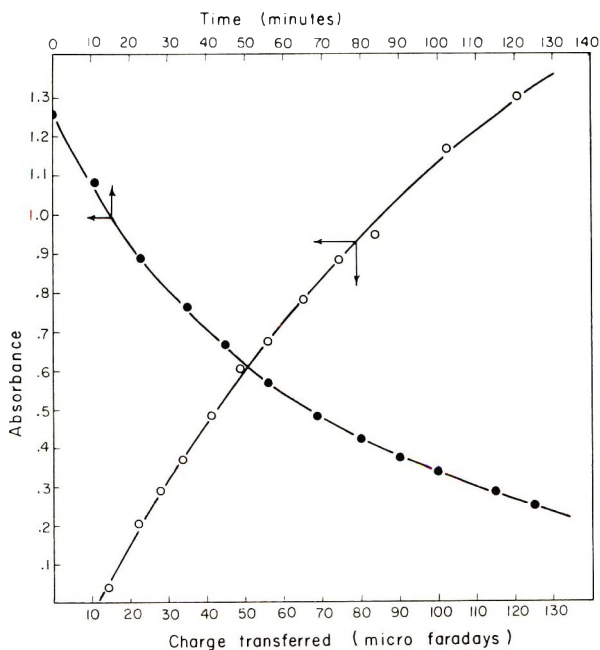


Fig. 6. Color formation on electrolysis and spontaneous decolorization of solution of $\text{LiB}(\text{C}_6\text{H}_5)_4$.

TABLE II
 Polymerization of α -Methylstyrene

Electrolyte	Monomer concn., moles/l.	Current, ma.	Monomer (cathode), g.	Polymer (cathode), g.	Mol. wt. $\times 10^{-4}$	Polymer formed per 2 Faradays, g. $\times 10^{-4}$
LiB(C ₆ H ₅) ₄	1.28	2.2	4.83	4.40	23.1	10.7
	1.28	1.3	4.38	3.22	27.4	8.8
	1.28	2.0	4.77	3.97	31.3	15.9
	1.28	1.3	4.86	2.17	48.6	8.9
	1.26	3.0	4.98	3.20	30.3	11.4
	0.64	1.3	2.98	2.04	21.3	6.7
	0.59	1.3	2.45	1.86	17.1	6.6
	0.51	1.3	2.34	1.66	17.6	6.8
NaB(C ₆ H ₅) ₄	0.42	2.4	1.92	1.90	5.17	5.0
	0.40	2.0	1.91	1.89	6.23	5.0
	0.87	2.0	4.09	4.05	7.85	8.0
	0.61	2.0	2.91	2.88	8.28	9.1
	0.61	3.0	2.63	2.61	10.5	10.2

rent was switched off, the solution spontaneously decolorized, and its change of absorbance with time is shown at the left of Figure 6.

When the living anions were transferred and cooled to -78.5°C ., polymer could be isolated. The amount of polymer obtained after 3 hr. reaction is shown in Table II. With further time of reaction the conversion of monomer to polymer could be made quantitative. However, the polymer formed per Faraday did not correspond to a polymer molecule per two electrons transferred at the electrode.

Szwarc has also reported anomalous results with styrene and lithium tetraphenylboron¹² and it appears likely that this salt undergoes complex formation, or other interaction, in the solution resulting in a decrease in the living anion concentration.

For NaB(C₆H₅)₄ as conducting electrolyte, these anomalies did not appear. The data are also shown in Table II, and it can be seen that the weight of polymer precipitated from the solution after a reaction time of 24 hr. represented a quantitative conversion of the monomer introduced. Furthermore, the molecular weight of the isolated polymer corresponded to that expected, on the assumption that two electrons were transferred per polymer molecule. The last column in Table II indicates the weight of polymer formed per two Faradays transferred. This is in remarkable agreement with the molecular weight as tabulated.

Effect of Impressed Current

Solutions of α -methylstyrene containing sodium tetraphenylboron were subjected to electrolysis at various currents between 0.6 and 5 ma., and the increase of absorbance was noted as a function of time. The data are shown in Figure 7. It is seen that there is an absolutely linear relationship

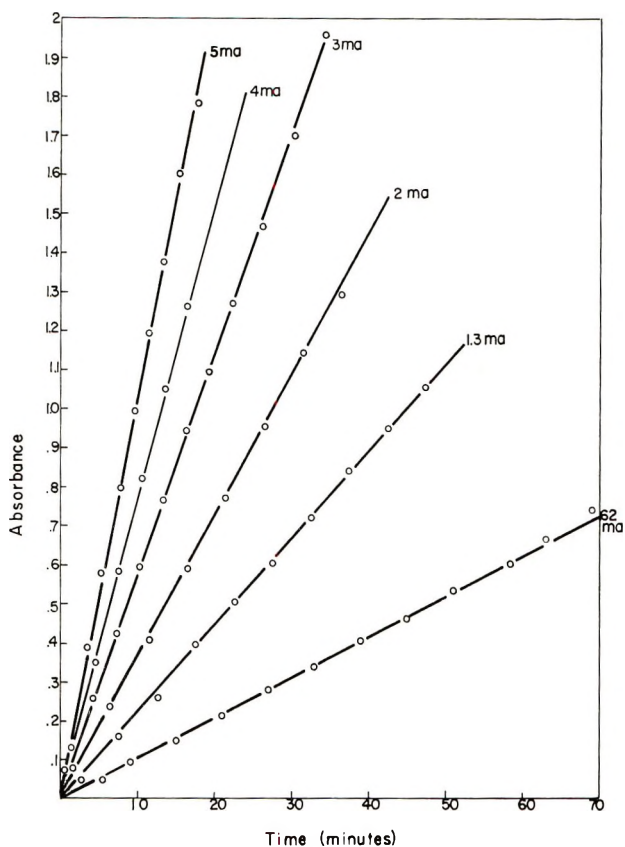


Fig. 7. Increase of absorbance with time of electrolysis at inscribed currents in solutions of $\text{NaB}(\text{C}_6\text{H}_5)_4$.

between the absorbance and time at each of the currents over the tenfold range. This is an unequivocal indication that diffusion effects are not limiting under the conditions of current density employed in this study. The slopes of the lines in Figure 7 indicate the living end concentration formed per unit time. When these slopes are plotted against current, a proportional relationship is found to exist. This shows that the concentration of living ends formed is determined by the number of Faradays passed through the solution, and is independent of the current density in the range investigated.

Experiments with Tetrabutylammonium Tetraphenylboron

This salt was of particular interest in that it did not contain an alkali metal as a cation. During electrolysis a red color formed around the cathode, but vanished quickly in the solution. Even prolonged electrolysis did not result in a persistent color of the living anion. However, the transient formation of color indicated the presence of α -methylstyrene living ions at the electrode. In other experiments with naphthalene and styrene we

have shown that the naphthalene complex can be formed under similar conditions.⁶ In the present work however, no polymer formation could be obtained with this salt. It is likely that there is an interaction between the salt and the living anion in the system.

Molecular Weights

The molecular weights of samples formed by cooling α -methylstyrene tetrameric anions to -78°C . were determined with a gel-permeation chromatograph. The molecular weight distribution was narrow, and high molecular weight polymer was isolated. Independent viscosity data also showed that molecular weights in excess of 200,000 were obtained by these methods, and the viscosity molecular weights¹³ are given in Table II. The sharp distribution obtained with the Li salt indicates that the interaction which was evident at room temperature (Fig. 6) does not persist at low temperatures.

Mechanism

This work is still consistent with Yamasaki's postulate of direct electron transfer to the monomer at the cathode. However, our experiments have shown that the killing species generated at the anode is formed in a one-to-one relationship with anions at the opposite electrode. Furthermore, the stability of the killing substance is convincing proof that it is not a radical or other transient species, but is a stable chemical entity. In the case of the boron compound it is tempting to postulate that the species is $\text{B}(\text{C}_6\text{H}_5)_3$. Similarly $\text{Al}(\text{C}_7\text{H}_5)_3$ could be postulated for the aluminum salt.

Synthetic Possibilities

The ability to change the living end population at will, and to determine quantitatively the number of living ends produced or remaining in the solution suggests a number of interesting experiments. By altering the concentration of living ends during the course of the polymerization it should be possible to produce polymers of unusual, but controlled, molecular weight distribution. Model experiments on such systems are being conducted in our laboratories.

Similar interesting work can be done by maintaining the living end concentration at a fixed value in the presence of monomers which can result in an attrition of the living end population. Furthermore, it is possible to program a current such that the rate of reaction remains constant throughout the course of polymerization, despite the change in monomer concentration as the reaction proceeds. These, and other interesting synthetic possibilities, result from the ready control of the living end concentration which can be achieved by electrolytic methods.

The authors thank the National Research Council for a grant and for the provision of a post-doctoral fellowship (D. R.). The financial assistance of the Dow Chemical Company of Canada is gratefully acknowledged.

References

1. J. W. Breitenbach and C. H. Srna, *Pure Appl. Chem.*, **4**, 245 (1962).
2. B. L. Funt and F. D. Williams, *J. Polymer Sci. A*, **2**, 865 (1964).
3. B. L. Funt and S. W. Laurent, *Can. J. Chem.*, **42**, 2728 (1964).
4. B. L. Funt and S. N. Bhadani, *Can. J. Chem.*, **42**, 2733 (1964).
5. N. Yamazaki, S. Nakahama, and S. Kambara, *J. Polymer Sci. B*, **3**, 57 (1965).
6. B. L. Funt, S. N. Bhadani, and D. Richardson, *Can. J. Chem.*, **44**, 711 (1966).
7. D. N. Bhattacharyya, C. L. Lee, J. Smid, and M. Szwarc, *J. Phys. Chem.*, **66**, 608 (1965).
8. D. J. Worsfold and S. Bywater, *J. Polymer Sci.*, **26**, 299 (1957).
9. M. Morton, A. A. Rembaum, and J. L. Hall, *J. Polymer Sci. A*, **1**, 461 (1963).
10. C. L. Lee, J. Smid, and M. Szwarc, *J. Phys. Chem.*, **66**, 904 (1962).
11. S. Bywater, *Fortschr. Hochpolymer. Forsch.*, **4**, 66 (1965).
12. D. N. Bhattacharyya, C. L. Lee, J. Smid, and M. Szwarc, *J. Phys. Chem.*, **69**, 612 (1965).
13. A. F. Siriani, D. J. Worsfold, and S. Bywater, *Trans. Faraday Soc.*, **55**, 2124 (1959).

Résumé

L'électrolyse de solutions d'alpha-méthylstyrene dans le THF entraîne la formation de spectres caractéristiques d'anions vivants dans le compartiment cathodique. L'accroissement d'absorption de la solution est strictement proportionnelle à la charge transférée aux électrodes, et est indépendante de l'électrolyte pour $\text{NaAl}(\text{C}_2\text{H}_5)_4$, $\text{NaB}(\text{C}_6\text{H}_5)_4$, $\text{KB}(\text{C}_6\text{H}_5)_4$. Pour des solutions de $\text{LiB}(\text{C}_6\text{H}_5)_4$ la couleur décroît spontanément par repos et une relation linéaire entre l'absorbance et la charge n'a pas pu être obtenue. Par mélange des solutions anodiques et cathodiques il y a destruction des groupes terminaux vivants et disparition de la couleur qui peut être régénérée par électrolyse ultérieure. Le renversement de la polarité des électrodes produit une destruction stœchiométrique des groupes terminaux vivants et une décroissance de l'absorbance en relation directe avec les charges transférées. La dépendance stœchiométrique exacte fournit un moyen d'estimer le taux d'impureté, la concentration en anions vivants, les coefficients d'extinction optique sur la base du nombre de faradays passés à travers la solution. Le contrôle de la distribution des poids moléculaires et de la vitesse de réaction par ces méthodes est indiqué.

Zusammenfassung

Die Elektrolyse von α -Methylstyrollösungen in THF führte zum Auftreten des charakteristischen Spektrums des lebenden Anions im Kathodenabteil. Die Zunahme der Extinktion der Lösung war der an der Elektrode umgesetzten Ladung streng proportional und bei $\text{NaAl}(\text{C}_2\text{H}_5)_4$, $\text{NaB}(\text{C}_6\text{H}_5)_4$ und $\text{KB}(\text{C}_6\text{H}_5)_4$ als Elektrolyt vom Elektrolyt unabhängig. Bei $\text{LiB}(\text{C}_6\text{H}_5)_4$ -Lösungen nahm die Farbe beim Stehen spontan ab und es wurde keine lineare Beziehung zwischen der Extinktion und der umgesetzten Ladung erhalten. Mischung der Anoden- und Kathodenlösung führte zu einer Zersetzung der lebenden Enden und einem Verschwinden der Farbe, welche durch weitere Elektrolyse regeneriert werden konnte. Eine Umkehr der Polarität der Elektroden führte zu einer stöchiometrischen Zersetzung der lebenden Enden und einer der umgesetzten Ladung direkt proportionalen Abnahme der Extinktion. Die exakte stöchiometrische Abhängigkeit lieferte eine Mittel zur Bestimmung des Gehalts an Verunreinigungen, der Konzentration des lebenden Anions und des optischen Extinktionskoeffizienten auf Grundlage der Zahl der durch die Lösung geschickten Faradays. Eine Kontrolle der Molekulargewichtsverteilung und der Reaktionsgeschwindigkeit durch die angegebenen Methoden erscheint möglich.

Received March 7, 1966
Prod. No. 5147A

Deviations from Topotaxy in Trioxane Polymerization

GEORGE ADLER, *Brookhaven National Laboratory,
Upton, New York 11973*

Synopsis

It is shown by photomicrographic techniques that the polymer does not always form in a unique crystallographic direction in the solid-state polymerization of trioxane. The polymerization in these instances cannot therefore be considered topotactic in the usually accepted sense. The crystallization of the polymer is attributed to factors which are, in a sense, secondary to the actual reaction mechanism.

Introduction

In the explanation of reactions in the solid state—particularly those involving molecules of a complex geometry such as organic compounds—it has been tempting to invoke “topotactic” mechanisms. This is often done on rather vague evidence. Topotactic has been defined in various ways. However, as used by most workers, it seems to imply more than that the reaction is affected by the lattice. Little orientation or diffusion of the reactant molecules from their equilibrium lattice position should be involved. As a result, the product molecules should have a structure and orientation which bears a simple and straightforward relation to that of the reactant lattice. To quote Glasser et al.,¹ “In topotaxy a single crystal of a starting material is converted to a pseudomorph containing one or more products in a definite crystallographic orientation: the conversion takes place throughout the entire volume of the crystal. For true topotaxy there must be some three-dimensional correspondence between the structures of the product and its host.” This would minimize the amount of motion necessary for reaction. Since extensive motion within a relatively rigid matrix is always a difficult problem, the attractiveness of such a hypothesis is readily apparent. This is especially true in the case of solid-state polymerizations, where many small molecules must join to form a single large one.

Initially, topotaxy had at times been inferred simply on the ground that the polymerization took place in the solid state. This made the reaction easier to understand. However, it was soon shown that many, if not most, of the polymerizations produce amorphous and disoriented polymer. (For examples, see Mesrobian et al.² and Adler.³) In the case of acrylamide, for example, it has been shown that only the first addition step usually, but not invariably, proceeds in a definite crystallographic direc-

tion.⁴ Therefore, this could not be a topotactic reaction in the usual sense, even though the lattice does influence the reaction. Indeed, it probably is because of the complex interrelationship between the monomer lattice, the possible polymer structures and the modes of motion required for reaction and which are allowable by the crystal that the polymer becomes amorphous.

It has since become customary to assume topotactic mechanisms in those instances where the polymer formed is crystalline and/or oriented in a specific way relative to some crystallographic direction of the monomer crystal from which it arose. Thus, trioxane polymerization has been widely cited as an example of a reaction having a topotactic type of mechanism because the polymer is highly crystalline and has been reported to be oriented in a specific manner with respect to the monomer *c* axis.^{5,6} This procedure, too, seems questionable since crystallization may arise in some manner that is indirectly related to the reaction mechanism.

There are several peculiarities in the behavior of trioxane that made us suspect that this may be the case. Trioxane forms soft, flexible crystals that may easily be twisted into knots. The polymerization is usually carried out above 40°C., but the monomer sublimes very rapidly even at room temperature. It was observed that the polymer crystals at the end of the reaction were occasionally larger though fewer in number than the monomer crystals present initially.⁷ This suggests that monomer recrystallization is taking place and that sublimation may play a role in the reaction. The published literature states that the polymer has a helical structure with approximately 29 monomer units for each 16 turns of the helix, or almost a 2:1 ratio.^{8,9} Trioxane, however, has three monomer units per ring molecule. For this to happen, the monomer molecule had to open by splitting a bond, the ring had to contract until the two open ends overlapped each other quite a bit. If normal bond angles and bond lengths are to be maintained, there had to be some contraction in the *a* and *b* lattice directions and extensive rearrangement in the *c* direction. This would put the polymer out of phase with the monomer lattice. These observations indicated that the proposed topotaxy of trioxane should be reexamined. This communication reports the first results of this new look, which was here taken with a microscope.

Experimental

Trioxane was purified by two successive sublimations. Small amounts of it were then melted on glass microscope slides underneath cover slips and then cooled until it recrystallized. This provided polycrystalline samples that were thin enough for good microscopy. The edges of the cover slip were then sealed with epoxy resin to prevent sublimation. These specimens were first examined carefully with a microscope to make sure that there was no polymer present. They were then given radiation dose of 1 Mrad from a Co⁶⁰ source at 24°C. Dose rate was 0.5 Mrad/hr. After irradiation the slides were again examined to see if any polymer was present.

Some specimens were then stored at 24°C., some heated to 46°C. and the rest to 54°C. The polymer in these preparations was then photographed under the microscope with the use of polarizing, dark-field, and phase-contrast techniques.

Results and Discussion

The mechanisms for the solid-state polymerization of trioxane which have been proposed to date all require that the resulting polymer should be crystalline with its long axis lying in some fixed direction relative to the crystallographic axes of the monomer. This direction is usually parallel to the *c* axis. The process was pictured as only requiring a simple rearrangement of atoms such as a ring opening followed by joining with the next molecule in line. The photomicrographs, Figures 1-5, are not entirely consistent with this picture. The actual situation appears to be much more complex.

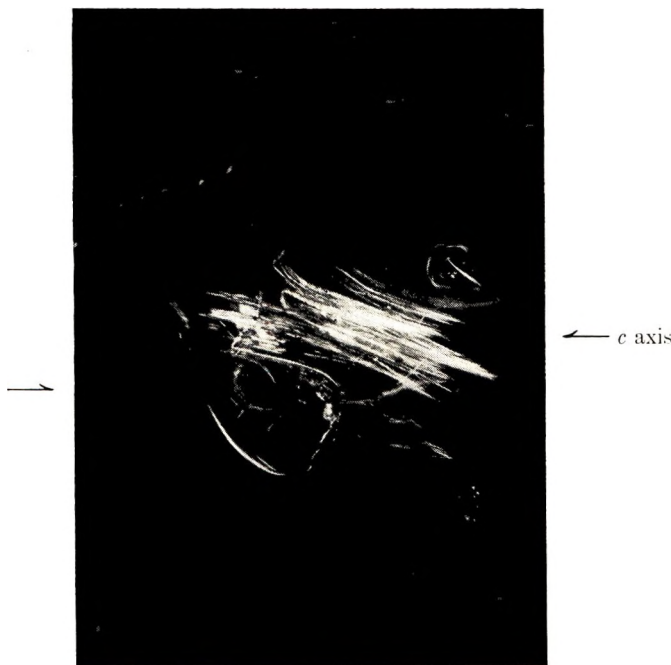


Fig. 1. Polyoxymethylene produced from trioxane at 24°C. Magnification 125 \times .

It was found that a small amount of polymerization occurred after irradiation and storage at temperatures below those usually quoted for trioxane polymerization. Thus, some polymer was found even at room temperature. However, the yield under these conditions was evidently very low.

Figure 1 is typical of the polymer seen at room temperature. It was taken with a polarizing microscope with the monomer at the extinction

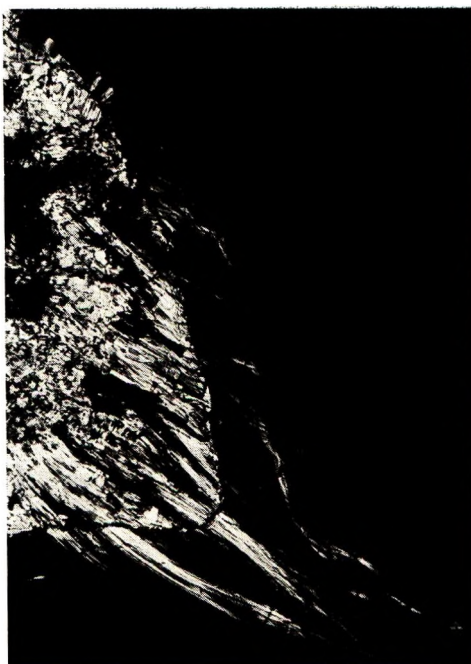


Fig. 2. Polyoxymethylene produced from trioxane at 46°C. Magnification 125 \times .

position. The direction of the monomer c axis is indicated by the long direction of the faintly outlined pits in the c crystal surface.

Several things are immediately obvious. The polymer, as expected, is found as a distinct phase separate from the monomer, apparently on the monomer surface. It is highly birefringent and presumably crystalline. Since the polymer fibers are not at the extinction position whereas the monomer is, and since the fibers do not lie parallel to the long direction of the pits, the polymer is obviously not oriented parallel to the monomer c axis. Most of the polymer seems to be in two bundles of fibers which lie at slightly different orientations. In addition, there are some fibers that twist through large changes of direction. It seems therefore that the polymer need not even lie in a definite crystallographic direction. It cannot be argued here that the polymer first formed in a given direction and then became misaligned. This would require the expenditure of energy and, as will be shown later, the polymer formed at higher temperatures shows far better orientation with respect to the monomer c axis. It seems, therefore, that no so-called topotactic mechanism can explain its formation. Apparently, considerable reorientation and motion on a molecular scale must have occurred. It should be kept in mind that even at room temperature trioxane anneals and sublimates rapidly.

Figure 2 was taken with a polarizing microscope with phase optics and a first-order compensator added. The specimen was heated at 46°C. for 21.5 hr. after irradiation. This is within the temperature range that has

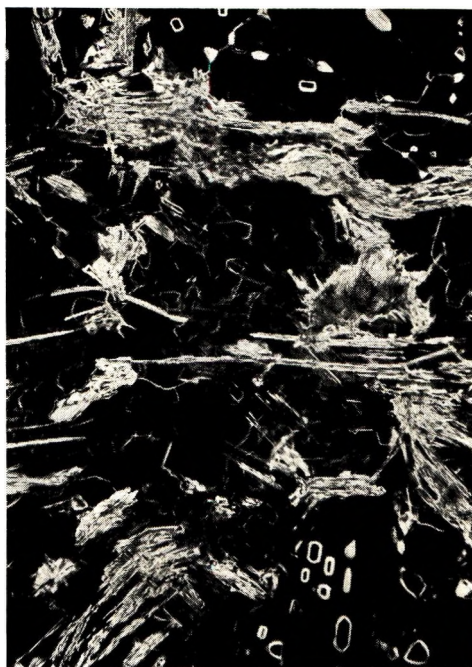


Fig. 3. Polyoxymethylene produced from trioxane at 46°C. Magnification 125 \times .

been reported for extensive polymerization. The bright area shows monomer crystals whose *c* axes lie perpendicular to the axis of the microscope. Bundles of more or less parallel and birefringent polymer fibers can be seen growing from the end of the crystalline mass. These fibers also show some variation in the direction of growth. The important thing is that the polymer fibers extend far beyond the crystals in which they originated and are in this sense like the whiskers which sometimes grow from inorganic crystals. This is reminiscent of the observation that the polymer crystals were often larger than the initial monomer crystals. It seems to imply that the polymer grows at the end of the fibers and that large amounts of motion and reorientation of the monomer molecules are involved.

Figure 3 shows polymer formed under the same conditions as Figure 2. It was photographed by use of a dark-field microscope with crossed polarizers. Here, it can be seen that the polymer forms fiber bundles that are often long enough to cross the boundaries between several grains of the polycrystalline monomer mass with no change in direction. This is most clearly seen in those areas where the conversion to polymer is relatively low and the grain boundaries can still be seen through the polymer. Since these crystal grains differ in orientation, the fiber could be parallel to the *c* axis in only one. In other words, the orientation of the fiber is more important in determining the direction of further growth than the orientation of the monomer substrate upon which it lies. This, again, implies that reaction at the fiber ends cannot be topotactic and that migration and re-

orientation of molecules over large distances in terms of molecular dimensions must take place. It is possible, even probable, that polymer at these temperatures forms as an oriented or "epitactic" growth on the monomer surface parallel to the c axis of the crystallite on which it initiated. However, in growing beyond the grain boundary it maintains its own orientation.

Figure 4 shows polymer as seen through a dark-field microscope after heating 4 hr. at 54°C . This is about 10°C . less than the melting point.

The monomer shown in Figure 4 seems to have recrystallized extensively, since the average size of the monomer crystallite is greater than has been seen previously. However, the significant feature is that here the polymer seems to be almost entirely parallel to the c axis. This case is therefore similar to what has been reported by other workers.

The polymer here, as in the other cases, seems to form a second phase which lies on the surfaces of the monomer crystals. However, even at this temperature not all the polymer is precisely oriented. A very small fraction, probably less than 2 or 3%, still grows in a disoriented fashion. This can be seen in Figure 5. This is also a dark field photomicrograph. The bulk of the polymer is oriented parallel to the c axis as expected. However, a small fraction, separate from the rest, seems to have grown very much misoriented. It is still birefringent and therefore presumably crystalline. Indeed, we have on occasion seen polymer that grew as a cluster of tangled fibers, very much like a bit of cotton fluff.



Fig. 4. Polyoxymethylene produced from trioxane at 54°C . Magnification $100\times$.



Fig. 5. Polyoxymethylene produced from trioxane at 54°C. Magnification 100 \times .

These photomicrographs point to the conclusion that crystalline and even aligned polymer can form in the solid state by a mechanism that is not topotactic in the sense defined in the introduction. It suggests that the crystallization of the polymer occurs by some process which is secondary to the reaction mechanism. It cannot be argued that the reaction occurs by two simultaneous mechanisms, one of which is nontopotactic, and the other topotactic, the latter favored by higher temperatures. This would not explain the difference in number of monomer units per helix turn between monomer and polymer nor the fact that occasionally the polymer crystals are larger than the monomer, the very observations that led us to experiments described here.

This leaves us with two important questions. How does one reconcile these observations with the x-ray diffraction data which have been published and why does one obtain a crystalline polymer if the mechanism is not topotactic?

There is little doubt that the x-ray work which has been published, such as that of Okamura et al.,⁶ indicates very precise alignment of monomer and polymer. The author has had very similar results in his laboratory. This is not inconsistent with the microscopic results as would appear at first glance. The conditions under which the x-ray data are obtained should be kept in mind. Data such as those of Lando et al.,¹⁰ which are for the polymer crystal after the extraction of the monomer, gives no direct evidence as to orientation relative to the monomer. Most of the rest of

the data, such as those of Okamura et al.,⁶ is derived from partially polymerized single crystals and shows monomer in the presence of polymer. When polymerization is done near room temperature, the polymer yields are so low that it is difficult to find by diffraction techniques. As was explained above, at temperatures near 46°C. the polymer probably initiates parallel to the *c* axis on a particular crystallite in a polycrystalline sample and then grows beyond the grain boundaries. Then the deviation from alignment with the monomer would only be apparent in a polycrystalline sample but not in the single crystal specimens usually used in x-ray diffraction. Finally, at the highest temperatures, both the x-ray data and the photomicrographs show good alignment. The small amount of misoriented polymer that is formed would be difficult to detect by the usual diffraction techniques. It would appear, therefore, that the x-ray and the microscopic data are not inconsistent with each other.

As seen above, the x-ray data are compatible with either topotactic or nontopotactic mechanisms. Since the photomicrographs are not easily explainable by a strictly topotactic mechanism, the latter is more probable.

The problem of the crystallinity of the misoriented polymer is more easily explained. Polyoxymethylene has a regular structure and is probably easily crystallizable, no matter how it is formed. The fact that alignment of monomer and polymer is better at higher temperatures can be explained by annealing of both reactant and product. In the case of polymer, annealing need only occur at the growing chain end. The mobility of the monomer molecules also helps in this process. It is instructive in this regard to compare trioxane with hexamethylcyclotrisiloxane. This, like trioxane, is a ring monomer and also forms rhombohedral crystals. The polymer, however, is less easily crystallizable. It is suggestive that amorphous polymer is formed in the solid-state polymerization of this compound.³

Conclusion

The purpose of this communication is not to present a new mechanism for trioxane or any other solid-state polymerization but rather it is to point out that crystallinity and alignment of the polymer and monomer molecules are not by themselves conclusive proof of a topotactic mechanism. As we shall show in a subsequent communication, trioxane is not unique in its behavior. Trithiane, for example, shows very similar results. This is not to say that no topotactic polymerizations exist or that the monomer lattice has absolutely no effect on the reaction. Indeed, consideration of lattice energies alone indicates that there must be some lattice effect in every reaction involving solids. However, topotaxy, as usually used, has a much more restrictive meaning and it is in this sense the above statements must be considered. In the light of the results here demonstrated, it is suggested that the proposed topotactic mechanisms in solid-state polymerization be reexamined.

The author wishes to thank R. F. Smith of the Photography Division, Brookhaven National Laboratory, for taking the photomicrographs used as illustrations. Without his skill at the camera, the reader could only take the author's word for what he saw, always a dangerous procedure.

This research was supported by the U.S. Atomic Energy Commission.

References

1. L. S. Dent Glasser, F. P. Glasser, and H. F. W. Taylor, *Quart. Rev.*, **16**, 343 (1962).
2. R. B. Mesrobian, P. Ander, D. S. Ballantine, and G. J. Dienes, *J. Chem. Phys.*, **22**, 565 (1954).
3. G. Adler, *J. Chem. Phys.*, **31**, 848 (1959).
4. G. Adler and J. H. Petropoulos, *J. Phys. Chem.*, **69**, 3712 (1965).
5. S. Okamura, K. Hayashi, and Y. Kitanishi, *J. Polymer Sci.*, **58**, 925 (1962).
6. S. Okamura, K. Hayashi, and M. Nishi, *J. Polymer Sci.*, **60**, 526 (1962).
7. D. S. Ballantine, private communication.
8. G. Carazzolo, S. Leghissa, and M. Mammi, *Makromol. Chem.*, **60**, 171 (1963).
9. G. Carazzolo, *J. Polymer Sci. A*, **1**, 1573 (1963).
10. J. Lando, N. Morosoff, H. Morawetz, and B. Post, *J. Polymer Sci.*, **60**, S24 (1962).

Résumé

On montre par technique photomicrographique que le polymère ne se conforme pas toujours dans une seule direction cristallographique au cours de la polymérisation à l'état solide du trioxane. La polymérisation dans ces cas ne peut dès lors pas être considérée comme topotactique dans le sens habituel de ce mot. La cristallisation du polymère est attribuée à des facteurs qui sont, dans un sens, secondaires par rapport au mécanisme de réaction actuel.

Zusammenfassung

Mikrophotographische Aufnahmen zeigen, dass bei der Polymerisation von Trioxan in fester Phase das Polymere sich nicht immer in einer einzigen kristallographischen Richtung bildet. Die Polymerisation kann daher in diesen Fällen nicht als topotaktisch im üblichen Sinne betrachtet werden. Die Kristallisation des Polymeren wird auf Faktoren zurückgeführt, welche in gewissem Sinn sekundäre Bedeutung für den tatsächlichen Reaktionsmechanismus besitzen.

Received April 20, 1966
Prod. No. 5162A

Polymerization of Some Sulfur-Containing Oxetanes

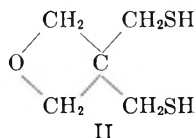
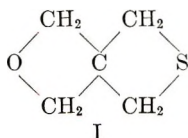
E. J. GOETHALS and E. DU PREZ, *Laboratory of Organic Chemistry, State University of Ghent, Ghent, Belgium*

Synopsis

Polymerization under the influence of boron trifluoride of 2-oxa-6-thia[3,3]spiroheptane gives two products: a linear polyether containing oxetane groups and a crosslinked polyether polysulfide. When the polymerization was carried out at -3°C ., up to 60% of soluble polysulfide is obtained. This does not prove that the thietane group polymerizes more rapidly than the oxetane group but rather that oxetane polymerization is inhibited by the presence of thietane groups. Polymerization under the influence of boron trifluoride etherate of 3,3-bis(mercaptomethyl)oxetane leads to a polyether containing free thiol groups. The degree of polymerization of the polymer, however, is low. In order to obtain higher degrees of polymerization several compounds with masked thiol groups were polymerized. 2-Oxa-6,7-dithia-6-thio[3,4]spirooctane and 2-oxa-6,8-dithia-7,7-dimethyl[3,5]-spirononane gave crosslinked products. The diacetate of 3,3-bis(mercaptomethyl)oxetane gave a linear polyether containing thiolacetate groups. Hydrolysis of this polymer leads to poly-3,3-bis(mercaptomethyl)oxetane with a softening temperature of $125\text{--}135^{\circ}\text{C}$.

Introduction

During the last decade much attention has been given to the polymerization of oxetanes¹ and especially to 3,3-bis(chloromethyl)oxetane (BCMO). Starting from BCMO or its bromo analog, several sulfur-containing oxetane derivatives have been synthesized.² In the present work the polymerization of 2-oxa-6-thia[3,3]spiroheptane (I), 3,3-bis(mercaptomethyl)oxetane (II), and derivatives is examined. The first compound was ex-



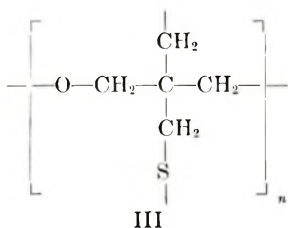
amined in order to compare the ease of polymerization of the thietane and oxetane groups. It has indeed been found that in some cases sulfur heterocycles polymerize more rapidly than the corresponding oxygen compounds (e.g., thiiranes and oxiranes)³ whereas in other cases the reverse is true (e.g., cyclic dithioketals and ketals).³

Polymerization of 3,3-bis(mercaptomethyl)oxetane (II) or its derivative leads to polyethers containing free thiol groups. The interest of such compounds as reversible mercaptide-forming reagents as well as their recent

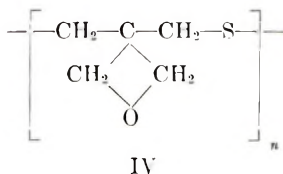
applications as radioactive prophylactics has made their synthesis of practical significance.⁴

Polymerization of 2-Oxa-6-Thia[3,3]Spiroheptane

When a solution of 2-oxa-6-thia[3,3]spiroheptane (I) in dichloromethane is treated with boron trifluoride etherate at 30°C., polymerization is complete after 30 min., giving an insoluble, infusible product. The infrared spectrum of the product shows a broad ether peak at 1050 cm.⁻¹ while the oxetane peak at 980 cm.⁻¹ has disappeared. It has obviously a three-dimensional structure (III) due to simultaneous polymerization of the oxetane and thietane ring. At -3°C. the reaction proceeds much more slowly;



and the main product is a soluble polymer, a small quantity of insoluble product also being formed. The soluble polymer is isolated by pouring the solution into a large volume of methanol. The infrared spectrum of the product shows a strong peak at 980 cm.⁻¹ due to the presence of the oxetane ring, and no linear ether peak at 1050 cm.⁻¹ is observed. This compound thus is a polysulfide of structure IV.



This polymer is highly crystalline as judged by its x-ray diffraction pattern and it has a softening point of 75–80°C. When a solution of polysulfide IV is treated with boron trifluoride etherate, an insoluble

TABLE I
Polymerization of 2-Oxa-6-thia[3,3]spiroheptane in Dichloromethane

Temperature, °C.	[M], mole/l.	$\frac{[M]}{[BF_3]}$	Reaction time, hr.	Conversion, %		η_{sp}/c of soluble polymer ^a
				Insoluble	Soluble	
30	3.1	30	0.5	100	0	—
-3	2.12	38	5.0	7.1	11.6	0.22
-3	2.12	19	5.0	7.4	13.3	0.22
-3	1.45	30	9.0	8.0	39.0	—
-3	1.45	30	14.0	9.0	49.0	—

^a Measured in dichloromethane at 25.0°C.; concentration = 0.500 g./dl.

polysulfide polyether (III) precipitates. Some results of the polymerization under different conditions are shown in Table I. Preliminary experiments have demonstrated that the concentration of water in the reaction mixture is of great importance. At low water concentration the rate of polymerization is proportional to the water concentration. In contrast with the results for the polymerization of BCMO⁵ where the rate falls off rapidly beyond the ratio H₂O/BF₃ of ca. 0.5, in this case, the rate continues to increase even at H₂O/BF₃ ratio of ca. 2.

The molecular weight of the soluble polymer decreases with increasing water concentration.

Polymerization of 3,3-Bis(mercaptomethyl)oxetane and Derivatives

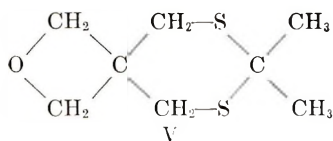
When 3,3-bis(mercaptomethyl)oxetane dissolved in dichloromethane is treated with boron trifluoride etherate, a white precipitate is formed. The product is difficultly soluble in DMF but is readily soluble in aqueous sodium hydroxide. The infrared spectrum shows peaks at 2550 and at 1050 cm.⁻¹ due to the thiol group and linear ether group, respectively. The oxetane peak at 980 cm.⁻¹ is absent. The specific viscosity of the product in DMF at 25°C. (concentration = 0.500 g./dl.) is 0.030 which indicates that the degree of polymerization is low. In order to obtain products with a higher degree of polymerization it is necessary to protect the thiol groups before polymerization.

A method often used for protection of thiol groups is oxidation of thiols to disulfides. The corresponding disulfide in our case is 2-oxa-6,7-dithia-[3,4]spirooctane. This compound however, polymerizes very rapidly to a polydisulfide² so that it is not an appropriate starting material.

The corresponding trisulfide, 2-oxa-6,7-dithia-6-thio[3,4]spirooctane,² is stable. It polymerizes under the influence of boron trifluoride etherate to an insoluble, infusible polymer. When the polymerization is carried out at 30°C., the infrared spectrum of the polymer still contains a peak at 980 cm.⁻¹ due to the presence of oxetane groups. This indicates that under the conditions used, the dithiacyclopentane ring polymerizes more rapidly than the oxetane ring.

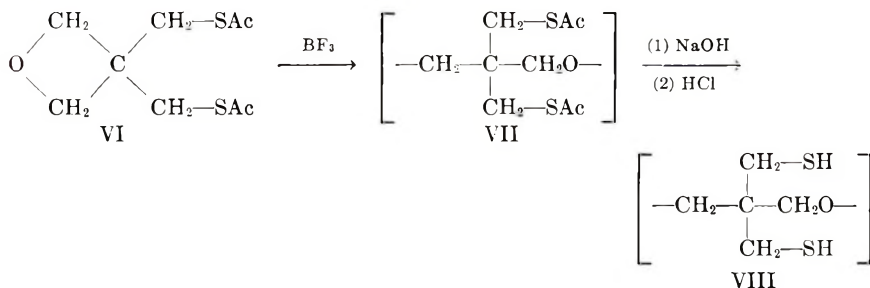
When the polymerization is carried out at 10°C. in nitrobenzene, the oxetane peak at 980 cm.⁻¹ is not seen in the product and instead, a broad ether peak at 1050 cm.⁻¹ is observed. Reduction of this polymer with sodium in liquid ammonia leads to a product that is soluble only in aqueous sodium hydroxide and that gives a positive nitroprusside test, indicating that free thiol groups are present. The product, however, is of low molecular weight and is difficult to purify.

Thioacetal formation is also often used to protect thiols. Under the influence of zinc chloride, 3,3-bis(mercaptomethyl)oxetane reacts with acetone with formation of cyclic dithioacetal (V). When a solution of this compound is treated with boron trifluoride etherate, a precipitate is formed immediately. The amount of precipitated product is proportional to the quantity of catalyst used and does not increase with prolonged reaction



time. The product is insoluble and infusible. Its infrared spectrum contains no oxetane peak at 980 cm.^{-1} ; instead, an ether peak at 1050 cm.^{-1} is present. These properties suggest that here also, the polymer is three-dimensional due to simultaneous polymerization of the thioether and oxetane rings.

Finally 3,3-bis(mercaptomethyl)oxetane diacetate (VI) was synthesized from dithiol (II) and acetyl chloride in the presence of pyridine. When a solution of this compound in dichloromethane is treated with boron trifluoride etherate, no precipitate is formed; the polymer is isolated by precipitation into methanol. Poly[3,3-bis(mercaptomethyl)oxetane diacetate] (VII) is a waxy amorphous substance. Its infrared spectrum shows a peak at 1675 and at 1050 cm.^{-1} due to the carbonyl and linear ether functions, respectively. Table II shows some results. Hydrolysis of the polythiolacetate was accomplished by stirring a suspension of the polymer in a methanolic sodium hydroxide solution at 50°C . After 1 hr. all material has dissolved. Polythiol (VIII) is isolated by precipitation into $2N$ hydrogen chloride solution.



Poly [3,3-bis(mercaptomethyl)oxetane] obtained by hydrolysis of the thiolacetate is soluble only in alkaline medium (water or alcohol). The polymer is amorphous, as judged by its x-ray diffraction pattern, and has a softening temperature of $125\text{--}135^\circ\text{C}$. Its infrared spectrum is practically identical to that of the product obtained by direct polymerization of 3,3-bis(mercaptomethyl)oxetane.

TABLE II
Polymerization of 3,3-Bis(mercaptomethyl)oxetane Diacetate

Temperature, $^\circ\text{C}$.	[M], mole/l. $^{-1}$	$\frac{[M]}{[\text{BF}_3]}$	Time, hr.	Conversion, %	η_{sp}/c^a
30	2.0	30	24	28	—
-3	1.0	7	48	33	0.38

^a Measured in DMF at 25°C .; concentration = 0.500 g./dl .

Experimental

2-Oxa-6-thia[3,3]spiroheptane (I) was prepared by dropping a solution of 46.5 g. of BCMO in 50 ml. of alcohol into a well-stirred boiling solution of 132 g. of sodium sulfide nonahydrate in 1500 ml. of water. The mixture was boiled for 2 hr. and cooled. It was extracted with dichloromethane, the dichloromethane solution was dried over anhydrous sodium sulfate, and the solvent was evaporated. The resulting 24.0 g. of 2-oxa-6-thia[3,3]-spiroheptane was distilled at 78°C./12 mm. (69%). The monomer was stored over calcium hydride and freshly distilled under purified nitrogen before use.

3,3-Bis(mercaptomethyl)oxetane (II) was prepared by reduction of 2-oxa-6,7-dithia-6-thio[3,4] spirooctane.² For polymerization purposes, it was distilled *in vacuo* and under nitrogen.

2-Oxa-6,8-dithia-7,7-dimethyl[3,5]spirononane (V) was synthesized as follows. To a cooled solution of 4.2 g. of 3,3-bis(mercaptomethyl)oxetane (II) in 30 ml. of acetone was added 2.0 g. of zinc chloride. After an exothermic reaction, the solution was allowed to stand overnight at room temperature and then poured into 100 ml. of water. The precipitate was filtered off, washed with water, and dried in a vacuum desiccator at room temperature. It was sublimated at 110°C./12 mm., yielding 3.05 g. of pure 2-oxa-6,8-dithia-7,7-dimethyl[3,5]spirononane (V) (58%), m.p. 128°C.

ANAL. Calcd. for $C_8H_{14}OS_2$: C, 50.5%; H, 7.40%; S, 33.7%; molecular weight 190. Found: C, 49.9%; H, 7.50%; S, 34.1%; molecular weight (by mass spectrometry), 190.

3,3-Bis(mercaptomethyl)oxetane diacetate (VI) could not be obtained by the action of sodium thioacetate upon BCMO. It was prepared as follows. Under stirring, 16.6 g. (0.23 mole) of acetyl chloride was added to 21.5 g. (0.27 mole) of dry pyridine. The mixture is kept between 0 and 5°C. by external cooling. To this solution, 17.6 g. (0.115 mole) of 3,3-bis(mercaptomethyl)oxetane (II) in 60 ml. of dichloromethane was added slowly and the reaction mixture stirred for 5 hr. at room temperature. The unreacted pyridine is neutralized with dilute hydrogen chloride. The organic layer is washed with dilute sodium hydroxide solution, with water, and is dried over sodium sulfate. The solvent was evaporated *in vacuo* and the residue fractionated; 7.75 g. (36%) of pure 3,3-bis(mercaptomethyl)oxetane diacetate (VI) was collected at 133–137°C./0.5 mm. n_D^{25} 1.5374;

ANAL. Calcd. for $C_8H_{14}O_3S_2$: C, 46.1%; H, 5.98%; S, 27.3%; molecular weight 234. Found: C, 45.8%; H, 5.91%; S, 26.9%; molecular weight (by mass spectrometry), 234.

Polymerizations were carried out in reaction tubes provided with a stopcock. After the solution of monomer was introduced, the tube was closed with a rubber capsule and cooled to about -25°C. Through the stopcock the tube was evacuated and filled with dry purified nitrogen three times. Still at -25°C., a 10% solution of boron trifluoride etherate in

dichloromethane was introduced by means of a hypodermic syringe. The tube was then placed in a thermostat.

To stop polymerization, methanol containing enough ammonia to neutralize all the boron trifluoride was added. The insoluble polymers were isolated by filtration, the soluble ones by precipitation in methanol.

Viscosities were measured in an Ubbelohde viscometer.

Dichloromethane was purified as described⁶ and stored over calcium hydride.

Commercial boron trifluoride etherate was distilled and stored as a 10% solution in dichloromethane.

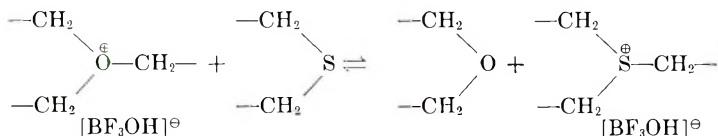
Water was added by means of a 10- μ l. capacity Hamilton syringe.

Infrared spectra were obtained with a Perkin-Elmer Model 237 infrared spectrometer (KBr pellet technique).

Conclusions

From the experiments on the polymerization of 2-oxa-6-thia[3,3]spiroheptane (I) it may be concluded that, under the influence of boron trifluoride etherate and in the presence of each other, the thietane group polymerizes more rapidly than the oxetane group. However, this does not mean that thietanes in general polymerize more rapidly than oxetanes. Indeed, from the slope of the time-conversion curve the rate of propagation was calculated to be 0.8×10^{-3} mole/l.-min. Penczek and Penczek have measured the propagation rate of the polymerization of BCMO under similar conditions as ours and they found a value of 1.25×10^{-3} mole/l.-min., a somewhat higher rate.⁵

The reason why, in the case of 2-oxa-6-thia[3,3]spiroheptane, practically only the thietane ring polymerizes, is that sulfonium salts, which are without doubt intermediates in the propagation of the polymerization of the thietane,^{7,8} are more stable products than are oxonium salts⁹ which are intermediates in the polymerization of oxetanes. Thus, the equilibrium between them lays practically entirely at the right side:



Thus the polymerization of the oxetane group is inhibited by the presence of the thietane group.

Under the influence of boron trifluoride etherate, 3,3-bis-(mercapto-methyl)oxetane (II) polymerizes to a polyether containing free thiol groups. Because of the presence of these free thiol groups, chain transfer is important and the degree of polymerization of the obtained polymer is low. When the thiol groups are acetylated, a polythiolacetate of higher degree of polymerization is obtained, and this can be transformed into a polythiol by alkaline hydrolysis.

The properties of poly 3,3-bis(mercaptomethyl)oxetane (VIII) are under investigation.

References

1. E. J. Goethals, *Ind. Chim. Eng.*, **30**, 559 (1965).
2. E. J. Goethals, *Bull. Soc. Chim. Belg.*, **72**, 396 (1963).
3. O. C. Dermer, WACD Technical Report TR 55-447 (1956).
4. C. G. Overberger, J. J. Ferraro, and F. W. Orttung, *J. Org. Chem.*, **26**, 3458 (1961).
5. I. Penczek and S. Penczek, *Makromol. Chem.*, **67**, 203 (1963).
6. A. Weissberger, E. S. Proskauer, J. A. Riddick, and E. E. Toops, Jr., Eds., *Organic Solvents*, Technique of Organic Chemistry, Vol. VII, Interscience, New York, 1955, p. 409.
7. J. L. Brode, *A.C.S. Polymer Preprints*, **6**, No. 2, 626 (1965).
8. J. K. Stille and J. A. Empen, *A.C.S. Polymer Preprints*, **6**, No. 2, 619 (1965).
9. H. Meerwein, G. Hinz, P. Hofmann, E. Kroning, and E. Pfeil, *J. Prakt. Chem.*, **255**, 257 (1936).

Résumé

La polymérisation sous l'influence de trifluorure de bore du 2-oxa-6-thia[3,3]-spiroheptane fournit deux produits; un polyéther linéaire contenant des groupes oxétaniques et un polyéther polysulfure ponté. Lorsque la polymérisation est effectuée à -3°C , jusque 60% de sulfure soluble est obtenu. Ceci ne prouve pas que le groupe thiétane polymérise plus rapidement que le groupe oxétanique mais plutôt que la polymérisation oxétanique est inhibée par la présence des groupes thiétanes. La polymérisation sous l'influence de l'éthérate de trifluorure de bore de 3,3-bis-mercaptométhyl oxétane fournit un polyéther contenant des groupes thiolés. Le degré de polymérisation du polymère est bas toutefois. Afin d'obtenir des degrés de polymérisation plus élevés de nombreux composés avec groupes thiolés masqués ont été polymérisés. Le 2-oxa-6,7-dithia-6-thia-[3,4]spirooctane et 2-oxa-6,8-dithia-7,7-diméthyl[3,5]spirononane fournissent des produits pontés. Le diacétate de 3,3-bis(mercaptométhyl)oxétane fournit un polyéther linéaire contenant des groupes thiolacétate. L'hydrolyse de ce polymère fournit le poly-3,3-bis(mercaptométhyl)oxétane, avec un point de fusion de 125 à 135°.

Zusammenfassung

Die Polymerisation von 2-Oxa-6-thia[3,3]spiroheptan unter der Einwirkung von Bortrifluorid liefert zwei Produkte: einen linearen Polyäther mit Oxtangruppen und ein vernetztes Polyäther-Polysulfid. Bei der Polymerisation bei -3°C werden bis zu 60% an löslichem Polysulfid erhalten. Das bedeutet nicht, dass die Thietangruppe schneller polymerisiert als die Oxetangruppe, sondern dass die Oxetanpolymerisation durch die Anwesenheit der Thietangruppen inhibiert wird. Die Polymerisation von 3,3-Bis(mercaptomethyloxetan) unter Einwirkung von Bortrifluorid-ätherat führt zu einem Polyäther mit freien Thiolgruppen. Das Polymere hat aber einen niedrigen D.P. Um einen höheren D.P. zu erhalten, wurden einige Verbindungen mit maskierten Thiolgruppen polymerisiert. 2-Oxa,6-7dithia-6-thio[3,4]spirooctan und 2-Oxa-6,8-dithia-7,7-dimethyl[3,5]spirononan ergaben vernetzte Produkte. Das Diacetat von 3,3-Bis(mercaptomethyl)oxetan lieferte einen linearen Polyäther mit einem Gehalt an Thiolacetatgruppen. Die Hydrolyse dieses Polymeren führt zu Poly-3,3-bis(mercaptomethyl)oxetan mit einem Erweichungspunkt von 125–135°C.

Received January 25, 1966

Revised May 2, 1966

Prod. No. 5163A

NOTES

Use of Labeled Oxygen ^{18}O in the Oxidation of Polyformaldehyde

Polyformaldehyde, heated in oxygen, is known to depolymerize mainly to monomer. This is accompanied also by formation of many volatile oxygen-containing products,¹ such as water, formic acid, methyl formate, trioxane, dioxolane, and linear fragments of macromolecules. Carbonyl groups with an absorption frequency of 1735 cm^{-1} accumulate in the solid residue.^{2,3,4} It was shown^{2,4} that the 1735 cm^{-1} band appears when the polymer is heated in an inert atmosphere as well, but the band intensity is weaker.

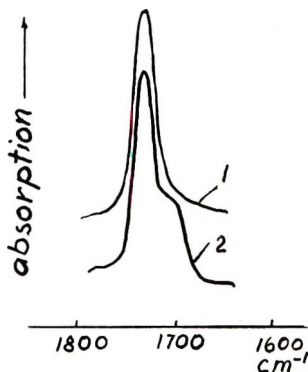


Fig. 1. The IR spectrum region for oxidized polyformaldehyde films as a function of non-oxidized films: (1) oxidation with oxygen of a normal isotopic composition; (2) oxidation with labeled oxygen.

The volatile oxygen-containing products and carbonyl groups may be formed at the expense of gaseous oxygen or from oxygen atoms, heteroatoms of the polymer chain, $\text{PCH}_2\text{OCH}_2\text{OCH}_2\text{O}\sim$. In order to find out the origin of oxygen in these compounds, polyformaldehyde was oxidized with labeled oxygen ^{18}O . The ratio of ^{18}O atoms to ^{16}O atoms was about 30% in the molecules of this oxygen. Before the oxidation the specimen of polyformaldehyde diacetate was evacuated at the temperature of the experiment in order to remove all substances absorbed in the polymer, and to destroy monoacetylated part of the polymer.

Additional peaks with mass numbers of 19, 20, and 48 were observed in comparing the mass spectra exhibited by the sums of volatile products formed in the oxidation with labeled and with ordinary oxygen. The 20 and 48 peaks were ascribed to molecular ions, H_2^{18}O and HCO^{18}OH . The ratio of 20 to 18 peak intensities was 6–7%, and that of 48/46 approximately 12%.

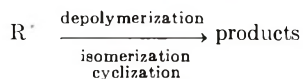
Thus, experiments have shown that water and formic acid are formed only partially as a result of the polymer oxidation with gaseous oxygen, and the rest of water and formic acid and all other products are due to oxygen heteroatoms of polymer chain.

The participation of gaseous oxygen in the formation of carbonyl groups of aldehydes was investigated by means of IR spectroscopy. Two polyformaldehyde films of equal

thickness were oxidized at 150°C. for 14 hr. One film was oxidized with labeled oxygen, and the other with oxygen of normal isotopic composition. The figure shows IR spectra of oxidated films, taken by a two-ray device, as a function of non-oxidized films. It may be seen that for labeled oxygen there is absorption at a frequency of 1700–1703 cm.^{-1} , besides the 1735 cm.^{-1} band. This is not observed for nonlabeled oxygen.

The isotopic shift value of the 32–35 cm.^{-1} group is equal to that obtained by other researchers for carbonyl-containing compounds.^{5,6} The ratio of the value of the band at 1700 cm.^{-1} to the value of the band at 1735 cm.^{-1} is much less than the 30% isotope ratio in gaseous oxygen. This result indicates that carbonyl groups of aldehydes which are formed by oxidation of polyformaldehyde are mainly due to oxygen heteroatoms of the polymer chain.

Thus, our results show that there are two methods of formation of products in oxidation of polyformaldehyde. The first method is a traditional mechanism of oxidation: $\text{RH} \rightarrow \text{R} \cdot \rightarrow \text{RO}_2 \cdot \rightarrow \text{ROOH} \rightarrow \text{products}$. The second method is intra- and intermolecular reactions in a polymer chain without participation of gaseous oxygen:



References

1. A. B. Blumenfeld, M. B. Neiman, and B. M. Kovarskaya, *Vysokomolekul. Soedin.*, **8**, N10 (1966).
2. S. Igarashi, J. Mita, and H. Kambe, *Bull. Chem. Soc. Japan*, **37**, 1160 (1964).
3. P. G. Kelleher and L. B. Jassie, *J. Appl. Polymer Sci.*, **9**, 2501 (1965).
4. F. Kurihara, *Kobunshi Kagaku*, **22**, 539 (1965).
5. M. Halmann and S. Pinchae, *J. Chem. Soc.*, **1958**, 1703.
6. E. Lippert, D. Samuel, and E. Fisher, *Ber. Bunsengesellsch. Phys. Chem.*, **69**, 155 (1965).

M. NEIMAN
A. BLUMENFELD
B. KOVARSKAYA

Institute of Chemical Physics
Academy of Sciences, USSR

Received April 7, 1966

Revised June 3, 1966

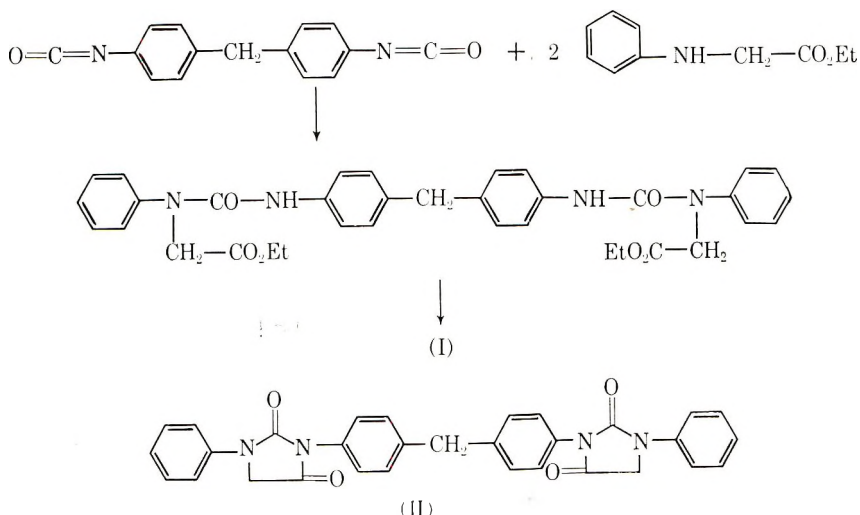
A New Class of Heterocyclic Polymers: Polyhydantoin

The preparation of polyhydantoin with aliphatic linkages in the chain has been previously reported.¹ They were obtained by the reaction of formaldehyde with 3,3'-methylene bis(5,5'-dialkyl hydantoin). In this communication we wish to report the preparation of new aromatic polyhydantoin obtained by a process of polyheterocyclization.

The synthesis of diphenyl-1,3-hydantoin was described in 1911 by Wheeler and Hoffman.² By the reaction of phenyl isocyanate on the *N*-phenyl glycine ethyl ester, at room temperature, the 1,3-diphenyl ureido ester was obtained. This latter compound, when heated, either in an inert solvent or in acidic media, was then cyclized to the corresponding hydantoin.

This reaction was extended to the polycondensation of *m*-phenylene diglycine diethyl ester with 4,4'-diphenyl methane diisocyanate.

At first, we synthesized model compounds of the polymer as follows:



Four mmole (1 g.) of pure 4,4'-diphenyl methane diisocyanate and 8 mmole (1.43 g.) of *N*-phenyl ethyl glycinate, freshly prepared (m.p. 57°C.) were dissolved in 50 ml. of anhydrous benzene. The solution was stirred for 15 hr. under nitrogen at room temperature. The benzene was removed at room temperature under reduced pressure. The resulting resinous material was triturated with methanol, and the white crystalline hydantoinic ester (I) was collected and dried under vacuum at room temperature to yield 2.13 g. (85%), m.p. 138°C.

ANAL. Calcd. for $C_{33}H_{36}N_4O_8$: C, 69.07%; H, 5.92%; N, 9.21%; Found: C, 69.05%; H, 6.11%; N, 9.10%.

The cyclization of the preceding ester to the hydantoin II occurred by heating for 15 hr. in boiling *N*-methyl pyrrolidone (yield, 70%) or acetic acid (yield, 62%) m.p. 232°C.

ANAL. Calcd. for $C_{31}H_{34}N_4O_4$: C, 72.08%; H, 4.68%; N, 10.85%; Found: C, 72.10%; H, 4.99%; N, 10.44%.

The IR spectra of these products are given in Figures 1 and 2. The cyclization of the ester to the hydantoin is shown by the disappearance of the peaks at 3333 cm^{-1} (NH), 1195 and 1018 cm^{-1} (C—O—C), and by the shift of the peaks due to the carbonyl groups (1745 to 1780 cm^{-1} and 1672 to 1724 cm^{-1}).

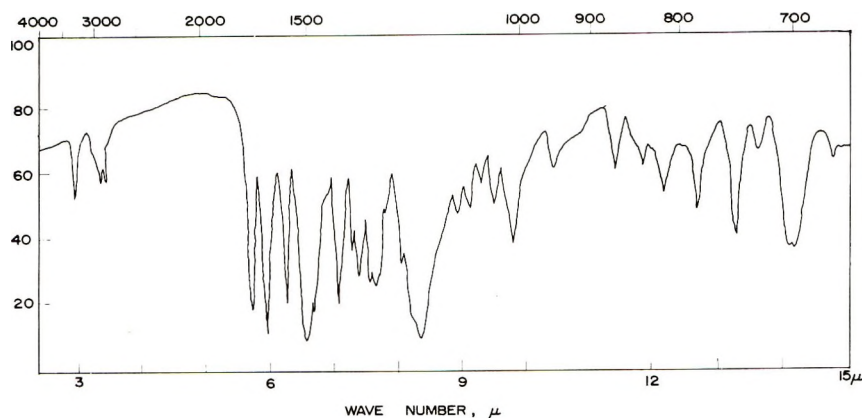


Fig. 1. Infrared spectrum of the hydantoic ester I (KBr).

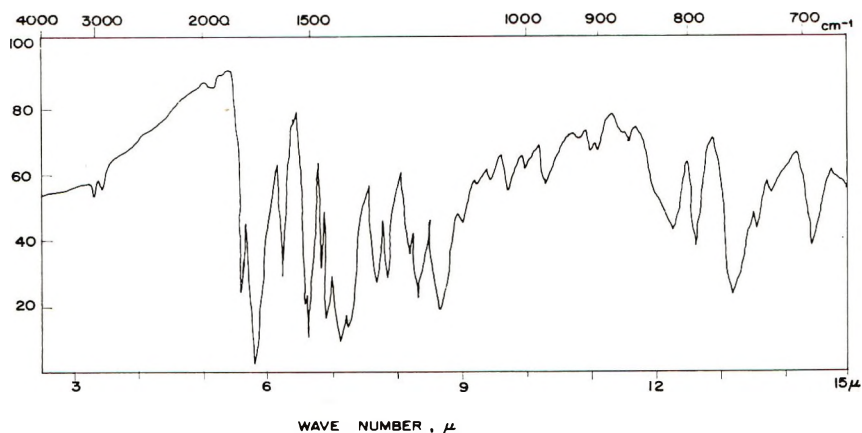


Fig. 2. Infrared spectrum of the hydantoin II (KBr).

The starting materials used for the polycondensation reactions were the diethyl *m*-phenylene glycinate and the 4,4'-diphenylmethane diisocyanate or its diphenyl diurethane derivative.

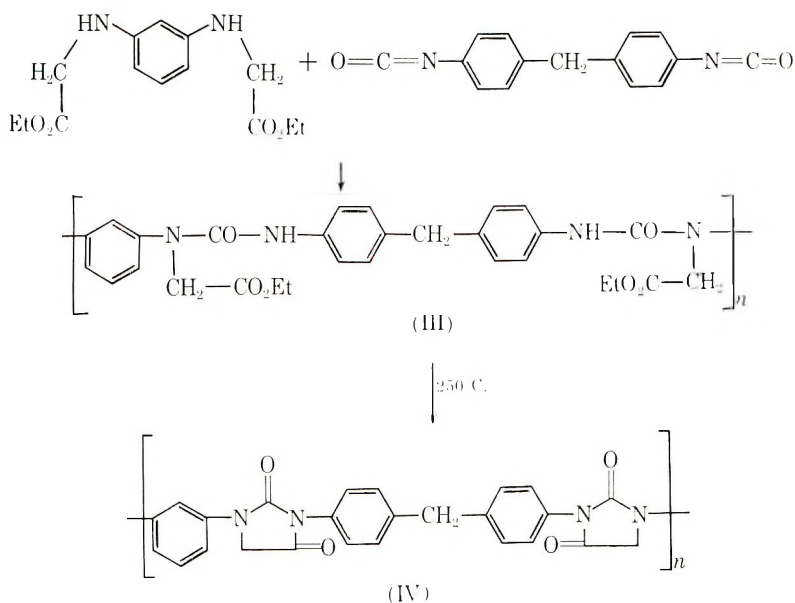
The diester was easily prepared from *m*-phenylenediamine, by reaction of ethyl chloroacetate in the presence of sodium acetate. The product was carefully purified by distillation under high vacuum, m.p. 72°C., reported 73°C.³ The IR spectrum showed peaks at 3333 cm^{-1} (NH), 1730 cm^{-1} (C=O), 1212 and 1030 cm^{-1} (C—O—C).

The commercial diisocyanate was purified by distillation under vacuum; its diphenyl diurethane derivative was prepared by heating a toluene solution of pure phenol and diisocyanate, affording 4,4'-methylene dicarbanilic diphenyl ester, m.p. 205°C., reported 168°C.⁴ IR spectrum showed peaks at 3311 cm^{-1} (NH) and 1724 cm^{-1} (C=O).

The polycondensation reactions were carried out by heating equimolar quantities of the reactants under a nitrogen atmosphere.

Using free diisocyanate, the mixtures were heated during 8 hr. at 200°C. After cooling, the products were ground, washed with ether, and dried; faintly yellow powders were obtained in nearly quantitative yields. The inherent viscosities, measured at 30°C. in dimethylacetamide (DMAC) at a concentration of 0.5%, were low (0.06–0.1)

and showed that only prepolymers were formed. These prepolymers were highly soluble (50 g./100 ml.) in polar solvents such as dimethylformamide (DMF) or DMAC. They were convenient for the preparation of laminated materials. The examination of their IR spectra showed that these prepolymers were mixtures of the polyhydantoic ester III and polyhydantoin IV.



These prepolymers were reheated 5 hr. at 250°C. under 10^{-2} mm. Hg, in order to complete the polycondensation and the heterocyclization. This was made apparent by the inherent viscosity, 0.25 (0.5% in DMAC, 30°C.) and was further confirmed by the IR absorption (disappearance of the peaks at 3333, 1190, and 1029 cm^{-1}), and by the elementary analysis as shown in following Table I.

TABLE I

	C, %	H, %	N, %
Calcd. for polyhydantoic ester III ($\text{C}_{29}\text{H}_{30}\text{N}_4\text{O}_6$) _n	65.66	5.66	10.56
Calcd. for polyhydantoin IV ($\text{C}_{25}\text{H}_{18}\text{N}_4\text{O}_4$) _n	68.48	4.14	12.78
Found for polymer obtained at 200°C.	67.54	4.96	11.55
Found for polymer after treatment at 250°C.	68.63	4.19	13.05

Using the diurethano derivative instead of the free diisocyanate, the melt polycondensations were carried out at 250°C. for 7 hr., and occurred without prepolymer stage. The formed phenol and ethanol were removed from the reaction flask by the flow of nitrogen. After cooling, the reaction products were dissolved in *m*-cresol and precipitated by pouring the solution into ethanol. The precipitates were filtered and thoroughly washed with ethanol, then dried, to give white powders in nearly quantitative yields. Under these conditions, high polymers were obtained. They had inherent vis-

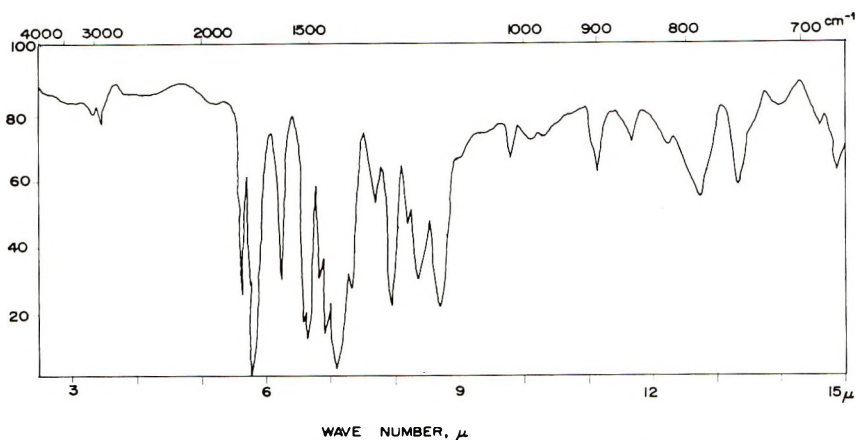


Fig. 3. Infrared spectrum of the polyhydantoin (film).

cosities of 0.9 (0.5% in *m*-cresol at 30°C.). A further treatment at 325°C., for 5 hr. under vacuum did not affect the viscosity. The resulting polymers were only slightly soluble in DMF or DMAC, but soluble at 10 g./100 ml. in *m*-cresol. Films were cast from these solutions; they were tough and almost colorless.

ANAL. Calcd. for $(C_{23}H_{18}N_4O_4)_n$: C, 68.48%; H, 4.14%; N, 12.78%; Found: C 68.57%; H, 4.30%; N, 12.31%.

The IR spectrum of the film of polymer (Fig. 3) was compared to the spectra of the model compounds and also showed clearly that the obtained polymer was the polyhydantoin entirely cyclized.

The thermal stability of the polymer was studied, in air and under argon atmosphere, using a heating rate of 60°C./hr. Decomposition of the polymer occurred at 330°C. in air and at 375°C. under inert atmosphere.

Further work on other polyhydantoin is in progress and will be reported in the near future.

This work is supported by the Délégation Générale à la Recherche Scientifique et Technique, to whom grateful acknowledgment is hereby made.

References

1. E. I. du Pont de Nemours & Co., Inc., French Pat. 1,386,691 (1964).
2. H. L. Wheeler and C. Hoffman, *Am. Chem. J.*, **45**, 383 (1911).
3. J. Zimmerman and M. Knyrim, *Ber.*, **16**, 514 (1883).
4. V. V. Korshak and I. A. Gribova, *Izv. Akad. Nauk. SSSR, Otd. Khim. Nauk.*, **1961**, 550.

R. H. SALLÉ
B. J. SILLION
G. P. DE GAUDEMARIS

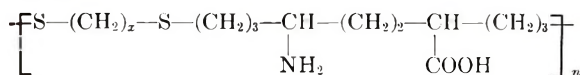
Département de Recherche
Institut Français du Pétrole
Grenoble, France

Received February 28, 1966

Revised May 10, 1966

The Use of Dialysis in Polymer Purification

In the synthesis of a series of regular polyampholytes,¹ copolymers of 3,6-diallyl-2-piperidone and α,ω -dithiols were hydrolyzed with dilute sulfuric acid to open the piperidone ring; this was followed by neutralization of the acid with sodium hydroxide to yield the polyampholyte:



The residual sodium sulfate proved to be difficult to remove. Such inorganic salts and other low molecular weight impurities are commonly removed from aqueous protein solutions by dialysis through a semipermeable membrane.² Dialysis against distilled water with the polyampholyte encased in seamless cellulose dialyser tubing (1.25 in.) was not effective for removing residues of around 1% which we had not been able to remove by washing. We found, however, that dialysis was accomplishing a fractionation of the polyampholyte as evidenced by increased inherent viscosity of 20% and more when dialysed for 96 hr. in an aqueous system. The most striking result was in the polyampholyte in which x is 4; here the inherent viscosity increased from 0.19 ($c = 0.455$ g./100 ml. formic acid at 30°C.) to 0.34 ($c = 0.436$ g./100 ml. formic acid at 30°C.).

The use of membranes such as methoxymethylnylon for the fractionation of polystyrene in non-aqueous systems has been described.³ But despite the very common reliance on dialysis for fractionating natural products such as proteins,^{4,5} enzymes,⁵ polysaccharides,⁶ and ligninsulfonates,⁷ we are not aware of its use for fractionating high polymers in aqueous systems. Work on proteins has shown that the arbitrary division between proteins (molecular weight $> 10,000$) and natural polypeptides (molecular weight $< 10,000$) corresponds to the division between nondialysability and dialysability through cellophane.⁸ In accordance with that work, we suggest that the higher viscosity of the polyampholytes after dialysis results from the diffusion into the solvent of the smaller molecules present in the polymer mixture.

In order to investigate the scope of applicability of this technique, several polymers and copolymers were studied. We prepared a copolymer consisting of 60 parts of methyl methacrylate and 40 parts of acrylic acid. This copolymer would be expected to be somewhat hydrophilic. The inherent viscosity of this material increased over 10% during 48 hr. of dialysis against distilled water, from 2.99 ($c = 0.462$ g./100 ml. formic acid at 30°C.) to 3.31 ($c = 0.443$ g./100 ml. formic acid at 30°C.). Nine per cent of the material dialysed out of the cellulose tubing into the solvent. When the nondialysed copolymer was reprecipitated from acetone with petroleum ether (30–60°C.), the inherent viscosity increased only very slightly, from 2.99 to 3.03 ($c = 0.581$ g./100 ml. formic acid at 30°C.).

Two hydrophobic polymers, polyacrylonitrile ($\eta_{\text{inh}} = 1.65$; $c = 0.439$ g./100 ml. formic acid at 30°C.) and poly(methyl methacrylate) ($\eta_{\text{inh}} = 1.05$; $c = 0.241$ g./100 ml. formic acid at 30°C.) showed no significant change in viscosity after 48 hr. of dialysis. The latter polymer did, however, show an improved agreement between theoretical and experimental carbon and hydrogen content.

The technique of dialysis is one which we feel has a place in synthetic polymer chemistry and its scope requires further study.

This study was supported in part by the National Science Foundation under N.S.F. grant G 15828.

References

1. C. H. H. Neufeld and C. S. Marvel, *J. Polymer Sci. A1*, in press.
2. H. D. Springall, *The Structural Chemistry of Proteins*, Academic Press, New York, 1954.

3. J. H. S. Green, H. T. Hookway, and M. F. Vaughan, *Chem. Ind. (London)*, **1958**, 862.
4. J. W. Pence and A. H. Elder, *Cereal Chem.*, **30**, 275 (1953).
5. L. C. Craig, Wm. Konigsberg, A. Stracher, and T. P. King, in *Symposium on Protein Structure*, A. Neuberger, Ed., Wiley, New York, 1958.
6. K. C. B. Wilkie, J. K. N. Jones, B. J. Excell, and R. E. Semple, *Can. J. Chem.*, **35**, 795 (1957).
7. J. L. Gardon and S. G. Mason, *Can. J. Chem.*, **33**, 1477 (1955).
8. R. L. M. Synge, *Quart. Rev. Chem. Soc., London*, **3**, 245 (1949).

C. H. H. NEUFELD*
C. S. MARVEL

Department of Chemistry
University of Arizona
Tucson, Arizona

Received June 30, 1966

* Visiting Professor of Chemistry, 1965-1966; on leave from Western Regional Research Laboratory, Western Utilization Research and Development Division, Agricultural Research Service, United States Department of Agriculture, Albany, California.

BOOK REVIEWS

Diffraction of X-Rays by Chain Molecules. B. K. VAINSHTEIN, Ed. American Elsevier Publishing Co., Inc., New York, 1966. xiii + 414. \$23.50.

There is a Spanish proverb which says "When the monkey likes to fish he needs to wet his tail." The philosophy behind it is that if anybody wants to achieve an end he must apply himself to it in spite of the difficulties. This is the case with this book. The subject is appealing to most polymer workers because at one time or another they have been exposed to the importance of x-ray diffraction in clarifying structural problems in their field. Unfortunately, people are continuously coming into polymer research from different origins and to them the book will require various amounts of effort to go through it. To x-ray crystallographers educated in single-crystal work, it will be an open door toward the understanding of polymer structure and morphology that will probably help "to trap" some of them for this fascinating field. To the physicists, working in other aspects of polymer science, it will require a formal reading to grasp the implication of the work presented. To biologists, chemists, and chemical engineers, it will demand first, a good brush-up of their mathematical background, especially the series and Fourier transform theories; second, a general reading on x-ray diffraction theory by single crystals, and finally a conscientious study of the book. To this introduction, it is necessary to add that the effort required in every case is worthwhile.

The book is essentially a textbook that in one way or another will come into the curriculum of most polymer physicists. Its organization is good. It starts by giving a summary of the diffraction theory and the necessary mathematical background which is extended into other chapters of the book. Alternating with them the problem of polymer diffraction is presented, initially in general terms in Chapter 2 and thoroughly in the following chapters. The analysis departs from the diffraction effect of an isolated polymer chain—linear or helical—toward the diffraction effect of association of chains, not as perfect geometrical systems but as real entities with various degrees of order—due to thermal motion, statistical disorder, strain, etc. Finally, the diffraction effects of amorphous polymers are analyzed in light of the precedent study, and a review of the meaning of low-angle scattering added. The author calls attention to the power of optical transforms to overcome the mathematical barrier, however, it is perhaps unfortunate that greater emphasis was not placed on this technique since mathematical relations of more general availability elsewhere have been included in the text. Similar comments can be made to the lack of a good glossary of the symbols used which demands a continuous concentration and extra work. On the other hand, a good feature is that most of the references cited are in journals of books available in English. Also, the book must be commended for having none of the defects normally found in translations, being adequately printed and attractively presented.

In conclusion, this book is recommended to everyone working in x-ray diffraction of polymers and proteins from the structural point of view.

Luis G. Roldan

Allied Chemical Corporation
Central Research Laboratory
Morristown, New Jersey

Polymeric Sulfur and Related Polymers. ARTHUR V. TOBOLSKY and WILLIAM J. MACKNIGHT. Interscience, New York, 1965. viii + 140. \$7.75.

This small volume may well become a classic for the growing number of scientists and engineers interested in the specialized field of polymeric sulfur, organic and inorganic polysulfide polymers. The treatment of the subject is in terms familiar to the physical chemist and the polymer scientist. It brings together the remarkably clarifying work of the authors, their co-workers, and others on the equilibrium polymerization of sulfur at all temperatures up to its boiling point. The role played by the supercooled, most stable form of sulfur, the S_8 ring, on the stress-strain properties of polymeric sulfur and organic polysulfide polymers is brought clearly to light. Many of us were aware of the confused situation and incomplete understanding that existed for many years in this area.

The authors put their emphasis on the effect of polymeric structures containing the polysulfide unit $-S_n-$ where n is at least equal to four. The dissociation energy of scission and the interaction of such groups with each other are exactly related to the chemical stress relaxation of the polysulfide polymers and also of the polymers containing predominantly a repeating disulfide structure. The activation energy of stress relaxation, the energy of dissociation of polysulfide structures, and other thermodynamic properties are the probes used to explain the viscoelastic properties of these polymers at widely varying crosslink levels. What can be said of the obscuring and complicating role played by crystallization in these predominantly elastomeric polymers of sulfur and its organic and inorganic copolymer? Here, again, the authors carefully isolate these effects by describing experiments in which the polymers are subjected to very low temperature quenchings. As a result, the various polymer transitions such as the glassy and rubbery states, and the region of chemical and rheological flow, can be demonstrated. A satisfying aspect of this book is the copious data in the form of tables, graphs and experimental description supporting the important deductions.

The chapter on the inorganic sulfur-containing copolymers discusses the viscoelastic properties of the systems sulfur-selenium, sulfur-arsenic, sulfur-selenium-arsenic, selenium-arsenic, and sulfur-phosphorous. The crosslinking effects of trivalent phosphorous and arsenic are demonstrated. In order to properly understand the effect of the comonomer of selenium, it was necessary to investigate its homopolymer. An interesting section on the viscoelastic properties of amorphous selenium and its stress relaxation at various temperatures is included.

This volume is a very welcome addition to the Polymer Review series under the editorship of H. F. Mark and E. H. Immergut.

E. R. Bertozzi

Thiokol Chemical Corporation
Trenton, New Jersey

ERRATUM

Properties of *p*-Polyphenyl. Pellet Formation, Radiation Resistance, and Electrical Behavior

(article in *J. Polymer Sci. A*, **3**, 4297-4298, 1965)

By PETER KOVACIC, VINCENT J. MARCHIONNA, and JAN P. KOVACIC

Department of Chemistry, Case Institute of Technology, Cleveland, Ohio

On page 4298, the first sentence under the Experimental section should read: *p*-Polyphenyl was prepared [$C_6H_6:CuCl_2:AlCl_3 = 8:1:2$ (molar), $32 \pm 1^\circ C.$, 2 hr.] according to the published procedure.²